US Army Corps of Engineers

CONTRACT REPORT GL-89-2

RE-EVALUATION OF THE LOWER SAN FERNANDO DAM

Report 2

EXAMINATION OF THE POST-EARTHQUAKE SLIDE OF FEBRUARY 9, 1971

by

H. Bolton Seed, Raymond B. Seed, Leslie F. Harder
Hsing-Lian Jong

H. Bolton Seed, Inc.
623 Crossridge Terrace
Orinda, California 94563

September 1989
Report 2 of a Series

Approved For Public Release; Distribution Unlimited

Prepared for DEPARTMENT OF THE ARMY
US Army Corps of Engineers
Washington, DC 20314-1000

Under Contract No. DACW39-85-C-0048

Monitored by Geotechnical Laboratory
US Army Engineer Waterways Experiment Station
3909 Halls Ferry Road, Vicksburg, Mississippi 39180-6199

GEOTECHNICAL LABORATORY

SECURITY CLASSIFICATION OF THIS PAGE

REPORT DOCUMENTATION PAGE

Form Approved OMB No. 0704-0188

1a. REPORT SECURITY CLASSIFICATION Unclassified	1b. RESTRICTIVE MARKINGS
2a. SECURITY CLASSIFICATION AUTHORITY	3. DISTRIBUTION/AVAILABILITY OF REPORT Approved for public release; distribution unlimited
2b. DECLASSIFICATION/DOWNGRADING SCHEDULE	
4. PERFORMING ORGANIZATION REPORT NUMBER(S)	5. MONITORING ORGANIZATION REPORT NUMBER(S) Contract Report GL-89-2
6a. NAME OF PERFORMING ORGANIZATION H. Bolton Seed, Inc. — 6b. OFFICE SYMBOL (If applicable)	7a. NAME OF MONITORING ORGANIZATION USAEWES Geotechnical Laboratory
6c. ADDRESS (City, State, and ZIP Code) 623 Crossridge Terrace Orinda, California 94563	7b. ADDRESS (City, State, and ZIP Code) 3909 Halls Ferry Road Vicksburg, Mississippi 39180-6199
8a. NAME OF FUNDING/SPONSORING ORGANIZATION US Army Corps of Engineers — 8b. OFFICE SYMBOL (If applicable)	9. PROCUREMENT INSTRUMENT IDENTIFICATION NUMBER
8c. ADDRESS (City, State, and ZIP Code) Washington, DC 20314-1000	10. SOURCE OF FUNDING NUMBERS PROGRAM ELEMENT NO. / PROJECT NO. / TASK NO. / WORK UNIT ACCESSION NO.

11. TITLE (Include Security Classification) Re-Evaluation of the Lower San Fernando Dam; Report 2: Examination of the Post-Earthquake Slide of February 9, 1971

12. PERSONAL AUTHOR(S)
Seed, H. Bolton; Seed, Raymond B.; Harder, Leslie F; Jong, Hsing-Lian

13a. TYPE OF REPORT	13b. TIME COVERED	14. DATE OF REPORT (Year, Month, Day)	15. PAGE COUNT
Report 2 of a Series	FROM _____ TO _____	September 1989	270

16. SUPPLEMENTARY NOTATION This report is available from the National Technical Information Service, 5285 Port Royal Road, Springfield, VA 22161.

17. COSATI CODES			18. SUBJECT TERMS (Continue on reverse if necessary and identify by block number)
FIELD	GROUP	SUB-GROUP	See reverse

19. ABSTRACT (Continue on reverse if necessary and identify by block number)

This report presents the results of an investigation performed to re-evaluate the slide in the upstream portion of the Lower San Fernando Dam which was triggered by the San Fernando Earthquake of February 9, 1971. Data from seismoscopes located on the crest and one abutment indicated that the main slide movements occurred about 20 to 30 sec after the strong earthquake shaking had stopped. It can thus be inferred that the earthquake shaking triggered a loss of strength in the soils comprising the embankment, and that it was this loss of strength in the soils comprising the embankment, and that it was this loss of strength, rather than the inertial forces induced by the earthquake shaking, which led to the sliding of the upstream slope.

The studies reported herein were performed for the following purposes: (a) to determine whether recently developed techniques for evaluating in-situ undrained steady state strength based on laboratory testing and post-test corrections would accurately predict the

(Continued)

20. DISTRIBUTION/AVAILABILITY OF ABSTRACT	21. ABSTRACT SECURITY CLASSIFICATION
☒ UNCLASSIFIED/UNLIMITED ☐ SAME AS RPT ☐ DTIC USERS	Unclassified
22a. NAME OF RESPONSIBLE INDIVIDUAL	22b. TELEPHONE (Include Area Code) / 22c. OFFICE SYMBOL

DD Form 1473, JUN 86 — Previous editions are obsolete — SECURITY CLASSIFICATION OF THIS PAGE

18. SUBJECT TERMS (Continued).

Case study	Hydraulic fill	Residual strength	Standard Penetration Test
Cyclic loading	Laboratory testing	Seismic stability	
Earth dams	Liquefaction	Soil dynamics	

20. ABSTRACT (Continued).

observed residual strength of the San Fernando Dam hydraulic fill materials; (b) to determine whether the use of improved sampling procedures would lead to different results for undrained cyclic load tests on "undisturbed" samples taken from the dam (relative to those obtained in earlier investigations performed in 1971-73); (c) to explore the reproducibility of laboratory steady state strength test data used for seismic stability evaluations as measured in different laboratories; and (d) to evaluate the feasibility of basing both pore pressure generation ("triggering") and undrained residual strength (post-triggering stability) assessments on SPT data using new standardized SPT procedures.

Reproducibility of laboratory steady state strength test data was found to be very good. Tests of reconstituted samples of a sandy silt material (Bulk Sample No. 7) from the base of the downstream hydraulic fill zone performed at four different laboratories (Stanford Geotechnical Laboratory, Waterways Experiment Station, GEI Consultants, Inc., and Rensselaer Polytechnic Institute) yielded very similar steady state lines. Tests of 10 undisturbed samples of sandy silt from this zone, corrected for disturbance effects and earthquake-induced densification, resulted in an average estimated pre-earthquake steady state stregnth of $S_{us} \approx 880$ psf for the base of the downstream slope. This agrees well with an average value of $S_{us} \approx 1100$ psf based on 15 tests of undisturbed samples performed by GEI, Inc. and the same set of corrections.

Overall assessment of a suitable value of S_{us} for re-analysis of the 1971 upstream slide based on the laboratory testing program is complicated by (a) the heterogeneity of the hydraulic fill, (b) possible differences in density between the upstream and downstream hydraulic fill zones due to different effective consolidation stresses, and (c) uncertainty in assessment of earthquake induced densification of various fill zones. A conservative assessment of these factors leads to an average laboratory-based estimate of the pre-earthquake $S_{us} \approx 800$ psf, and a lower 35-percentile estimate of $S_{us} \approx 580$ psf. These values are somewhat higher than the observed residual field strength of $S_r \approx 300$ to 500 psf, but are lower than the initial average driving shear stresses in the hydraulic fill of $\tau_{dr,i} \approx 900$ psf. Accordingly, these laboratory-based steady state strength estimates would correctly predict the initiation of slide movements, but would not predict the large displacements actually observed and would provide a somewhat unconservative assessment of the actual observed strength.

Results of undrained cyclic triaxial tests performed on undisturbed samples of hydraulic fill were found to be in good agreement with those of earlier studies. Cyclic strengths (stress ratios causing 5 percent strain in a given number of cycles) were about 5 to 15 percent lower in these studies than those measured in 1971-73, and both the current and earlier cyclic strength data sets provide a good basis for evaluation of the observed performance of the upstream and downstream slopes. It should be noted, however, that this is probably due to a fortuitous compensation of the effects of sampling disturbance and sampling densification, and does not mean that cyclic testing of undisturbed samples will necessarily provide a consistently reliable basis for assessment of the in situ liquefaction resistance of other materials.

Standard penetration test (SPT) results from 1971 and 1985 field investigations, after correction for procedural and equipment effects to a new proposed standard $(N_1)_{60}$, provided good agreement with the liquefaction resistance assessment based on cyclic tests of undisturbed samples, and by analogy provided a good assessment of observed pore pressure generation behavior of the hydraulic fill zones. With an additional correction for fines content, the SPT resistance of $(N_1)_{60}$-clean sand ≈ 13.5 blows/ft and the observed residual strength of the hydraulic fill fit well with the pattern of $(N_1)_{60}$-clean sand versus S_r developed by back-analysis of a number of other liquefaction slides. It thus appears that this type of correlation between $(N_1)_{60}$-clean sand versus S_r provides a reasonably and reliable basis for evaluation of in situ residual undrained strengths.

PREFACE

This study was a part of an investigation of the strength of soils that have been weakened by earthquake shaking, and the stability of embankment dams containing or founded on susceptible soils. This report is one of a series which documents the investigation. The project was carried out jointly by Geotechnical Engineers, Inc. (GEI), H. Bolton Seed, Inc., Rensselaer Polytechnic Institute (RPI), and the US Army Engineer Waterways Experiment Station (WES). Principal Investigators were Dr. Gonzalo Castro for GEI, Professor H. Bolton Seed, Professor Ricardo Dobry for RPI, and Dr. A. G. Franklin for WES. Mr. Edward Pritchett, Office of the Chief of Engineers, Washington, DC, was responsible for recognizing the importance and timeliness of this research to the Corps of Engineers, and for generating Corps support for the project. Funding was provided through the US Army Engineer District, Kansas City, for whom oversight was provided by Mr. Francke Walberg.

Essential to the overall investigation was an exploration and records review effort at the Lower San Fernando Dam, in order to obtain crucial data and soil samples for laboratory testing. This effort included an extensive drilling and penetration testing program, excavation of a large-diameter shaft, in-situ testing, collection of samples, and review of historical records. The Los Angeles Department of Water and Power, owner of the Lower San Fernando Dam, provided access to the site and to the historical records, and other assistance. The California Department of Water Resources provided information from their files.

Drilling, Standard Penetration Testing, and undisturbed sampling from borings were performed by WES, under the supervision of Mr. Joseph Gatz. Cone Penetration Test soundings were performed by Earth Technology Corporation (ERTEC). Excavation of the exploratory shaft was done by Zamborelli Drilling Company, under the direction of GEI. Investigations and sampling in the shaft, and the review of historical records, were done by and under the supervision of Mr. Tom Keller of GEI.

The results presented in this report were developed by H. Bolton Seed, Inc., in cooperation with the Stanford University Geotechnical Laboratory. The work was carried out under WES Contract No. DACW39-85-C-0048.

The technical monitor and Contracting Officer's Representative at WES was Dr. A. G. Franklin, Chief of the Earthquake Engineering and Geosciences Division, Geotechnical Laboratory. The primary WES reviewer was Dr. Paul F. Hadala, Assistant Chief of the Geotechnical Laboratory. Chief of the Geotechnical Laboratory was Dr. William F. Marcuson III.

Commander and Director of WES during the preparation of this report was COL Larry B. Fulton, EN. Dr. Robert W. Whalin was Technical Director.

CONTENTS

CONTENTS (Contd.)

LIST OF TABLES

LIST OF FIGURES

LIST OF FIGURES (Contd.)

LIST OF FIGURES (Contd.)

LIST OF FIGURES (Contd.)

LIST OF FIGURES (Contd.)

LIST OF FIGURES (Contd.)

LIST OF FIGURES (Contd.)

LIST OF FIGURES (Contd.)

CONVERSION FACTORS, NON-SI TO SI (METRIC) UNITS OF MEASUREMENT

Non-Si units of measurement used in this report may be converted to metric (SI) units as follows:

Multiply	By	To Obtain
cubic feet	0.02831685	cubic metres
inches	2.54	centimetres
pounds (force)	4.448222	newtons
pounds (force) per square inch	6.894757	kilopascals
square inches	6.4516	square centimetres

RE-EVALUATION OF THE LOWER SAN FERNANDO DAM
REPORT 2:
EXAMINATION OF THE POST-EARTHQUAKE SLIDE OF FEBRUARY 9, 1971

by

H. Bolton Seed, Raymond B. Seed, Leslie F. Harder and Hsing-Lian Jong

1. Introduction

The Lower San Fernando Dam in California developed a major slide in the upstream slope and crest as a result of the 1971 San Fernando earthquake. An investigation of the slide, including trenches and borings, in situ density tests, undisturbed sampling, index testing, static and cyclic load testing, and analyses was performed and reported by Seed et al. (1973), Seed et al. (1975a), Seed et al. (1975b), and Lee et al. (1975). The field investigation showed that the slide occurred due to liquefaction of a zone of hydraulic sand fill near the base of the upstream shell.

Two cross sections of the Lower San Fernando Dam are presented in Fig. 1-1, one showing the observations made in a trench excavated through the slide area and the other showing a reconstructed cross section of the dam, illustrating the zone in which liquefaction occurred. Large blocks of essentially intact soil from the upstream section of the dam moved into the reservoir, riding over or "floating" on the liquefied soil. After movements stopped, the liquefied soil was found to have extruded out below the toe of the dam and up between the intact blocks, with maximum movements as much as 200 ft (61 m) beyond the toe of the dam. The block of soil which contained the toe of the dam moved about 150 ft (46 m) into the reservoir.

Data from seismoscopes located on the abutment and on the crest of the embankment indicated peak accelerations of about 0.55g and 0.5g, respectively, and an analysis of the seismoscope record on the dam crest indicated that the slide occurred about 20 to 30 seconds after the earthquake shaking had stopped

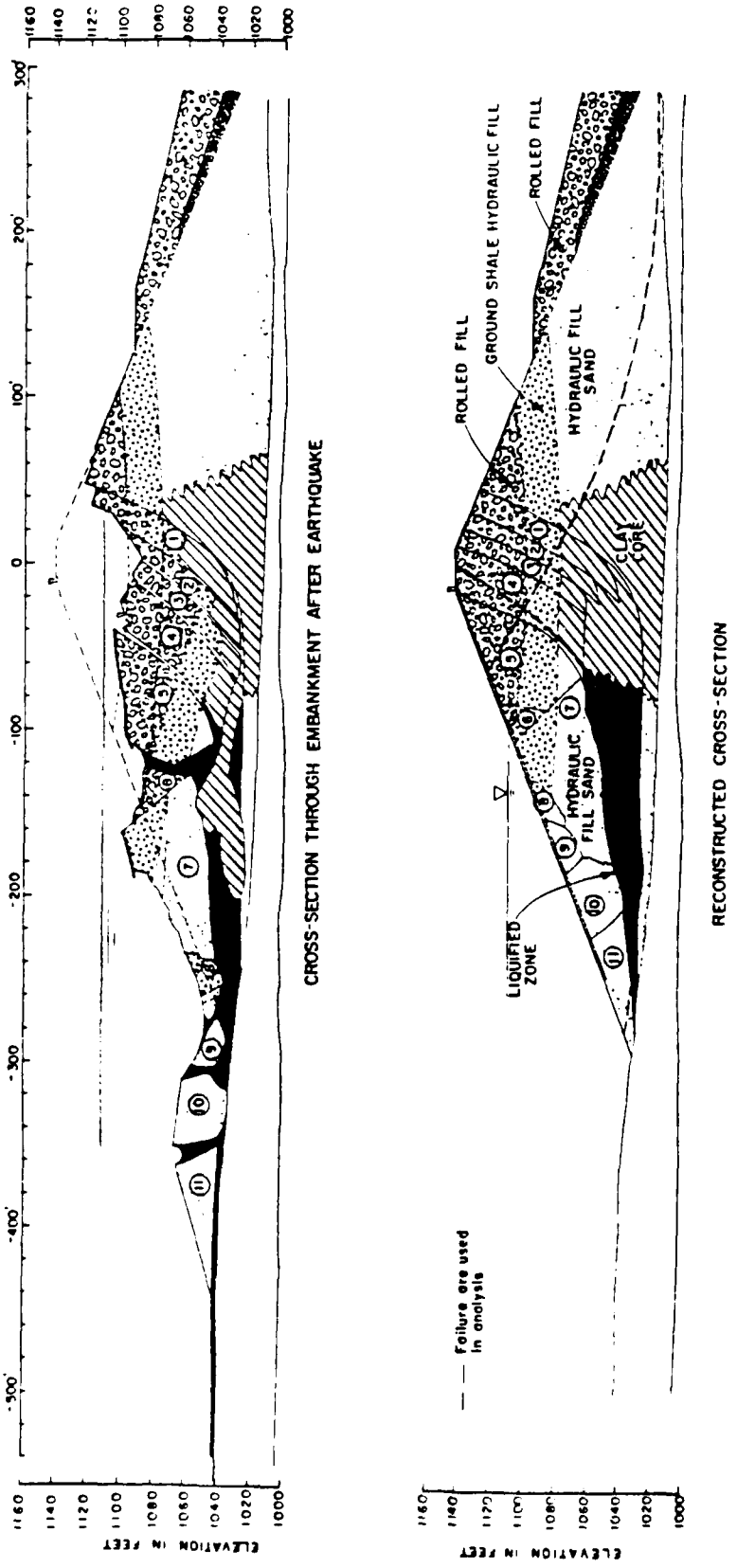

Fig. 1-1 FAILURE AND RECONSTRUCTED CROSS SECTION, LOWER SAN FERNANDO DAM

(After Seed et al., 1983)

(Seed, 1979). Thus the large slide movements apparently developed in the absence of earthquake-induced stresses and were caused only by the static stresses due to the weight of the materials in the embankment. It can thus be inferred that the earthquake shaking triggered a loss of strength in the soils comprising the embankment and it was this loss of strength, rather than the inertia forces induced by the earthquake shaking, which led to the sliding of the upstream slope.

It has been estimated that the slide movements in the Lower San Fernando Dam developed mainly in about 40 seconds, suggesting that the average rate of movement was about 5 ft/sec or 3 mph (5 kph). This comparatively slow rate of movement indicates that the soil in the slide zone was in a marginal state of limiting equilibrium during the period of sliding and that the factor of safety was only slightly less than 1.0. However the flow of liquefied sand into cracks in the embankment and the flow of sand beyond the toe of the embankment suggests that the strength of the liquefied sand in some zones must have been quite low.

While it is readily apparent that sliding due to liquefaction occurred in the upstream shell of the embankment, performance data from the files of the City of Los Angeles Department of Water and Power show that the water levels measured in wells installed in the downstream shell showed only small changes in elevation as a result of the earthquake shaking (see Figs. 1-2 and 1-3). Thus it would appear that while the earthquake caused a small increase in pore pressure ratio in the downstream shell and its foundation, there was no significant extent of soil liquefaction in this part of the embankment.

The analysis of the dynamic response of the dam, performed as part of the investigation in 1973, was made using a method of analysis proposed by Seed, Lee and Idriss (Seed et al., 1975b). This method of analysis involves the following steps:

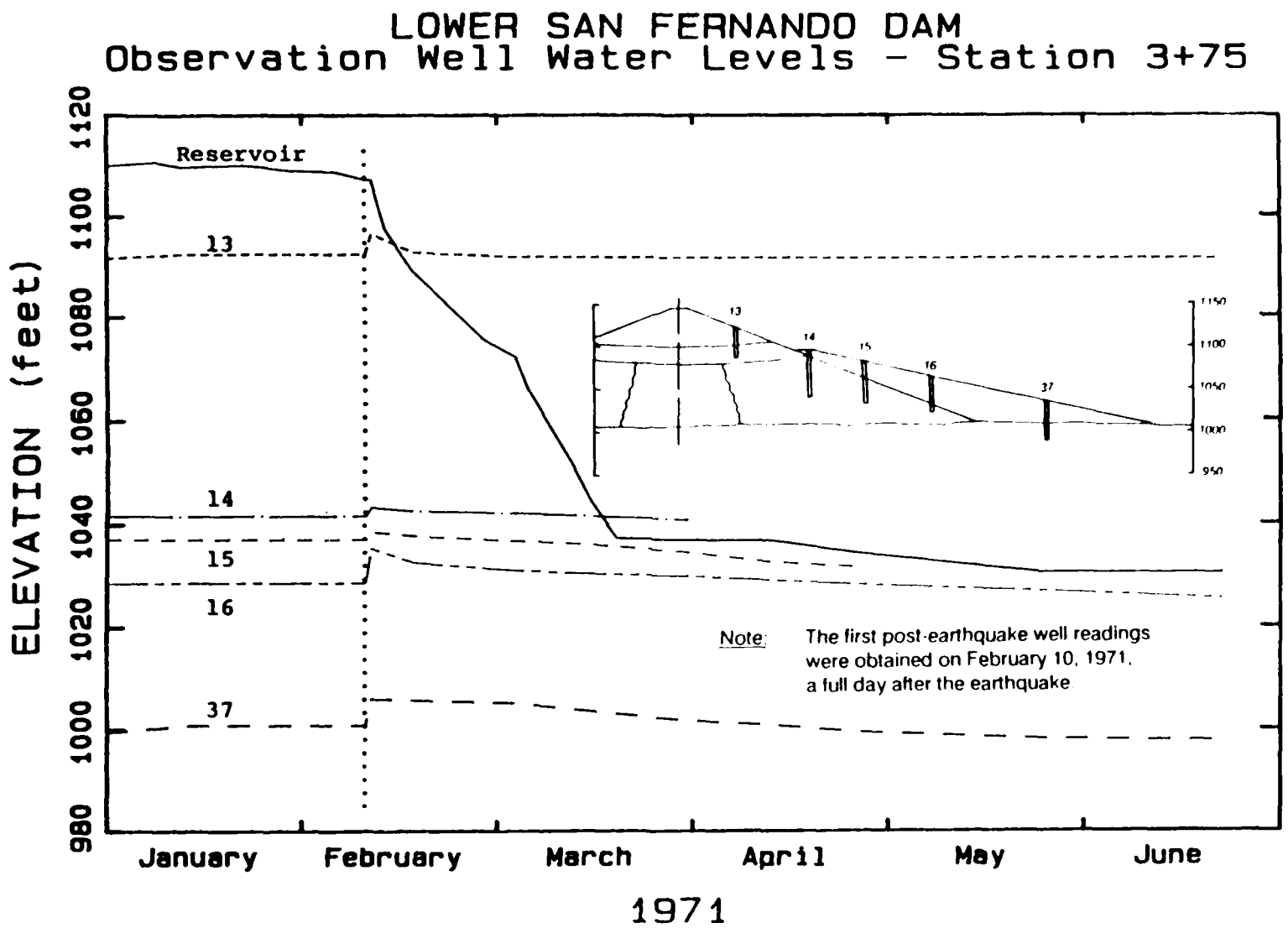

Fig. 1-2 OBSERVED WATER LEVEL CHANGES IN WELLS IN DOWNSTREAM SHELL AND FOUNDATION OF LOWER SAN FERNANDO DAM

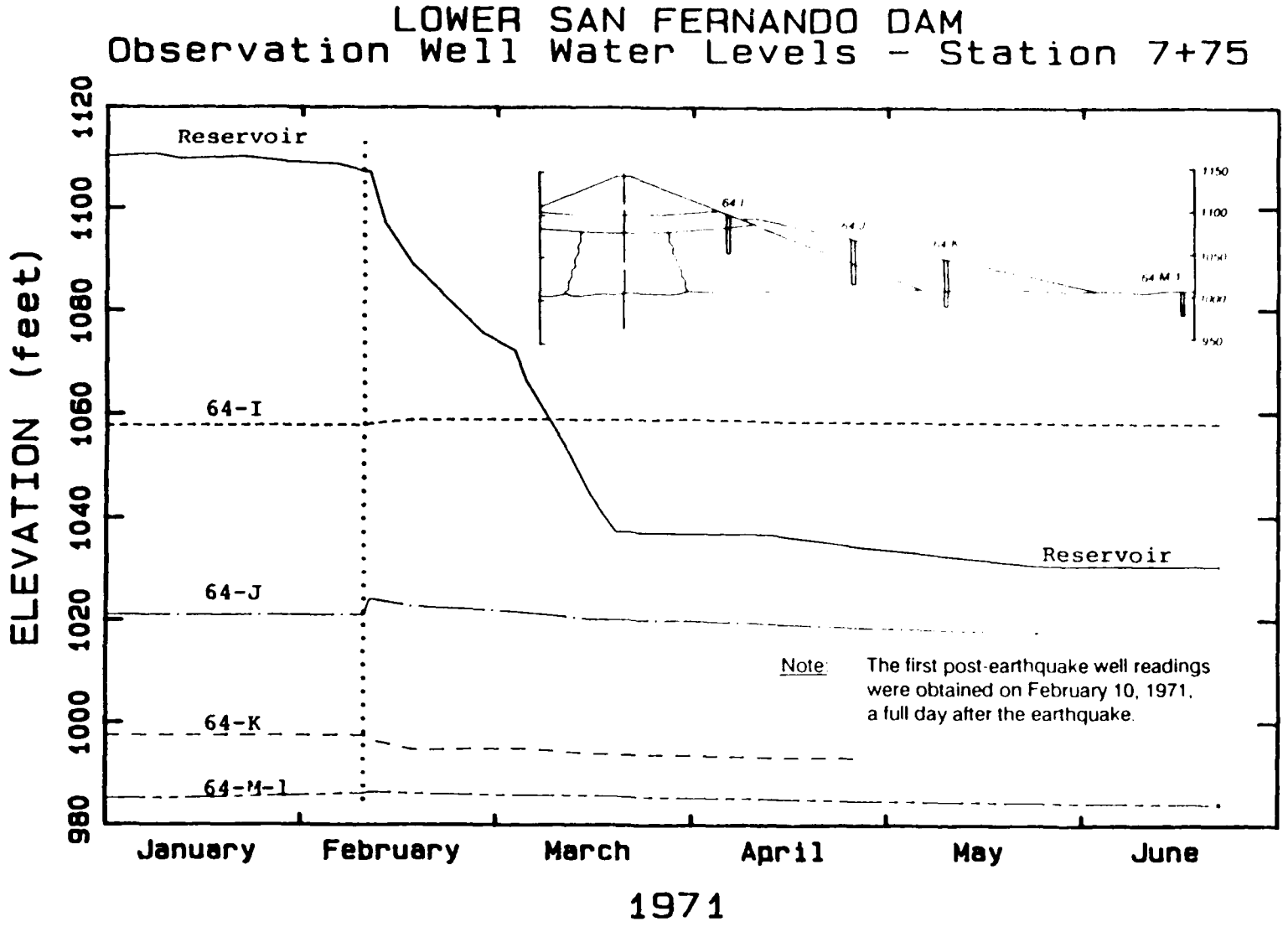

Fig. 1-3 OBSERVED WATER LEVEL CHANGES IN WELLS IN DOWNSTREAM SHELL AND FOUNDATION OF LOWER SAN FERNANDO DAM

1. Determine the cross-section of the dam to be used for analysis.
2. Determine, with the cooperation of geologists and seismologists, the maximum time history of base excitation to which the dam and its foundation might be subjected.
3. Determine, as accurately as possible, the stresses existing in the embankment before the earthquake; this is probably done most effectively at the present time using finite element analysis procedures.
4. Determine the dynamic properties of the soils comprising the dam, such as shear modulus, damping characteristics, bulk modulus or Poisson's ratio, which determine its response to dynamic excitation. Since the material characteristics are nonlinear, it is also necessary to determine how the properties vary with strain.
5. Compute, using an appropriate dynamic finite element analysis procedure, the stresses induced in the embankment by the selected base excitation.
6. Subject representative samples of the embankment materials to the combined effects of the initial static stresses and the superimposed dynamic stresses and determine their effects in terms of the generation of pore water pressures and the potential development of strains. Perform a sufficient number of these tests to permit similar evaluations to be made, by interpolation, for all elements comprising the embankment.
7. From the knowledge of the pore pressures generated by the earthquake, the soil deformation characteristics and the strength characteristics, evaluate the factor of safety against failure of the embankment either during or following the earthquake.

8. If the embankment is found to be safe against failure, use the strains induced by the combined effects of static and dynamic loads to assess the overall deformations of the embankment.
9. Be sure to incorporate the requisite amount of judgment in each of steps (1) to (8) as well as in the final assessment of probable performance, being guided by a thorough knowledge of typical soil characteristics, the essential details of finite element analysis procedures, and a detailed knowledge of the past performance of embankments in other earthquakes.

Application of the method to the Lower San Fernando Dam led to the conclusion that it provided a reasonable basis for evaluating the location and extent of the zone of liquefaction in the upstream shell, as shown in Fig. 1-4. The analysis also indicated that liquefaction would be expected in limited zones of the downstream shell, as shown in Fig. 1-4. When the liquefied soil was considered to have no residual strength the computed factor of safety of the upstream shell was about 0.8 and it was thus concluded that the analysis would indicate that failure would have occurred. However because of the location and limited extent of the zones of liquefaction in the downstream shell there was no danger of sliding in the downstream direction. The same method of analysis also indicated failure of the Sheffield Dam in an earthquake in 1925, and it correctly indicated no failures, and in fact no liquefaction, in typical hydraulic fill dams subjected to earthquake motions from Magnitude 6.5 earthquakes producing a peak acceleration of about 0.2g (Seed et al., 1973). This is in accordance with the observed behavior of a number of such dams including Fairmont, Silver Lake, and Lower Franklin dams in the 1971 San Fernando earthquake. The method also seemed to explain

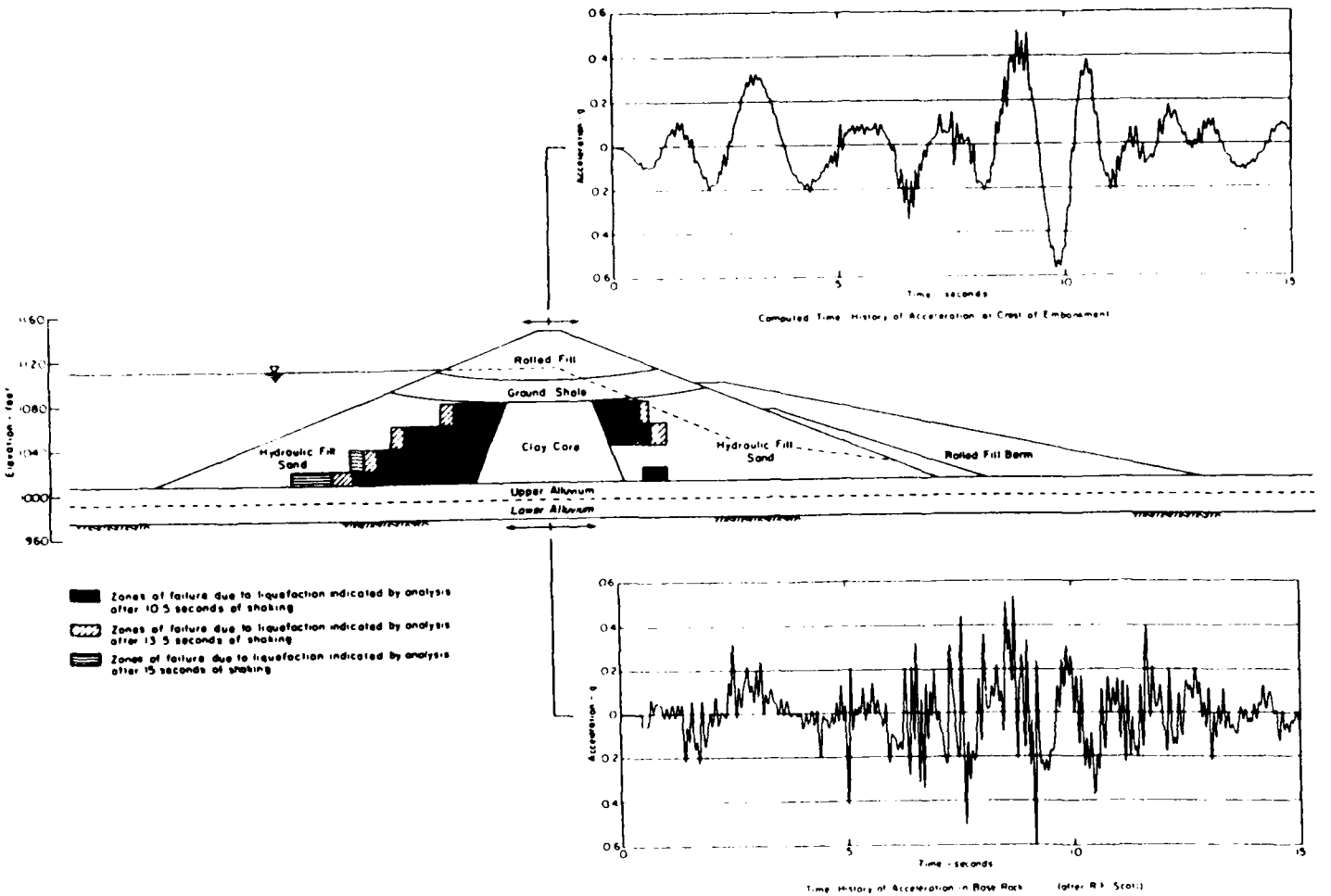

Fig. 1-4 ANALYSIS OF RESPONSE OF LOWER DAM DURING SAN FERNANDO EARTHQUAKE TO BASE MOTIONS DETERMINED FROM SEISMOSCOPE RECORD (After Seed et al., 1973)

reasonably well the performance of the Upper San Fernando Dam, in which there was a downstream slide of about 5 ft in the same earthquake.

As a result of these successful analyses of embankment behavior, the method, in its original form or in slightly modified forms, has been used for seismic stability evaluations of a number of dams in the past 15 years (Babbitt et al., 1983; Marcuson et al., 1983; Smart and Von Thun, 1983). During that period, however, certain limitations of the method have been noted, including the facts that:

1. The method sometimes predicts large potential deformations accompanying soil liquefaction which may not develop in the field.
2. The method does not provide any basis for evaluating the residual strength of the soil in zones which are predicted to liquefy.

and 3. The San Fernando Dam samples used for laboratory testing in the 1973 studies were probably slightly disturbed and densified prior to testing and thus may have given somewhat erroneous results.

At the same time, studies of the steady-state strength of liquefied soils by Castro and Poulos (Castro et al., 1982; Poulos et al., 1985) have clearly shown that even after liquefaction, many sands do retain a significant resistance to shear deformations, and laboratory test procedures have been developed for evaluating this steady-state or residual strength (Poulos et al., 1985).

The procedure proposed by Poulos et al. for this purpose is based on careful laboratory testing of good-quality undisturbed samples. It is described in detail in Poulos et al. (1985) and illustrated schematically in Fig. 1-5. Basically it recognizes that samples of loose to medium dense sands are likely to be densified in the sampling, transportation, handling and testing procedures. Thus the steady state strength of the soil is measured at the

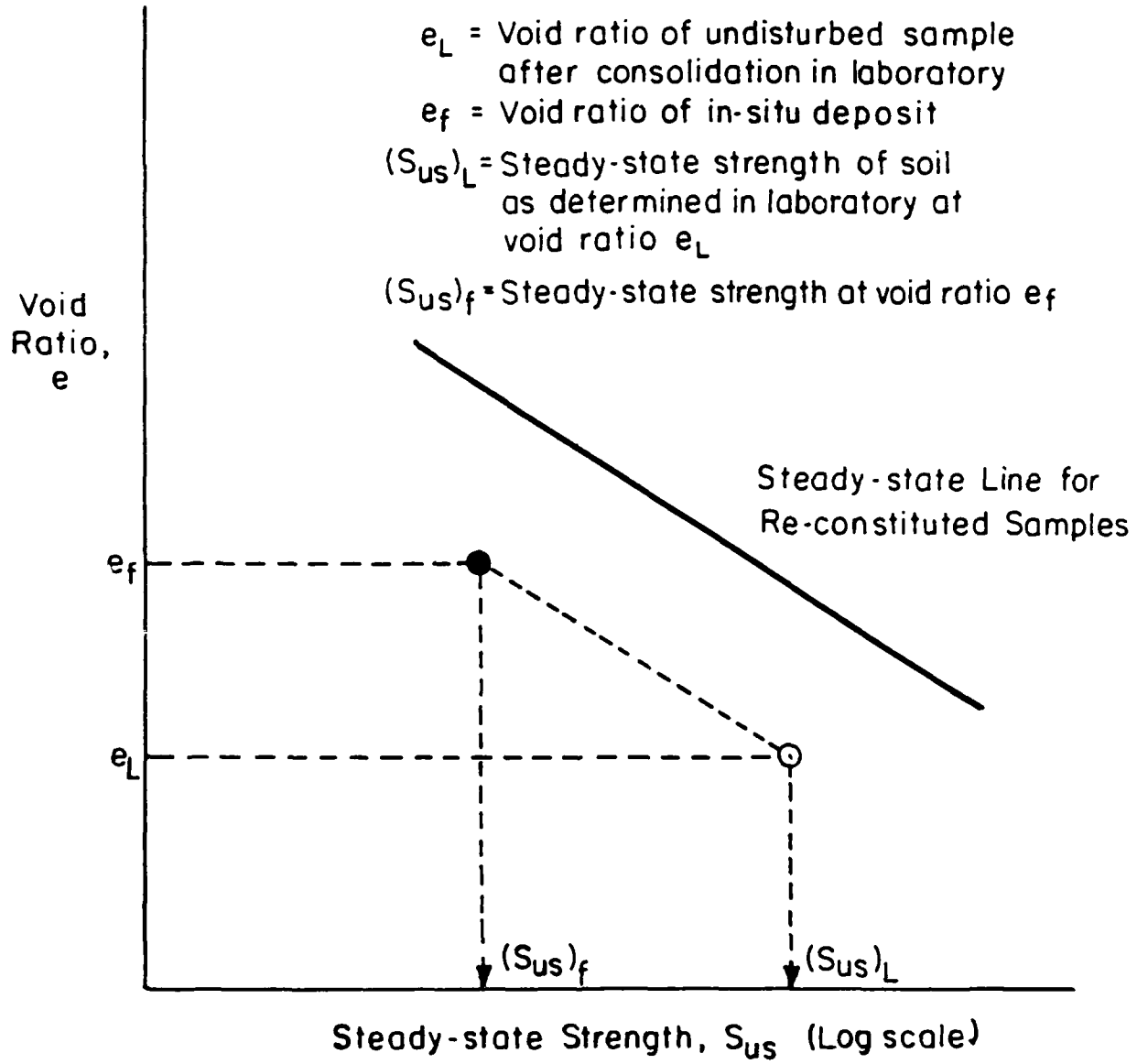

Fig. 1-5 PROCEDURE FOR DETERMINING STEADY-STATE STRENGTH FOR SOIL AT FIELD VOID RATIO CONDITION (AFTER POULOS ET AL., 1985)

void ratio at the time of failure in the laboratory and then, assuming that the slope of the steady state line (the relationship between steady state strength and void ratio) is the same for undisturbed and remolded samples, the steady state strength measured in the laboratory is corrected to a lower value corresponding to the void ratio of the soil in its field condition. Associated with the development of this procedure has been the development of improved procedures for obtaining undisturbed samples of sand for laboratory testing purposes.

More recently Seed (1986, 1987) has analyzed the stability, after liquefaction, of a number of field cases of instability resulting from liquefaction. The most recent (1988) values of the residual strength of the liquefied soils determined in this way, including several data points recently obtained from studies of embankment failures during the 1985 Chilean earthquake (De Alba et al., 1987) are shown in Fig. 1-6. Such values provide a useful guide to residual strengths likely to be developed in other deposits of liquefied sand and they provide an important basis for evaluating the applicability of laboratory testing procedures for determining such values.

In using case studies such as these to evaluate the residual or steady-state strength of a liquefied soil, however, it is important to keep in mind the meaning of this soil strength characteristic. As described by Poulos et al. (1985), it is the lowest value of resistance to deformation which a liquefied soil exhibits during deformation, at constant composition, over a large range of deformations (see Fig. 1-7). This being the case it is correct to conclude that if the steady-state strength of a deposit in which liquefaction occurs over the full length of the potential slip surface is greater than the average driving stress on this slip surface, including any inertia effects, no significant deformations (i.e., failure) can develop. Thus

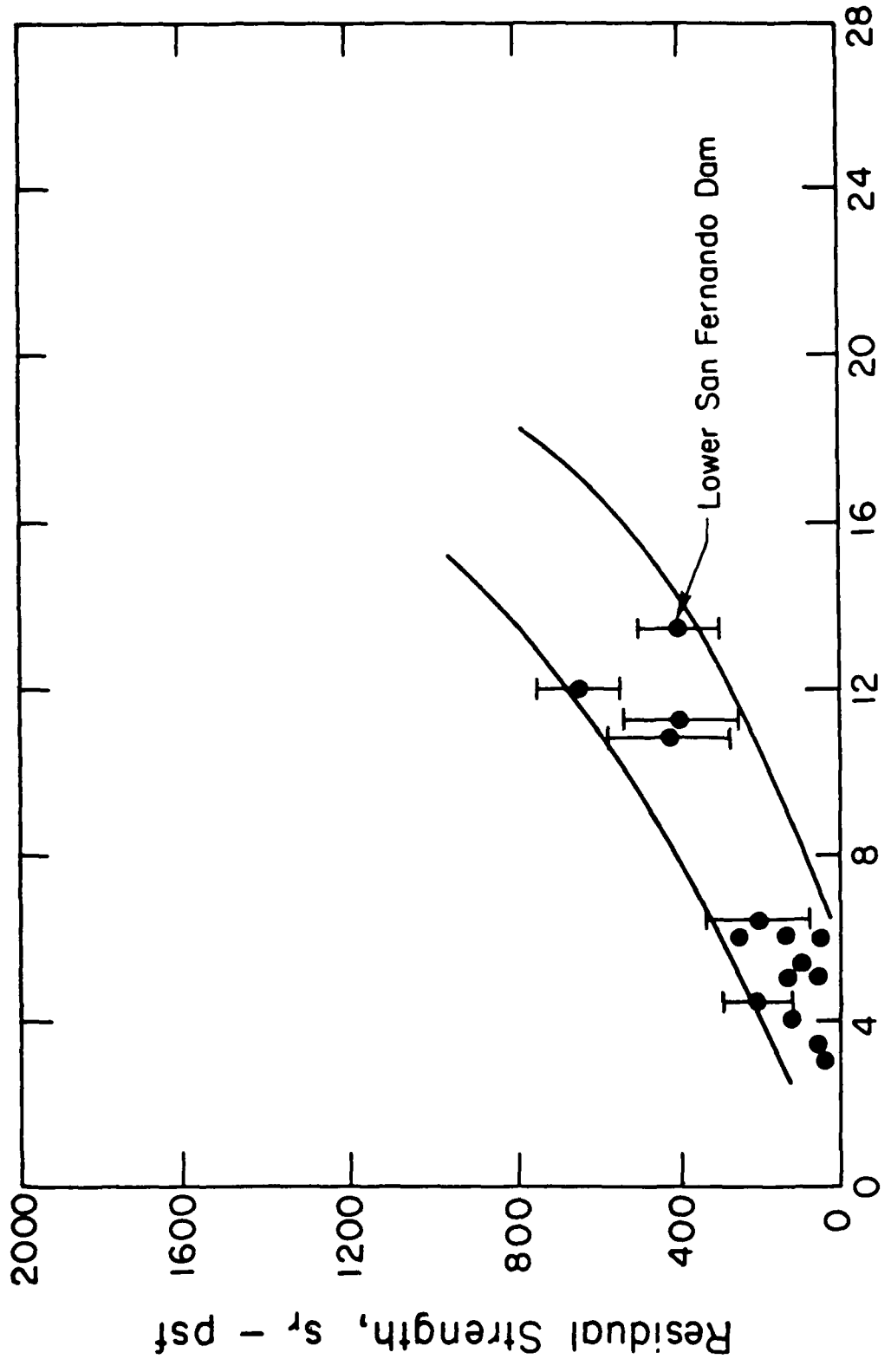

Fig. 1-6 TENTATIVE RELATIONSHIP BETWEEN RESIDUAL STRENGTH AND SPT N VALUES FOR SANDS

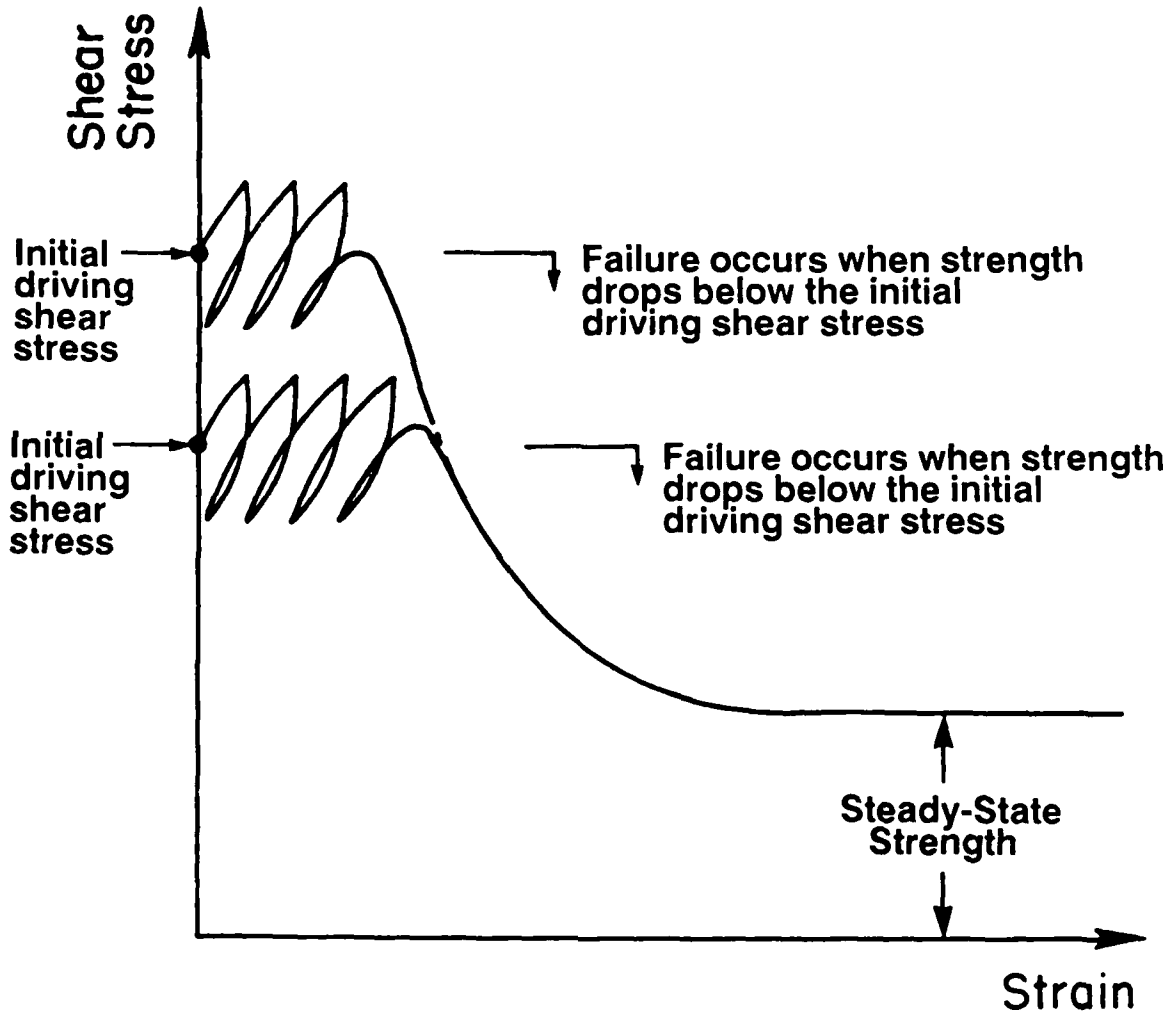

Fig. 1-7 SCHEMATIC ILLUSTRATION OF STRESS CONDITIONS WHEN LIQUEFACTION FAILURE OCCURS IN LABORATORY CYCLIC LOAD TESTS

comparison of the driving stress and the steady-state strength is a useful design technique for evaluating the possibility of major sliding occurring under these conditions. Its validity however will clearly depend on the accuracy with which the residual or steady-state strength is determined and on the computed value of the average driving stress for the pre-failure configuration of the deposit under consideration.

When case histories are used to evaluate actual values of residual or steady-state strength, however, the average driving stress on the potential failure surface for the pre-failure configuration does not have the same level of significance. The conditions when failure is initiated may be complicated by the fact that liquefaction does not extend all the way along the failure surface, or that sliding begins before all the soil has attained its minimum resistance to deformation. Thus, as failure develops, the soil resistance may still be dropping to its steady-state value, represented by the fact that the theoretical factor of safety when the sliding was initiated may have been significantly less than 1. Such conditions will probably always exist whenever a major flow-type failure occurs. If the factor of safety were in fact unity, then a small change in configuration would reduce the driving stress, raise the factor of safety, and quickly arrest the slide movements. Large deformations indicate that large reductions in driving stress were required to bring the slide movements to a stop and thus the factor of safety based on the residual or steady-state strength of the soil being developed all along the sliding surface could not have been unity for the pre-slide configuration. In fact, if the residual or steady-state strength of the liquefied soil is developed over the full length of the failure surface, then the factor of safety must be unity only when the slide movements stop, and thus it is the post-

failure configuration which provides the most reliable basis for evaluating the residual or steady-state strength of a liquefied soil deposit.

This differentiation between the role of the driving stress in the pre-failure and post-failure configurations is an important consideration in the use of case histories to evaluate residual or steady-state strengths under field conditions. It is directly analagous to the stress conditions illustrated for laboratory tests in Fig. 1-7 where the steady-state strength bears no direct relationship to the pre-failure driving stresses acting on the soil samples and is the same for both samples, even though they have different driving stresses. Clearly the samples would not fail if the steady-state strength were not less than the driving stress, but the steady-state strength is not determined by the value of the driving stress. Similarly for design evaluations the driving stress for the pre-slide configuration serves a very useful purpose for evaluating stability, but for case study evaluations of residual strength, it can only be regarded as providing a theoretical upper-bound value which may bear no resemblance to the actual residual strength of the soil.

In the case of the Lower San Fernando Dam slide, for example, the configuration of the upstream shell of the embankment when sliding was initiated was approximately as shown in Fig. 1-8. Analyses indicate that the average driving stress along the potential failure surface was about 850 psf. If it is assumed that all the soil along the failure surface was liquefied and that the factor of safety at this time was unity, then it would be concluded that the residual or steady-state strength of the liquefied soil was about 850 psf in this case.

If the residual or steady-state strength of the soil were indeed close to 850 psf, however, then only a relatively small movement of the slide mass,

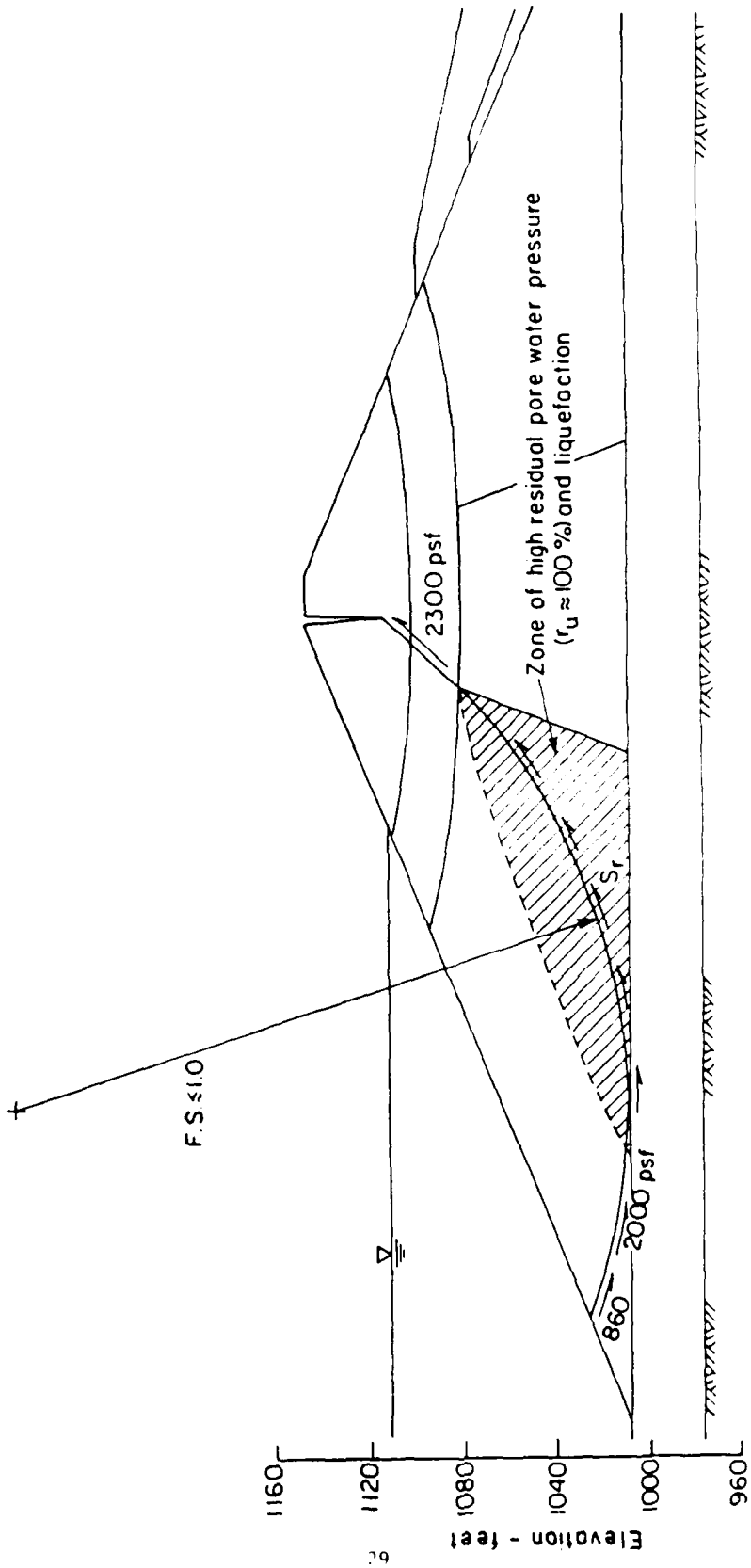

Fig. 1-8 CROSS SECTION OF LOWER SAN FERNANDO DAM AT END OF EARTHQUAKE

say 10 to 15 ft, would have brought the slide movement to a stop. The fact that very large movements, of the order of 150 ft occurred before sliding stopped indicates that either the factor of safety was significantly less than unity, and the residual strength of the liquefied soil significantly less than 850 psf, or that more complex considerations were involved in determining the onset of sliding. In either case the value of 850 psf can only be considered, as previously indicated, as a theoretical upper bound value for the residual strength of the liquefied soil and it cannot be assumed that the residual or steady-state strength of the soil in the liquefied zone was necessarily equal to or even nearly equal to the average driving stress at the time the slide movements started.

Possible complexities involve the recognition that the configuration of the embankment and the approximate extent of the zone of liquefaction at the time of initiation of sliding were similar to those shown in Fig. 1-8. It may be seen that there is a zone of non-liquefied soil near the toe of the upstream shell, probably associated with the starter dike, which apparently did not liquefy. It has been hypothesized (Seed, (1979)) that it was the development of the undrained strength of the soil in this dilatant zone, after liquefaction occurred in the interior zone of the upstream shell, which prevented failure from occurring during and immediately following the earthquake; furthermore that it was the gradual reduction in strength of the soil in this zone from its undrained value to the drained value, as water migrated from the reservoir to this zone of reduced pore-water pressures, which ultimately led to a sufficient reduction in strength to cause the failure to be initiated. However there can be no assurance that the strength had dropped to the drained strength values shown in Fig. 1-8 when sliding started. All that is known is that for the configuration shown, the factor of safety dropped to a value of

about 1. Assuming that the drained strength was developed in the non-liquefied dilatant zone near the toe of the upstream shell, stability analyses indicate that the residual or steady-state strength of the liquefied soil must have been about 800 psf. However if the strength of the soil in the dilatant toe zone was only reduced part-way towards the drained strength, the residual strength of the soil in the liquefied zone would be significantly less than this value. Because of this uncertainty and uncertainties about the extent of the non-liquefied zone at the toe of the upstream shell, the residual or steady-state strength of the liquefied soil cannot be determined with any high degree of accuracy from the conditions existing when failure was initiated.

These uncertainties are minimized, however, if the residual or steady-state strength of the liquefied soil is computed from the conditions and configuration of the embankment when slide movements stopped. At this stage, as shown in Fig. 1-9, virtually the entire surface of sliding was covered with the liquefied soil and, since the rate of sliding was relatively slow, inertia effects were relatively small. Knowing that sliding would stop when the factor of safety attained a value of unity, the residual or steady-state strength, based on the configuration of the slide mass at the end of sliding, can be computed to have values as low as 300 psf. Somewhat higher values, up to about 500 psf, are determined if allowance is made for the inertia effects associated with the rate of movement and a possible 70% reduction in strength of the liquefied soil as it moves into the reservoir. There is other evidence, such as the flow of liquefied sand into cracks which developed in the embankment, to indicate that the lower bound values of residual strength were indeed probably attained in some zones however. Allowing for all these sources of uncertainty, a good representative value for the residual strength

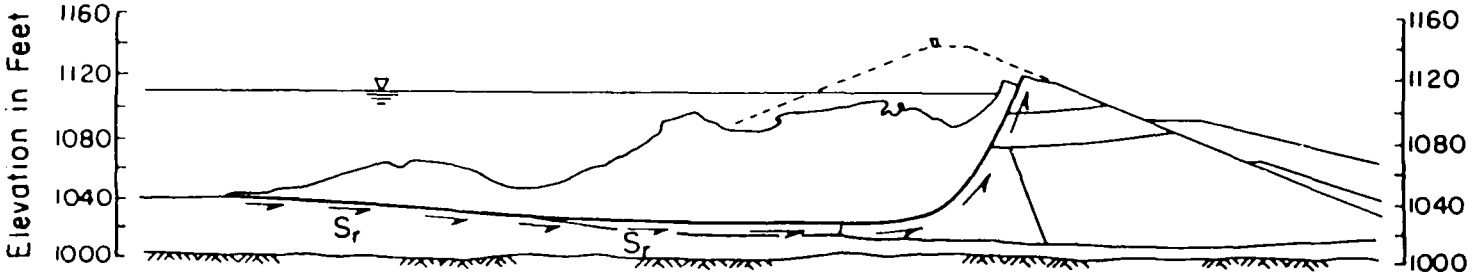

Fig. 1-9 POST-FAILURE CONFIGURATION OF UPSTREAM SHELL OF LOWER SAN FERNANDO DAM

of the liquefied soil in this case can thus be determined to be about 400 ± 100 psf.

Similar analyses can be made, but usually with lesser levels of accuracy, for other cases where liquefaction-type slides and failures have occurred. The residual strengths determined from such case studies seem to be related in a general way to the standard penetration resistance of the sands, as indicated in Fig. 1-6, and these results also provide a basis for estimating the residual strength of soils on other projects.

In the light of new developments in sampling techniques and in procedures for evaluating the residual or steady-state strength of liquefied sands and silty sands, it was concluded in 1985 that considerable benefits and clarification of the current state of knowledge might be gained through a cooperative re-evaluation of the Lower San Fernando Dam. This study was sponsored by the U.S. Army Corps of Engineers for the following purposes:

1. To determine whether laboratory testing procedures for evaluating steady-state strengths would predict the known residual strength of the sand in the Lower San Fernando Dam.
2. To determine whether the use of improved sampling procedures would lead to different results for cyclic load tests on undisturbed samples taken from the dam.
3. To explore the reproducibility of laboratory test data used for seismic stability evaluations as measured in different laboratories.
4. To examine the standard penetration resistance of the sands in the Lower San Fernando Dam using new standardized procedures.

The cooperating agencies involved were the Waterways Experiment Station of the U.S. Army Corps of Engineers, Geotechnical Engineers Inc. of Winchester,

Massachusetts, and H. Bolton Seed Inc. in cooperation with the Soil Mechanics Laboratory of Stanford University, California.

This report presents the results of the study by H. Bolton Seed Inc. Section 2 presents a brief description of the Lower San Fernando Dam and the field investigations made in 1985 to explore its properties. Section 3 presents an analysis of the probable changes in properties of the soils in the embankment since the earthquake occurred in 1971. Section 4 presents a review of the standard penetration test data for the sands in the dam in the 1971 and 1985 investigations. Section 5 presents the results of cyclic load tests performed on the samples obtained in the 1985 investigation and a comparison of these results with those obtained in 1971 and those expected based on past field performance. Section 6 presents the results of steady-state strength tests on samples obtained in the 1985 field exploration program. Section 7 presents an evaluation of the properties of the hydraulic fill near the base of the upstream shell, based on the test results and other studies summarized in this report. Section 8 discusses the practical significance of the results obtained, including a comparison of steady state strengths determined by laboratory testing with those estimated from the known field performance of the upstream shell in this dam and other dams where liquefaction-type failures have occurred, and a general review of the applicability of analytical methods for evaluating the seismic stability of the Lower San Fernando Dam. Section 9 presents overall conclusions.

2. Field Investigations in 1985

Since the failure of the upstream slope of the Lower San Fernando Dam in 1971, the dam has been reconstructed to serve as an emergency water retaining structure with the configuration shown in Fig. 2-1. The original upstream shell has been replaced by a compacted fill but the downstream shell below El. 1100 remains essentially as it was at the time of the 1971 earthquake. Since the original hydraulic fill embankment was probably reasonably symmetrical in configuration and properties about the center line of the crest, the properties of the soil forming the upstream shell can be evaluated with a reasonable degree of accuracy on the basis of the properties of the hydraulic fill comprising the present downstream portion of the embankment.

For this purpose a field exploration program was performed by Geotechnical Engineers Inc. in 1985. The program involved:

1. The performance of 6 borings (S101, S102, S103, S104, S105, and S111) in which, with the exception of Boring S104, split spoon samples were obtained continuously through the hydraulic fill portion of the dam and intermittently above and below the hydraulic fill. In Boring S104 samples were taken at 5 ft intervals for the entire boring.
2. The performance of CPT soundings at 12 locations, designated C101 to C112. Six of the 12 CPT soundings were performed adjacent to the SPT sampling holes.
3. The performance of 6 borings (U102, U103, U104, U105, U111, and U111A) in which undisturbed samples were taken in selected zones of the dam.

and 4. The construction of an exploration shaft from which hand carved

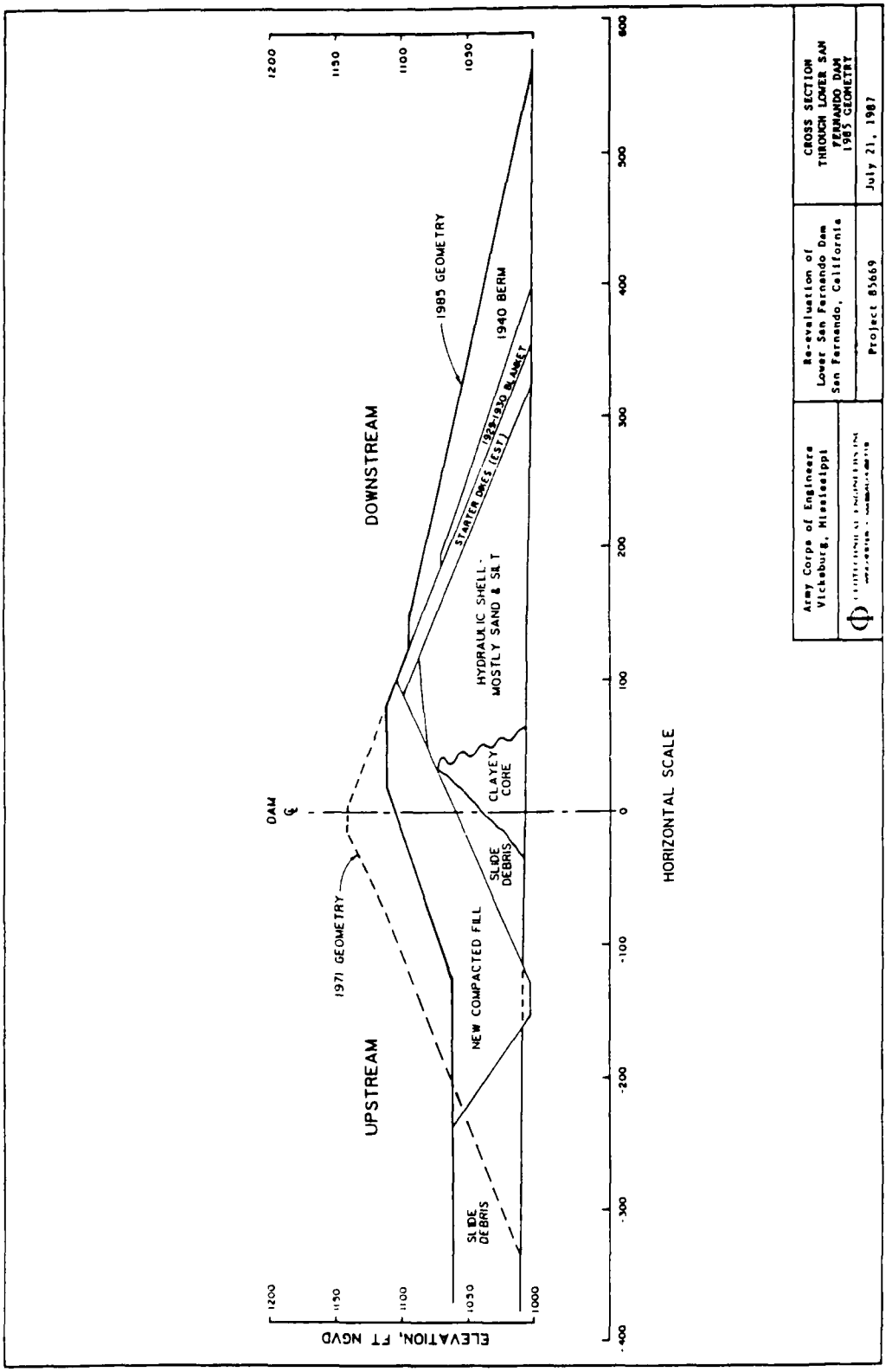

Fig. 2-1 CROSS-SECTION THROUGH LOWER SAN FERNANDO DAM IN 1985 (after GEI)

undisturbed samples were recovered using a special "tripod" sampling procedure developed by GEI.

The locations of the various field tests and borings are shown in Fig. 2-2. The investigation program was laid out along four cross-sections located at Stations 5+85, 9+35, 12+95, and 16+40 along the axis of the dam.

In the field investigation the SPT boring showing the most consistently low blowcounts near the base of the hydraulic fill was found to be S111 on the cross-section through Station 5+85. The exploration shaft was thus constructed near boring S111 in order to obtain high quality undisturbed samples of this material, in addition to those obtained from undisturbed sample borings. The material was found to be a layer of stratified silty sand and sandy silt as shown by the results of SPT and CPT investigations at this location in Fig. 2-3. The relative relationship between the exploration shaft and Boring S111 is shown in Fig. 2-2. A cross-section at Station 9+35 showing the SPT N-values measured in Borings S103, S104 and S105 is shown in Fig. 2-4.

In interpreting the stratification in the hydraulic fill, GEI identified 5 major zones in each boring, designated as Zones 1 to 5 in Figs. 2-3 and 2-4. A detailed analysis of these zones for Boring S111 is shown in Table 2-1. In this table the measured SPT N-values of the soils in the various zones are expressed in terms of values of $(N_1)_{60}$, the normalized N-values for an overburden pressure of 1 tsf as measured in an SPT test providing a driving energy in the drill rod of 60 percent of the theoretical free-fall energy of the falling weight, and an appropriate correction for the absence of liners in the SPT sampling tube.

In addition small corrections (ΔN_1) have been made for the silt contents of the different layers to establish the equivalent clean sand values of $(N_1)_{60}$ for the soils in the different zones. The representative soil profile

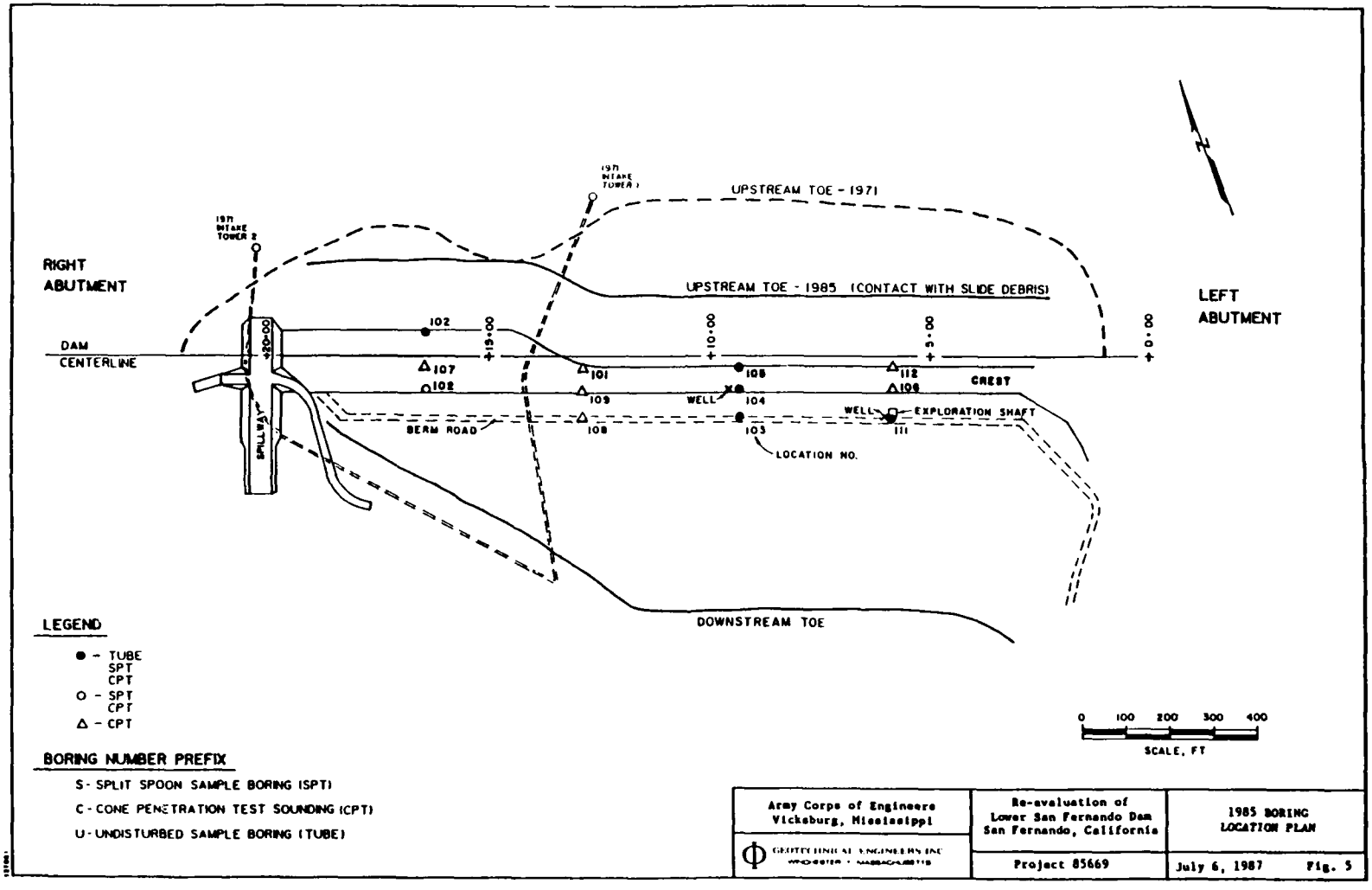

Fig. 2-2 PLAN OF LOWER SAN FERNANDO DAM SHOWING LOCATIONS OF BORINGS AND EXPLORATION SHAFT (after GEI)

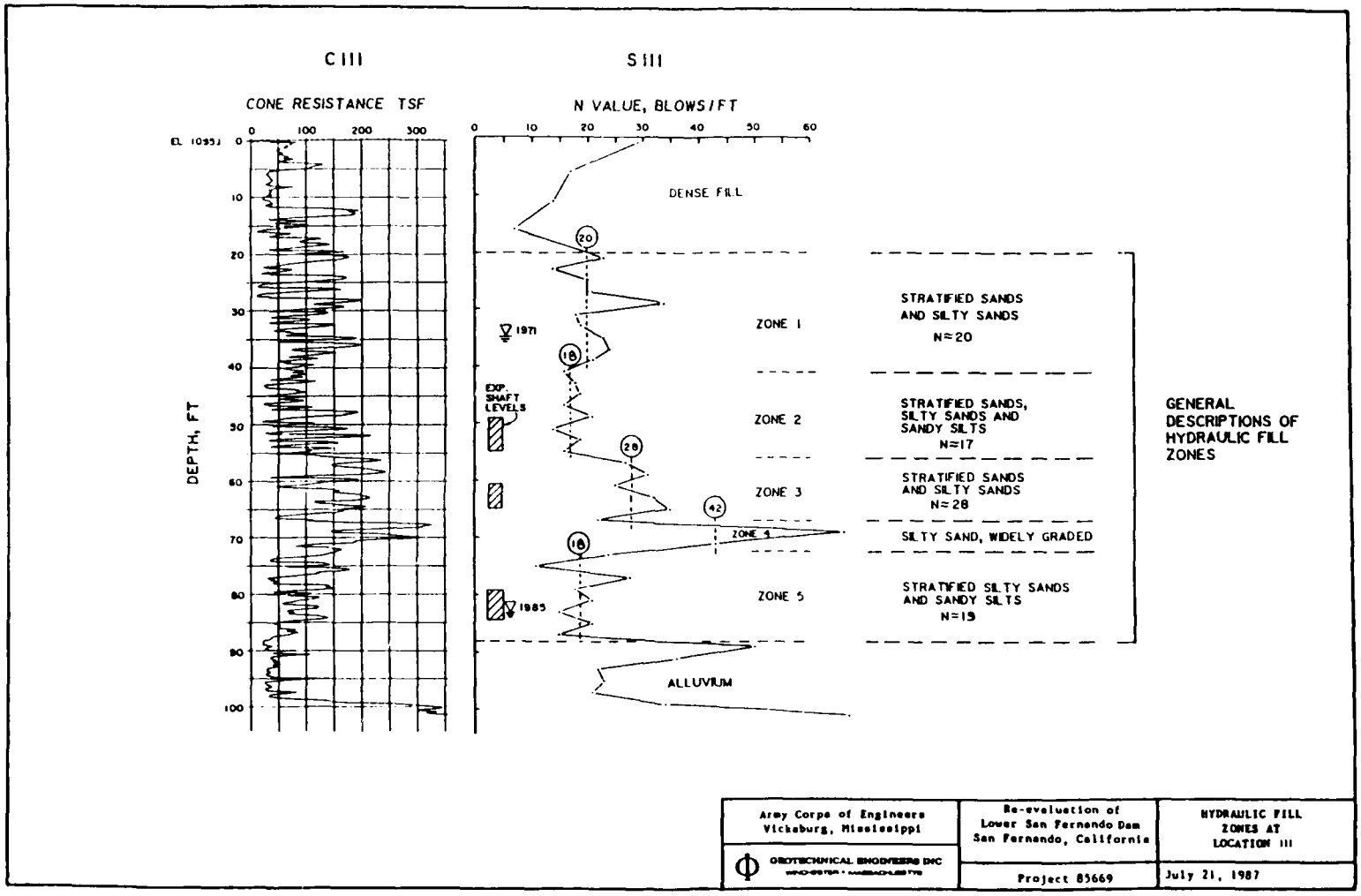

Fig. 2-3 SOIL CONDITIONS AND PENETRATION RESISTANCE VALUES NEAR BORING S111 (after GEI)

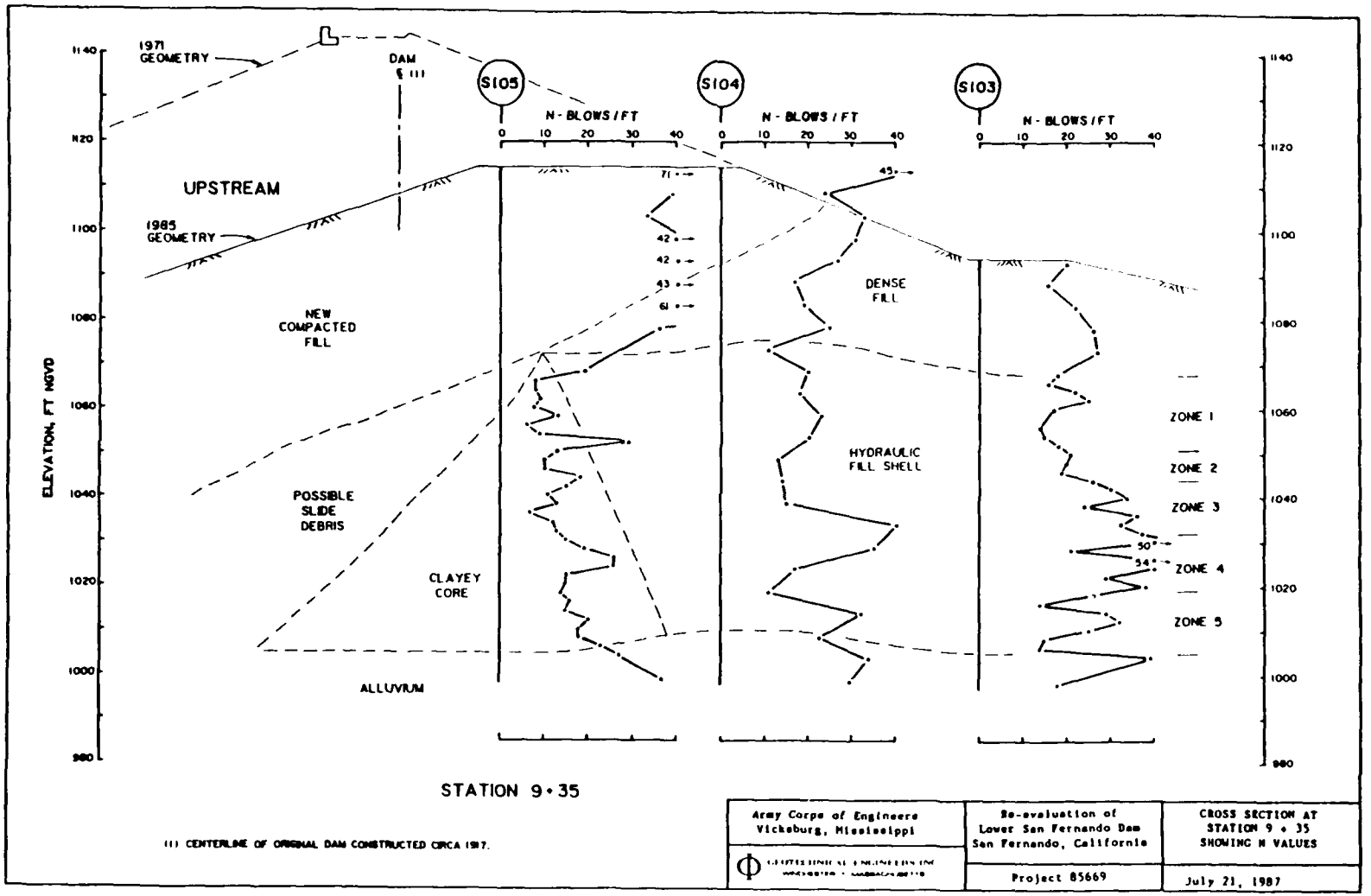

Fig. 2-4 SOIL PROFILE AT STATION 9+35
(after GEI)

TABLE 2-1 SOIL PROFILE NEAR BORING S111

Elevation	Thickness	Soil Type	Measured $\bar{N}$	Average σ_o' psf	C_N	Measured $\bar{N}_1$	$(\bar{N}_1)_{60}$	ΔN_1	Equivalent Clean Sand $(\bar{N}_1)_{60}$
1095 to 1075	20 ft	Denser Fill	15	1100	1.4	≈21	≈28	Varies	≈29
1075 to 1054	21 ft	Hyd. fill - Zone 1	20	3350	0.76	≈15	≈20.5	0.5	≈21
1054 to 1039	15 ft	Hyd. fill - Zone 2	17	5050	0.60	≈10	≈14	2	≈16
1039 to 1028	11 ft	Hyd. fill - Zone 3	28	6500	0.50	≈14	≈19.5	1	≈20.5
1028 to 1022	6 ft	Hyd. fill - Zone 4	42	7450	0.47	≈19.5	≈27	1	≈28
1022 to 1007	15 ft	Hyd. fill - Zone 5	19	8400	0.44	≈ 8.5	≈12	3	≈15
1007 to		Foundation soils							

for conditions near Boring S111 as indicated by the data in Table 2-1 and Fig. 2-3 is shown in Fig. 2-5. It may be seen that the soil conditions in Zones 2, 3 and 5 identified by GEI are very similar and samples for the various laboratory tests were therefore taken almost exclusively from these zones.

The undisturbed samples and representative bulk samples from the field explorations were distributed by GEI among the participating laboratories, the GEI laboratory in Winchester, Mass., the Waterways Experiment Station, Vicksburg, Miss., and Stanford University, Palo Alto, California.

Full details of the field explorations are presented in the report on the study prepared by Geotechnical Engineers Inc.

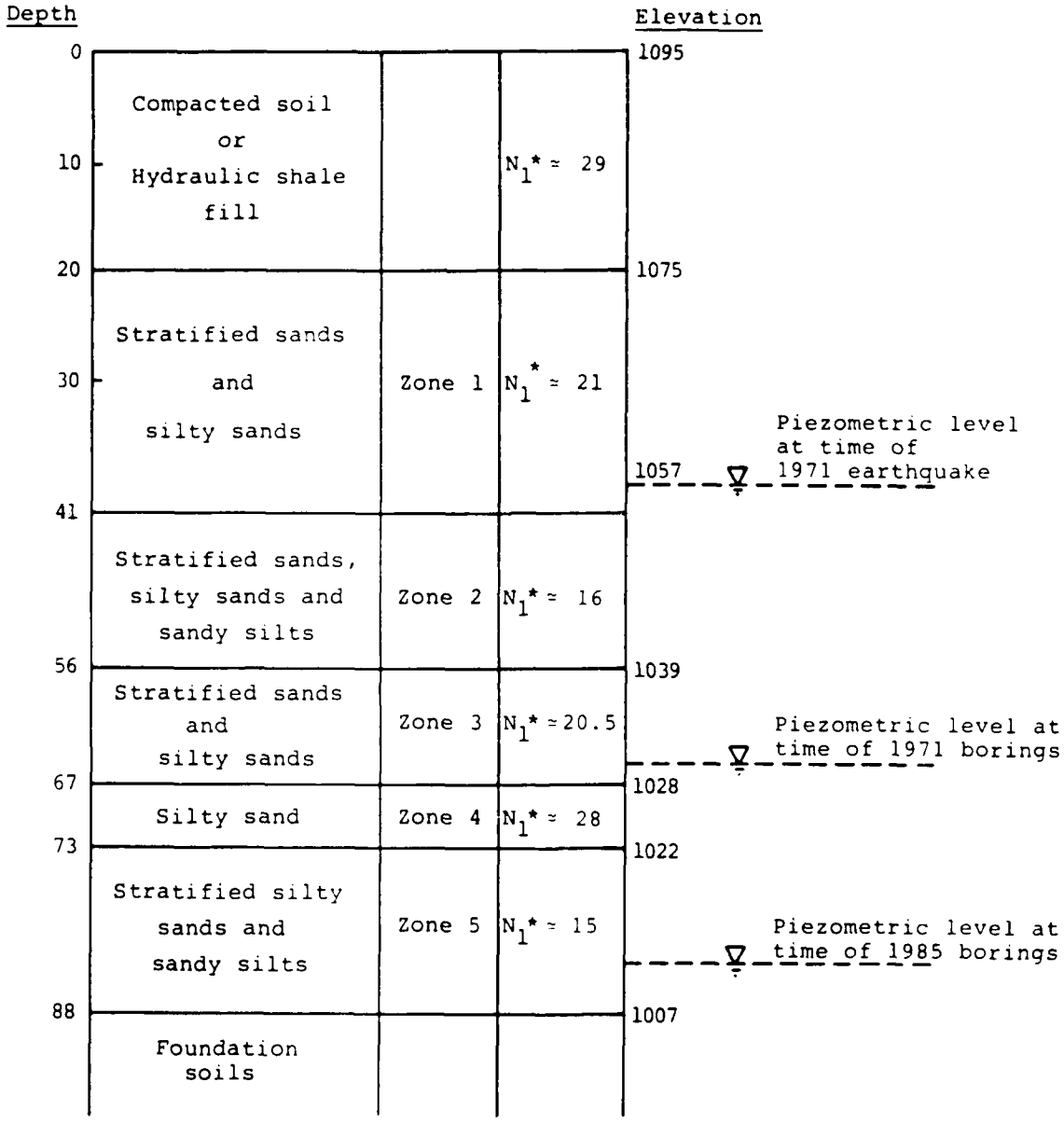

*Denotes equivalent clean sand $(N_1)_{60}$-value.

Fig. 2-5 SOIL PROFILE NEAR BORING S111

3. Changes of Density of Hydraulic Fill Since 1971 Earthquake

In order to evaluate the behavior of the Lower San Fernando Dam during the earthquake in 1971, it is necessary to determine the properties of the hydraulic fill for the conditions at the time the earthquake occurred. For some properties, any changes since the earthquake may be of minor significance but for others, such as the steady-state strength, the results are highly dependent on an accurate evaluation of the void ratio of the soil in its pre-earthquake condition. Estimates of the changes in void ratio in Zone 5 of the hydraulic fill since the earthquake and just prior to sampling in 1985, for sections along Stations 9+00 and 5+00, are therefore presented below.

Station 9+00

Estimates of the changes in dry density or void ratio of the hydraulic fill since the time of the earthquake can be made from comprehensive settlement observations made on the downstream shell of the dam by the Los Angeles Department of Water and Power both prior to and following the 1971 earthquake. Fig. 3-1, for example, shows settlements measured on the surface of the embankment normal to the axis of the dam at Station 9+00. The test shaft is located 122 ft south of the axis at Station 5+85. For point A, located on the horizontal berm at about the same distance from the axis as the test shaft, it may be seen from Fig. 3-1 that the settlement in the period from December 1970, just before the earthquake, to February 1985, the year the samples were taken from the embankment, was about 0.82 ft. This represents the combined compression of the dense soil above the hydraulic fill, the zone of hydraulic fill above the piezometric surface at the time of the earthquake, the saturated zone of hydraulic fill and the foundation soils. This comprises about 40 ft of compacted soil and partially saturated hydraulic fill above Elevation 1057,

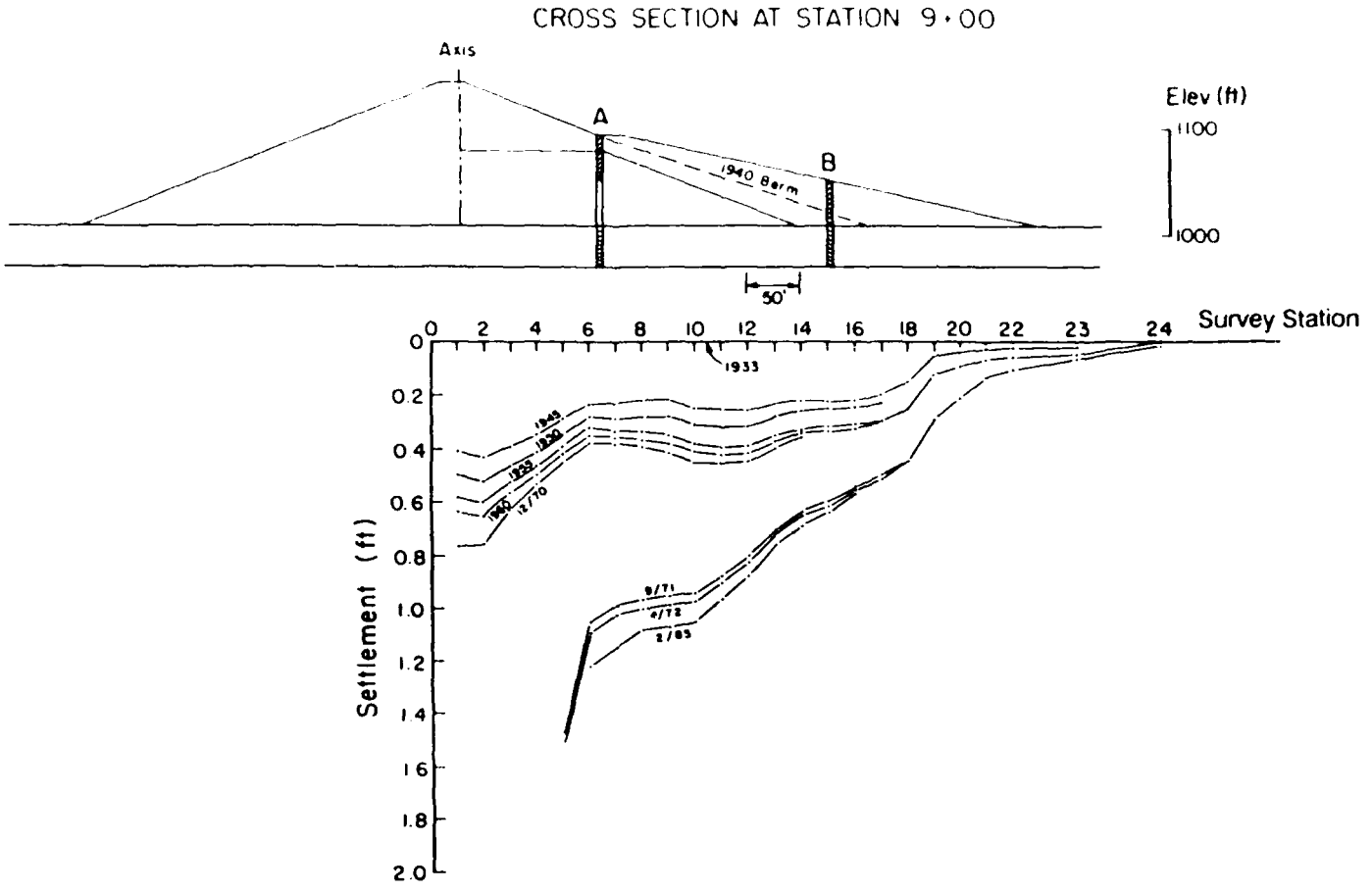

Fig. 3-1 OBSERVED SETTLEMENTS ALONG CROSS-SECTION THROUGH STATION 9+00
(Data provided by Geotechnical Engineers Inc.)

about 50 ft of hydraulic fill in Zones 2, 3, 4 and 5, and about 30 ft of foundation soils, as shown in Fig. 3-2.

It may also be seen from Fig. 3-1, that significant settlement has occurred on the top of the 1940 rolled fill berm at point B where the height of the layer of hydraulic fill in the underlying soil column is zero. The settlement at point B in the period between the earthquake and sampling in 1985 is about 0.32 ft. This represents the settlement of a 40 ft column of partially saturated denser soils and the underlying 30 ft depth of foundation soil. A comparison between the soil conditions in the columns underlying points A and B, and the settlements of points A and B is shown in Fig. 3-2.

The difference between the observed settlements at points A and B is presumably due to the vertical compression of Zones 2, 3, 4 and 5 of the saturated hydraulic fill in the period Feb. 1971 to October 1985, i.e. about 0.82-0.32 = 0.50 ft. The total depth of saturated (at the time of the earthquake) hydraulic fill contributing to this settlement is about 50 ft as shown in Fig. 3-2. Zone 5 of the hydraulic fill comprises only about 15 ft of this thickness but it probably contributes disproportionately to the settlement. A conservative estimate would be that Zone 5 contributes about 45% of the total compression although it makes up only about 30% of the thickness.

Thus it may be estimated that:

$$\text{Compressive strain in Zone 5 of the hydraulic fill since the 1971 earthquake} \approx \frac{0.45 \times 0.50 \text{ ft}}{15 \text{ ft}}$$

$$\approx 1.5\%$$

$$\text{Corresponding change in void ratio} \approx \frac{1.5}{100}(1+e)$$

where e = void ratio of soil = 0.72 for the hydraulic fill

$$\text{Hence change in void ratio of Zone 5 of hydraulic fill at St. 9+00 along axis of dam since earthquake occurred} \approx \frac{1.5}{100}(1 + 0.72)$$

$$\approx \underline{0.026}$$

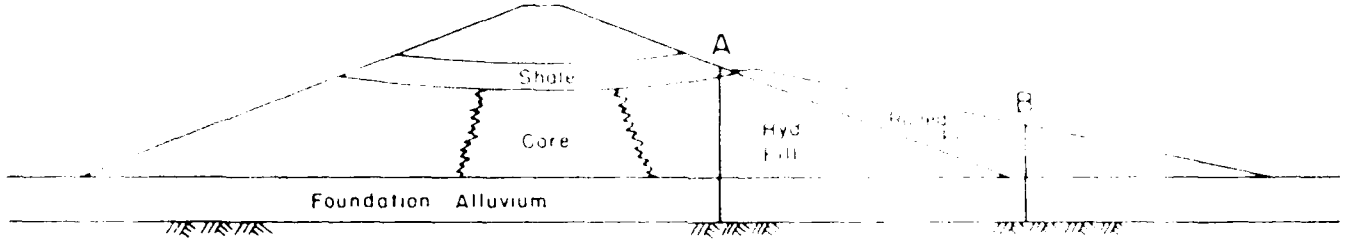

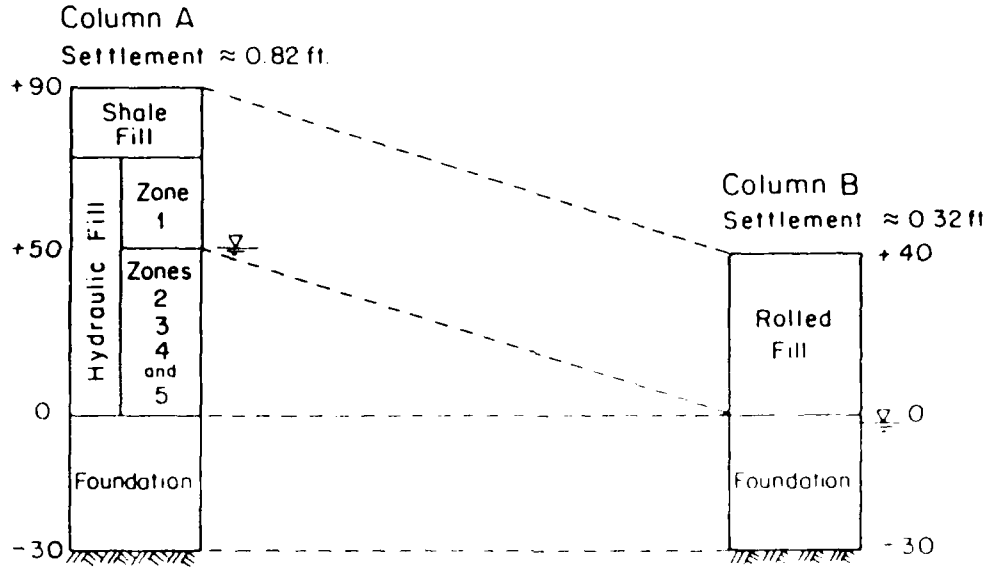

Post EQ Settlement in Zones 2 to 5 of Hydraulic Fill ≈ 0.82 − 0.32 ≈ 0.50 ft

CROSS SECTION AT STATION 9+00

Fig. 3-2 OBSERVED SETTLEMENTS ALONG CROSS-SECTION THROUGH STATION 9+00
(Data provided by Geotechnical Engineers Inc.)

Station 5+00

Settlement data for the section through the embankment at Station 5+00 on the axis of the dam are shown in Fig. 3-3. Although this data is not so complete as for the section at St. 9+00 (records were discontinued in May, 1975) it never-the-less provides a good basis for evaluating the change in void ratio of the lower part of the hydraulic fill, especially with the data at St. 9+00 to serve as a guide. Thus, following the same procedure as that outlined above, the following results are obtained:

Estimated post-earthquake settlement of point A	$\approx$ 0.57 ft
Estimated post-earthquake settlement of point B	$\approx$ 0.26 ft
Estimated change in thickness of Zones 2-5 of hydraulic fill from pre-earthquake condition to time of sampling in 1985	$\approx$ 0.31 ft
Estimated compressive strain in Zone 5 of hydraulic fill	$\approx \frac{0.45 \times 0.31}{15}$
	$\approx$ 0.9%
Estimated change in void ratio of Zone 5 since earthquake	$\approx \frac{0.9}{100}(1 + 0.72)$
	$\approx \underline{0.016}$

In addition to void ratio changes due to vertical compression there may also have been some densification due to lateral compression of the hydraulic fill. Fig. 3-4 shows the lateral movements of survey points along the downstream section of the embankment through Station 9+00 from 1945 to 1972. It is clear that the earthquake caused a marked increase in lateral movements of the survey points. However it is not clear whether these movements were due to lateral compression of the embankment or to shear deformations of the embankment and it seems highly probable that they were due mainly to shear

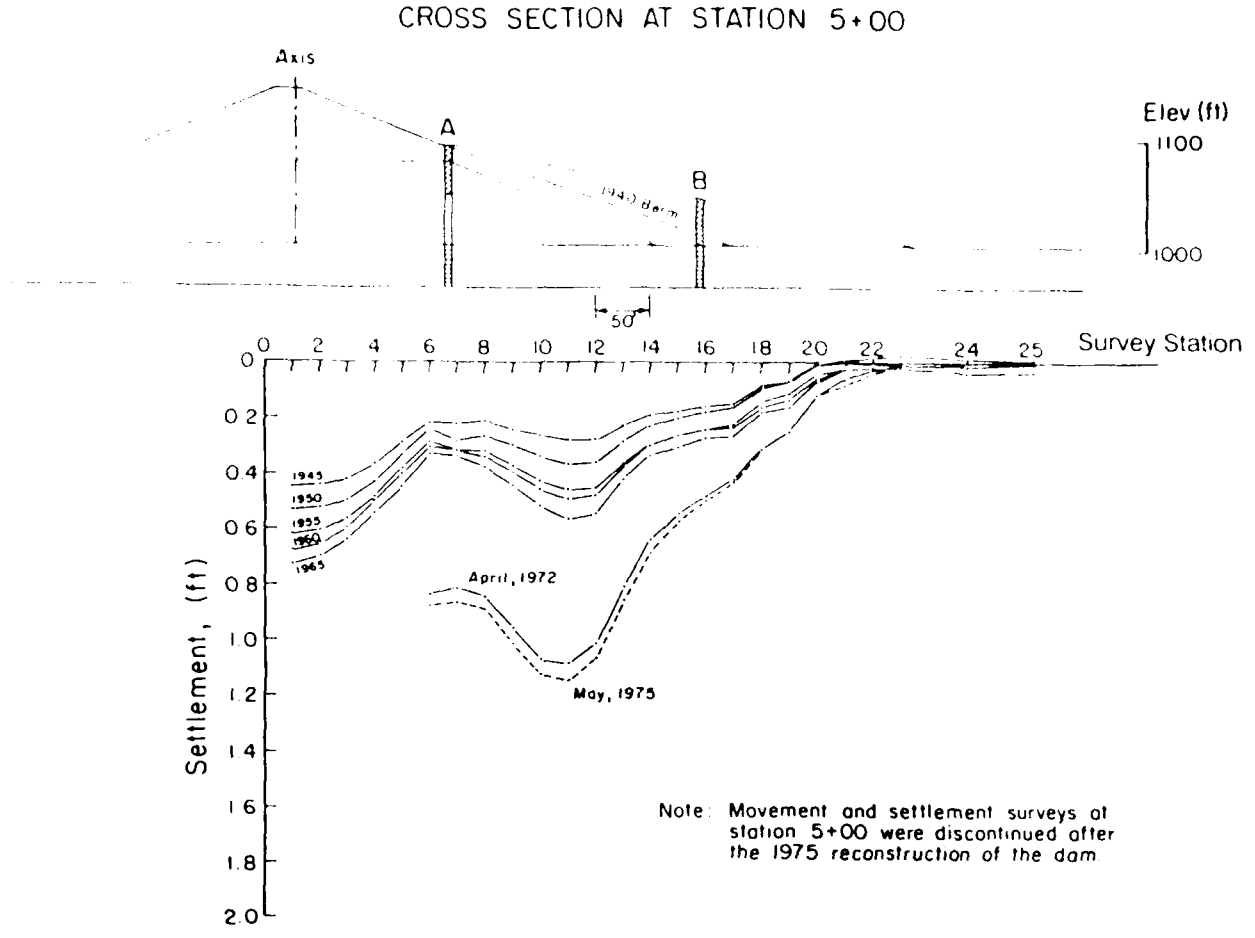

Fig. 3-3 COMPARISON OF POST-EARTHQUAKE SETTLEMENTS FOR COLUMNS A AND B ALONG CROSS-SECTION THROUGH STATION 5+00

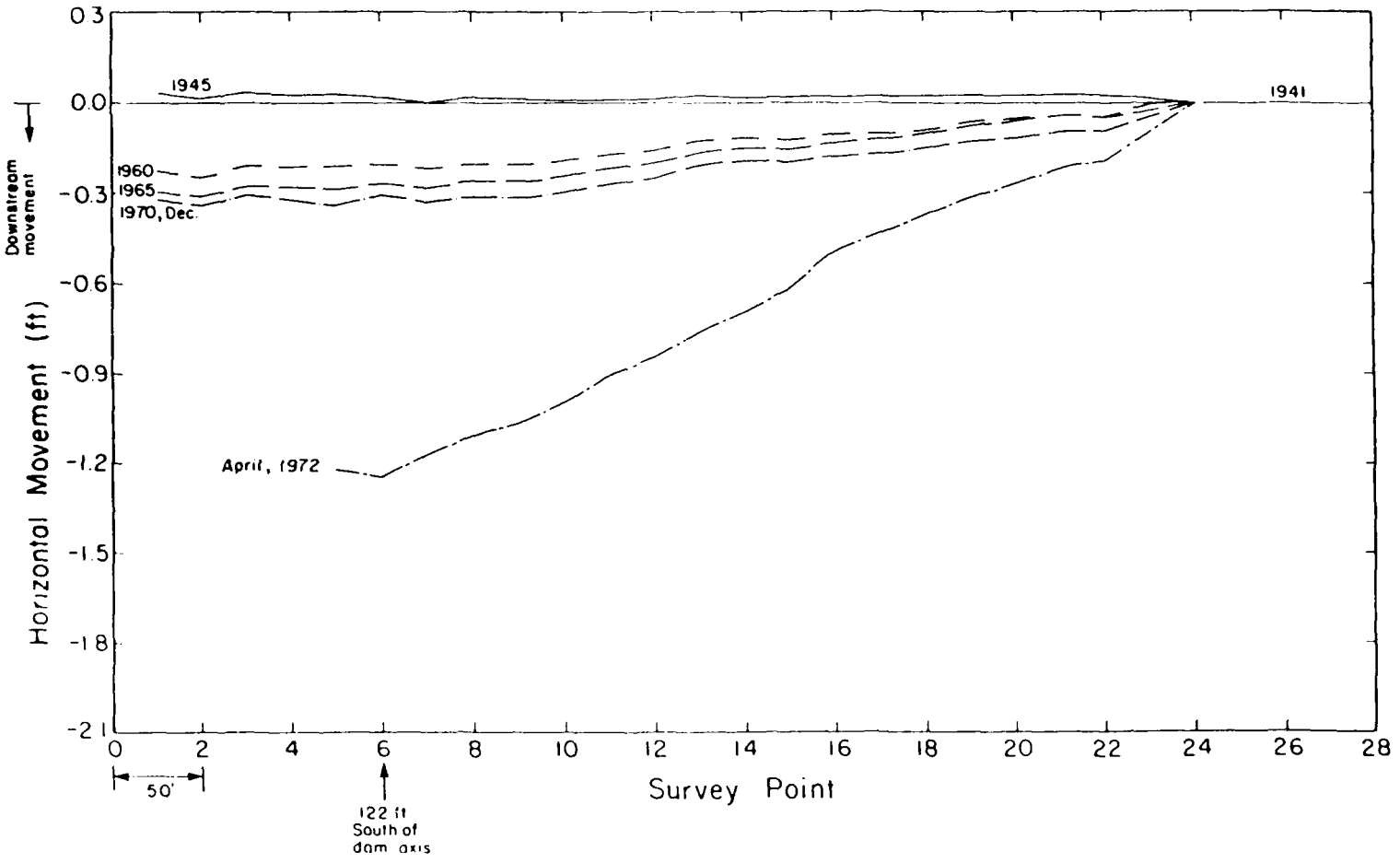

FIG. 3-4 OBSERVED HORIZONTAL MOVEMENTS OF SURVEY POINTS ALONG CROSS-SECTION THROUGH STATION 9 + 00
(Data provided by Geotechnical Engineers Inc.)

deformations. Thus it is unlikely that the observed movements at the surface of the embankment are indicative of movements along the base of the embankment; in fact, it seems highly unlikely that there would be any significant lateral deformations of points along the base of the embankment or in the underlying foundation soil.

These considerations make it difficult to estimate the possible changes in void ratio of the embankment soils due to the observed horizontal movements. Fortunately the observed movements in the vicinity of the exploration shaft (i.e., near Survey Point No. 6), shown in Fig. 3-4, do not contribute significantly to the overall densification of the hydraulic fill. Based on data such as that shown in Fig. 3-4, it can be estimated that the average change in void ratio of the soil near Survey Point No. 6 due to lateral movements is about 0.0005 and 0.003 for sections through St. 9+00 and St. 5+00 respectively.

The results presented above may thus be summarized as follows:

	Station 5+00	Station 9+00
Estimated void ratio change in Zone 5 of hydraulic fill due to vertical settlement	≈ 0.016	≈ 0.026
Estimated void ratio change in Zone 5 of hydraulic fill due to lateral compression	≈ 0.003	≈ 0.0005
Estimated change in void ratio between time of earthquake and time of sampling in 1985	≈ 0.019	≈ 0.026

The main exploratory shaft is located on the section through Station 5+85. Interpolating in the above values determined for sections at Stations 5+00 and Stations 9+00 leads to an estimated change in void ratio of the hydraulic fill, in the period between the earthquake of 1971 and sampling in 1985 of about 0.020.

It may be noted that the observed post-earthquake settlement of point A on the horizontal berm at Station 5+00 is about 0.57 ft while the corresponding settlement of point A on the berm at Station 9+00 is about 0.82 ft. Interpolation between these values for the settlement of a similar point A on a cross-section at Station 5+85 would lead to an estimated value of 0.62 ft. This is in good agreement with the observed settlement for a similar point close to the test shaft at Station 6+00, where the post-earthquake settlement was observed to be 0.63 ft, see Fig. 3-5.

Finally, it is interesting to note that an independent estimate of the void ratio changes in the different zones of the hydraulic fill, near the test shaft, following a totally different procedure from that described previously (Franklin, 1987) led to the following values:

Zone	Estimated change in void ratio between time of earthquake and time of sampling
1	0.000
2	0.011
3	0.024
4	0.000
5	0.023

Since the samples used in the testing program described in this report were obtained principally from Zones 2 and 5 of the hydraulic fill, it would appear that a representative value for this void ratio change based on these results would be somewhere between 0.011 and 0.023.

Based on the preceding analyses of void ratio changes since the 1971 earthquake, it was considered appropriate in interpreting the test data to allow for an average post-earthquake change in void ratio of 0.020 for all samples prior to their extraction from the ground in the 1985 sampling program.

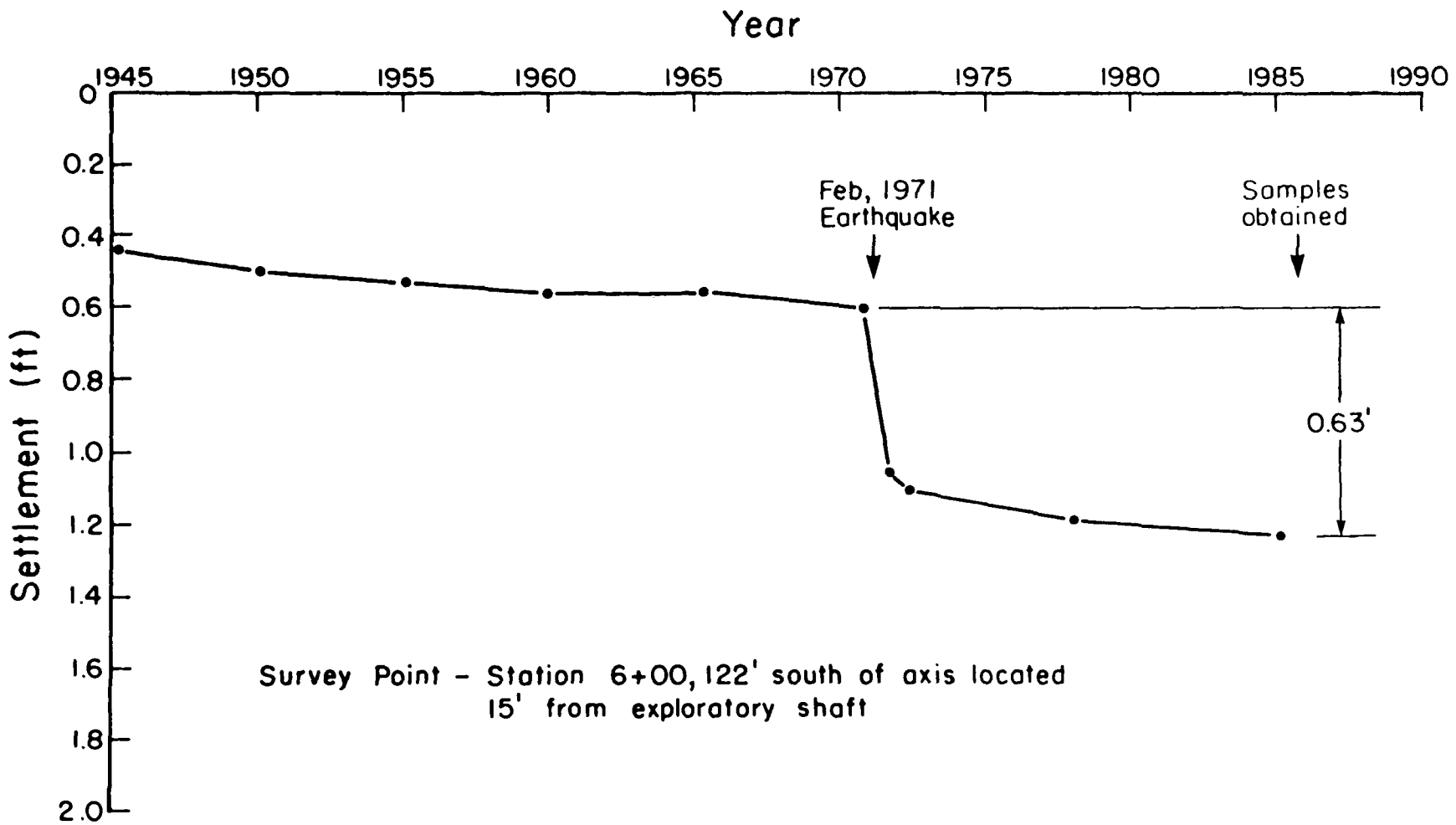

Fig. 3-5 SETTLEMENT RECORDS FOR SURVEY POINT LOCATED 15 FT FROM EXPLORATORY SHAFT
(Data provided by Geotechnical Engineers Inc.)

4. Analyses of Standard Penetration Test Data for Downstream Shell of Embankment

Considerable insight into the properties of the soils comprising the embankment can be obtained from the results of standard penetration tests. Such tests were performed in a limited study in 1967, in the comprehensive study performed in 1971 following the earthquake, and again in the investigation performed in 1985.

1971 Investigation

A plan showing the locations of SPT borings made in the 1971 investigations is shown in Fig. 4-1. In this study borings D-1, E-1, E-2, F-1, F-2, G-1 and G-2 were made in the downstream shell, primarily to determine the in-situ properties of the hydraulic sand fill. These borings showed that the hydraulic fill was highly stratified with soil types ranging from poorly graded sand to highly plastic clays. A summary of the soil stratification revealed by these seven borings is shown on the right hand side of Fig. 4-2. The results of all the penetration tests performed in the hydraulic fill are shown on the left of Fig. 4-2. In order to provide meaningful comparisons, the SPT data have been converted to values of $(N_1)_{60}$, the normalized standard penetration resistance under an overburden pressure of 1 tsf for an SPT test performed with a hammer providing 60% of the theoretical free-fall energy, in accordance with the conditions listed in Table 4-1 (Seed et al., 1985).

The main corrections to the field data required to determine values of $(N_1)_{60}$ were as follows:

1. The tests were performed using drilling rigs belonging to the State of California Dept. of Water Resources. These rigs are believed to have used a safety hammer operated by a rope and pulley technique, a

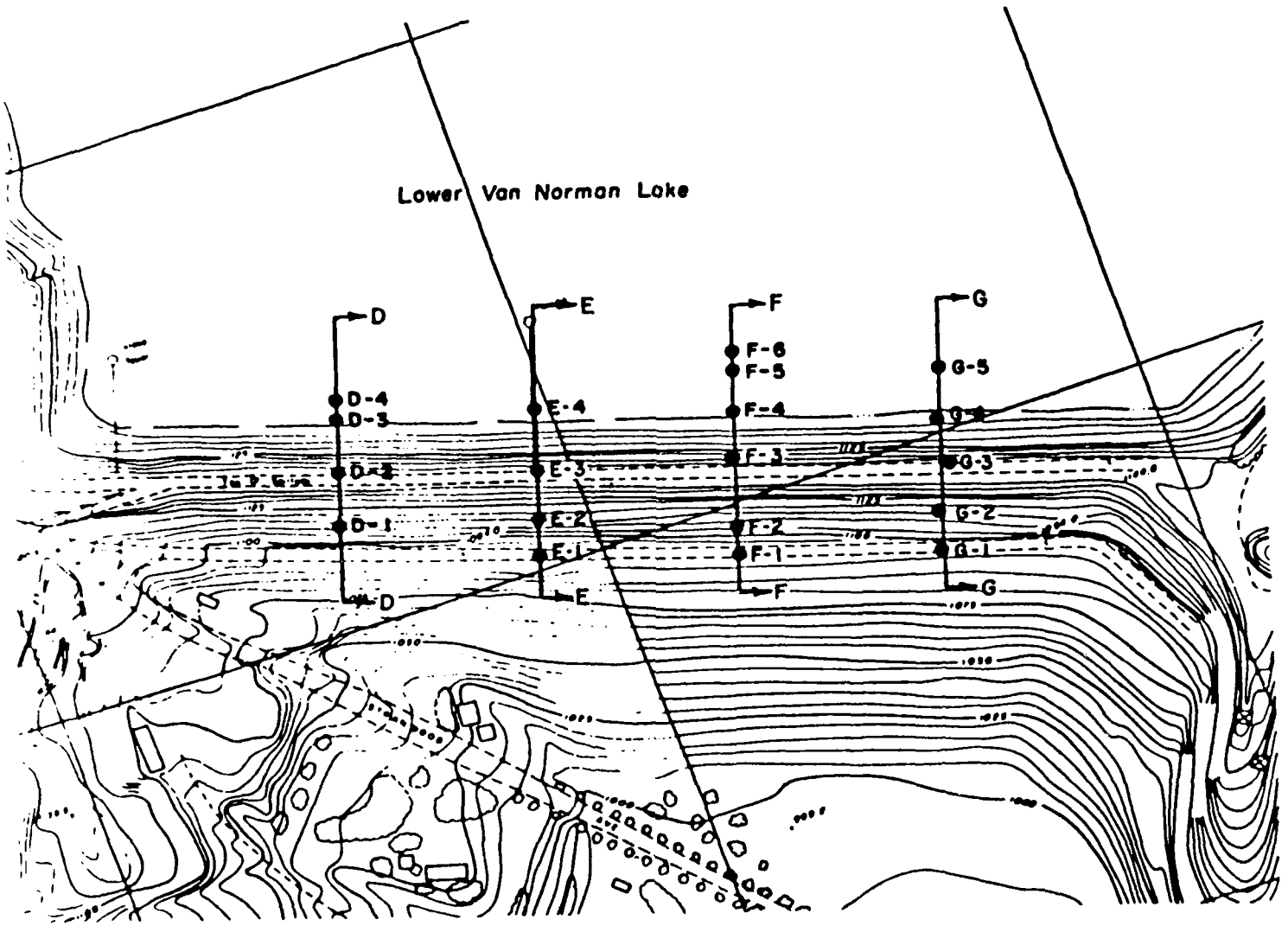

Fig. 4-1 PLAN OF LOWER SAN FERNANDO DAM SHOWING BORING LOCATIONS IN 1971 INVESTIGATION

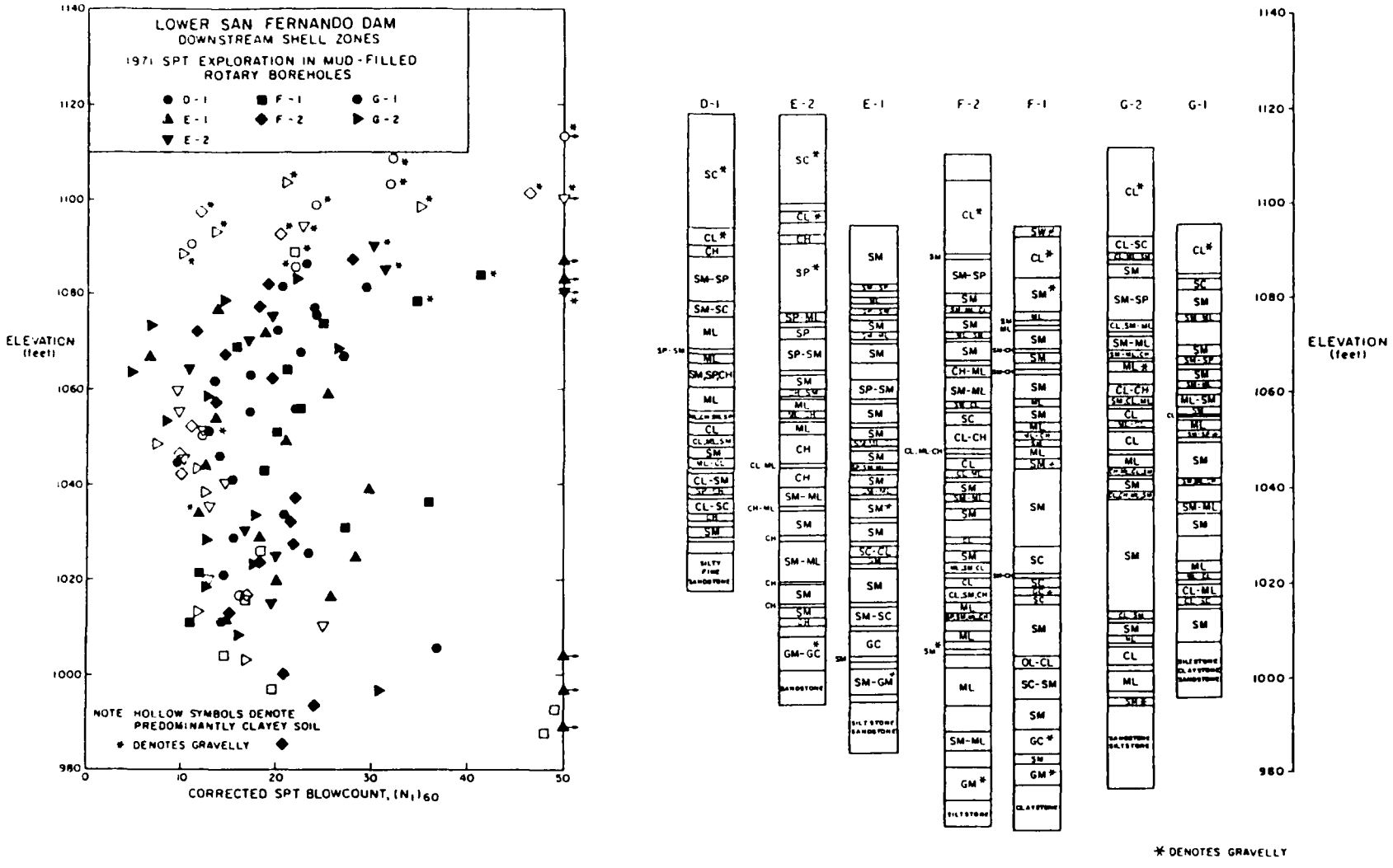

Fig. 4-2 RESULTS OF STANDARD PENETRATION TESTS IN DOWNSTREAM SHELL IN 1971 INVESTIGATIONS

TABLE 4-1 RECOMMENDED SPT PROCEDURE FOR USE IN LIQUEFACTION CORRELATIONS

A.	Borehole:	4 to 5-inch diameter rotary borehole with bentonite drilling mud for borehole stability
B.	Drill Bit:	Upward deflection of drilling mud (tricone of baffled drag bit)
C.	Sampler:	O.D. = 2.00 inches I.D. = 1.38 inches - Constant (i.e. no room for liners in barrel)
D.	Drill Rods:	A or AW for depths less than 50 feet N or NW for greater depths
E.	Energy Delivered to Sampler:	2520 in.-lbs. (60% of theoretical maximum)
F.	Blowcount Rate:	30 to 40 blows per minute
G.	Penetration Resistance Count:	Measures over range of 6 to 18 inches of penetration into the ground

procedure which characteristically provides an energy ratio of 60%. Thus no energy correction was required.

2. The Dept. of Water Resources test procedures at that time used the ASTM sampling tube without the liners. The measured N-values were increased by 10 to 30% to allow for this deviation from standard procedures (Seed et al., 1985).

3. The measured SPT N-values were corrected to N_1 values using the equation

$$N_1 = C_N \cdot N$$

where C_N is determined by the curve for loose to medium dense sand proposed by Seed (1979a,b) and shown in Fig. 4-3.

The corrected values of $(N_1)_{60}$ for all tests performed in 1971 are shown in Fig. 4-2. It was observed that some of these tests, indicated by open symbols in Fig. 4-2, were performed in predominantly clayey soils. Since the SPT test data were only intended to indicate the properties of the cohesionless soils, the data from Fig. 4-2 are replotted in Fig. 4-4 for the cohesionless soils only. An analysis of this data indicated four main zones of cohesionless soil with mean and median values of $(N_1)_{60}$ as shown in Fig. 4-5. It may be noted that the two upper layers and the lowest layer have very similar characteristics with mean $(N_1)_{60}$ values of 16.5, 15.5 and 16 respectively. The third layer which corresponds approximately with the Zones 3 and 4 as identified by the GEI studies, shows higher $(N_1)_{60}$ values, with a mean value of 21.5. These results may be interpreted to indicate that with the exception of the apparently denser layer between Elevations 1024 to 1038, the cohesionless soils in the hydraulic fill have generally similar characteristics.

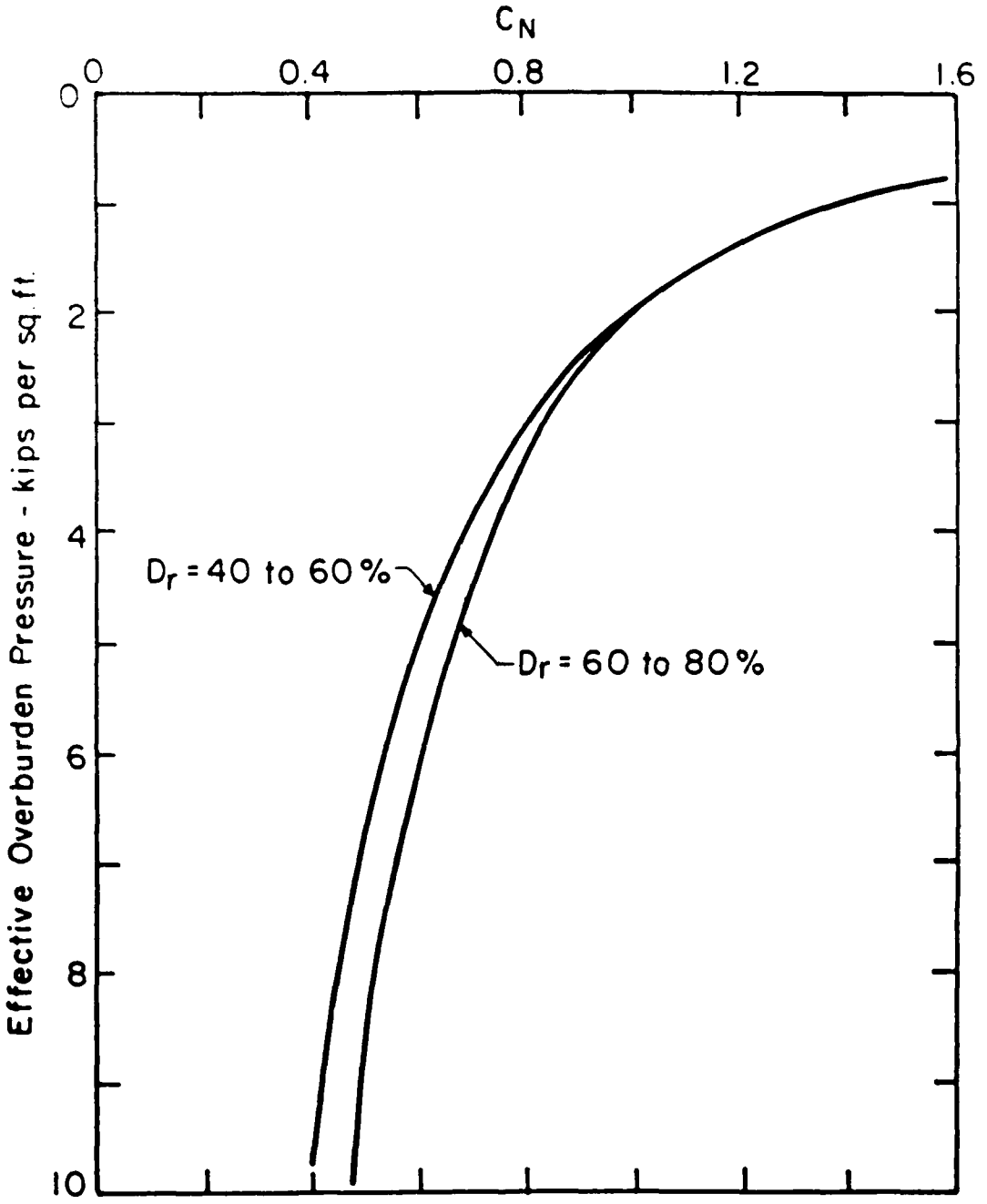

Fig. 4-3 VALUES OF C_N

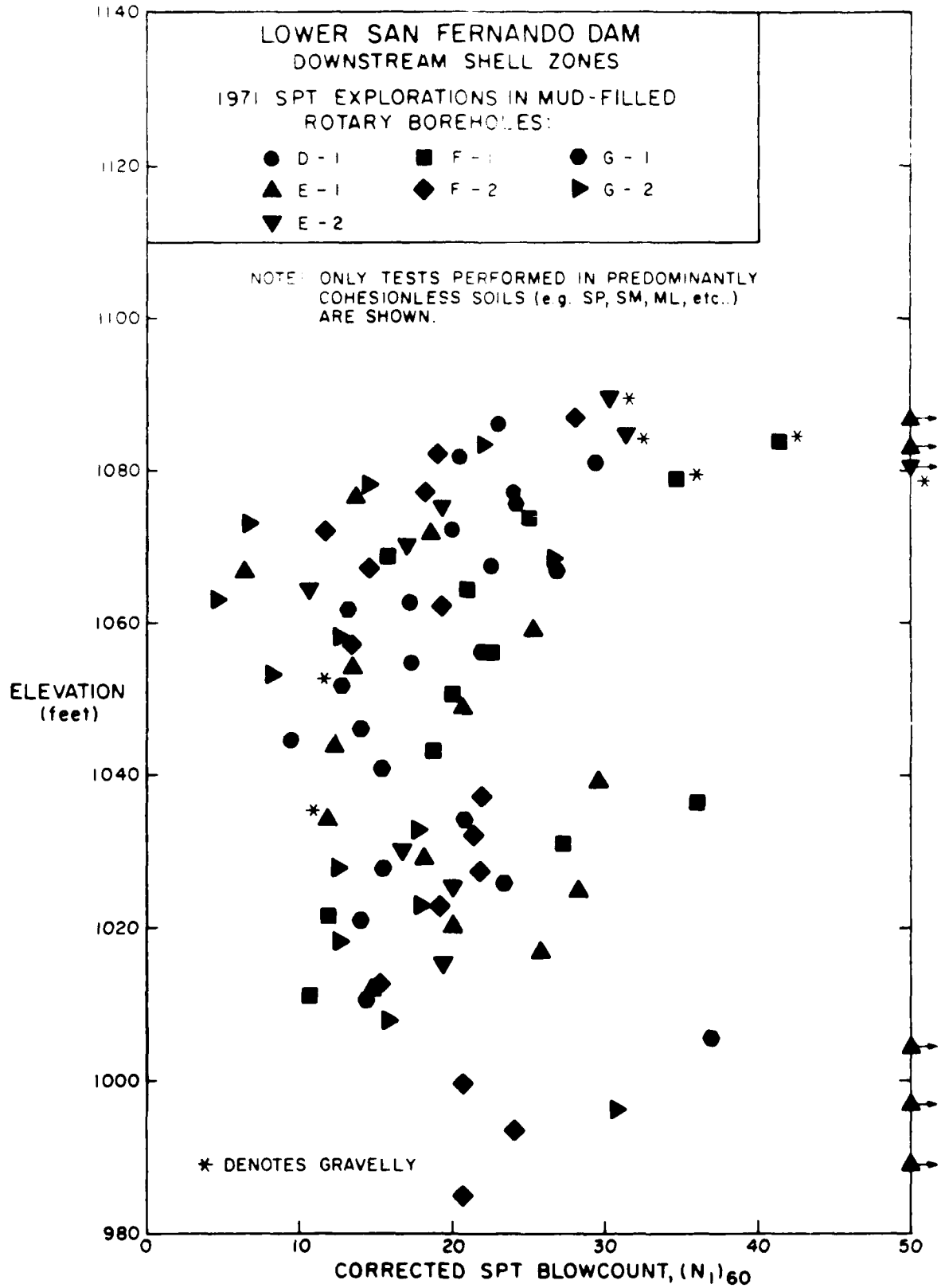

Fig. 4-4 RESULTS OF STANDARD PENETRATION TESTS IN COHESIONLESS SOILS IN DOWNSTREAM SHELL IN 1971 INVESTIGATION

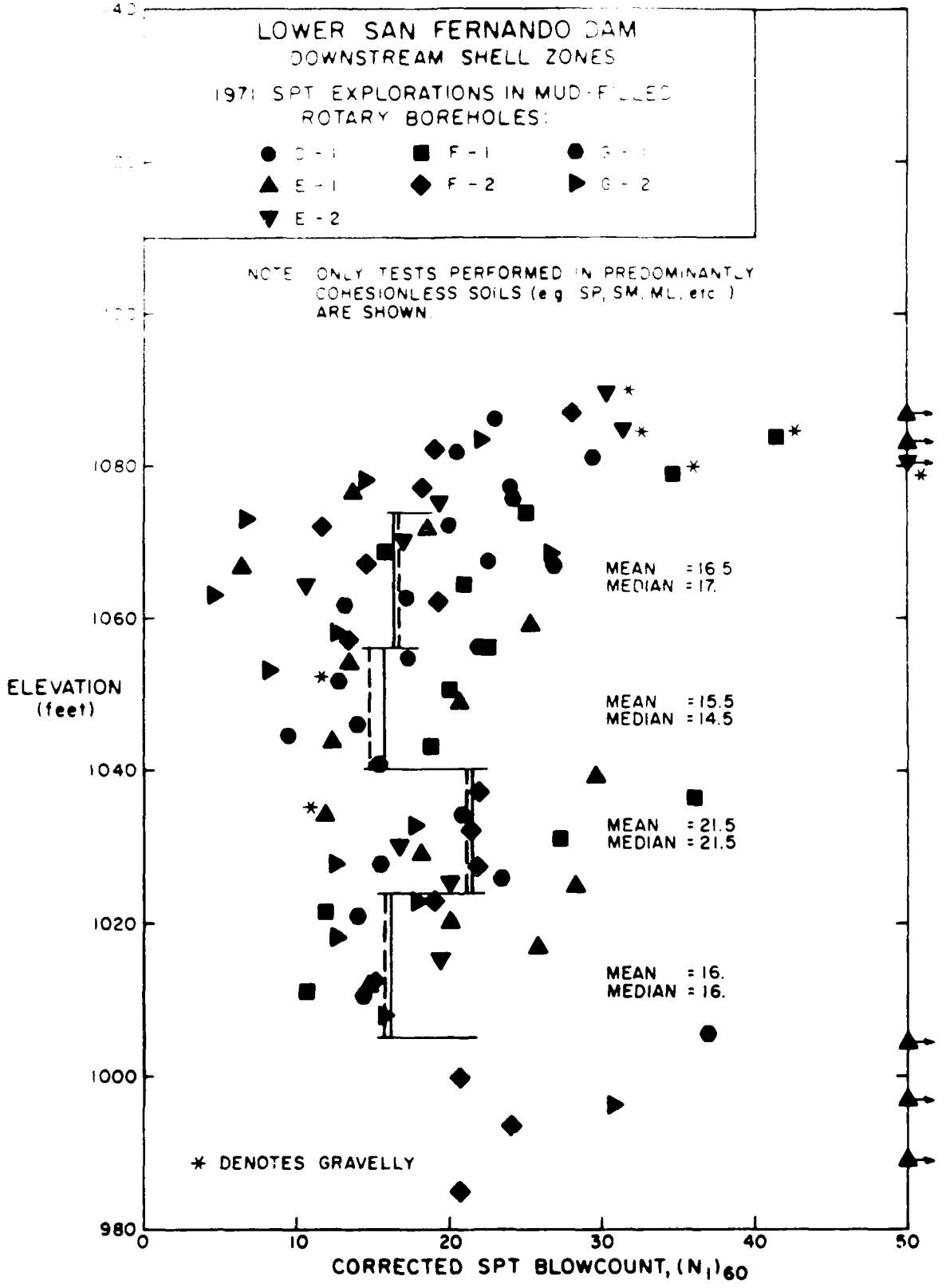

Fig. 4-5 ANALYSES OF SPT DATA FOR COHESIONLESS SOILS IN DOWNSTREAM SHELL - 1971 INVESTIGATION

For comparison purposes, the six SPT N-values measured in the 1967 investigation were converted to $(N_1)_{60}$ values and these results are superimposed on the results of the 1971 investigation in Fig. 4-6. The 1967 data were believed to be obtained using a conventional Donut Hammer and a rope and pulley test procedure. Consequently the energy ratio used in this test was considered to be about 50% and the field data were corrected accordingly. The data were also corrected for the presumed absence of liners in the sampling tubes. In addition, because the N-values measured in the 1967 investigation were counted for 0 to 12 inches of penetration rather than the 6 to 18 inches range required in the standard procedure, the values were increased by 15% to allow for this deviation from standard practice. This correction was proposed by Schmertmann (1979). The results are shown in Fig. 4-6. It may be seen that they reflect near upper and lower bounds for the 1971 data.

1985 Investigation

Values of $(N_1)_{60}$ determined in the 1985 investigation based on measurements made in Borings Nos. S101, S103, S104 and S111 in the downstream shell are shown in Fig. 4-7. As before, measured values were corrected for energy ratio effects (the energy ratio for the hammer used in the 1985 program was measured to be 72%) and for the absence of liners in the sampling tube, and then normalized to an overburden pressure of 1 tsf using the value of C_N shown in Fig. 4-3.

The resulting values of $(N_1)_{60}$ are shown in Fig. 4-7, and the results of statistical analyses of the values in the same four layers as those shown in Fig. 4-5, are presented in Fig. 4-8. The presence of a more resistant layer

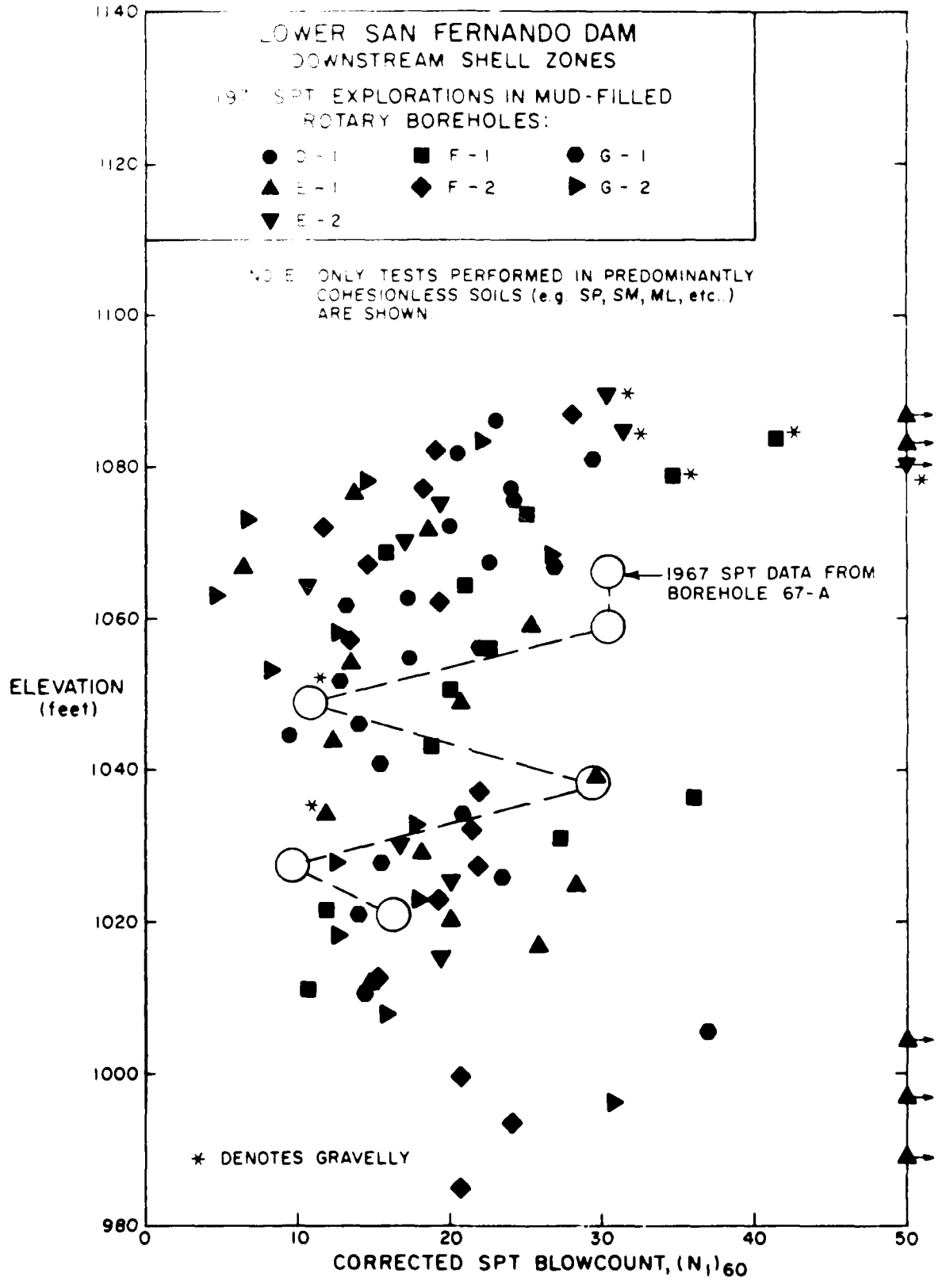

Fig. 4-6 COMPARISON OF SPT DATA IN 1967 AND 1971 INVESTIGATIONS

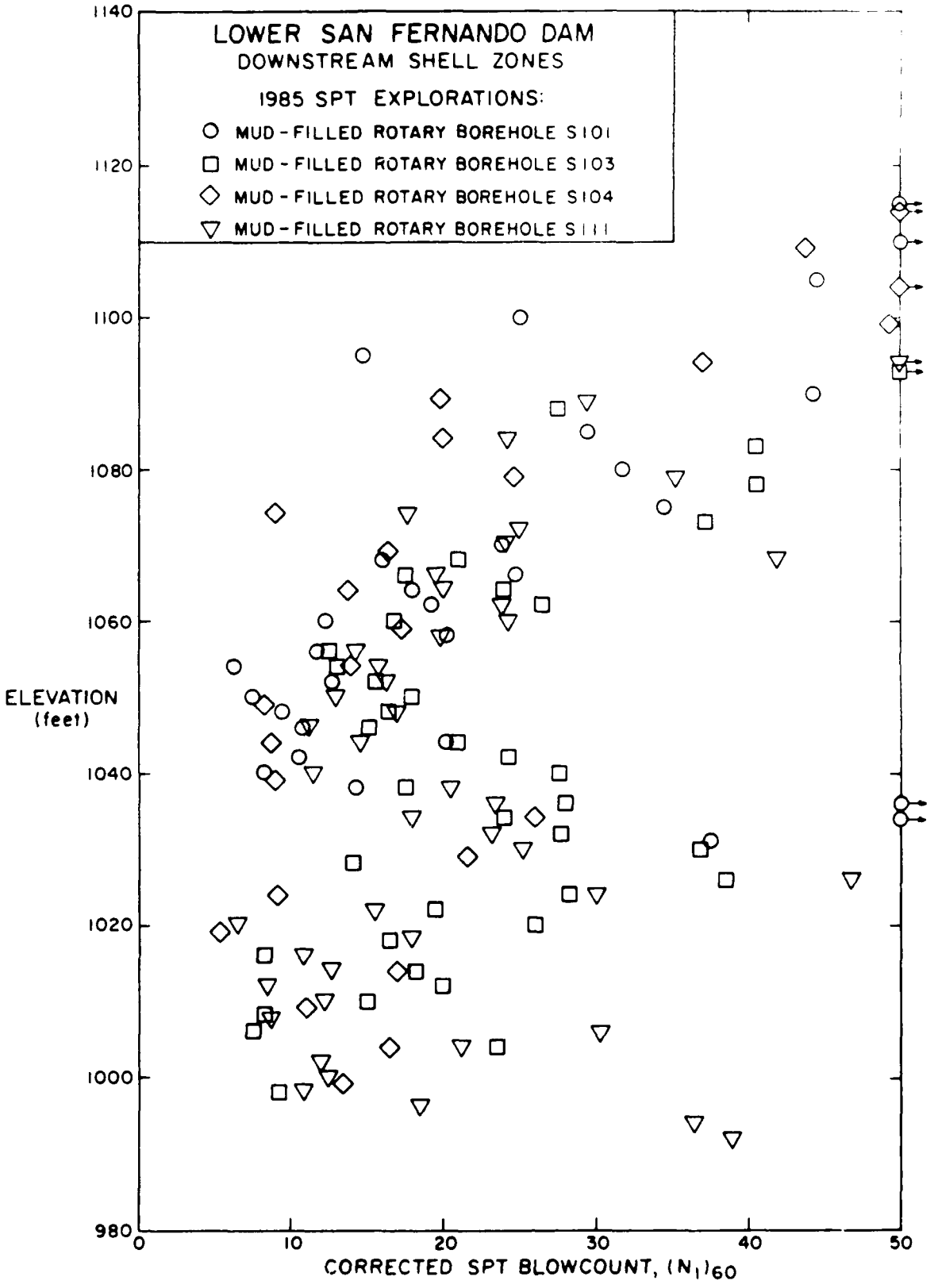

Fig. 4-7 RESULTS OF STANDARD PENETRATION TESTS IN DOWNSTREAM SHELL IN 1985 INVESTIGATION

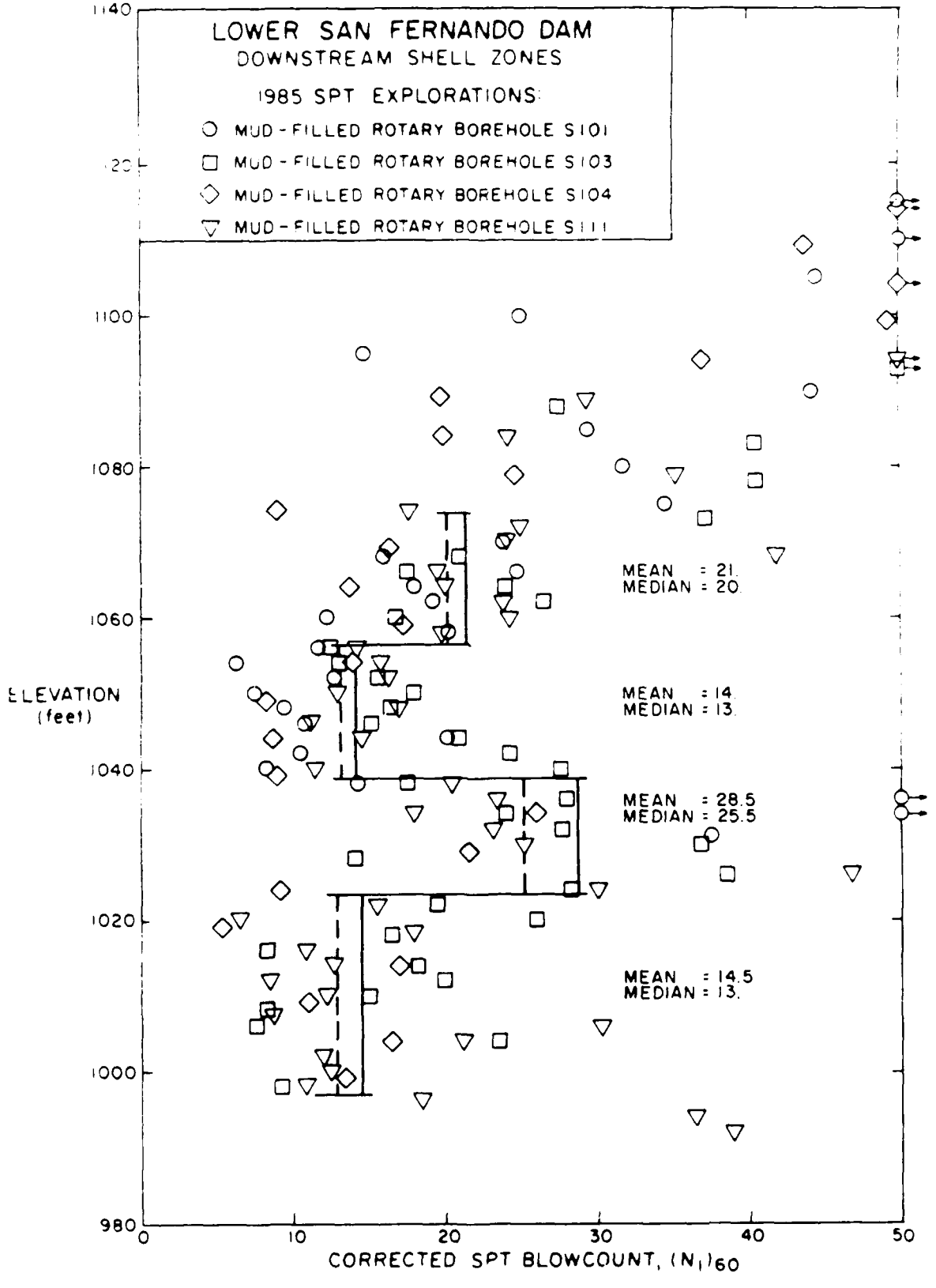

Fig. 4-8 ANALYSES OF SPT DATA FOR BORINGS IN DOWNSTREAM SHELL IN 1985 INVESTIGATION

of fill between approximately Elevations 1024 and 1038 is readily observable in these data also.

For comparison purposes, the values of $(N_1)_{60}$ measured in cohesionless soil in the downstream shell in the 1985 investigation are compared with values determined in the 1971 investigation in Fig. 4-9. The general distribution seems to be about the same for both studies.

Summary

The standard penetration resistance of the cohesionless soils in the downstream shell of the embankment, expressed in terms of $(N_1)_{60}$ may be summarized as follows:

Elevation (ft)	Median values of $(N_1)_{60}$ 1971 Data	1985 Data	Avg. values of $(N_1)_{60}$ 1971 Data	1985 Data	Representative Avg. $(N_1)_{60}$
1074-1057	17	20	16.5	21	≈ 19
1056-1039	14.5	13	15.5	14	≈ 14.5
1038-1024	21.5	25.5	21.5	28.5	≈ 24
1023-1000	16	13	16	14.5	≈ 14.5

In general the soil in the Elevation zones 1000-1023 and 1039 to 1056 corresponds to that in Layers 2 and 5 identified by GEI. The cohesionless silty sand in these layers appears to be very similar with an overall average value of $(N_1)_{60}$ of about 14.5.

As noted previously, the density of this soil has probably changed since the earthquake as evidenced by the settlement of observation points on the downstream side of the embankment. Density changes at the time of the 1985 borings are significantly greater than those at the time of the post-

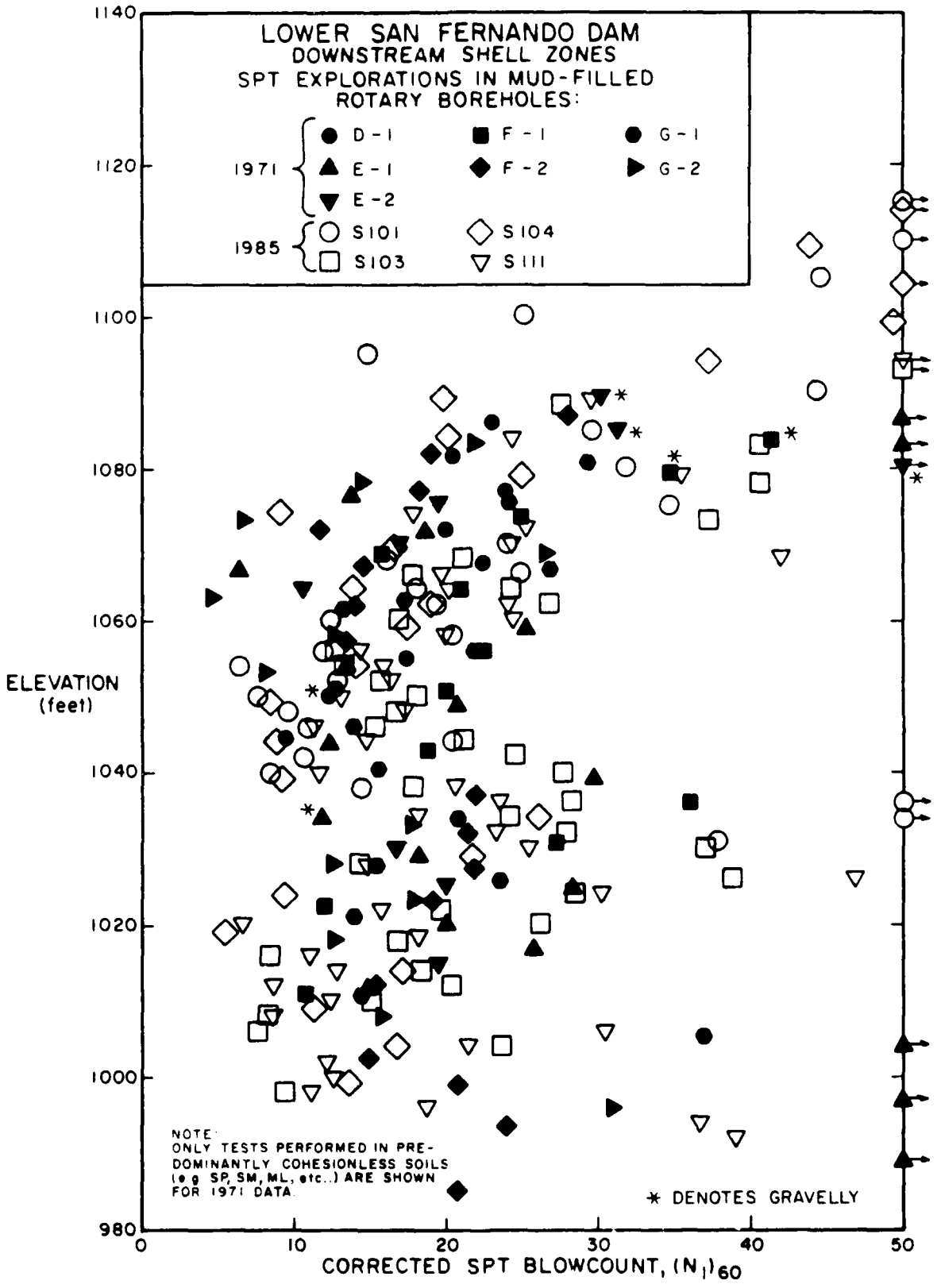

Fig. 4-9 COMPARISON OF RESULTS OF SPT DETERMINATIONS IN DOWNSTREAM SHELL IN 1971 AND 1985 INVESTIGATIONS

earthquake 1971 borings (April and May, 1971). Conservatively a representative average change in void ratio appears to be about 0.02 as shown in Section 3 of this report. This corresponds to a volumetric compression strain of about 1.15% in the silty sands and to a corresponding change in dry density of about 1.1 pcf. For the silty sands in the Lower San Fernando Dam, the range between maximum and minimum dry densities was found to be about 25 pcf in the 1971 investigations. Thus a change in density of about 1.1 pcf corresponds to a change in relative density of about 4%, with the relative density increasing from a value of, say, about 48% before the earthquake to about 52% at the time of the investigations after the earthquake. Such a change in relative density, using a typical correlation between relative density and $(N_1)_{60}$ corresponds to an increase in $(N_1)_{60}$ of about 2 blows/ft.

In a recent paper, Skempton (1986) has suggested that the ratio of $(N_1)_{60}/D_r^2$ has values of about 65 for coarse sands and 55 for fine sands. With a slight extrapolation, a suitable approximate relationship for silty sands might be

$$\frac{(N_1)_{60}}{D_r^2} \approx 50$$

Thus $$\Delta(N_1)_{60} \approx 100 \cdot D_r \cdot \Delta(D_r)$$

and if $D_r \approx 0.5$ and $\Delta(D_r) \approx 0.04$ as discussed above

$$\Delta(N_1)_{60} \approx 100 \cdot 0.5 \cdot 0.04 \approx 2 \text{ blows/ft.}$$

Based on the above, the average pre-earthquake penetration resistance of the silty sand in the most critical layers of the downstream shell would be about $(N_1)_{60} \approx 12.5$.

Finally it may be noted that the penetration resistance of silty sands is somewhat lower than that for clean sands. Seed (1987) has recently

proposed that for equal relative densities, values of $(N_1)_{60}$ determined for silty sands could be corrected to equivalent clean sand values by adding small increments to the measured values of $(N_1)_{60}$ as follows:

Fines content	$\Delta(N_1)_{60}$
10%	1
25%	2
50%	4
75%	5

For the average silty sand in the Lower Dam, the fines content appears to be about 25 percent and the corresponding value of $\Delta(N_1)_{60}$ would be about 2. In these terms a representative average value of the equivalent clean sand $(N_1)_{60}$-value for pre-earthquake conditions would be about 14.5.

5. Results of Cyclic Load Tests on Silty Sand

Laboratory Test Data

During the investigation of the slide in the San Fernando Dam (1971-73), it was observed in the field that the hydraulic fill in the upstream shell was highly stratified with layers of silt and clay frequently occurring between thicker layers of silty sand. Thus, since the clayey soils were not likely to be vulnerable to liquefaction, the studies of cyclic loading resistance were performed on undisturbed samples of silty sand taken by undisturbed sample borings. A total of 49 cyclic load tests were performed on both isotropically and anisotropically-consolidated samples obtained from the hydraulic fill and the foundation alluvium. Details of the testing procedures, together with the results of the tests are described by Seed et al. (1973). The relationships between cyclic stress ratio and number of stress cycles required to cause a pore-pressure ratio of $r_u \approx 100\%$ and ±5% strain determined by this study for samples consolidated under pressures of 2 kg/cm^2 are shown by the dashed line in Fig. 5-1.

In the 1985 investigation samples were obtained both from undisturbed sample borings and from a test shaft. Many of the samples were sandy silt but many were silty sand. Since the number of samples available, however, was limited it was decided to concentrate the cyclic load test program on the silty sand samples to provide a direct comparison with the data obtained in the 1971 investigation. Furthermore, in view of the limited number of silty sand samples available, tests were performed mainly on samples consolidated isotropically under a confining pressure of 2 kg/cm^2. Details of the testing program are provided in the Appendix to this report.

The results of these tests are also shown in Fig. 5-1. It was found that for samples which developed a condition of $r_u \approx 100\%$ and cyclic strains

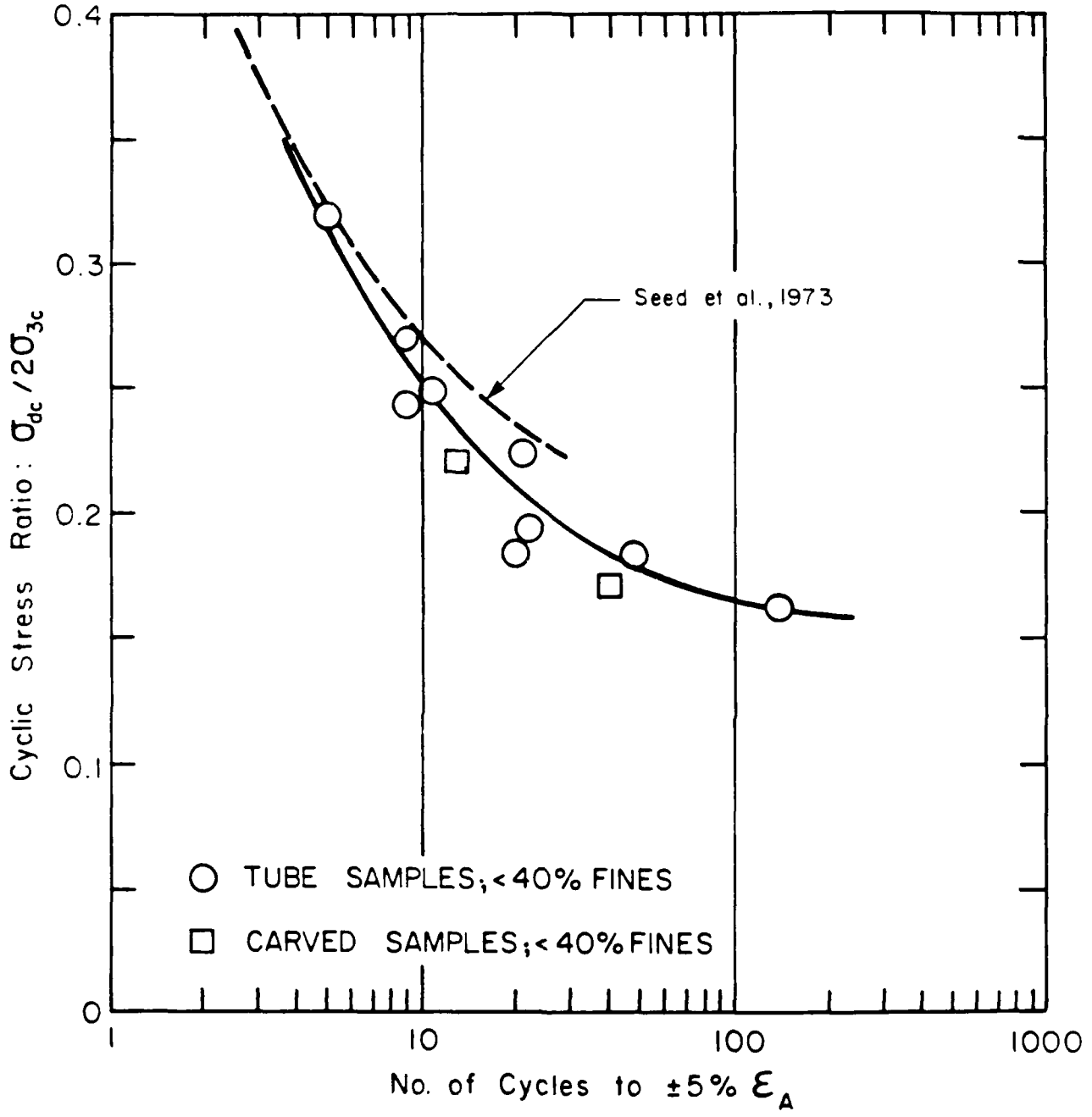

Fig. 5-1 RESULTS OF CYCLIC LOAD TESTS ON UNDISTURBED SAMPLES OF SILTY SAND

of ±5% strain in low numbers of cycles (say less than 10), the cyclic stress ratios were very similar to those determined in the 1971 investigation. However for samples reaching the prescribed failure condition in larger numbers of cycles, say 15 to 40 cycles, the cyclic loading resistance was 10 to 15 percent lower than that determined in the 1971 investigation. No reason for this small difference in behavior could be determined. There appeared to be no significant difference between the results of tests on samples obtained from borings or from the test shaft. The range of grain size distribution curves for the samples for which data is shown in Fig. 5-1 is presented in Fig. 5-2.

Cyclic load tests were also performed on samples of sandy silt. The grain size curves for these samples are shown in Fig. 5-3 and it will be seen that the fines content was substantially higher than that for the samples of silty sand. However, as shown by the test data in Fig. 5-4, there was no significant difference in the cyclic loading resistance of these samples. Details of the test conditions and results for all samples are presented in Table 5-1.

A limited number of tests were also performed on samples of silty sand consolidated anisotropically under a minor principal stress of 2 kg/cm^2 and a major principal stress of 3.5 kg/cm^2. The grain size distribution curves for these samples are shown in Fig. 5-5 and the test results are summarized in Table 5-2. All of these samples were obtained from Zone 3 of the hydraulic fill (see Appendix I, Table I-3 and Fig. I-1). The cyclic stress ratio required to cause a pore pressure ratio $r_u \approx 100\%$ and an axial strain of 5% in these tests for each of the samples is plotted in Fig. 5-6. It may be seen that the cyclic loading resistance of the anisotropically-consolidated samples

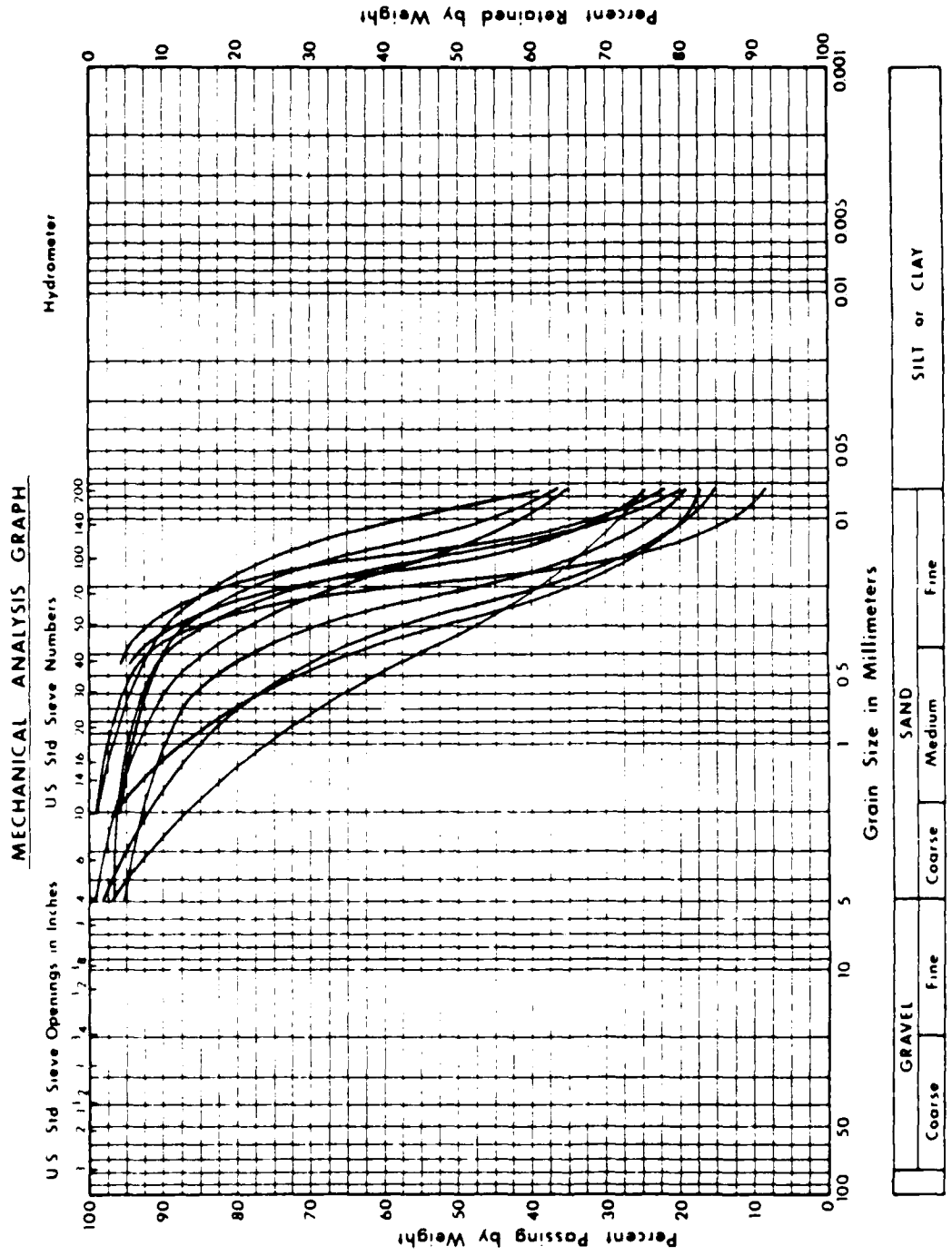

Fig. 5-2 GRAIN-SIZE DISTRIBUTION CURVES FOR UNDISTURBED SAMPLES OF SILTY SAND SUBJECTED TO CYCLIC LOAD TESTS (IC-U)

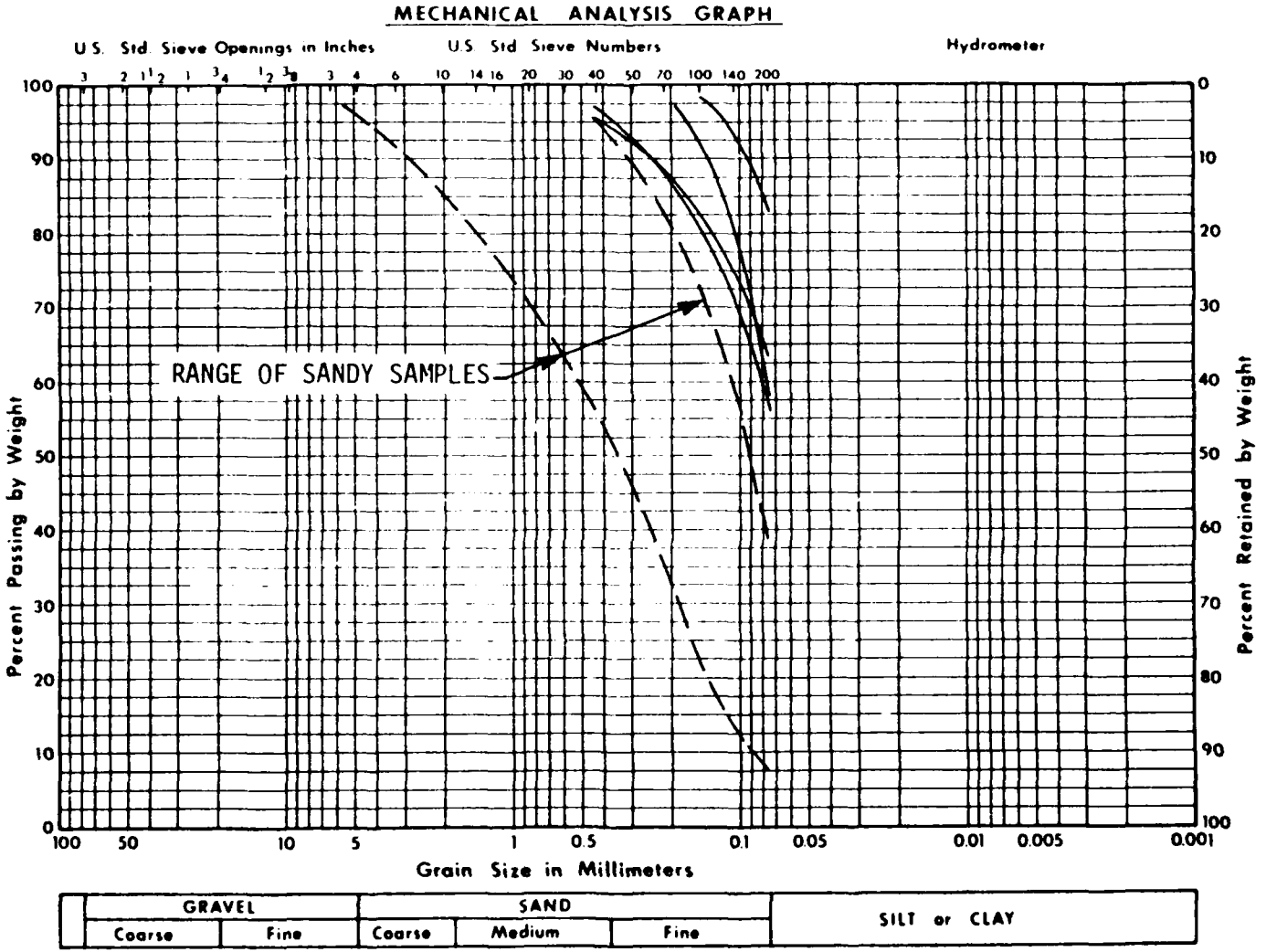

Fig. 5-3 GRAIN-SIZE DISTRIBUTION CURVES FOR UNDISTURBED SAMPLES OF SANDY SILT SUBJECTED TO CYCLIC LOAD TESTS (IC-U)

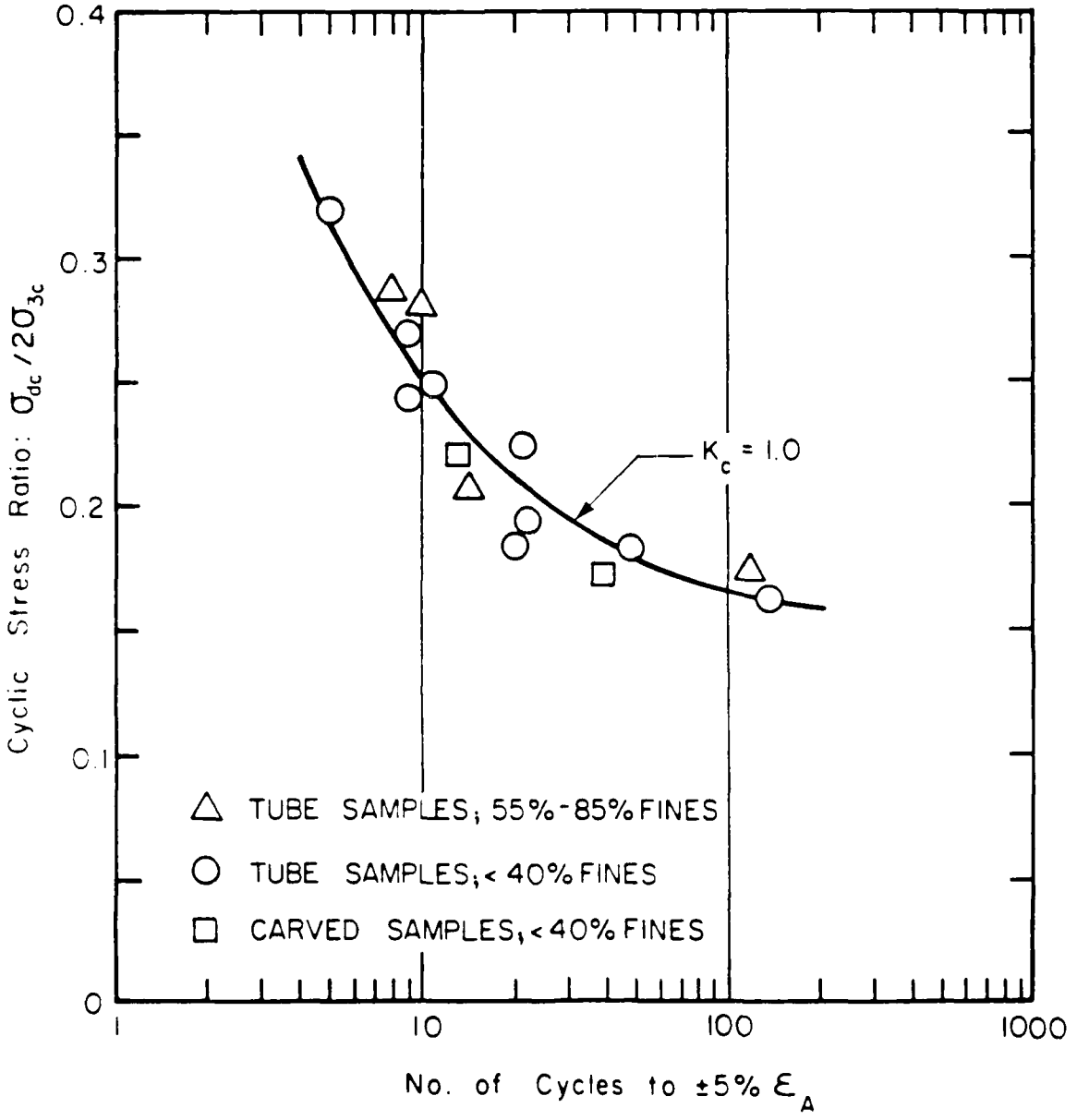

Fig. 5-4 RESULTS OF CYCLIC LOAD TESTS ON UNDISTURBED SAMPLES OF SILTY SAND AND SANDY SILT

TABLE 5-1 TEST DATA FOR ISOTROPICALLY CONSOLIDATED-UNDRAINED CYCLIC TRIAXIAL TESTS ON UNDISTURBED SAMPLES OF HYDRAULIC FILL FROM LOWER SAN FERNANDO DAM

Test No.	Boring No.	Sample No.	Sample Elev. (ft.)	Void Ratio as Tested*	Void Ratio After Sampling*	Void Ratio In Situ (1985)*	$\sigma'_{3,i}$ (kg/cm^2)	"B-value"	$\sigma_{d,c}/2\sigma'_{3,i}$	No. of Cycles to ±5% ε_A	% Finer Than #200 Sieve
1	U104	UF8	1022	0.664	0.730	0.741	2.00	0.989	0.249	11	20
2	U104	UF8	1021	0.611	0.651	0.661	2.00	0.996	0.319	5	8
3	U111A	UF18	1014	0.549	0.615	0.607	2.00	0.997	0.270	9	15
5	U111A	UF18	1013	0.487	0.537	0.559	2.00	0.995	0.224	21	19
8	U111	UF18	1017	0.680	0.707	0.708	2.00	0.995	0.288	8	56
15	U102	UF1	1054	0.592	0.637	0.628	2.00	0.986	0.193	22	35
17	U111	UF21	1011	0.587	0.566	0.577	2.00	0.989	0.184	20	25
18	U111	UF21	1011	0.504	0.543	0.554	2.00	0.998	0.162	139	17
21	U103	UF4	1011	0.624	0.689	0.675	2.00	0.988	0.282	10	63
22	U103	UF4	1010	0.670	0.721	0.736	2.00	0.996	0.243	9	39
30	U111	UF4	1044	0.709	0.761	0.789	2.00	0.987	0.183	48	24
31	U111	UF4	1043	0.670	0.735	0.762	2.00	0.994	0.208	14	58
39	U111	UF16	1021	0.689	0.758	0.734	2.00	0.995	0.174	118	83
47	Shaft**	TS117	1041	0.708	0.759	0.737	2.00	0.991	0.221	13	22
49	Shaft**	TS211	1031	0.691	0.786	0.779	2.00	0.998	0.172	39	36

*Based on G_s = 2.69. Void ratio after consolidation.

**Hand-carved samples from exploratory shaft.

TABLE 5-2 TEST DATA FOR ANISOTROPICALLY CONSOLIDATED-UNDRAINED CYCLIC TRIAXIAL TESTS ON UNDISTURBED SAMPLES OF HYDRAULIC FILL FROM LOWER SAN FERNANDO DAM

Test No.	Boring No.	Sample No.	Sample Elev. (ft.)	Void Ratio as Tested*	Void Ratio After Sampling*	Void Ratio In Situ (1985)*	$\sigma'_{3,i}$ (kg/cm^2)	"B-value"	$\sigma_{d,c}/2\sigma'_{3,i}$	No. of Cycles to ±5% ϵ_A	% Finer Than #200 Sieve
32	U111	UF9	1035	0.569	0.638	0.669	2.00	0.993	0.293	153	24
33	U111	UF9	1034	0.543	0.589	0.621	2.00	0.991	0.357	24	14
40	U111A	UF6	1037	0.605	0.667	0.680	2.00	0.989	0.287	281	12
41	U111A	UF6	1036	0.520	0.602	0.614	2.00	0.974	0.325	57	17
42	U111A	UF7	1034	0.585	0.671	0.690	2.00	0.997	0.297	82	15

*Based on G_s = 2.69. Void ratio after consolidation.

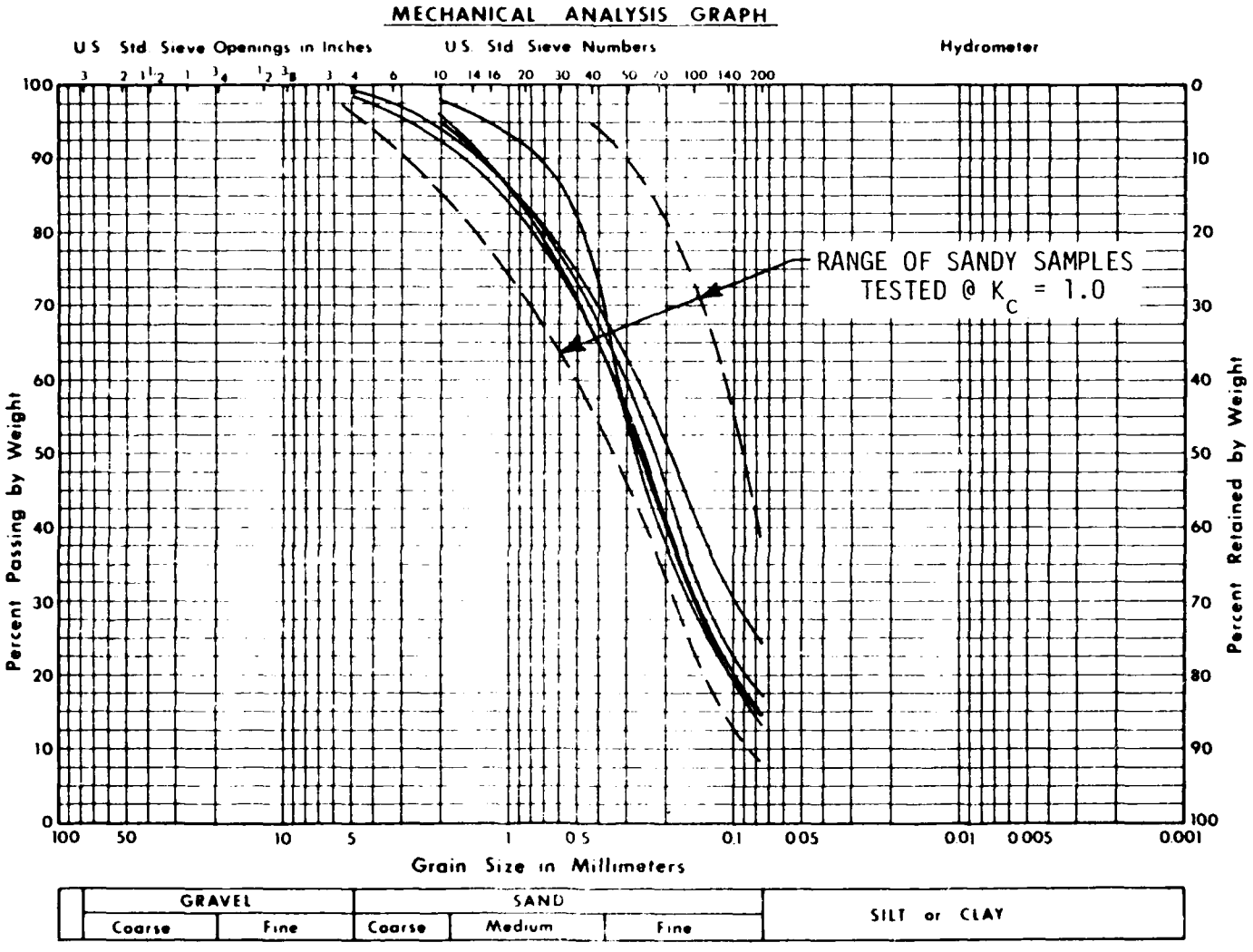

Fig. 5-5 GRAIN-SIZE DISTRIBUTION CURVES FOR UNDISTURBED SAMPLES OF SILTY SAND SUBJECTED TO CYCLIC LOAD TESTS (AC-U)

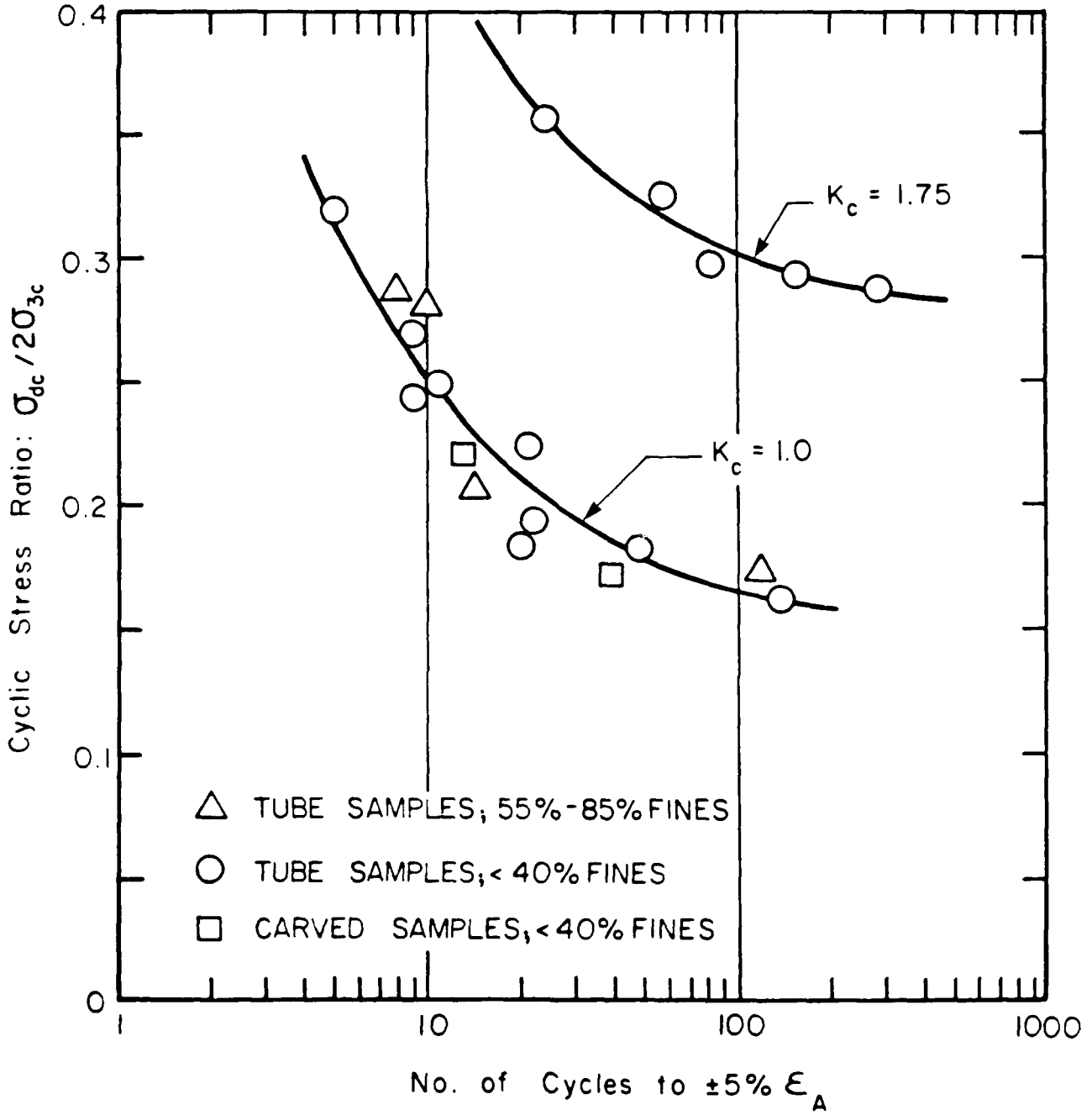

Fig. 5-6 COMPARISON OF IC-U AND AC-U CYCLIC LOAD TEST DATA FOR UNDISTURBED SAMPLES OF SILTY SAND

is considerably higher than that required to cause similar conditions in the tests on isotropically consolidated samples. These results were also similar to those obtained in the 1971 investigation.

Effect of Void Ratio Changes on Test Results

It may be noted from the test data presented in Table 5-1 that there was a significant reduction in void ratio of the samples between their condition in the field and their condition at the end of consolidation in the laboratory tests. This change occurred during the sampling and handling processes. For the 15 samples listed in Table 5-1, the average change in void ratio due to these effects was about 0.052 which corresponds to a volumetric strain of about 3%. Since the range of $(\gamma_d)_{max} - (\gamma_d)_{min}$ for the silty sand was typically about 25 pcf, and the in-situ dry density was about 100 pcf, such a change in volume corresponds to a change in relative density of about 11%. Thus considering that the field relative density was about 52%, the average relative density of the samples at the time of testing was probably about 63%.

In addition to this change it was shown in Section 4 that the relative density of the silty sand was probably increased by about 4% due to the earthquake shaking in 1971. Thus the test data shown in Fig. 5-1 represents the behavior of the silty sand at a relative density about 15% higher than that of the soil prior to the 1971 earthquake. It is necessary to consider what effect this may have had on the test results.

The probable effects of sampling and handling on the results of cyclic load tests on sands have been discussed by Seed et al. (1982). It was noted that during sampling and handling of medium dense sands several effects occur:

(1) There is a loss of strength previously gained by aging resulting from the disturbance of the grain structure, and

(2) There is a gain in strength due to densification of the samples.

Thus it was suggested that in most cases, for sands with a relative density of about 50%, these effects are compensating and somewhat fortuitously, the results of tests on undisturbed samples are about the same as those for the soil in its in-situ condition. If this is so, then it is unnecessary to correct the test data for changes occurring during sampling and handling. However it would be appropriate to correct the results for the effects of densification during the earthquake of 1971. Such a correction, since cyclic loading resistance is approximately proportional to relative density, would require that the laboratory test data be reduced slightly, by about 8% to determine the cyclic loading resistance for the pre-earthquake conditions in 1971.

Some insight into the appropriateness of this evaluation may be obtained by noting that the cyclic loading resistance of sands and silty sands can also be evaluated from the results of standard penetration tests (Seed et al., 1983; Seed et al., 1985), using correlations between cyclic loading resistance and $(N_1)_{60}$-values determined from field cases of level ground liquefaction and non-liquefaction in Magnitude 7.5 earthquakes. Such a correlation developed by Seed et al. (1985) is shown in Fig. 5-7. For any given value of $(N_1)_{60}$ it is a simple matter to read off from such a chart the value of τ_{av}/σ_o' at which liquefaction will occur under level ground conditions. This cyclic stress ratio, applicable to simple shear conditions, can than be converted to a corresponding value of stress ratio causing liquefaction in triaxial tests conditions using the relationship (Seed, 1979a,b):

$$\left(\frac{\tau_{av}}{\sigma_o'}\right)_{\ell\text{-ss}} = c_r \left(\frac{\sigma_{dc}}{2\sigma_{3c}}\right)_{\ell\text{-triaxial}} \qquad (1)$$

where c_r has a value of about 0.6 for normally consolidated silty sands.

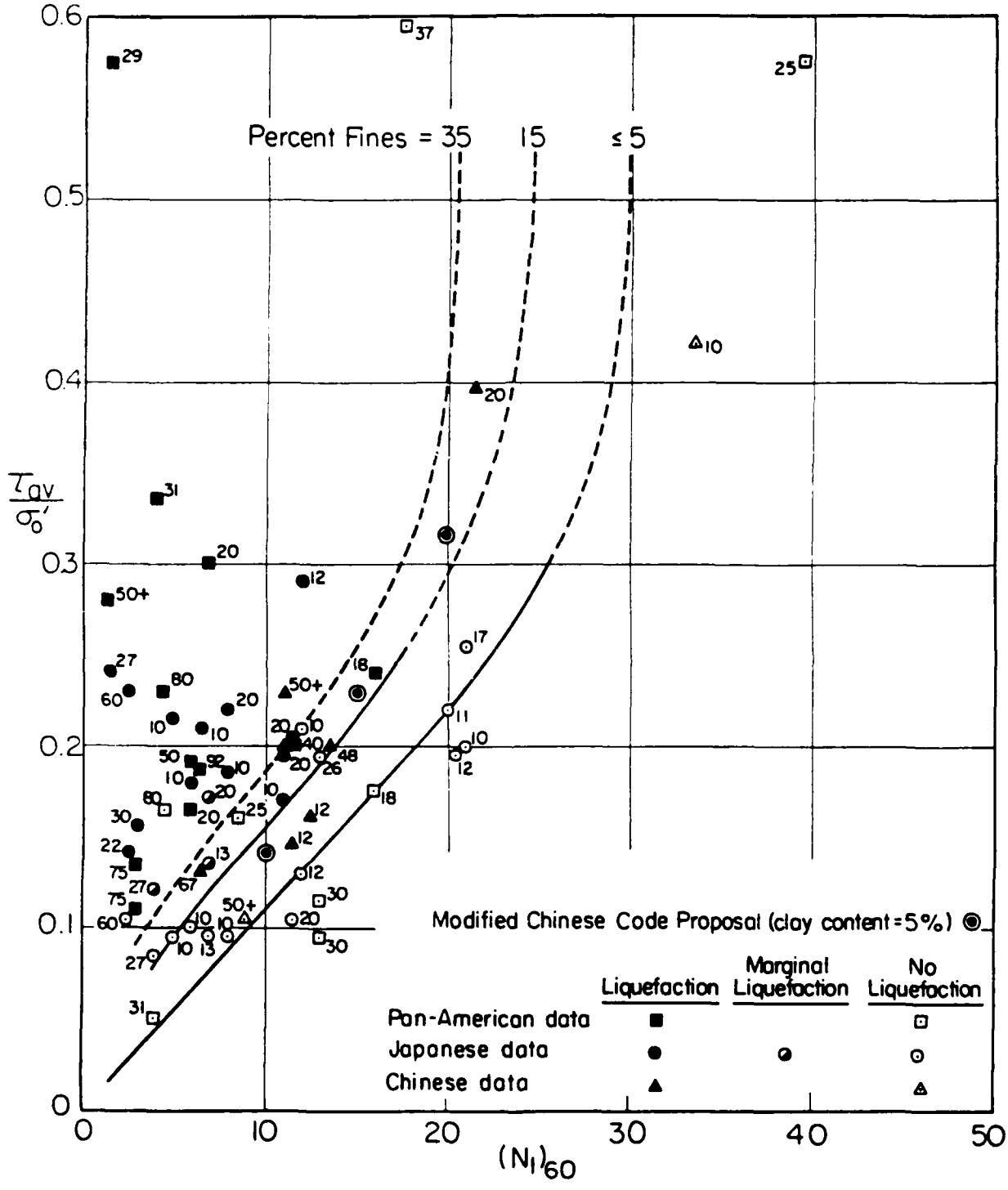

Fig. 5-7 RELATIONSHIPS BETWEEN STRESS RATIOS CAUSING LIQUEFACTION AND $(N_1)_{60}$-VALUES FOR SANDS AND SILTY SANDS IN M ≈ 7 1/2 EARTHQUAKES (after Seed et al., 1985)

It was shown in the previous section of this report that a representative pre-earthquake value of $(N_1)_{60}$ for the silty sands in the critical zones of the downstream shell of the San Fernando dam embankment is about 12.5 and the fines content is about 25%. From Fig. 5-7, it may be observed that this corresponds to a value of τ_{av}/σ_o' causing liquefaction of about 0.2. Converting this to a cyclic stress ratio for triaxial test conditions, with the aid of Eqn. (1), leads to a value of

$$\frac{\sigma_{dc}}{2\sigma_{3c}} \approx \frac{0.2}{0.6} \approx 0.33 \quad \text{for a Mag. 7.5 earthquake.}$$

Since a Magnitude 7.5 earthquake typically corresponds to about 15 uniform stress cycles, this result can be compared with the results of the cyclic load tests on undisturbed samples tested under a confining pressure of 1 kg/cm^2; and having determined one point on the cyclic loading resistance curve in this way, other points can readily be determined following the procedure described by Seed et al. (1983). The resulting comparison is shown in Fig. 5-8. It may be seen that the cyclic loading resistance determined in this way is in good agreement with the results obtained in the 1973 investigations.

This would seem to indicate that the effects of densification and sample disturbance during sampling and handling are largely compensating for the cyclic load test for hydraulic fill, and that no significant correction needs to be applied to the test data to determine the probable cyclic loading resistance for the pre-1971 earthquake conditions.

The fact that the samples were densified both by the 1971 earthquake and during sampling and handling has, however, significant implications regarding the possibility of determining the post-liquefaction strength of the hydraulic fill from tests on undisturbed samples. This strength is determined, for any

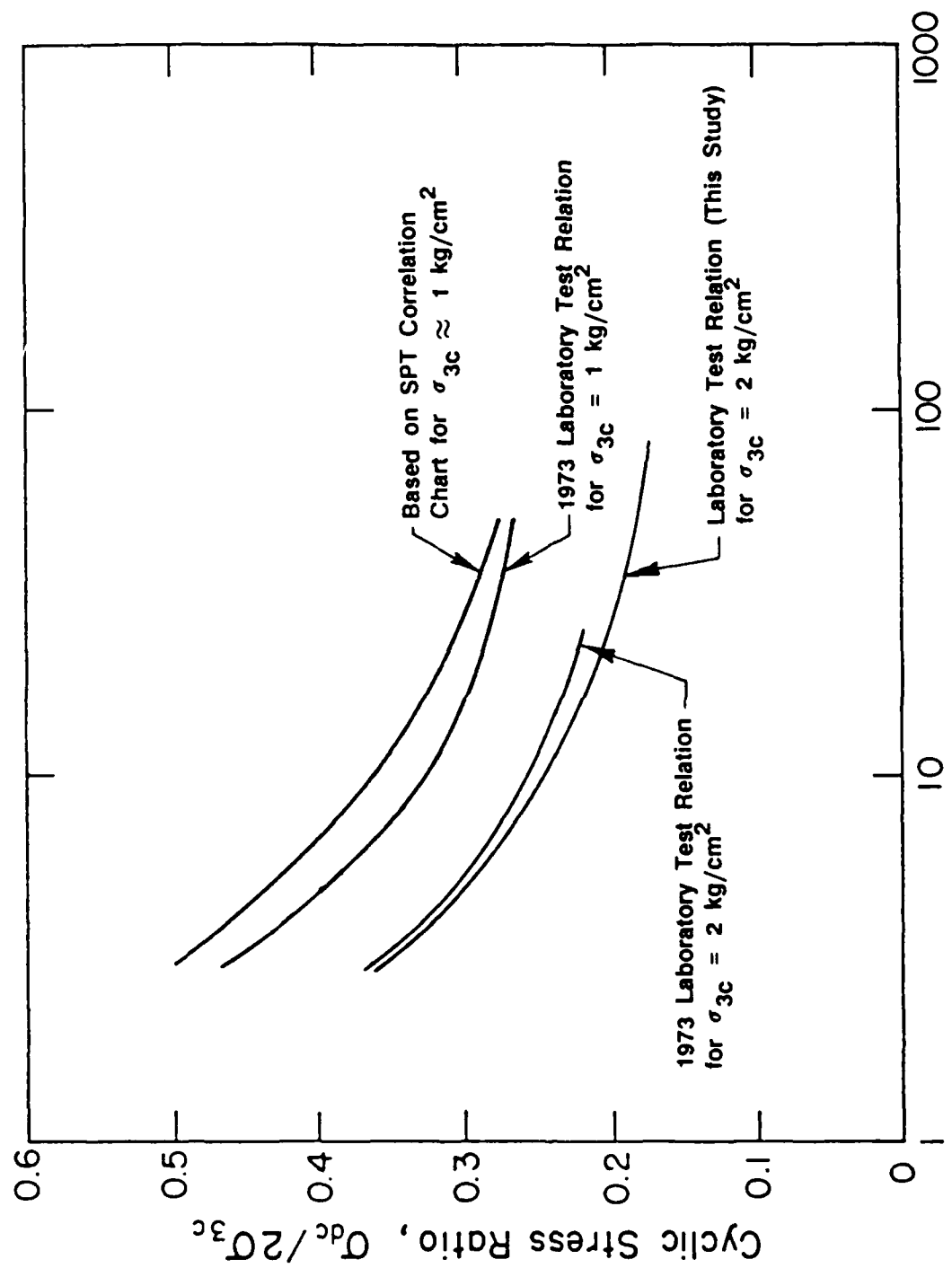

Fig. 5-8 COMPARISON OF RESULTS OF LABORATORY CYCLIC LOAD TESTS WITH DATA DETERMINED FROM FIELD CASE STUDIES

given soil, mainly by the void ratio or relative density of the soil and a change in relative density of 15%, say from about 48% to 63% could change the soil from a compressive to a dilatant condition. Thus there is no possibility that the post-liquefaction strength of a loose to medium dense sand could be determined directly from tests performed on undisturbed samples. Such a determination would require that test data be corrected for void ratio changes occurring both during sampling and handling as well as during the event causing liquefaction. The corrections for void ratio changes occurring during sampling and handling of the test specimens are best made by means of steady-state strength tests as described in the following section of this report.

6. Results of Steady-State Strength Tests

To investigate the steady-state strength of the soils in the Lower San Fernando Dam, a number of steady-state strength tests were performed on undisturbed samples taken during the 1985 sampling program. The majority of these samples were obtained from undisturbed sample borings Nos. U111 and U111A and the exploratory test shaft, but five of the samples tested were obtained from Borings U102, U104 and U105. The criteria for selection of samples were

1. That they should consist of the same type of soil throughout the height of the sample; i.e., contain no visual non-homogeneity

and 2. Be obtained from the zones of the hydraulic fill identified as Zones 2, 3 or 5 by GEI.

A schematic section of the existing embankment showing the locations of all samples judged to meet these criteria is shown in Fig. 6-1.

The samples obtained in this way generally fell into two groups: (a) samples of sandy silt and (b) samples of silty sand. Steady-state strength tests were performed on:

4 samples of sandy silt taken from the test shaft

7 samples of sandy silt taken from undisturbed sample borings

3 samples of silty sand taken from the test shaft

2 samples of silty sand taken from undisturbed sample borings.

Details concerning the testing program are provided in the Appendix to this report.

It was recognized in the exploration program that different soils existed in the hydraulic fill and representative bulk samples of the silty sand (designated Bulk Sample No. 3) and the sandy silt (designated Bulk Sample No. 7) were selected by GEI and distributed to the participating laboratories.

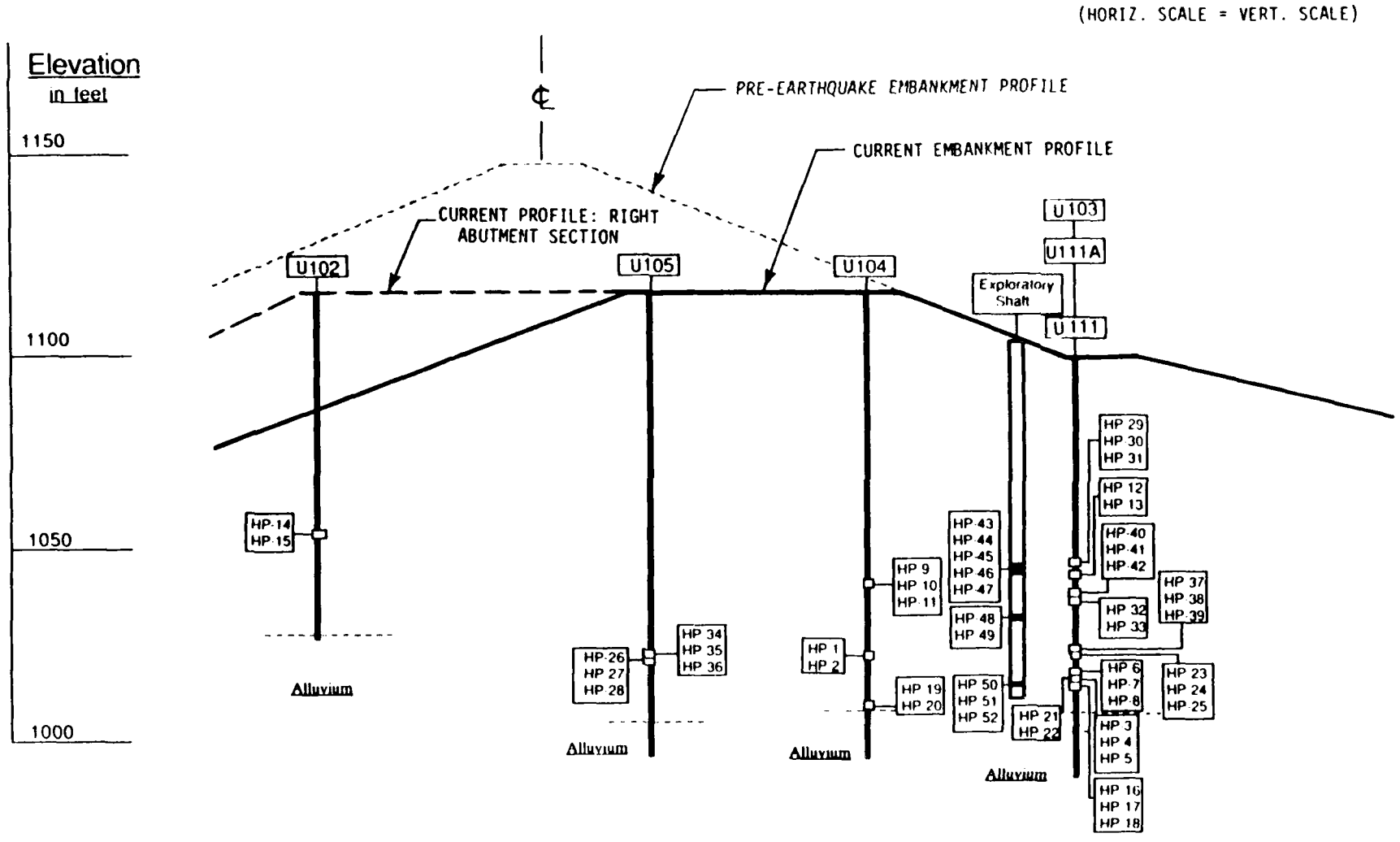

Fig. 6-1 CROSS-SECTIONAL PROJECTION OF EXPLORATORY TEST SHAFT AND CONVENTIONAL BOREHOLE SAMPLE LOCATIONS

Grain size distribution curves for these two materials are shown in Figs. 6-2 and 6-3 respectively. In order to determine the steady state lines for these two soils it was first necessary to perform steady-state strength tests on reconstituted samples of these materials. For this purpose 9 tests were performed on samples of Bulk Sample No. 3 (silty sand) prepared by moist tamping to different void ratios in the range of 0.55 to 0.8. Similarly 11 tests were performed on samples of Bulk Sample No. 7 (sandy silt), eight of the samples being prepared by moist tamping and three of the samples by wet pluviation. There was no significant difference in the results of the tests for the two different methods of sample preparation.

Test Results

The results of the steady-state strength tests performed on soil from Bulk Samples Nos. 3 and 7 are shown in Figs. 6-4 and 6-5 respectively. The steady-state lines for these two materials are shown in the figures. It may be noted that the position of the line for Bulk Sample No. 7 is almost identical with that determined in the test program performed by GEI indicating very good reproducibility of the results.

Grain size distribution curves for all of the undisturbed samples subjected to steady-state strength tests are shown in Fig. 6-6. It may be seen that they fall generally into two groups: (a) Samples with fines contents ranging from about 45% to 85%. These samples were classified as sandy silt for the purposes of this investigation and the slope of their steady state line was assumed to be parallel to that of Bulk Sample No. 7. (b) Samples with fines contents less than about 25%. These samples were classified as silty sand and the slope of their steady state line was assumed to be parallel to that for Bulk Sample No. 3. The grain size distribution curves for Bulk Samples Nos. 3 and 7 are also shown on Fig. 6-6 for comparison purposes.

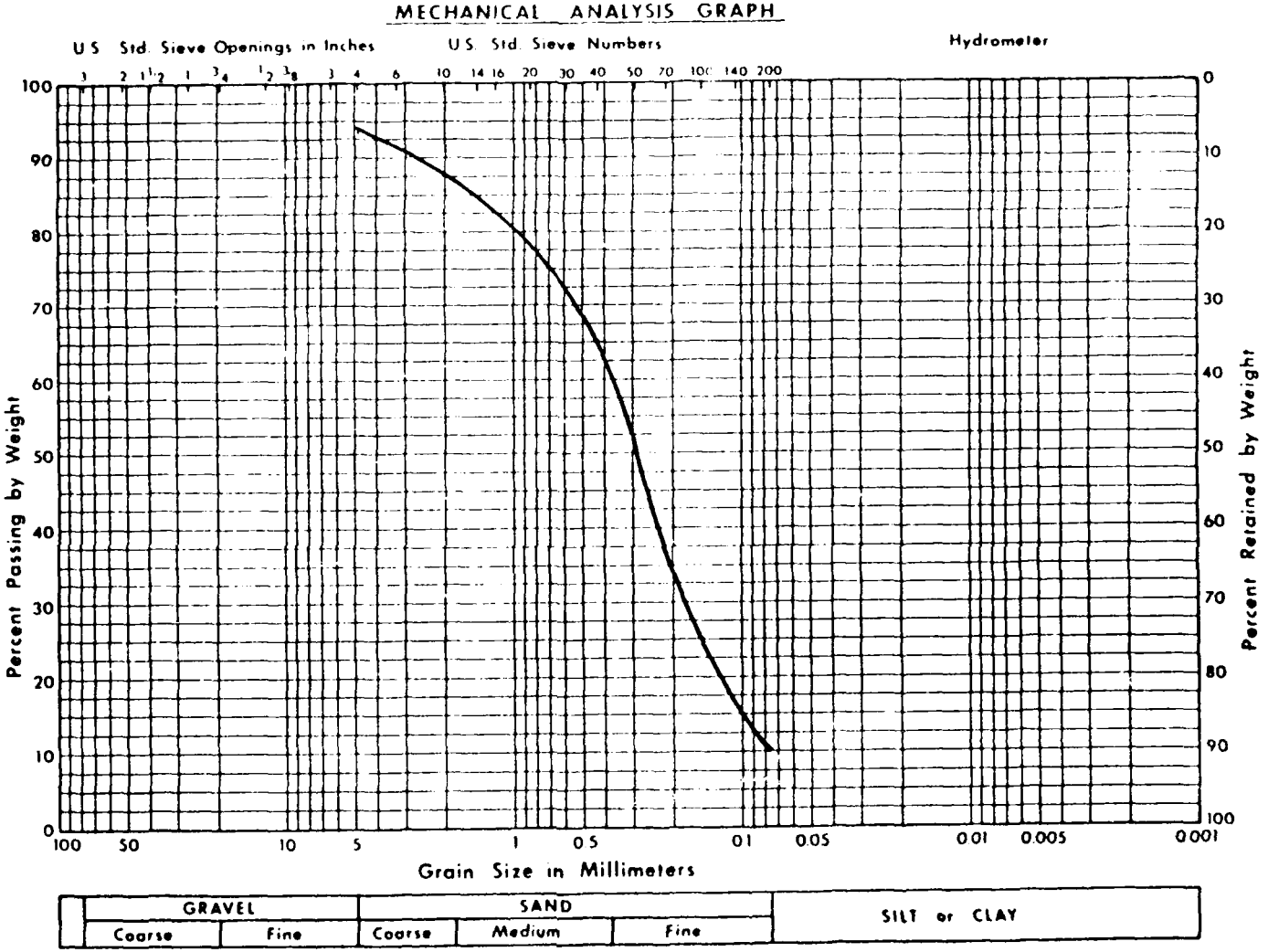

Fig. 6-2 GRAIN-SIZE DISTRIBUTION FOR BULK SAMPLE NO. 3

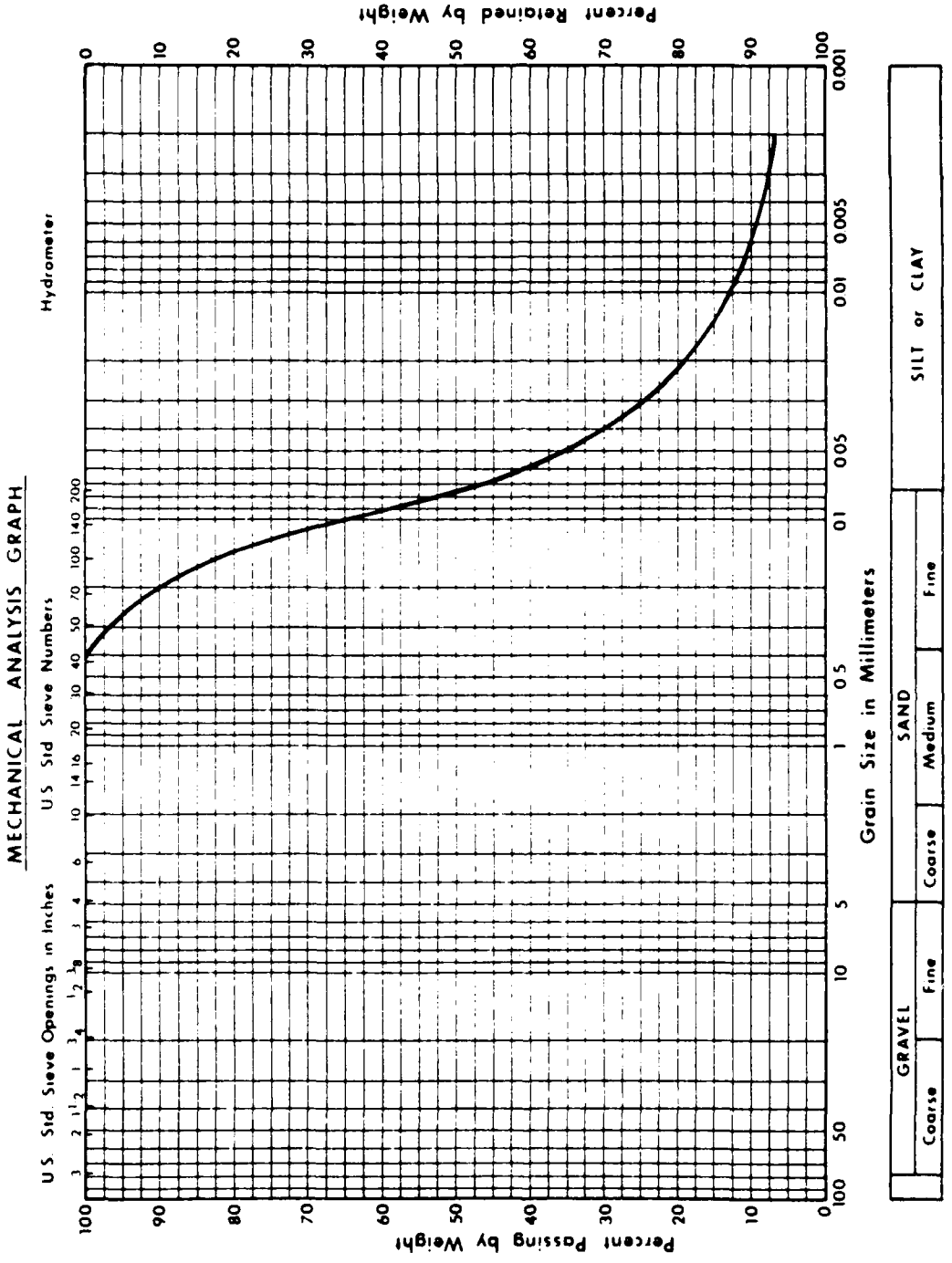

Fig. 6-3 GRAIN-SIZE DISTRIBUTION FOR BULK SAMPLE NO. 7

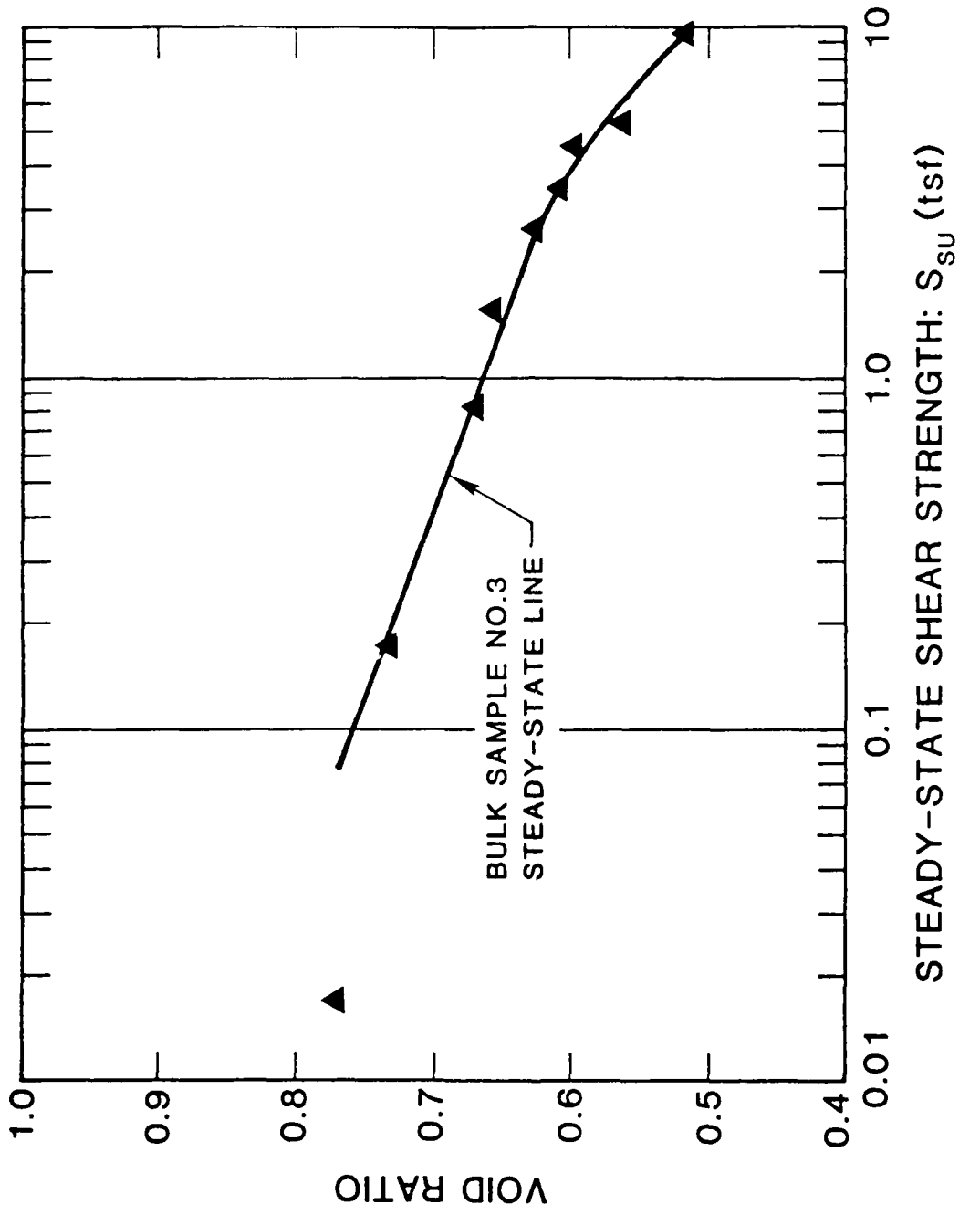

Fig. 6-4 STEADY STATE LINE FOR BULK SAMPLE NO. 3 (SILTY SAND)

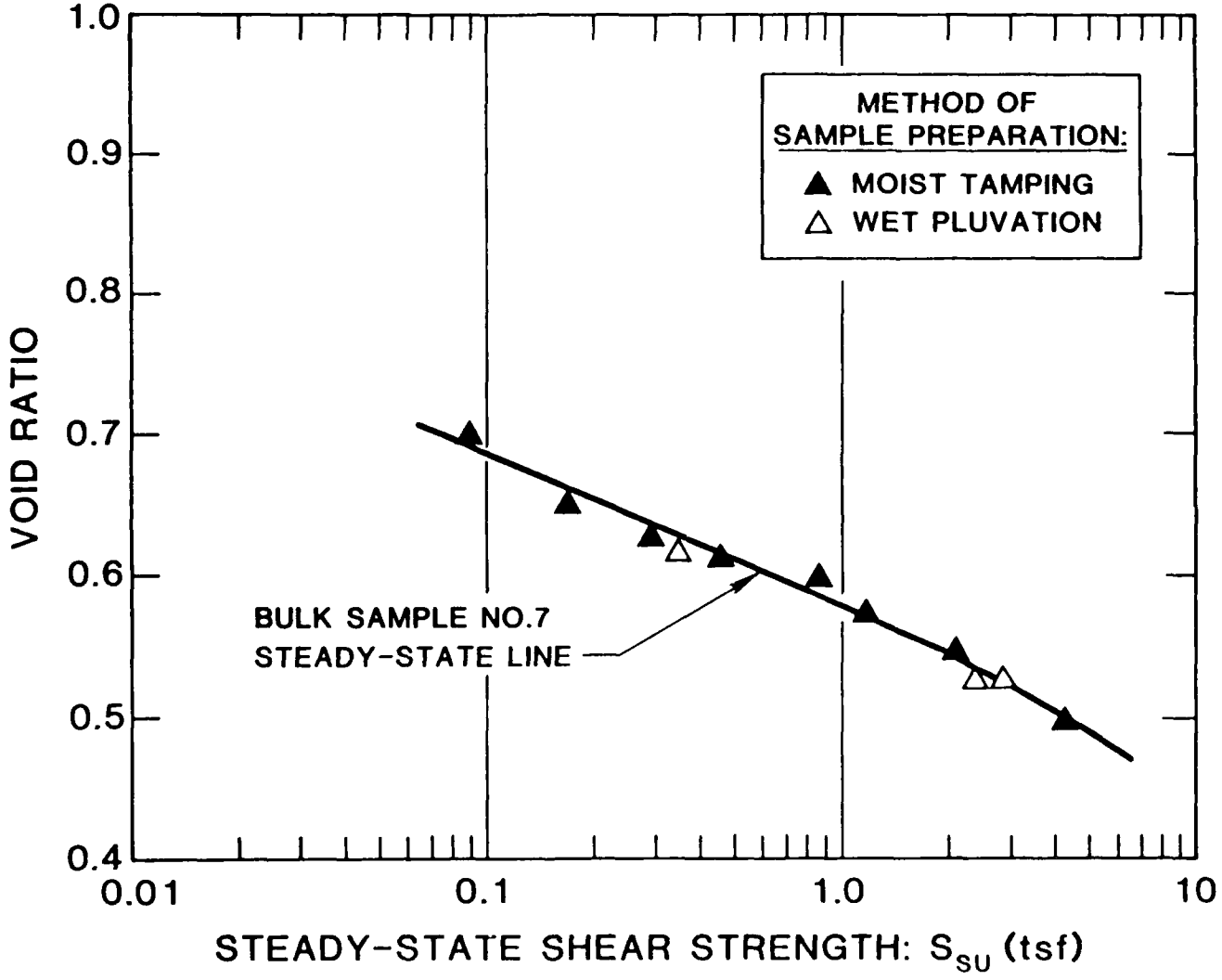

Fig. 6-5 STEADY STATE LINE FOR BULK SAMPLE NO. 7 (SANDY SILT)

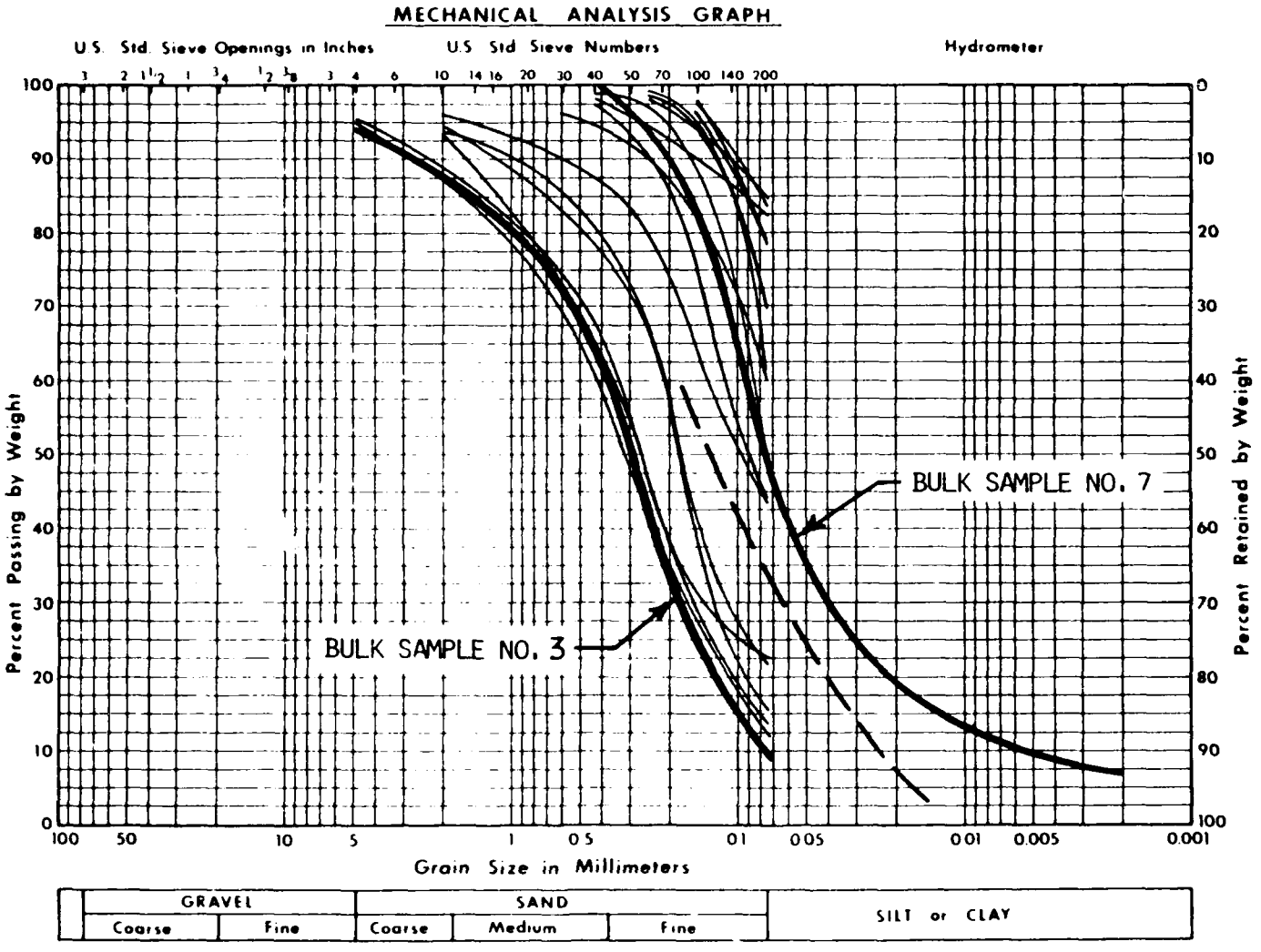

Fig. 6-6 GRAIN SIZE DISTRIBUTION CURVES FOR UNDISTURBED SAMPLES SUBJECTED TO IC-$\bar{U}$ TRIAXIAL TESTS

The results of the steady-state strength tests on the undisturbed samples of sandy silt are shown in Fig. 6-7. For each sample the steady-state strength is shown for four different void ratios:

1. The void ratio at the time of testing in the laboratory
2. The void ratio after the sample was recovered from the ground
3. The void ratio corresponding to the in-situ condition of the sample

and 4. The void ratio the sample would have had in the ground before the 1971 earthquake if the void ratio change occurring after the start of the earthquake and prior to sampling in 1985 had been 0.020.

In all cases these void ratios could be determined from the changes in volume of the samples in the sampling and handling processes as described in the Appendix. The steady state lines for all samples were assumed to be parallel to that for Bulk Sample No. 7 as shown in Fig. 6-7. In this way the pre-earthquake in-situ steady state strengths for the sandy silt samples could be determined. The results for the void ratios at different stages of the sampling and handling process are shown in Fig. 6-7. It should be noted that the test data for samples of sandy silt taken from the Test Shaft have been corrected for heave at the base of the shaft, following the procedures described by GEI (Castro and Keller, 1987) in addition to the void ratio changes described in the Appendix.

Similar results for the undisturbed samples of silty sand are shown in Fig. 6-8, the steady state lines for these samples being assumed to be parallel to that for Bulk Sample No. 3 as shown in the figure.

A summary of the steady-state strengths determined in this way for the samples of sandy silt is presented in Table 6-1 and a similar summary for the the samples of silty sand is presented in Table 6-2.

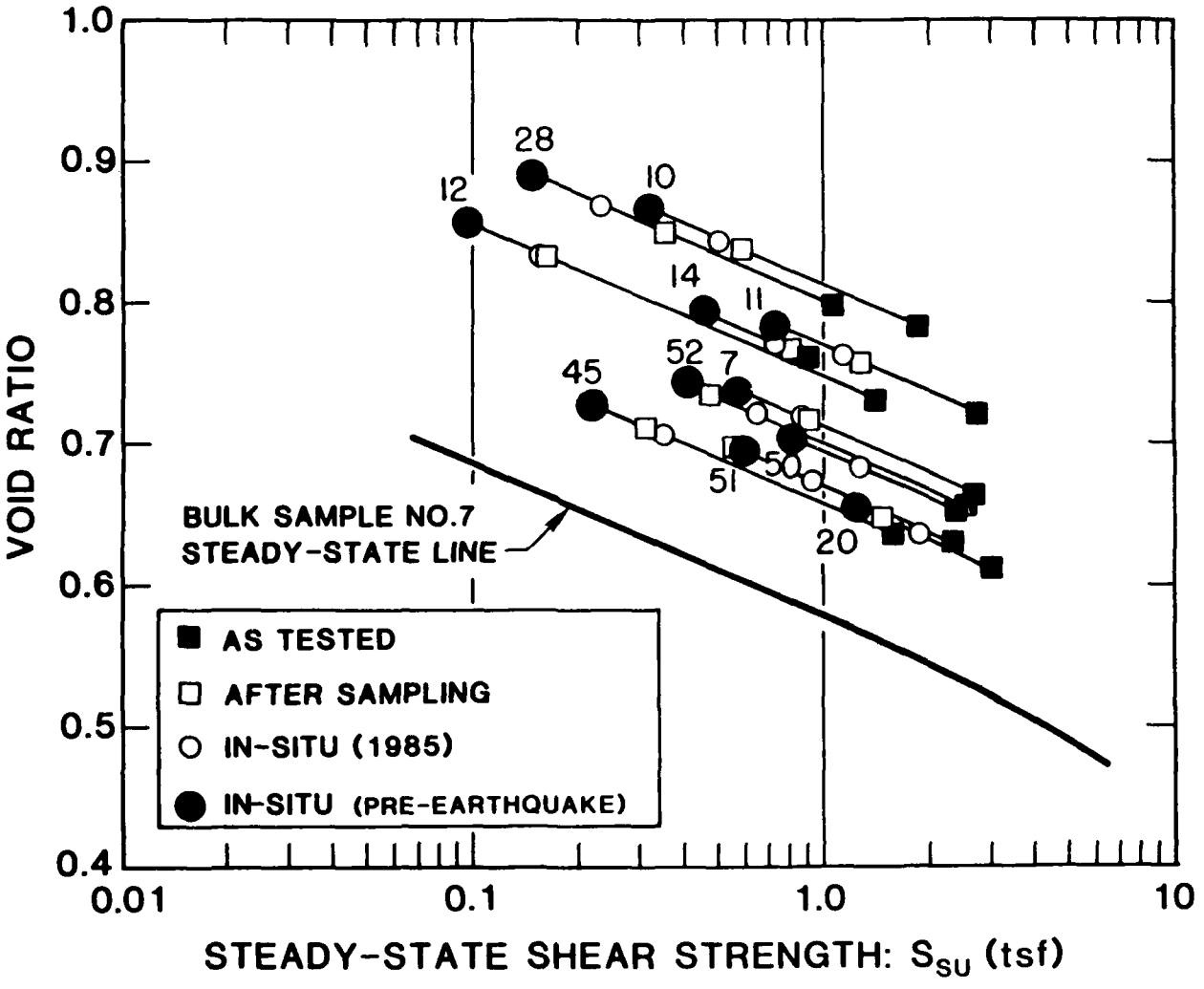

Fig. 6-7 STEADY STATE STRENGTH DATA FOR UNDISTURBED SAMPLES OF SANDY SILT

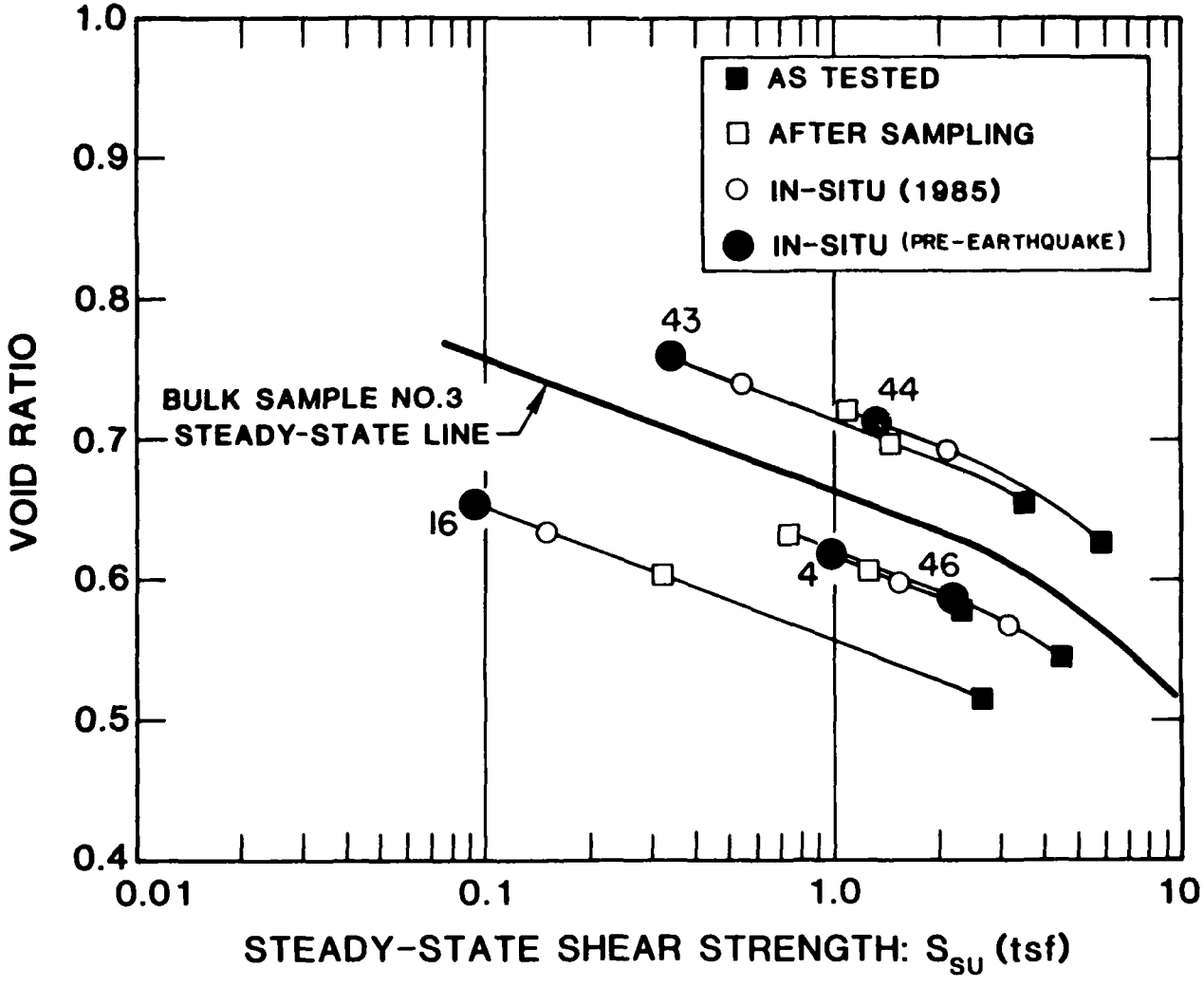

Fig. 6-8 STEADY STATE STRENGTH DATA FOR UNDISTURBED SAMPLES OF SILTY SAND

TABLE 6-1 SUMMARY OF ESTIMATED STEADY-STATE STRENGTHS FOR SILT SAMPLES

Sample No.	Source	Elev. (ft)	Percent Fines	Pre-earthquake* Void Ratio	S_{us} (psf)	S_{us} (tsf)
7	U-111	1017	70	0.738	1140	0.57
10	U-104	1040	85	0.863	630	0.31
11	U-104	1039	78	0.783	1470	0.74
12	U-111	1041	78	0.856	190	0.09
14	U-102	1054	84	0.792	920	0.46
20	U-104	1008	61	0.655	(2500)**	(1.25)**
28	U-105	1019	43	0.890	370	0.15
45	TS	1042	84	0.729	440	0.22
50	TS	1013	51	0.705	1600	0.80
51	TS	1013	44	0.694	1160	0.58
52	TS	1012	61	0.743	800	0.40
				Average =	880 psf	0.44 tsf

TABLE 6-2 SUMMARY OF ESTIMATED STEADY STATE STRENGTHS FOR SAND SAMPLES

Sample No.	Source	Elev. (ft)	Percent Fines	Pre-earthquake* Void Ratio	S_{us} (psf)	S_{us} (tsf)
4	U-111A	1013	22	0.620	2000	1.00
16	U-111	1017	15	0.890	200	0.10
43	TS	1044	21	0.758	680	0.34
44	TS	1044	16	0.712	2600	1.30
46	TS	1042	4	0.587	(4500)**	(2.25)**
				Average =	1380 psf	0.69 tsf

* Assuming change in void ratio in interval from just before earthquake in 1971 to time of sampling in 1985 is about $\Delta e = 0.020$.

**Sample not included in strength averages.

Discussion of Results

It may be seen from Table 6-1 that the estimated values of steady-state strength for the samples of sandy silt in their pre-earthquake condition range from about 200 to 1600 psf, with an average value of 880 psf. There does not appear to be any significant difference between the results of tests performed on samples from the test shaft and samples obtained from the undisturbed sample borings.

Table 6-2 shows the estimated values of steady-state strength for the samples of silty sand; again samples taken from the test shaft have been corrected for the effects of heave at the base of the shaft in addition to the changes described in the Appendix to this report. However swelling for these samples was considered to be only one half of that occurring in the sandy silt. It may be seen that values of steady-state strength range from about 200 psf to over 4900 psf, with an average value (excluding Sample No. 46 since it appears to represent an isolated condition) of about 1380 psf.

It is not clear how these results should be interpreted to determine a representative value for the soils in the zone of liquefaction in the upstream shell of the Lower San Fernando Dam. The soils which liquefied in the main slide area were considered at the time of the field studies of the slide to be mainly silty sands but it would seem, from the 1985 investigation, that they must have included considerable quantities of sandy silts. A review of photographs of the liquefied soils in the slide area shows that liquefaction and loss of strength clearly occurred in a variety of soil types including clean sands, some coarse sand, and silty sand, and that it was not limited to sandy silt. Such soils were evident in the failure zone and in samples taken from this zone. Under these conditions it does not seem reasonable to base an evaluation of the post-earthquake strength of the soil in the liquefied zone

on the results of tests on a single material. Viewed from this perspective, selection of a representative post-earthquake strength for the material in the liquefied zone of the upstream shell, from the available data, presents significant problems. The problems are compounded by the variability of the test results and the very limited number of samples on which tests could be performed.

If the average value determined for all samples tested in this study is taken as representative, then based on tests on 14 samples (excluding Samples Nos. 20 and 46) it would be about 1020 psf. On the other hand, if the average values for sandy silt and silty sand are given equal weight, the representative average value would be about 1130 psf. Alternatively if the sandy silt near the base of the embankment near Boring S111 is considered representative, the average steady-state strength would be 880 psf. In view of the variability of the soils and the extensive zone over which failure occurred (about 1100 ft along the embankment), it is not clear how a representative value can be determined from the data available. Based on the data, however, it seems reasonable to select a value of the order of 1000 psf for the steady-state strength of the hydraulic fill near the base of the downstream shell of the embankment.

It is interesting to note that the average steady-state strength for 15 samples of silt tested by GEI and corrected for post-earthquake void ratio changes in the same manner as that used in this investigation leads to an average value for steady strength of this soil, on the downstream side of the embankment, of about 1100 psf. This is in remarkably good agreement with the values discussed above. Averaging the results from the two laboratory programs results in a mean value of approximately 1050 psf.

7. Properties of Hydraulic Fill Near the Base of the Upstream Shell of the Embankment

In the preceding sections of this report, emphasis has been placed on determining the properties of the hydraulic fill near the base of the downstream shell of the embankment in the condition existing prior to the 1971 San Fernando earthquake. Since the slide occurred in the upstream shell of the embankment, however, it is necessary to question whether the properties of the hydraulic fill were the same on both sides of the embankment.

Castro and Keller (1987) have suggested that this was probably not the case for two reasons:

1. The placement of the stabilizing berm on the outside of the downstream shell in 1940 induced some compressive stress and thus some additional degree of densification of the hydraulic fill on the downstream side of the embankment.

and 2. The presence of water in the reservoir would necessarily cause the effective vertical stresses on the hydraulic fill in the upstream shell to be lower than those in the downstream shell, thereby leading to a somewhat less dense condition for the soil in the upstream shell. This would depend to some extent on whether the upstream shell ever existed, after construction was completed, with little or no water in the reservoir thus permitting the sand to compress under the full weight of the fill. Unfortunately this early history of the reservoir is not known and thus this question cannot be resolved definitively.

Never-the-less Castro and Keller (1987) have estimated that taking into account both of these considerations, the void ratio of hydraulic fill on the upstream side of the embankment may be as much as 0.011 higher than that of

corresponding hydraulic fill near the base of the downstream side of the embankment. This is a rather significant difference and it would cause corresponding changes in the penetration resistance, the cyclic loading resistance and particularly the steady state strength values of the hydraulic fill. Estimated values of these characteristics taking this change in void ratio into account are as follows:

(1) Penetration Resistance

It was shown in Section 4 of this report that a change in void ratio of the hydraulic fill of 0.020 would lead to a change in penetration resistance of the hydraulic fill of about 2 blows/ft. Following a similar line of reasoning, it may be shown that a void ratio change of 0.011 would lead to a change in penetration resistance of about 1 blow/ft. Thus the standard penetration resistance of the hydraulic fill near the base of the upstream shell of the embankment before the earthquake of 1971 can be expected to have had an average value of $(N_1)_{60} \approx 11.5$. The corresponding equivalent clean sand value of $(N_1)_{60}$ is about 13.5.

(2) Cyclic Loading Resistance

On the basis of the results presented in Section 5 of this report, it is found that a change in void ratio of 0.011 in the hydraulic fill could be expected to change the cyclic loading resistance of the hydraulic fill by about 4%. The estimated cyclic loading resistance of the hydraulic fill near the base of the upstream shell prior to the 1971 earthquake, obtained by reducing the values shown in Figs. 5-4 and 5-8 by 4% is shown in Fig. 7-1.

Also shown in Fig. 7-1 is the cyclic loading resistance of the hydraulic fill determined from the empirical correlation shown in Fig. 5-7, corresponding to soil with a value of $(N_1)_{60} \approx 11.5$ and a fines content of 25 to 30%. It may be seen that the cyclic loading resistance is about the same whether it

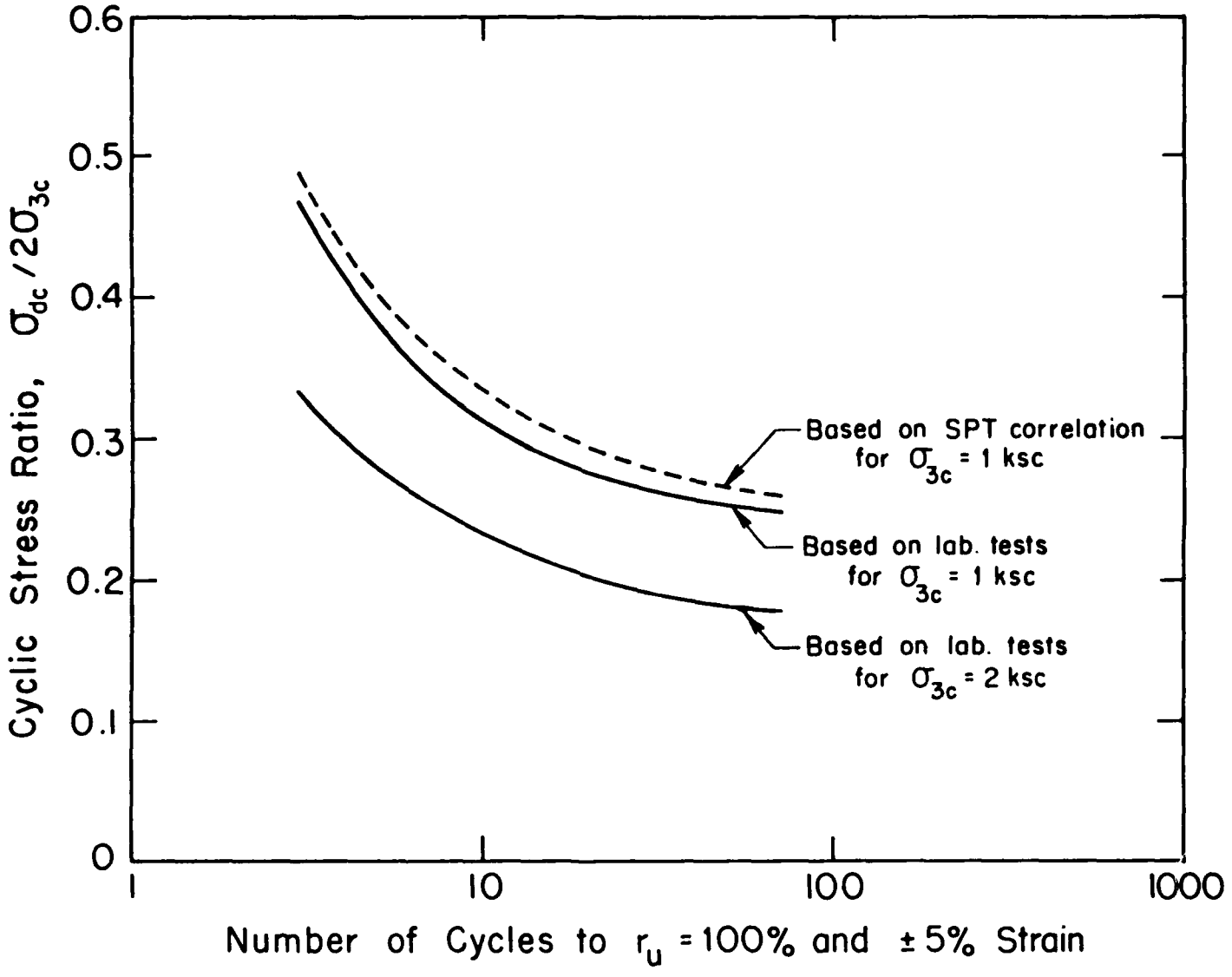

Fig. 7-1 COMPARISON OF ESTIMATED CYCLIC LOADING RESISTANCE CURVES FOR SAND NEAR BASE OF UPSTREAM SHELL OF LOWER SAN FERNANDO DAM

is determined by laboratory tests or by the correlation based on SPT data. Furthermore both procedures lead to values of cyclic loading resistance within a few percent of the values used for analysis of the seismic stability of the embankment in 1973 (Seed et al., 1973).

(3) Steady-State Strength

Steady-state strength values for the samples tested in this investigation, corrected for an additional increase in void ratio of 0.011, can readily be read off from the data presented in Figs. 6-7 and 6-8. The additional values of S_{us} determined from the steady-state strength test data in this way lead to the following values for the hydraulic fill near the base of the upstream shell:

Average of 10 samples of silt	= 640 psf
Average of 4 samples of silty sand	= 1020 psf
Average of 14 samples of silt and silty sand	= 750 psf.

For comparison purposes it may be noted that the average steady-state strength for 15 samples of silt tested by GEI and corrected for the same change in void ratio is 860 psf. The overall average for 29 samples tested in both studies is thus about 800 psf.

A more conservative interpretation of the steady-state strength test data, say by choosing 35-percentile values leads to the following values:

35-percentile value for 14 samples of silt and silty sand tested in this investigation	≈ 475 psf
35-percentile value for 15 samples of silt tested by GEI	≈ 680 psf.

The overall 35 percentile value for 29 samples tested in both studies is thus about 580 psf.

8. Practical Significance of Test Data

The main purposes of this study were:

1. To determine whether the steady-state testing procedure would provide values of post-earthquake strength for the liquefied soil in the Lower San Fernando Dam in reasonable agreement with those determined from back-analysis of the failure conditions.
2. To determine whether the results of steady-state tests performed in different laboratories would be in reasonable agreement.
3. To determine whether the cyclic loading resistance of the soils in the hydraulic fill of the Lower San Fernando Dam used in previous analyses of seismic stability were significantly affected by sample disturbance.
4. To explore how the cyclic loading resistance of undisturbed samples of the hydraulic fill material determined by laboratory tests compared with that determined from correlations between cyclic loading resistance and SPT values of $(N_1)_{60}$.

and 5. To determine whether the residual strength of the hydraulic fill in the failure zone of the San Fernando Dam could be anticipated based on correlations of values of residual strength determined from studies of other liquefaction-type failures and SPT $(N_1)_{60}$ values.

The results obtained in this study provide answers to most of these questions as discussed below. For ease of reference, the properties of the hydraulic fill determined in the preceding sections of this report are summarized in Table 8-1.

TABLE 8-1 SUMMARY OF STRENGTH PARAMETERS FOR LOWER SAN FERNANDO DAM HYDRAULIC FILL

Strength Parameter	Base of Upstream Hydraulic Fill Zone	Base of Downstream Hydraulic Fill Zone
Pre-Earthquake Average In Situ SPT $(N_1)_{60}$ (blows/foot)	≈ 11.5	≈ 12.5
Pre-Earthquake Average Clean Sand SPT $[(N_1)_{60}]_{CS}$ (blows/foot)	≈ 13.5	≈ 14.5
Pre-Earthquake Average Cyclic Stress Ratio Causing $r_u \approx 100\%$ in 15 Cycles in Isotropically Consolidated Cyclic Triaxial Tests with $\sigma_{3c} = 1$ ksc	≈ 0.31	≈ 0.33
Pre-Earthquake Average Steady-State Strength	≈ 800 psf	≈ 1050 psf
Pre-Earthquake 35th percentile Steady-State Strength	≈ 580 psf	≈ 750 psf
Actual Residual Shear Strength Determined from Configuration When Slide Mass Stopped Moving (psf)	400 ± 100 psf	NOT APPLICABLE D/S Hydraulic Fill did not liquefy

(a) Steady-State Strength Determination

1. It can be concluded that the use of the steady-state testing approach, as proposed by Poulos et al. (1985) and applied in this study, is capable of predicting the onset of sliding in the upstream slope of the Lower San Fernando Dam. The approach used involves the assumption that the soil in the embankment would liquefy and a very conservative interpretation of a comprehensive set of test data. Never-the-less following these procedures it can generally be determined that the initial (pre-slide) static driving stress in the hydraulic fill would be about 800 to 900 psf and the average post-earthquake residual or steady-state strength of this material after liquefaction would be about 800 psf. Such results would indicate that sliding would be initiated in the upstream slope, and this is a significant accomplishment of this re-evaluation program. Also important is the fact that similar results can be obtained independently in different laboratories and they can all be interpreted to indicate strengths which will lead to prediction of the onset of a failure.

This conclusion becomes more definitive if the steady-state strength test data is interpreted more conservatively by adopting a 35-percentile value (i.e. about 580 psf) for comparison with the initial driving stress. However there seems to be no special reason to select such a value in this case unless it is to allow for unknown factors not included in the testing and data-interpretation procedures.

It should be noted, however, that the results of the steady-state testing program must be interpreted carefully and very

conservatively to arrive at these results. In fact the procedure followed in this investigation involves the following steps and assumptions:

1. Locate, by a careful investigation, what appears to be the weakest zone in the embankment profile.
2. Assume that the soil in this layer or zone exists over the entire base of a long embankment, even though it is unlikely to do so because:
   (a) Other soil types are known to exist near the base of the embankment
   and (b) There was apparently a dilatant zone of soil near the toe of the upstream shell, probably related to the construction of the starter dike for the hydraulic fill construction operations.
3. Perform a steadv-state testing program on many samples from the most critical layer or zone identified to determine a representative strength for the most critical material in the zone, even though the zone may also include other material types.
4. Allow conservatively for the fact that the soil in the upstream shell of the embankment may be weaker than that in the downstream shell even though there may be some uncertainty about this question.
and 5. Interpret the test results conservatively--say by using the 35-percentile value of steady state strength from the test data on the weakest soil type encountered, and assume that

this strength applies for other soils comprising the liquefied zone.

Many of these procedures and assumptions are reasonable and their use leads to good results in this significant case study. However presumably comparable levels of care and conservatism would be required in any other project where steady-state testing is to be used for design or analysis purposes. Despite these cautionary observations, however, the present study provides a good indication of the ability of the steady-state strength approach, with conservative data interpretation and conservative assumptions regarding likely field behavior mechanisms, to predict the onset of a sliding failure for the conditions existing after liquefaction occurred in the upstream shell of the Lower San Fernando Dam. This is a significant advancement in the use of laboratory test data for such a purpose.

2. Also of importance, however, is the fact that even with conservative data interpretation, the steady-state strength determined from the laboratory tests does not indicate the best estimates of the actual residual strength apparently achieved by the liquefied soil (about 300 to 500 psf) in the Lower San Fernando Dam. Based on the results presented in Section 1, the best-estimates of the average pre-earthquake, post-earthquake and post-slide stresses and strengths in the hydraulic sand fill near the base of the upstream shell, and their variations with time after the start of earthquake shaking to the end of sliding, are shown in Fig. 8-1. As the slide movements progressed, the average driving stress was gradually reduced and, since inertia effects were small, sliding would stop when the average

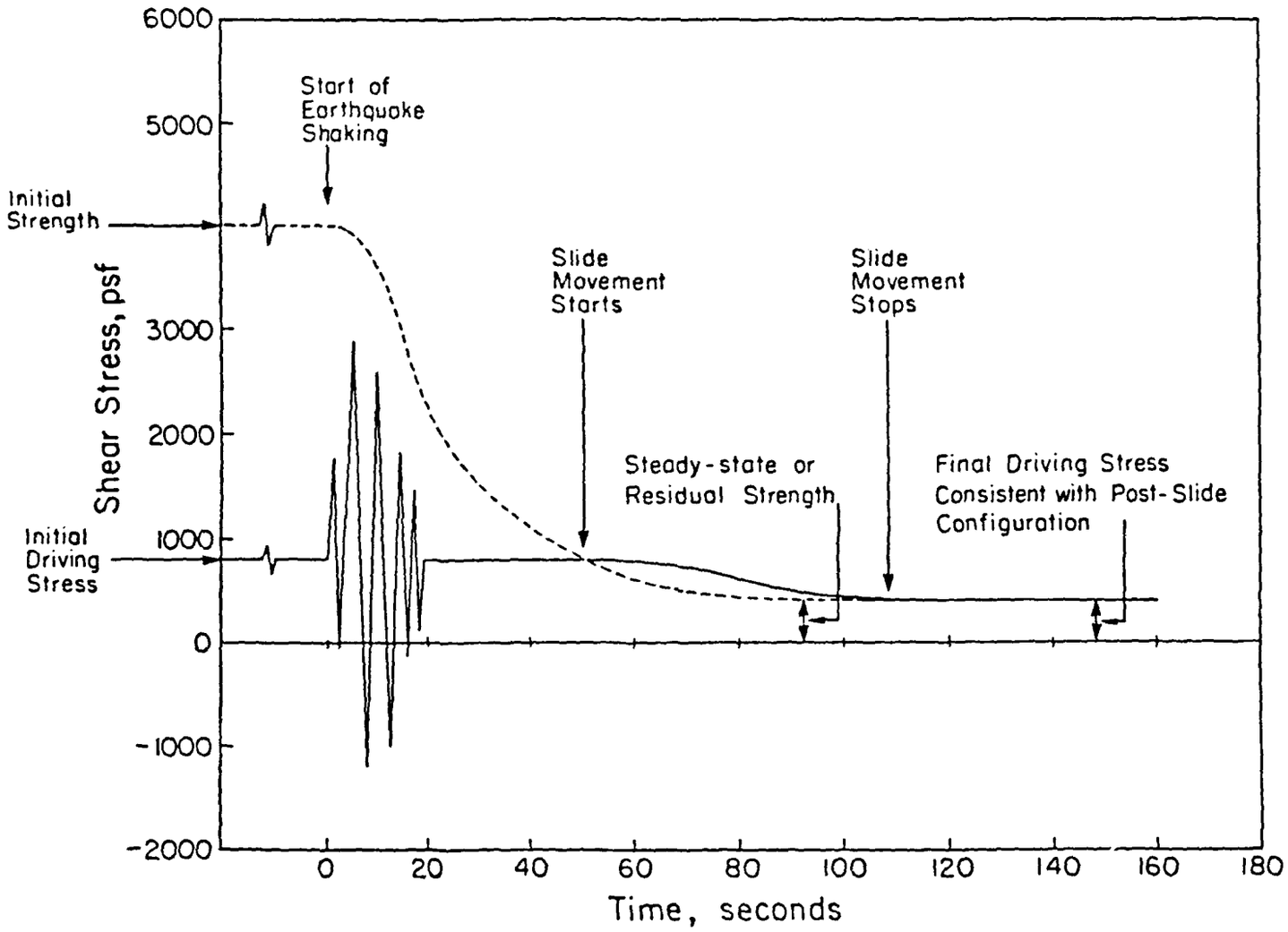

Fig. 8-1 ESTIMATED CHANGES IN AVERAGE DRIVING STRESS AND SHEAR RESISTANCE OF HYDRAULIC FILL NEAR BASE OF UPSTREAM SHELL AFTER START OF EARTHQUAKE UNTIL END OF SLIDE MOVEMENTS

driving stress became equal to the residual or steady-state strength of the liquefied sand. A comparison of the estimated range of residual strengths for the liquefied soil based on the configuration of the slide zone when the slide movements stopped (400 ± 100 psf as discussed in Section 1 of this report), and the probable average and 35-percentile values of steady state strength determined from the laboratory test program as indicated above is shown in Fig. 8-2. The range of values of steady-state strength determined from laboratory tests is significantly higher than the range of values of back-calculated residual strength, indicating that a more conservative interpretation of steady-state strength data than the use of a 35-percentile value may well be required to determine the actual residual or steady-state strength of liquefied soils.

The steady state strength values determined in this study are also significantly lower than those obtained for comparable materials in a number of other studies (Von Thun, 1986), further indicating the care required to assure the determination of representative values.

3. Possibly the main reason why it is necessary to interpret the test data conservatively, rather than simply taking the average value of steady state strength from a range of soil types as would seem appropriate for a failure investigation, is that the interpretation of the test results does not include any allowance for the possible effects of water content or void ratio redistribution which may well occur in the field during an earthquake. Arthur Casagrande discussed this possibility at length in his later writings on soil liquefaction. In fact in his Carillo Lecture, the text of which was published in 1984, he stated:

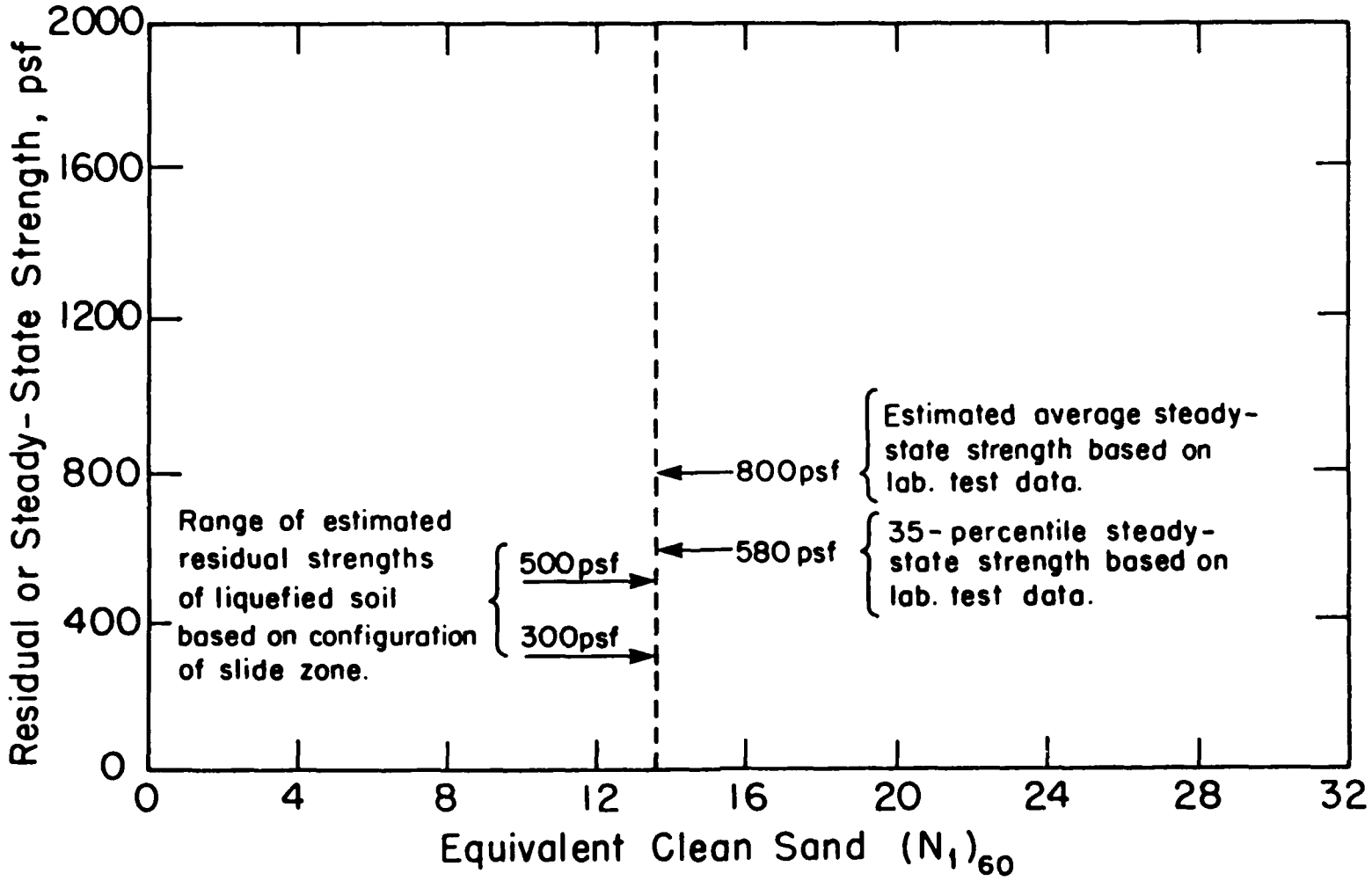

Fig. 8-2 COMPARISON OF STEADY-STATE STRENGTHS AND RESIDUAL STRENGTHS DETERMINED FROM FIELD CONDITIONS

> "The question that will arise is: If we have in the ground a large mass of the same sand material with an initial relative density of 40 or 41 percent, can the material actually liquefy? Can such a redistribution of water content occur, or is this redistribution a boundary effect that occurs in (test) specimens and depends even on the shape of the specimens?....I believe that many have tried to answer these questions by laboratory tests. We should do more in the field--investigate sand deposits in areas that are subject to frequent earthquakes and determine on an empirical basis which relative density can liquefy and which can-not liquefy. At the moment I do not have the answer to this problem."

More recently the possibility of water content redistribution has been discussed by Seed (1986,1987), Whitman (1985), and the report of the NRC Committee on Earthquake Engineering (1986). Model test data from China indicates that this phenomenon does occur in stratified sands and more recently, Arulanandan et al. (1989) have presented centrifuge model test data to show that it occurs in sands in layered deposits and Gilbert (1984) has shown that it occurs in undrained laboratory triaxial tests. To circumvent the problem, Seed (1986, 1987) developed an empirical correlation between the residual strength of liquefied sands and silty sands and the SPT blow count, as Casagrande had suggested.

The fact that this phenomenon may well occur both in the field and in the laboratory does not in any way invalidate the basic concepts of the steady state approach. It simply puts an additional obstacle in the path of determining an appropriate strength using this method. Since the tests do not include water content redistri

bution effects, it is necessary to allow for these effects by extrapolating the laboratory test data to somewhat higher void ratios than those existing in the field at the start of the earthquake so that the strength of the loosened sand zones can be determined. The problem is that we do not currently know how to determine these higher void ratios; but certainly a conservative interpretation of the test data is a step in the right direction. The alternative, which may seem preferable to many engineers, is to accept the fact that field case histories have this factor incorporated directly in the field performance to the extent that it actually occurs in nature, and thus determinations of residual strength from studies of liquefaction-type failures allow for the effects of the phenomenon in the field.

This seems to be a more practical approach than the inclusion of an arbitrary amount of conservatism in the interpretation of steady-state test data. It is also significantly less expensive, since penetration test data will inevitably be required in any case.

4. It may be noted that the overall average value of steady-state strength determined in this special study of the soils near the base of the upstream shell of the Lower San Fernando Dam (about 800 psf) is in reasonable accord with the values of residual strength indicated by other case studies of the residual strength of liquefied sands and silty sands, when the effects of variations in relative density, as measured by penetration resistance, are taken into account (see Fig. 8-3). This is not always the case (see data summarized by Von Thun, 1986) and thus a comparison of laboratory-determined values of residual or steady-state strength with values determined from case studies would seem to be necessary in all cases,

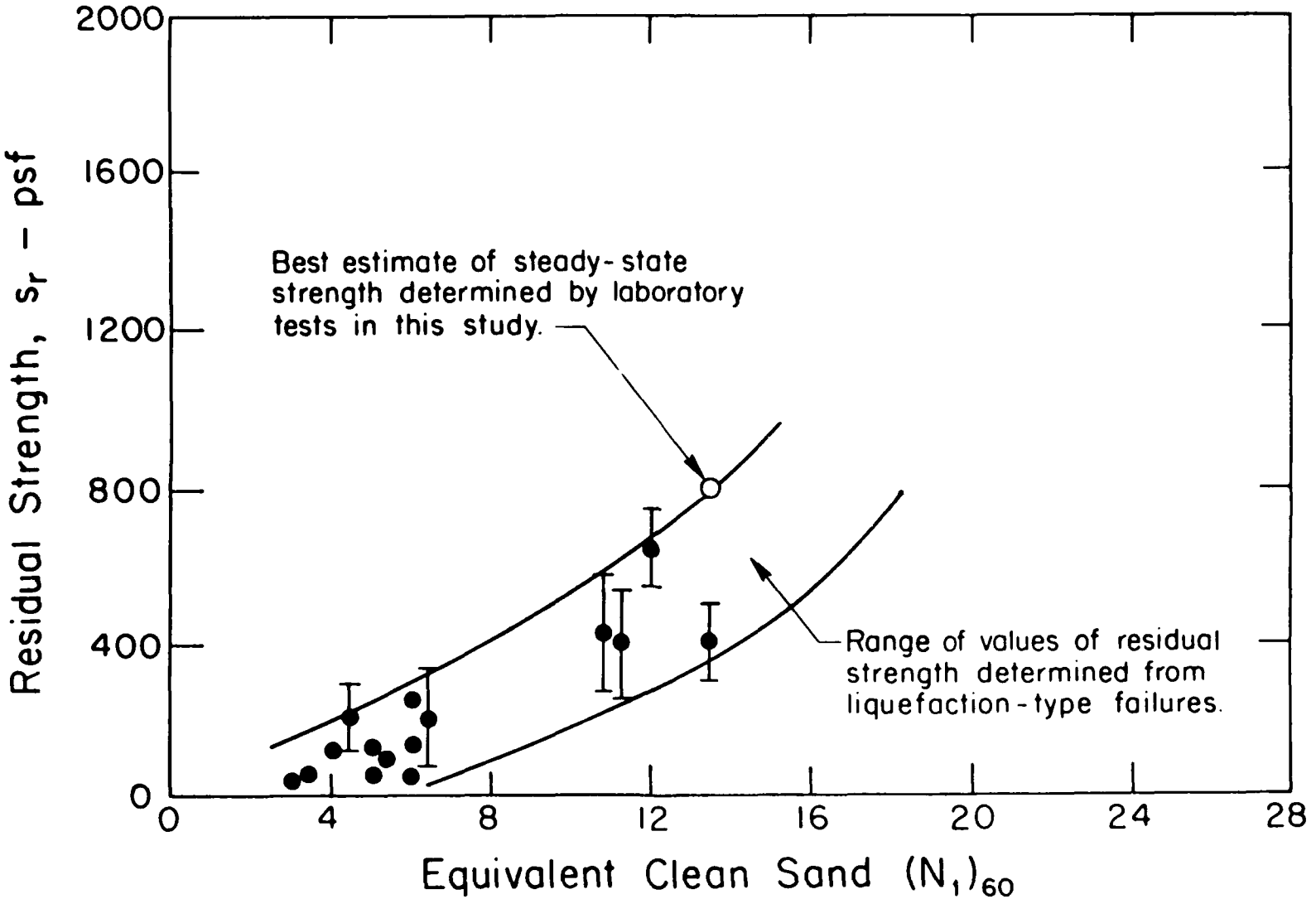

Fig. 8-3 COMPARISON BETWEEN VALUES OF RESIDUAL STRENGTH AND STEADY-STATE STRENGTH DETERMINED IN THIS STUDY

pending further studies and the development of appropriate bases for the use of laboratory test data for design and evaluation purposes.

5. Finally, it should be noted that field evidence indicates no significant degree of pore-pressure generation occurring in the downstream shell of the Lower San Fernando Dam during the earthquake shaking of 1971, and extensive sampling following the 1971 earthquake showed no evidence of soil liquefaction in this zone, with the exception of one sample taken from the upper layers of hydraulic fill near the core of the embankment. In the absence of liquefaction in the downstream shell it is not possible to judge the applicability of steady-state theory, which applies only when liquefaction occurs, to the conditions in the downstream shell of the embankment in this earthquake.

(b) Determinations of Cyclic Loading Resistance

1. The results of cyclic load tests performed on samples of silty sand and sandy silt obtained from the 1985 field investigation program are very similar (within a few percent) to those obtained in the 1971 study for samples which are tested under isotropic consolidation conditions and reach a condition of $r_u \approx 100\%$ and $\pm 5\%$ strain in numbers of cycles less than about 10.

2. The laboratory cyclic load test data for conditions producing a pore pressure ratio of 100% in isotropically-consolidated samples are also in good accord with values determined from the standard penetration test results and existing correlations between $(N_1)_{60}$ values and cyclic loading resistance based on field performance of level sites. This agreement is obtained despite the fact that the samples tested were probably about 10 to 15% higher in relative density at the time

of testing than for the field condition at the time of the earthquake. A correction to the data could be made for this relative density change, but it is apparently unnecessary because of compensating effects on the test specimens resulting from the disturbance and densification of loose to medium dense sands in the sampling process.

3. Because the cyclic loading resistance of the cohesionless soil in the hydraulic fill is essentially the same in the 1985 and 1971 investigations, it follows that the zones of liquefaction in the hydraulic fill, based on the 1985 studies, are about the same as those determined from the 1971 studies if the Seed-Lee-Idriss method of analysis is used to investigate the extent of this zone. The results of the earlier analyses are shown in Fig. 8-4. The predicted zone of liquefaction in the upstream shell is in good general accord with that determined from field investigations of the mechanism of sliding.

   Field evidence indicates no significant degree of pore pressure generation occurring in the hydraulic fill in the downstream shell of the Lower San Fernando dam due to earthquake shaking in 1971, and extensive sampling following the earthquake in 1971 showed no evidence of soil liquefaction in this zone with the exception of one sample taken from the embankment in the upper layers of hydraulic fill near the core of the embankment. Piezometer readings in the downstream shell following the 1971 earthquake show no evidence that a condition of liquefaction was even close to being triggered by the shaking. The general absence of significant pore-pressure generation in the downstream shell is also in accord with the analytical results shown in Fig. 8-4. However a limited degree of pore pressure build-up was observed to have occurred both in the downstream shell and in

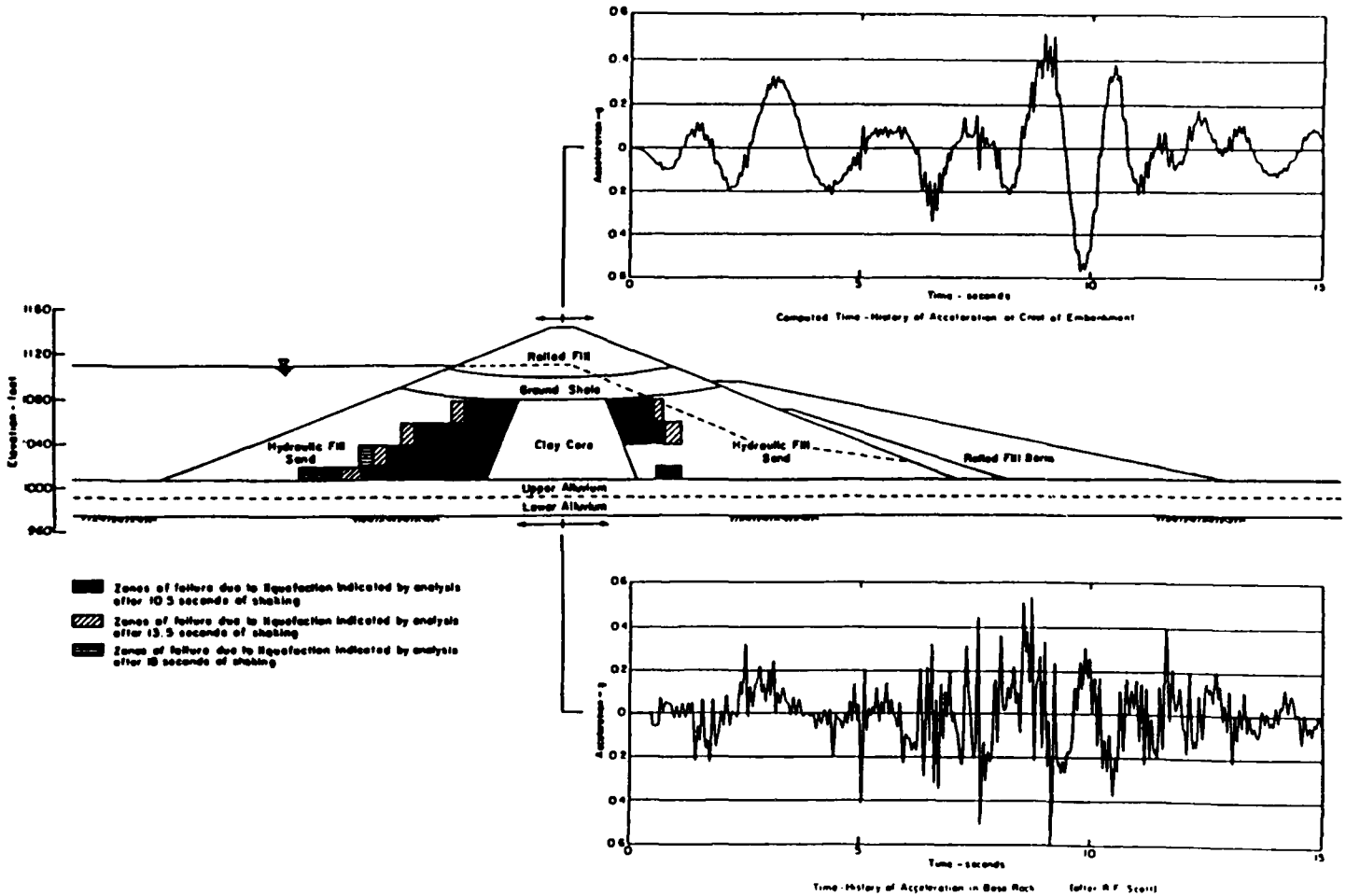

Fig. 8-4 ANALYSIS OF RESPONSE OF LOWER DAM DURING SAN FERNANDO EARTHQUAKE TO BASE MOTIONS DETERMINED FROM SEISMOSCOPE RECORD

the foundation soils, and this presumably corresponds to some of the settlements observed in the downstream slope since the 1971 earthquake.

4. The cyclic loading resistance of the hydraulic fill, either determined by the laboratory studies in the 1973 or 1985 investigations, or on the basis of the empirical correlation between cyclic loading resistance and standard penetration test data (Seed et al. 1983, 1985; Seed, 1981), used in association with the Seed-Lee-Idriss procedure for evaluating the seismic stability of embankments, also leads to the conclusion that there would be no large pore pressure build-up leading to the onset of sliding in the Lower San Fernando Dam if the Magnitude 6.6 earthquake in 1971 had produced motions at the dam-site having a maximum acceleration of about 0.2g. This is an important result because many hydraulic fill dams have withstood earthquake shaking with maximum accelerations up to about 0.2g in other earthquakes (Seed, 1984) and three hydraulic fill dams (Silver Lake, Fairmont and Lower Franklin dams) located in the Los Angeles area survived the 1971 San Fernando earthquake with no apparent damage despite the fact that the earthquake caused ground shaking with a maximum acceleration of about 0.2g at all three dam-sites.

It is also in reasonable accord with the known performance of the Lower San Fernando Dam in previous earthquakes to which it had been subjected. A review of earthquake shaking levels in the San Fernando area since the Lower dam was constructed in 1915-1916 up to the time of the earthquake in 1971 shows that the maximum level of earthquake shaking to which the Lower dam had been subjected prior to 1971 was that resulting from the 1952 Kern County earthquake

(Magnitude 7.6). Based on records obtained at stations in the vicinity of San Fernando, the 1952 earthquake probably produced a maximum acceleration of about 0.09g at the site of the Lower San Fernando dam. Two days after this earthquake a pore pressure increase of about 1 ft of water was observed in Observation Well No. 37, which has its tip in the foundation soils below the downstream rolled fill buttress. In comparison, this same well showed a pore pressure increase of about 5 ft of water about 1 day after the 1971 earthquake. Observation wells in the downstream hydraulic fill were not read until two weeks following the 1952 earthquake, at which time no increase in pore water pressure could be observed. In comparison, two weeks after the 1971 earthquake, one of these same wells (No. 16) showed a pore pressure increase of about 4 ft. These water pressure measurements indicate that the induced cyclic strains were significantly less during the 1952 earthquake than in the 1971 earthquake, suggesting that pore pressure increases in the upstream shell would also be correspondingly less and clearly insufficient to trigger liquefaction. This is also confirmed by the fact that there was no evidence of any type to indicate that the upstream shell of the embankment was even close to a failure condition in the 1952 event. This behavior helps to set a bound on the accelerations which would not cause a liquefaction-type failure in the upstream shell.

A ground motion with a peak acceleration of 0.09g in the 1952 Magnitude 7.6 earthquake would be equivalent in its damaging capability to a significantly higher level of peak ground acceleration developed in a Magnitude 6.6 event (which would have a shorter duration of shaking) such as that which occurred in 1971. Different

approaches may be used to determine the equivalent level of shaking. For example Bureau et al. (1985) have proposed the Earthquake Severity Index as a means of assessing the effects of earthquake shaking on embankment dams. The Earthquake Severity Index (ESI), which is intended to evaluate the combined effects of earthquake Magnitude and maximum ground accelerations, is defined by Bureau et al. as:

$$\text{Earthquake Severity Index} = a_{max} \cdot (M - 4.5)^3$$

Thus the ESI for the Lower San Fernando dam site in the 1952 earthquake was equal to $0.09g\ (7.6 - 4.5)^3 \approx 2.7g$. In a Magnitude 6.6 event the equivalent value of a_{max} required to produce the same severity of shaking would be:

$$(a_{max})_{equiv} = \frac{ESI}{(M - 4.5)^3} \approx \frac{2.7g}{(6.6 - 4.5)^3} \approx 0.3g.$$

Since there was no apparent damage to the dam in the 1952 event, it might be concluded from this result that the embankment would have safely withstood earthquake motions with a peak acceleration of about 0.3g in the 1971 San Fernando earthquake.

Alternatively if the incidence of liquefaction is due primarily to the effects of (a) the slightly higher spectral accelerations associated with M = 7.6 earthquakes as compared with M = 6.6 events and (b) the greater duration of shaking in M = 7.6 earthquakes as compared with M = 6.6 events, then the equivalent maximum acceleration for a Magnitude 6.6 would only be about 1.4 times that for a Magnitude 7.6 event, which would lead to an equivalent M = 6.6

acceleration, corresponding to the ground shaking in the 1952 earthquake, of only about 0.09g x 1.4 ≈ 0.13g.

In view of this range of values and the fact that the Lower dam showed no evidence of being even close to a failure condition in the 1952 earthquake, it seems reasonable to conclude that it would have safely withstood the 1971 San Fernando earthquake with no observable pore pressure changes in the downstream shell and no evidence of any significant strength loss in the upstream shell, if it had been further from the source and the maximum acceleration had been about 0.2g rather than the value of about 0.55g which actually occurred and led to the failure.

This same result is indicated by the analysis procedure. Thus the cyclic loading resistance of the hydraulic fill determined in both the 1973 and 1985 investigations, used in conjunction with the Seed-Lee-Idriss procedure for seismic stability evaluation, seems to provide satisfactory evaluations of the known performance of the Lower San Fernando Dam at both bounds for which failure or non-failure can be evaluated.

5. Because of the densification of samples in the sampling, handling, and testing process, it is unreasonable to expect that the residual or steady state strength measured on a sample, after it liquefies in a cyclic load test, could possibly be indicative of the residual or steady state strength of the soil in its field condition. To determine such a residual strength for the soil would require a major correction for void ratio changes and this is more easily accomplished by performing steady-state strength tests under static loading conditions as proposed by Poulos et al. (1985).

6. Although the residual strength of the silty sand in the Lower San Fernando Dam can not be determined directly by cyclic loading tests on undisturbed samples in the laboratory, it can be determined with a good degree of accuracy from a correlation of residual strength determined in other flow-failures with the SPT $(N_1)_{60}$ value of sands. Values determined in this way are in the range of 400 to 800 psf and, in conjunction with the indicated zones of liquefaction, they lead to the conclusion that a flow failure would occur in the Lower San Fernando Dam as a result of the 1971 earthquake shaking and that the soil could move through a distance of 150 to 200 ft as actually occurred.

7. Thus it follows that both the distribution of zones of liquefaction and the residual strength of the soil in these zones can be predicted with a satisfactory degree of accuracy from correlations of SPT values of $(N_1)_{60}$ with cyclic loading resistance and residual strength of sands, silty sands and sandy silts. This method of approach offers the practical advantage that representative values can be based on a larger number of data points which describe the non-homogeneity of the soils involved and permits a meaningful statistical analysis of this data for the determination of representative values. It also ensures that parameters selected for use in design and analysis are not inconsistent with those representative of a significant number of cases of failure and non-failure due to liquefaction under actual field conditions.

(c) <u>Post-liquefaction resistance of hydraulic fill determined from laboratory tests</u>

1. The only way to determine the post-liquefaction resistance of a sand or silty sand in its in-situ condition by means of laboratory tests

is to measure this resistance at the void ratio of the sample used in the test and then correct it to the in-situ void ratio of the soil, as proposed in the steady-state testing procedure. This procedure is necessary because of the very significant change in void ratio which takes place in the sampling, handling and reconsolidation processes.

Aspects of the procedure which should be carefully considered in determining the residual or steady-state strength of a soil by this method are the following:

(a) Whether it is appropriate to correct the results to the current in-situ void ratio of the sand or whether there may be some redistribution of water content during the earthquake which would change (increase) the void ratio to a higher value.

(b) The magnitude of the correction involved. In the present study the average steady-state strength of all samples, as tested, was about 5250 psf, while the average strength after correcting the results to the pre-1971 earthquake void ratio of the hydraulic fill in the upstream shell was about 750 psf. Thus the correction factor is very large and small changes in procedural details, such as the slope of the steady-state line, can have a large effect on the final results.

(c) The large variations in steady-state strength which occur from one sample to another, even when a major effort is made to limit the selection of samples to one type of soil. Because of the large scatter it is necessary to perform a large number of tests to obtain a representative body of data from which to select a reasonable value of residual or steady-state strength to be used in design. At the present time the selection of design strength can only be made on the basis of engineering judgment.

With appropriate consideration of these factors, the studies described previously show that reasonable values of post-liquefaction strength of a soil can be made by this procedure.

2. For the liquefied cohesionless soils in the upstream shell of the Lower San Fernando Dam, the post-liquefaction strength can be determined from slope stability analyses to be about 400 ± 100 psf. In this study the average steady-state strength for all samples tested, corrected to the pre-1971 earthquake condition in the upstream shell was found to be 800 psf, while the 35-percentile value for all the test data is about 580 psf. If the sandy silt and silty sand are considered to be representative of all the soil in the liquefied zone of the upstream shell, then with a conservative interpretation of the test data and conservative assumptions regarding the likely field behavior of the soil near the toe of the upstream shell of the embankment, the steady state-strength procedure correctly predicts the onset of sliding in the upstream shell. Use of the 35-percentile value of steady state strength for the samples tested would indicate that a flow-type failure would occur if liquefaction were triggered by the 1971 earthquake shaking. However, even the 35-percentile values of steady-state strength are still somewhat higher than the values of residual strength determined from back-analysis of the conditions in the failure zone of the dam after sliding stopped.

   Thus very conservative data interpretation and/or the avoidance of low factors of safety is required in interpreting the results of steady-state strength tests in order to arrive at a meaningful value for engineering analysis purposes.

9. Conclusions

The results presented in the preceding pages provide a basis for re-evaluating the soil conditions in the Lower San Fernando Dam prior to the failure of the upstream shell in the earthquake of 1971 and the applicability of currently-available procedures for evaluating the seismic stability of embankment dams. The main conclusions to be derived from the studies would appear to be as follows:

1. (a) The soil in the zone of liquefaction in the upstream shell appears to be a stratified sequence of layers of silty sand, sandy silt and clay. The sand becomes less fine towards the outer parts of the embankment. Representative average characteristics for the cohesionless zones of the upstream hydraulic fill, in the condition existing before the earthquake in 1971, appear to be as follows:

   Silty sand with fines content of about 25 to 30%

   $(N_1)_{60}$ in situ $\approx$ 11.5

   Equivalent clean sand $(N_1)_{60} \approx 13.5$.

   The results of the standard penetration tests performed in both the 1971 and 1985 investigations were remarkably similar and both sets of data are generally in accord with the average conditions noted above.

   (b) The average post-liquefaction strength of the soil in the liquefied zone of the upstream shell at the time of failure was about 400 $\pm$ 100 psf.

   (c) The combination of penetration resistance and residual strength of the liquefied silty sand is consistent with the correlation between these soil characteristics determined for other liquefaction failures (see Fig. 8-3).

2. The Seed-Lee-Idriss method for analyzing the seismic stability of earth dams provides a meaningful basis for evaluating the zone of liquefaction which developed in the upstream shell of the embankment of the Lower San Fernando Dam as a result of the ground shaking in the 1971 San Fernando earthquake and also indicating the absence of liquefaction in the downstream shell of the embankment. It also seems to provide a suitable basis for demonstrating that a liquefaction-type failure would not be triggered in a similar earthquake ($M \approx 6.6$) producing peak accelerations of the order of 0.2 to 0.25g, which would appear to be justified on the basis of the performance of the embankment in the 1952 Kern County earthquake ($M \approx 7.6$) and the performance of other hydraulic fill dams in the Los Angeles area in the 1971 San Fernando earthquake.

   However cyclic loading resistance as measured in cyclic triaxial tests on "undisturbed" samples cannot predict the residual strength of the liquefied sand and some supplementary procedure is required for this purpose.

3. The residual strength of a liquefied soil can only be determined at the present time by two methods:

   (a) Correlations based on past case studies (Seed, 1987).

   or (b) Steady-state strength testing in the laboratory as proposed by Poulos et al. (1985), followed by appropriately conservative corrections to the field void ratio condition taking all relevant factors into account.

   Both methods inevitably involve a significant degree of judgment due to the natural non-uniformity of cohesionless soils. Thus large numbers of tests are required to determine representative properties. However both methods, applied to the case of the liquefaction-type slide in the

upstream shell of the Lower San Fernando Dam correctly predict that such a slide would occur if liquefaction of the soils were induced by the earthquake shaking.

4. Both cyclic loading resistance (as measured by the development of 100% pore pressure ratio) and residual strength can be reasonably well correlated with values of $(N_1)_{60}$ determined by SPT values. Use of these correlations, in conjunction with appropriate analysis procedures, is likely to provide as reliable a method as any to evaluate the seismic stability of embankment dams.

10. Acknowledgments

The authors greatly appreciate the financial support for the study described in this report provided by the U.S. Army Corps of Engineers, and the cooperation of Dr. A. G. Franklin of the U.S. Army Corps of Engineers, Waterways Experiment Station and Drs. G. Castro and T. Keller of Geotechnical Engineers Inc. in providing important information and advice relating to the preparation of the report. Special thanks are also due to Mr. Peter Nicholson who performed a number of the soil tests at Stanford University. The authors also thank the Los Angeles Department of Water and Power, particularly Mr. Henry Mayeda of that Department, for providing valuable information concerning the performance of the San Fernando Dam.

References

Arulanandan, K., Seed, H. B., Seed, R. B., Yogachandran, C. and Muraleetharan, K. (1989) "Centrifuge Model Tests to Study the Effects of Volume Change Characteristics on the Dynamic Stability of Heterogeneous Earth Dams," Geotechnical Research Report, University of California at Davis, in press.

Babbitt, D. H., Bennett, W. J. and Hart, R. D. (1983) "California's Seismic Reevaluation of Embankment Dams," Procs., ASCE Symp. on Seismic Design of Embankments and Caverns, Philadelphia, PA, May 16-20, 1983, pp. 96-112.

Bieganousky, Wayne A. and Marcuson, William F., III (1976) "Liquefaction Potential of Dams and Foundations--Report 1: Laboratory Standard Penetration Test on Reid Bedford Model and Ottawa Sands," Report S-76-2, Waterways Experiment Station, Oct., 1976.

Bureau, Gilles, Volpe, Richard L., Roth, Wolfgang H. and Udaka, Takekazu (1985) "Seismic Analysis of Concrete Face Rockfill Dams," Procs., Symp. on Concrete Face Rockfill Dams--Design, Construction, and Performance, sponsored by the Geot. Div., ASCE in conjunction with the ASCE Convention in Detroit, MI, Oct. 21, 1985, edited by J. Barry Cooke and James L. Sherard, pp. 479-508.

Casagrande, A. (1984) "Reflections on Some Unfinished Tasks," First Nabor Carrillo Lecture of the Mexican Society for Soil Mechanics presented at the 6th National Meeting of the Society in November, 1972 and published in 1984.

Castro, G. and Keller, T. (1987) "Re-Evaluation of the Lower San Fernando Dam," Geotechnical Engineers Inc. Report to U.S. Army Corps of Engineers, W.E.S.

Castro, G., and Poulos, S. J. (1977) "Factors Affecting Liquefaction and Cyclic Mobility," Journal of the Geotechnical Engineering Division, ASCE, Vol. 103, No. GT6, 1977, pp. 501-516.

Castro, G., Poulos, S. J., France, J. W., and Enos, J. L. (1982) "Liquefaction Induced by Cyclic Loading," Report by Geotechnical Engineers, Inc. to the National Science Foundation, Washington, D.C., March, 1982, pp. 1-80.

De Alba, P., Seed, H. Bolton, Retamal, E., and Seed, R. B. (1987) "Residual Strength of Sand from Dam Failures in the Chilean Earthquake of March 3, 1985," Earthquake Engineering Research Center, Report No. UCB/EERC-87-11, University of California, Berkeley, September, 38 pp.

Franklin, A. G. (1987) Personal communication.

Gilbert, P. A. (1984) "Investigation of Density Variation in Triaxial Test Specimens of Cohesionless Soil Subjected to Cyclic and Monotonic Loading," Technical Report No. GL-84-10, U.S. Army Corps of Engineers, Waterways Experiment Station, Vicksburg, MS, September.

Lee, Kenneth L., Seed, H. Bolton, Idriss, Izzat M. and Makdisi, Faiz I. (1975) "Properties of Soil in the San Fernando Hydraulic Fill Dams," Journal of the Geotechnical Engineering Division, ASCE, Vol. 101, No. GT8, August, 1975, pp. 801-821.

Marcuson, W. F., III, and Bieganousky, W. A. (1976) "Laboratory Standard Penetration Tests on Fine Sands," Journal of the Geotechnical Engineering Division, ASCE, Vol. 103, No. GT6, June, 1976, pp. 565-588.

Marcuson, W. F., III, and Franklin, A. G. (1983) "Seismic Design, Analysis, and Remedial Measures to Improve Stability of Existing Earth Dams--Corps of Engineers Approach," Procs., ASCE Symp. on Seismic Design of Embankments and Caverns, Philadelphia, PA, May 16-20, 1983, pp. 65-78.

Poulos, Steve J., Castro, Gonzalo and France, John W. (1985) "Liquefaction Evaluation Procedure," Journal of the Geotechnical Engineering Division, ASCE, Vol. 111, No. 6, June, 1985, pp. 772-792.

Schmertman, J. H. (1979) "Statics of the SPT," Journal of the Geotechnical Engineering Division, American Society of Civil Engineers, Vol. 105, No. GT5, May, pp. 655-670.

Seed, H. Bolton (1979) "Soil Liquefaction and Cyclic Mobility Evaluation for Level Ground During Earthquakes," Journal of the Geotechnical Engineering Division, ASCE, Vol. 105, No. GT2, February, 1979, pp. 201-255.

Seed, H. Bolton (1979) "Considerations in the Earthquake-Resistant Design of Earth and Rockfill Dams," 19th Rankine Lecture of the British Geotechnical Society, Geotechnique, Vol. XXIX, No. 3, September, 1979.

Seed, H. Bolton (1983) "Earthquake-Resistant Design of Earth Dams," Paper presented at the Annual ASCE Convention, Philadelphia, PA, May 16-19.

Seed, H. Bolton (1986) "Design Problems in Soil Liquefaction," Report No. UCB/EERC-86/02, Earthquake Engineering Research Center, University of California, Berkeley, February, 1986, 33 pp.

Seed, H. Bolton (1987) "Design Problems in Soil Liquefaction," Journal of the Geotechnical Engineering Division, ASCE, Vol. 113, No. 8, August, 1987.

Seed, H. Bolton, Idriss, I. M. and Arango, Ignacio (1983) "Evaluation of Liquefaction Potential Using Field Performance Data," Journal of the Geotechnical Engineering Division, ASCE, Vol. 109, No. 3, March, 1983, pp. 458-482.

Seed, H. Bolton, Idriss, Izzat M., Lee, Kenneth L. and Makdisi, Faiz I. (1975b) "Dynamic Analysis of the Slide in the Lower San Fernando Dam during the Earthquake of February 9, 1971," Journal of the Geotechnical Engineering Division, ASCE, Vol. 101, No. GT9, September, 1975, pp. 889-911.

Seed, H. Bolton, Lee, K. L., Idriss, I.M. and Makdisi, F. (1973) "Analysis of Slides in the San Fernando Dams during the Earthquake of February 9, 1971," Report No. EERC-73-2, Earthquake Engineering Research Center, University of California, Berkeley, June, 1973.

Seed, H. Bolton, Lee, Kenneth L., Idriss, Izzat M. and Makdisi, Faiz I. (1975a) "The Slides in the San Fernando Dams During the Earthquake of February 9, 1971," Journal of the Geotechnical Engineering Division, ASCE, Vol. 101, No. GT7, July, 1975, pp. 651-688.

Seed, H. Bolton., Lee, Kenneth L., Idriss, Izzat M. and Makdisi, Faiz I. (1975b) "Dynamic Analyses of the Slide in the Lower San Fernando Dam During the Earthquake of February 9, 1971," Journal of the Geotechnical Engineering Division, ASCE, Vol. 101, No. GT9, pp. 889-911.

Seed, H. Bolton, Singh, Sukhmander, Chan, C. K. and Vilela, F. F. (1982) "Considerations in Undisturbed Samplingof Sands," Journal of the Geotechnical Engineering Division, ASCE, Vol. 108, No. GT2, February, 1982, pp. 265-283.

Seed, H. Bolton, Tokimatsu, K., Harder, L. F. and Chung, R. M. (1985) "Influence of SPT Procedures in Soil Liquefaction Resistance Evaluations," Journal of the Geotechnical Engineering Division, ASCE, Vol. 3, No. 12, December, 1985.

Seed, Raymond B., Jong, Hsing-Lian and Nicholson, Peter G. (1987) "Laboratory Evaluation of Undrained Cyclic and Residual Strengths of Lower San Fernando Dam Soils," Geotechnical Engineering Research Report No. SU/GT/87-01, Department of Civil Engineering, Stanford University, June, 1987, 168 pp.

Skempton, A. W. (1986) "Standard Penetration Test Procedures and the Effects of Overburden Pressure, Relative Density, Particle Size, Ageing and Over-consolidation, Geotechnique, 36, No. 3, pp. 425-447.

Smart, J. D. and Von Thun, J. L. (1983) "Seismic Design and Analysis of Embankment Dams Recent Bureau of Reclamation Experience," Procs., ASCE Symp. on Seismic Design of Embankments and Caverns, Philadelphia, PA, May 16-20, 1983, pp. 79-95.

Von Thun, J. Lawrence (1986) "Analysis of Dynamic Compaction Foundation Treatment Requirements, Stage I, Jackson Lake Dam," Technical Memorandum No. TM-JL-230-26, Bureau of Reclamation, Engineering and Research Center, Division of Dam and Waterway Design, Embankment Dams Branch.

Whitman, R. V. (1985) "On Liquefaction," Proceedings of the Eleventh International Conference on Soil Mechanics and Foundation Engineering, San Francisco, Vol. 4, pp. 1923-1926.

Appendix I: LABORATORY TESTING PROCEDURES AND TEST RESULTS

I-1 General:

This Appendix describes the sampling and testing procedures used in these studies, and presents individual plots of the results of each test performed. All tests reported herein were performed at the Stanford University Geotechnical Laboratory. Testing procedures employed are described in Sections I-2 and I-B.

Bulk samples as well as high quality "undisturbed" samples for this program were obtained and delivered to the Stanford Geotechnical Laboratory by Geotechnical Engineers, Inc. Bulk samples of hydraulic fill were obtained by hand from within a large-diameter exploratory shaft bored through the intact downstream portion of the hydraulic fill at approximately station 6+00. Figure 2-2 shows the location of this exploratory shaft. A total of seven different bulk samples from this test shaft were forwarded for possible investigation.

Two sampling methods were used to obtain high quality "undisturbed" samples of hydraulic fill. "Undisturbed" 2.8-inch diameter piston samples were retrieved from conventional boreholes, and hand-carved samples (also of 2.8-inch nominal diameter) were obtained at various elevations within the exploratory shaft. A brief description of sampling procedures and sample handling procedures is included in Appendix I - Section B. Figure 2-2 shows the locations of the sample borings and test shaft. Figure I-1 shows the locations of each "undisturbed" sample tested as part of this testing program, projected onto the existing embankment profile. This includes samples subjected to both monotonic and cyclic undrained loading.

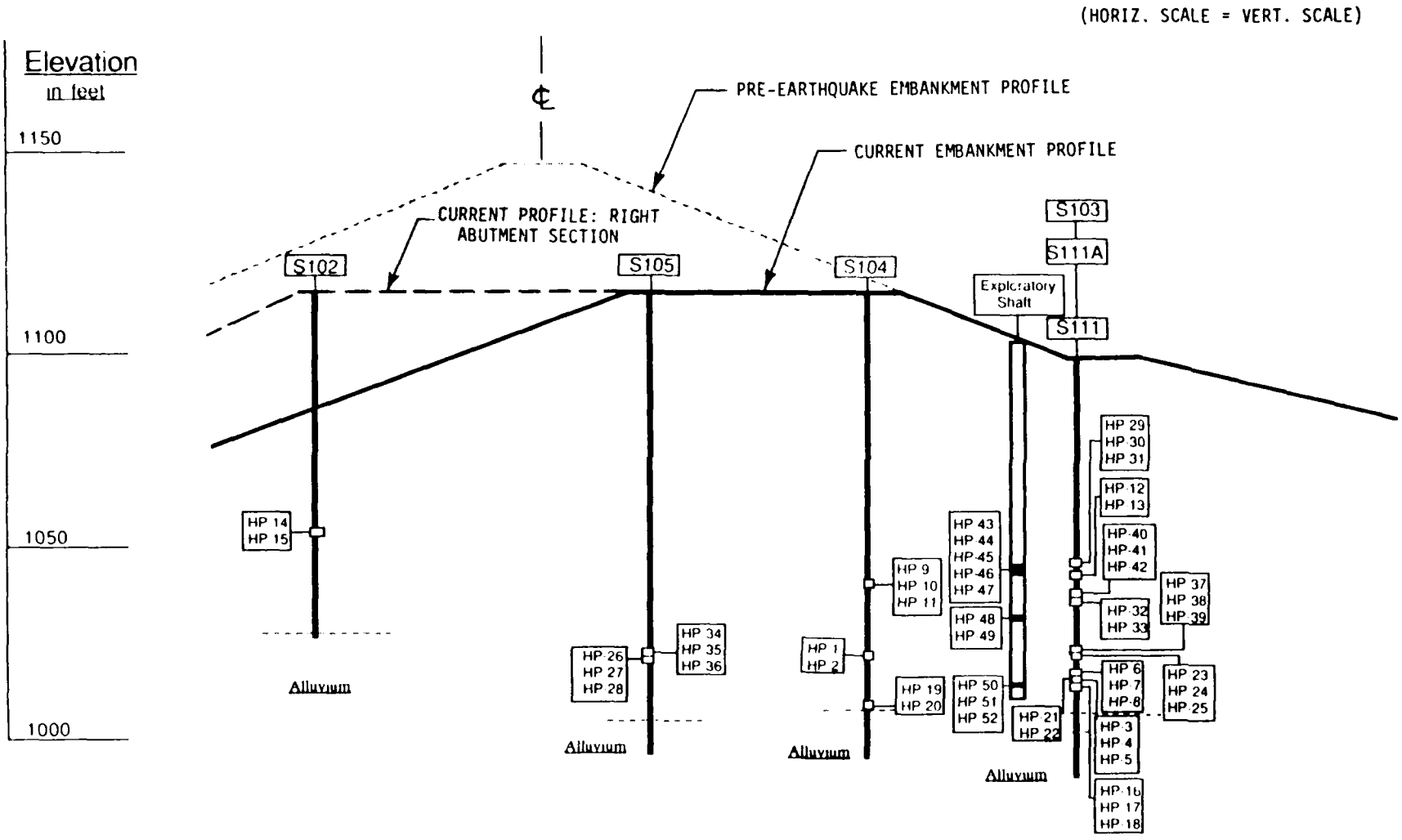

Figure I-1: CROSS-SECTIONAL PROJECTION OF EXPLORATORY TEST SHAFT AND CONVENTIONAL BOREHOLE SAMPLE LOCATIONS

Section I-A presents the results of $\overline{IC\text{-}U}$ triaxial tests performed on reconstituted bulk samples and Section I-C presents the results of $\overline{IC\text{-}U}$ triaxial tests performed on "undisturbed" samples to provide a basis for evaluation of in-situ steady state strengths of the hydraulic fill zones. Undisturbed samples for these tests were selected so that only silty sand and sandy silt samples of low plasticity obtained from within the elevation ranges of between +1008 to +1023 feet and between +1039 to +1056 feet (NGVD) were subjected to residual strength testing, as Standard Penetration Test (SPT) data suggests that these types of samples within these two elevation ranges are likely to represent the lowest in-situ steady-state strengths within the hydraulic fill zones.

Section I-D presents the results of undrained cyclic triaxial tests performed on undisturbed samples. Isotropically consolidated undrained cyclic tests were performed on "undisturbed" silty sand and sandy silt hydraulic fill samples obtained from elevations of between +1010 to 1054 feet (NGVD). Anisotropically consolidated undrained cyclic triaxial tests were performed on silty sand hydraulic fill samples obtained from within the same range of elevations to investigate the influence of initial static stress anisotropy on undrained cyclic pore pressure. In addition, a series of isotropically consolidated undrained cyclic triaxial tests were performed on "undisturbed" silty clay samples obtained from the hydraulic fill "core" zone at approximately elevation +1021 feet (NGVD) to investigate the cyclic loading behavior of this core material.

I-2 Steady State Line Evaluation:

The gradation characteristics of the intact downstream portion of the Lower San Fernando Dam hydraulic fill vary considerably, ranging from

fairly clean medium silty sands to clayey silts of low plasticity. It was judged that the "undisturbed" samples subjected to undrained steady-state strength testing could be divided into two general classes: (a) medium to fine silty sands (SM to SM-ML) and (b) finer sandy clayey silts (SM-ML to ML). The criterion for separating these two classes of hydraulic fill material was the samples' fines contents: samples with more than 40 percent by dry weight passing a No. 200 sieve were considered to represent "silty" materials and will be referred to as "sandy silts." Soils with less than 25 percent by dry weight passing a No. 200 sieve were considered to represent "sandy" materials, and will be referred to as "silty sands." Steady state lines were developed by testing reconstituted specimens from two bulk samples, one a medium to fine silty sand and the other a sandy clayey silt, in order to provide a basis for the void-ratio-based correction of S_{su} for samples of both soil types.

I-2.1 Steady-State Line for Silty Sands:

Bulk Sample No. 3, obtained from the exploratory test shaft at Elevation 2041, is a medium to fine silty sand with approximately 10 percent non-plastic silt fines as determined by "wet" hand-sieving through a No. 200 sieve. A gradation curve for this soil is presented in Figure 6-2. A series of nine isotropically consolidated-undrained ($\overline{IC\text{-}U}$) triaxial tests with pore pressure measurements were performed on reconstituted samples of Bulk Sample No. 3.

All samples tested were 2.8-inches in diameter, with a height vs. diameter ratio of approximately 2.3:1. All samples were prepared by moist-tamping. Each sample was prepared in nine even layers. Sufficient soil to achieve the desired void ratio within each layer was mixed to a

water content of approximately 8 to 10 percent and then deposited into a rubber membrane held by vacuum pressure to the sides of a rigid forming mold. A tamper with a fixed maximum drop was then used to tamp the new layer to a pre-determined thickness. The top of the layer was then scarified lightly to "knit" with the base of the next layer, and the process was repeated. Experience has shown that it is necessary to vary the weight of soil used in each layer, using slightly more in upper layers grading to slightly less in lower layers in order to achieve uniform final density, as lower layers are densified slightly by tamping of (upper) overlying layers.

Samples were saturated by a vacuum/back pressure saturation process. First an essentially full vacuum was applied internally to remove as much air as possible from the sample. An external vacuum "cell" pressure was applied to minimize the applied effective confining stress during this stage of sample preparation. Following vacuum application, the sample was filled with de-aired water flowing from base to top cap at approximately the rate of capillary rise (under slight positive vertical gradient). Positive internal back pressure was then applied sufficient to dissolve any remaining air and thus achieve full saturation. This application of back pressure was accompanied by simultaneous application of confining pressure in order to maintain constant isotropic effective confining stress. An effective confining stress of approximately 0.5 ksc (one-half atmosphere or 7.4 psi) was maintained during both the vacuum and back-pressure saturation stages. All vacuum and back pressures were applied slowly in increments in order to avoid differential overconsolidation of the ends of the samples. Achievement of full saturation was verified by monitoring the sample's

B-values ($B = \Delta u/\Delta\sigma_3$). B-values greater than or equal to approximately 0.98 were taken as acceptably close to full saturation.

Following back pressure saturation, each sample was isotropically consolidated to the desired density and initial effective confining stress $\sigma_{3,c}'$. The sample was then sheared to failure under undrained conditions at a constant rate of axial strain. Axial strain rates for loading were on the order of $\epsilon_A \approx 0.5\%$ per minute, in order to provide representative measurements of internal pore pressures during shearing. Table I-1 presents a summary of test conditions for each sample, and Section I-A presents individual plots of: (a) applied axial stress vs. axial strain, (b) σ_3' vs. axial strain, and (c) deviatoric stress $(\frac{1}{2})(\sigma_1 - \sigma_3)$ vs. effective mean volumetric stress $(\frac{1}{2})(\sigma'_1 - \sigma'_3)$ for each test performed.

Table I-1 summarizes the results of this $\overline{IC\text{-}U}$ triaxial test series. Figure 6-4 presents a plot of the results in the form of a plot of the $\log_{10}$ of undrained steady-state strength (S_{su}) vs. void ratio. The solid line in Figure 6-4 represents the "steady-state line" for Bulk Sample No. 3 as determined by this test series.

I-2.2 Steady-State Line for Sandy Silts:

Bulk Sample No. 7, obtained from the exploratory test shaft at Elevation 1013, is a sandy silt of low plasticity with approximately 52 percent fines. A gradation curve for this soil is presented in Figure 6-3. The gradation of material passing the No. 200 sieve was evaluated based on hydrometer analysis.

A series of eleven $\overline{IC\text{-}U}$ triaxial tests were performed on reconstituted samples of Bulk Sample No. 7. All samples tested were 2.8-inches in diameter with a height vs. diameter ratio of approximately

Table I-1: $\overline{\text{IC-U}}$ TRIAXIAL TESTS ON BULK SAMPLE NO. 3

Test No.	Method of Sample Preparation	γ_d (pcf)	Void Ratio[1]	"B-value"	$\sigma_{3,c}'$ (psi)	$\sigma_{3,r}'$ (psi)	ϕ_r' (°)	S_{su} (psi)
BS3-1	Moist Tamp.	101.40	.656	0.996	65.2	19.3	35.6	22.0
BS3-2	Moist Tamp.	103.20	.627	0.991	65.0	30.8	36.7	36.7
BS3-3	Moist Tamp.	107.40	.564	0.994	79.9	62.5	36.7	74.4
BS3-4	Moist Tamp.	110.57	.519	0.985	80.1	103.6	37.1	137.4
BS3-5	Moist Tamp.	105.24	.596	0.989	57.8	54.3	36.2	63.3
BS3-6	Moist Tamp.	94.77	.772	0.991	29.6	0.2	36.3	0.23
BS3-7	Moist Tamp.	96.86	.733	0.995	29.8	2.2	34.5	2.40
BS3-8	Moist Tamp.	100.56	.670	0.993	29.9	11.0	34.0	11.5
BS3-9	Moist Tamp.	104.37	.609	0.992	49.7	41.1	36.1	47.7

Note: 1. Based on G_s = 2.69 and γ_w = 62.43 pcf @ 4°C.

2.3:1. All samples were saturated using the vacuum/back pressure saturation procedures described in Section I-2.1. Two sample preparation procedures were used. Eight samples were prepared by "moist tamping" as described in Section I-2.1. Three additional samples were prepared by "wet pluviation" to investigate the influence of sample preparation method on steady-state strength behavior. The three "wet pluviation" samples were deposited by pluviation through standing water, and were then isotropically consolidated to different initial effective confining stresses ($\sigma_{3,c}'$) in order to achieve different void ratios. All samples were sheared to failure under undrained conditions at constant axial strain. Axial strain rates for loading were approximately 0.07% to 0.1% per minute. Table I-2 presents a summary of test conditions for each sample, and Section I-A presents individual plots of: (a) applied axial stress vs. axial strain, (b) σ_3' vs. axial strain, and (c) ½ of the principal effective stress sum vs. the maximum deviatoric stress (p vs. q or $(\sigma_1' + \sigma_3')/2$ vs. $(\sigma_1 - \sigma_3)/2$ for each test performed.

Table I-2 summaries the results of these $\overline{\text{IC-U}}$ triaxial tests on Bulk Sample No. 7. Figure 6-5 presents a plot of the results in the form of a plot of the $\log_{10}$ of undrained steady-state strength S_{su} vs. void ratio. As shown in this figure, there appears to be little significant difference in steady-state strength behavior between samples of this soil prepared by moist tamping and samples prepared by wet pluviation. The solid line in Figure 6-5 represents the "steady-state line" for Bulk Sample No. 7 as determined by this test series.

I-3 Evaluation of Steady State Strengths In-Situ:

A series of 16 $\overline{\text{IC-U}}$ triaxial tests were performed on "undisturbed" samples of hydraulic fill from the intact downstream portion of Lower

Table I-2: $\overline{\text{IC-U}}$ TRIAXIAL TESTS ON BULK SAMPLE NO. 7

Test No.	Method of Sample Preparation	γ_d (pcf)	Void Ratio[2]	"B-value"	$\sigma_{3,c}'$ (psi)	$\sigma_{3,r}'$ (psi)	ϕ_r' (°)	S_{su} (psi)	
BS7-1	Moist Tamp.	108.57	0.547	0.983	39.9	26.9	34.7	29.2	
BS7-2	Moist Tamp.	112.20	0.497	0.982	49.9	55.2	34.5	59.5	
BS7-3	Moist Tamp.	101.78	0.650	0.984	12.0	2.1	33.6	2.3	
BS7-4	Moist Tamp.	106.85	0.572	0.975	29.9	15.6	33.9	16.4	
BS7-5	Moist Tamp.	104.24	0.611	0.974	15.0	6.2	33.6	6.4	
BS7-6	Moist Tamp.	103.23	0.627	0.996	14.8	4.1	32.5	4.0	
BS7-7	Moist Tamp.	98.84	0.699	0.991	6.0	1.2	33.9	1.2	
BS7-8	Moist Tamp.	105.11	0.597	0.940	24.2	12.2	33.6	12.1	
BS7-1W	Wet Pluv.	109.98	0.527	0.987	65.1	28.2	33.7	33.3	(Note #3)
BS7-2W	Wet Pluv.	103.85	0.617	0.989	5.5	4.8	33.3	4.9	
BS7-3W	Wet Pluv.	109.96	0.527	0.991	69.3	35.3	35.5	39.8	

Notes:
1. Methods of Sample preparation: (a) moist tamping in layers, (b) wet pluviation and consolidation.
2. Based on G_s = 2.69, γ_w = 62.43 pcf @ 4°C.
3. Sample density not uniform, denser at top of sample. Also, data lost prior to plotting.

San Fernando Dam to provide a basis for estimation of in-situ steady-state strengths of this hydraulic fill material. Nine of these "undisturbed" samples were 2.8-inch diameter piston samples retrieved from conventional boreholes, and the other seven samples were hand-carved 2.8-inch diameter samples retrieved from the exploratory test shaft. Table I-3 and Figures 2-2 and I-1 summarize the locations from which these samples were obtained.

Section I-B provides a description of procedures used for sampling, sample extrusion and test set-up, sample saturation, sample consolidation and undrained testing. Sampling procedures used for both piston and hand-carved sampling permitted monitoring of sample void ratio changes during the sampling process. Subsequent void ratio changes during sample extrusion, test set-up and consolidation were also continuously monitored.

Table I-3 lists the void ratios of each of the "undisturbed" samples at various stages: (a) as tested (following consolidation), (b) after sampling but prior to extrusion and test set-up, (c) in-situ prior to sampling in 1985, and (d) in-situ prior to the 1971 San Fernando Earthquake. Pre-earthquake (1971) void ratios are based on an estimated average earthquake-induced void ratio decrease (densification of $\Delta e \approx 0.020$).

Table I-4 presents a summary of test conditions for each IC-U triaxial test performed on an "undisturbed" sample. All samples tested were 2.8-inches in diameter. Height vs. diameter ratios varied from 1.8:1 through 2.4:1, and all samples were tested with well-lubricated end platens. All samples were back pressure saturated, were isotropically consolidated to the desired initial effective confining stress ($\sigma_{3,c}'$),

Table I-3: RESIDUAL STRENGTHS BASED ON $\overline{IC-U}$ TRIAXIAL TESTS ON UNDISTURBED SAMPLES OF HYDRAULIC FILL FROM LOWER SAN FERNANDO DAM

Test No.	Boring No.	Sample Elev. (ft.)	Void Ratio as Tested	Void Ratio After Sampling	Void Ratio In Situ (1985)	Void Ratio In Situ (1971)*	Steady State Strength: S_{su} (psi)	
							As Tested	In Situ (1971)*
4	U-111A	1013	0.578	0.608	0.600	0.620	32.9	13.9
7	U-111	1017	0.665	0.717	0.718	0.738	37.3	7.9
10	U-104	1040	0.783	0.837	0.843	0.863	25.8	4.4
11	U-104	1039	0.722	0.757	0.763	0.783	38.1	10.2
12	U-111	1041	0.731	0.832	0.836	0.856	19.7	1.3
14	U-102	1054	0.761	0.764	0.772	0.792	12.6	6.4
16	U-111	1012	0.515	0.603	0.635	0.655	37.2	1.3
20	U-104	1008	0.611	0.647	0.635	0.655	41.8	17.4
28	U-105	1019	0.797	0.849	0.870	0.890	14.9	2.6
43	Shaft**	1044	0.654	0.697	0.751	0.771	49.7	3.5
44	Shaft**	1044	0.627	0.720	0.705	0.725	82.9	13.7
45	Shaft**	1042	0.636	0.712	0.736	0.756	22.9	1.7
46	Shaft**	1042	0.545	0.633	0.567	0.587	63.1	34.1
50	Shaft**	1013	0.651	0.705	0.719	0.739	34.5	5.5
51	Shaft**	1013	0.630	0.697	0.708	0.728	32.2	4.0
52	Shaft**	1012	0.664	0.734	0.757	0.777	36.0	2.7

* Corrected for an assumed earthquake-induced void ratio change of $\Delta e = 0.020$

** Hand-carved samples from exploratory shaft.

Table I-4: $\overline{\text{IC-U}}$ TRIAXIAL TESTS ON UNDISTURBED SAMPLES OF HYDRAULIC FILL FROM LOWER SAN FERNANDO DAM

SAMPLE ORIGIN			SAMPLE TESTING CONDITIONS				RESIDUAL OR STEADY STATE RESULTS		
Test No.	Boring No.	Sample No.	γ_d (pcf)	Void Ratio*	$\bar{B}$	$\sigma_{3,c}'$ (psi)	$\sigma_{3,r}'$ (psi)	ϕ_r' (°)	$\tau_{f,s}$ (psi)
4	U-111A	UF-18	106.42	0.578	0.994	65.1	33.2	33.2	32.9
7	U-111	UF-18	100.88	0.665	0.995	55.3	34.3	34.7	37.3
10	U-104	UF-4	94.21	0.783	0.996	54.9	24.4	34.1	25.8
11	U-104	UF-4	97.51	0.722	0.986	53.4	35.0	34.7	38.1
12	U-111	UF-6	97.02	0.731	0.991	54.5	17.9	35.0	19.7
14	U-102	UF-1	95.36	0.761	0.998	54.6	13.1	32.1	12.6
16	U-111	UF-21	110.81	0.515	0.991	65.1	33.5	35.2	37.2
20	U-104	UF-10	104.22	0.611	0.996	54.7	39.8	34.0	41.8
28	U-104	UF-10	93.47	0.797	0.996	54.6	13.6	34.8	14.9
43	Shaft**	TS-101	101.46	0.654	0.997	60.2	44.4	35.3	49.7
44	Shaft**	TS-106	103.21	0.627	0.988	60.2	73.7	35.5	82.9
45	Shaft**	TS-111	102.65	0.636	0.982	45.0	20.2	35.6	22.9
46	Shaft**	TS-113	108.68	0.545	0.994	60.1	53.3	36.6	63.1
50	Shaft**	TS-303	101.69	0.651	0.991	55.1	31.2	35.1	34.5
51	Shaft**	TS-308	103.00	0.630	0.993	60.2	29.8	34.6	32.2
52	Shaft**	TS-311	100.93	0.664	0.994	50.0	32.4	35.1	36.0

* Based on G_s = 2.69 and γ_w = 62.43 pcf @ 4°C.

** Hand-carved samples from exploratory shaft.

and were sheared to failure under undrained conditions at a constant rate of axial strain. Strain rates employed varied from sample to sample as a function of perceived sample permeability. Tables 6-1, 6-2, I-3 and I-4 present the results of these $\overline{IC\text{-}U}$ tests. Section I-C also presents (a) soil gradation curves, (b) plots of axial stress vs. axial strain, (c) plots of effective confining stress ($\sigma_{3'}$) vs. axial strain and (d) p-q effective stress path plots for each "undisturbed" sample tested.

I-4 Undrained Cyclic Triaxial Testing:

Both 2.8-inch diameter "undisturbed" tube samples as well as 2.8-inch diameter hand-carved samples were subjected to cyclic tests. Sample handling, test set-up and back pressure saturation procedures used were the same as described previously in Sections I-2 and I-B. Upon completion of back pressure saturation (to a "B-value" of not less than B = 0.98) most of the samples were isotropically consolidated to $\sigma'_{3,i}$ = 2.0 ksc. Some of the samples were anisotropically consolidated at K_c = 1.75 by applying an additional axial consolidation stress concurrent with the applied confining stress of $\sigma'_{3,i}$ = 2.0 ksc.

Uniform sinusoidal axial cyclic loading was applied using a computer-controlled pneumatic loading system. The rate of cyclic loading was 0.5 Hz for all cyclic tests performed. Testing results are evaluated herein primarily in terms of cyclic strains induced, as it was judged that many of the samples tested contained sufficient fine content as to be relatively impervious so that the pore pressure distributions within some of the samples might not have been fully uniform during testing. Pore pressures were measured at the sample bases.

Tables 5-1 and 5-2 present a summary of the results of cyclic tests. Actual test data for each individual cyclic test performed is

presented in Section I-D; this includes plots of (a) sample gradation curves, (b) cyclic axial load vs. time, (c) incremental pore pressure generation vs. time, and (d) axial strain vs. time.

In addition to the 15 cyclic tests performed on sandy and silty samples, a series of four additional isotropically consolidated undrained cyclic triaxial tests were performed on undisturbed samples of low plasticity silty clay obtained from the central "core" zone of the hydraulic fill. Table I-5 lists sample locations, sample characteristics, testing conditions and test results for these cyclic tests. All four samples tested were silty clays of low plasticity, and all consisted of more than 97% by dry weight finer than a No. 200 sieve.

Figure I-2 shows the results of these tests on clayey samples, along with the cyclic strength curves for sandy and silty samples from Figures 5-4. Inspection of the individual test records (Figures D-21, D-31, D-33 and D-35) show that these samples do progressively soften and develop positive pore pressures under repeated cyclic loading. However, as shown in Figures I-2 and Figures D-21, D-31 , D-33 and D-35, they do so only at relatively high cyclic stress ratios and large numbers of loading cycles. It may be concluded from these test results that the clayey hydraulic fill from the central "core" region of Lower San Fernando Dam would not develop significant pore pressures and would not be significantly softened by the cyclic loading likely to have been induced by the 1971 San Fernando Earthquake.

Table I-5: ISOTROPICALLY CONSOLIDATED-UNDRAINED CYCLIC TRIAXIAL TESTS ON UNDISTURBED SILTY CLAY HYDRAULIC FILL SAMPLES FROM LOWER SAN FERNANDO DAM

Test No.	Boring No.	Sample No.	Sample Elev. (ft.)	Void Ratio as Tested*	Void Ratio After Sampling*	Void Ratio In Situ (1985)*	$\sigma'_{3,i}$ (ksc)	"B-value"	$\sigma_{d,c}/2\sigma'_{3,i}$	No. of Cycles to ±5% ε_A
27	U105	UF12	1020	0.818	0.857	0.878	2.00	0.990	0.255	179
34	U105	UF11	1022	0.807	0.832	0.884	2.00	0.988	0.345	14
35	U105	UF11	1021	0.851	0.889	0.901	2.00	0.981	0.298	50
36	U105	UF11	1020	0.880	0.903	0.915	2.00	0.991	0.339	17

*Based on G_s = 2.69, γ_w = 62.43 @ 4°C.

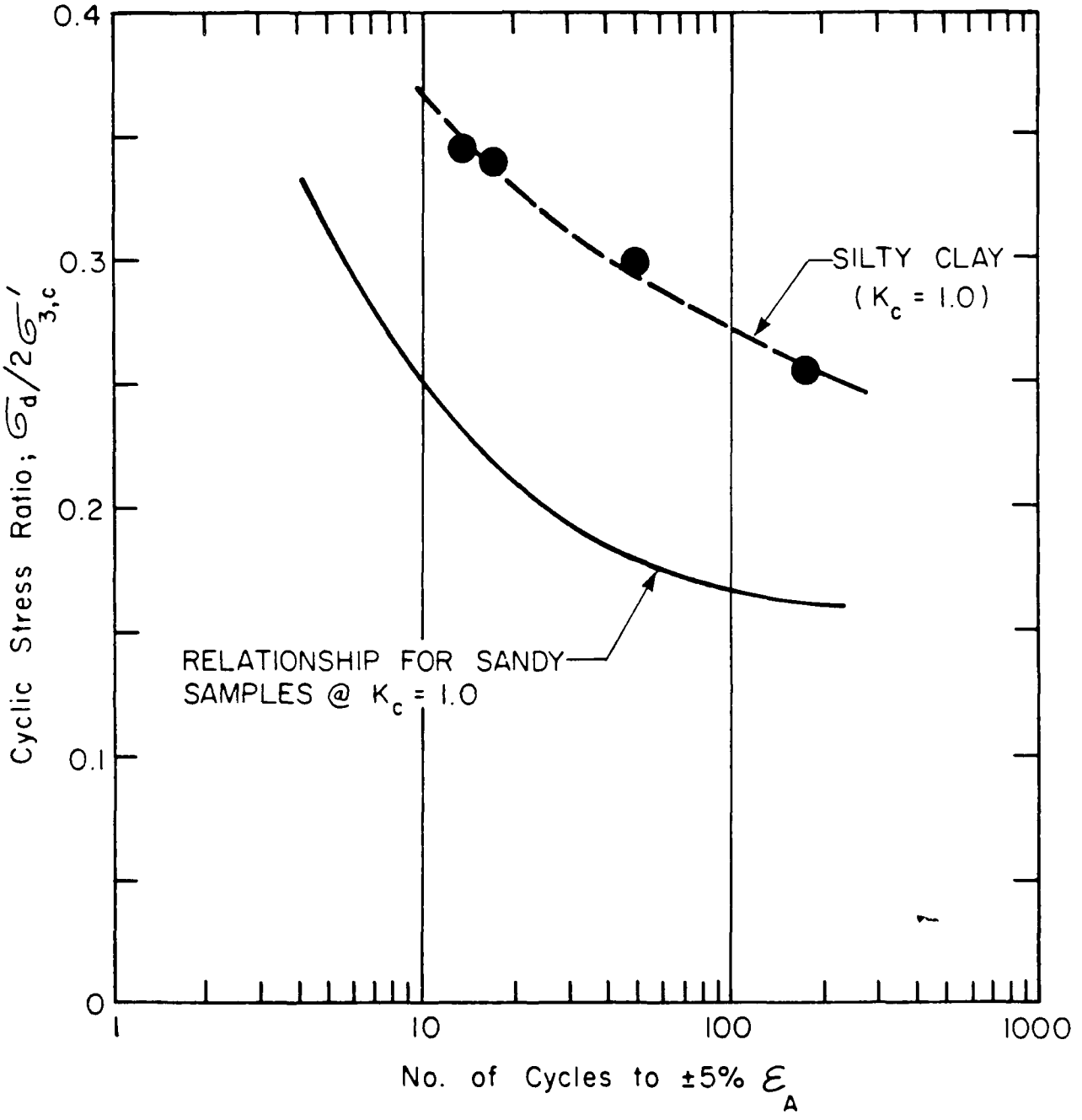

Figure I-2: ISOTROPICALLY CONSOLIDATED UNDRAINED CYCLIC TRIAXIAL TESTS ON UNDISTURBED SAMPLES OF CLAYEY HYDRAULIC FILL

Section I-A: IC-$\bar{U}$ TRIAXIAL TESTS ON RECONSTITUTED SAMPLES

Figures A-1 through A-9 present plots of (a) applied axial stress vs. axial strain, (b) effective confining stress (σ_3') vs. axial strain and (c) one-half of the principal effective stress sum $(1/2)(\sigma_1' + \sigma_3')$ vs. the maximum deviatoric stress $(1/2)(\sigma_1 - \sigma_3)$ for the isotropically consolidated undrained (IC-$\bar{U}$) triaxial tests of reconstituted samples of the hydraulic fill material "Bulk Sample No. 3." A gradation curve for this medium to fine silty sand is presented in Figure 6-2.

Figures A-10 through A-19 present similar plots of IC-$\bar{U}$ triaxial tests of reconstituted samples of the hydraulic fill material "Bulk Sample no. 7." A gradation curve for this non-plastic sandy silt (ML) is presented in Figure 6-3.

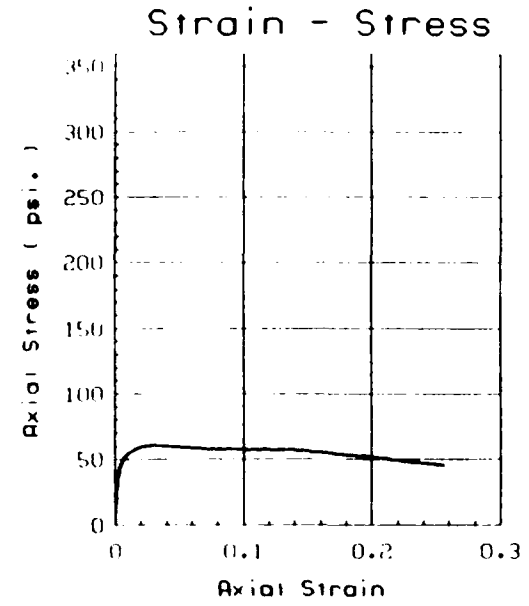

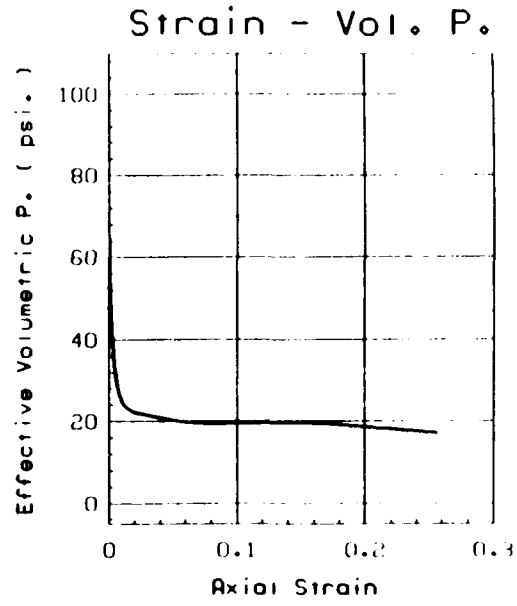

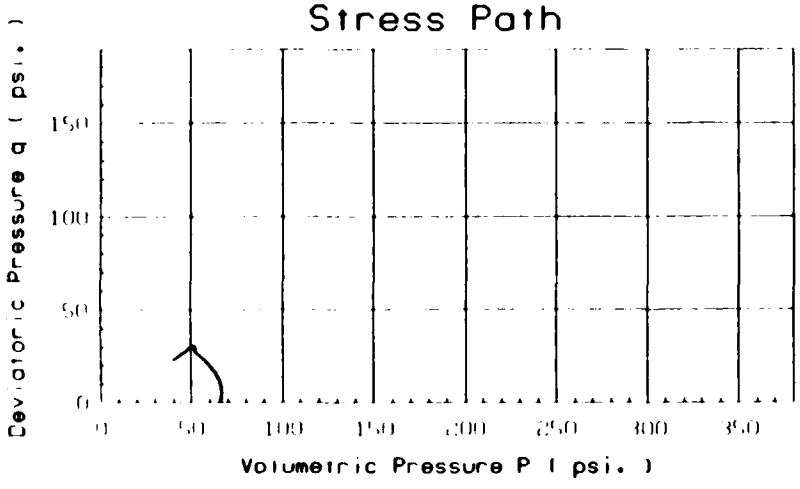

Test No. : BS3-1

Test Date : 5/27/86

Material : Bulk Sample #3

Silty Sand (SM), 8.1% fines.

γ_d = 101.40 pcf

$\bar{B}$ = 0.996

$\sigma_{3,c}'$ = 65.2 psi

Strain RATE = 25.3% per hour

Figure A-1: IC-$\bar{U}$ TRIAXIAL TEST NO. BS3-1

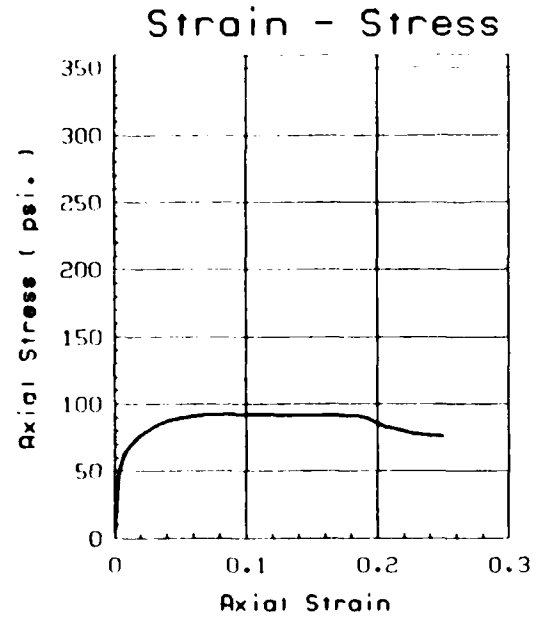

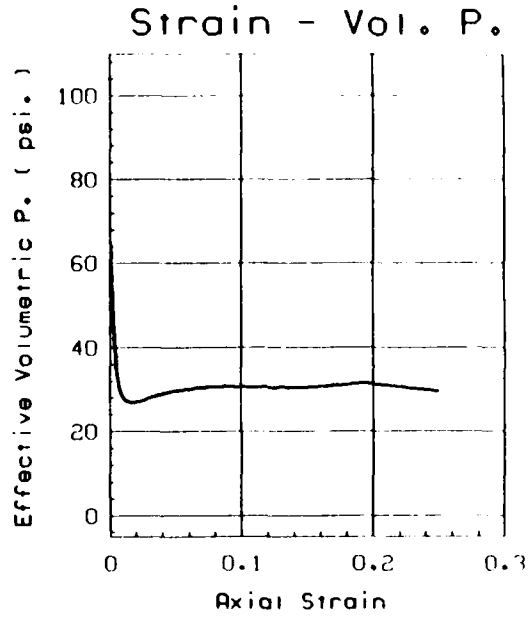

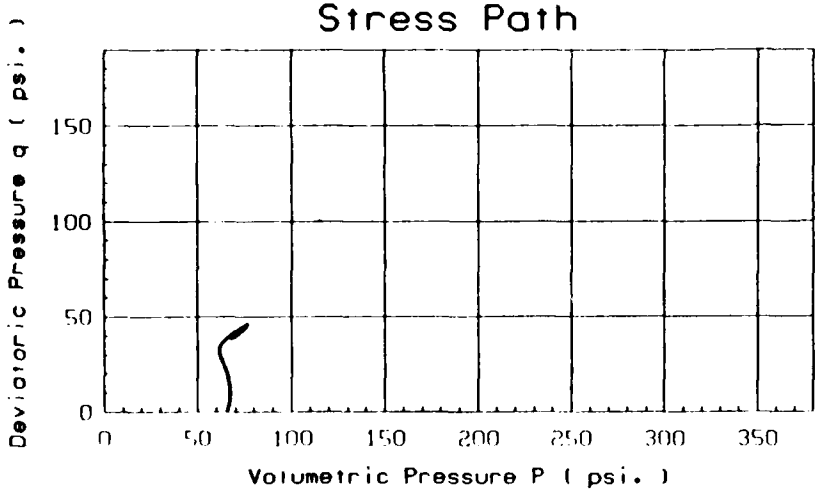

Test No. : BS3-2
Test Date : 5/27/86
Material : Bulk Sample #3
Silty Sand (SM), 8.1% fines.
γ_d = 103.20 pcf
$\overline{B}$ = 0.991
$\sigma_{3,c}'$ = 65.0 psi
Strain RATE = 25.4% per hour

Figure A-2: IC-$\bar{U}$ TRIAXIAL TEST NO. BS3-2

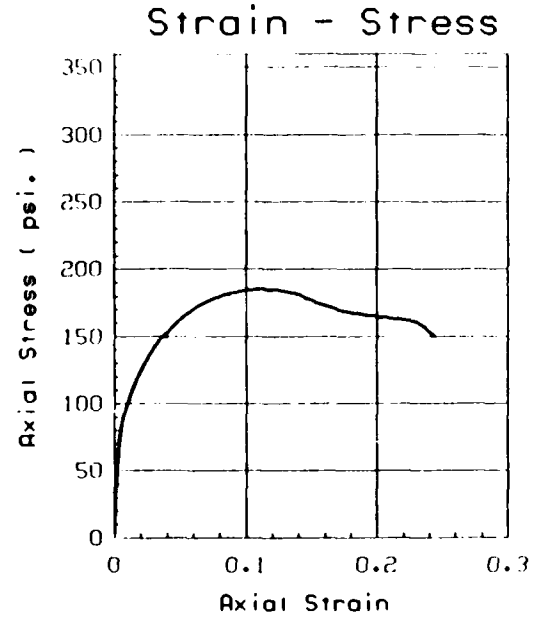

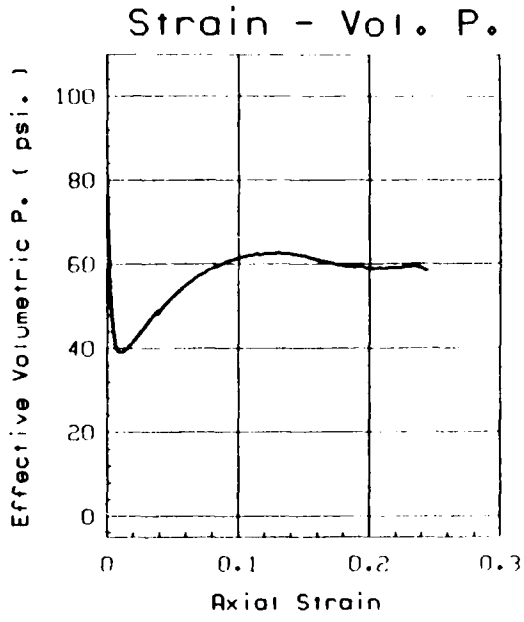

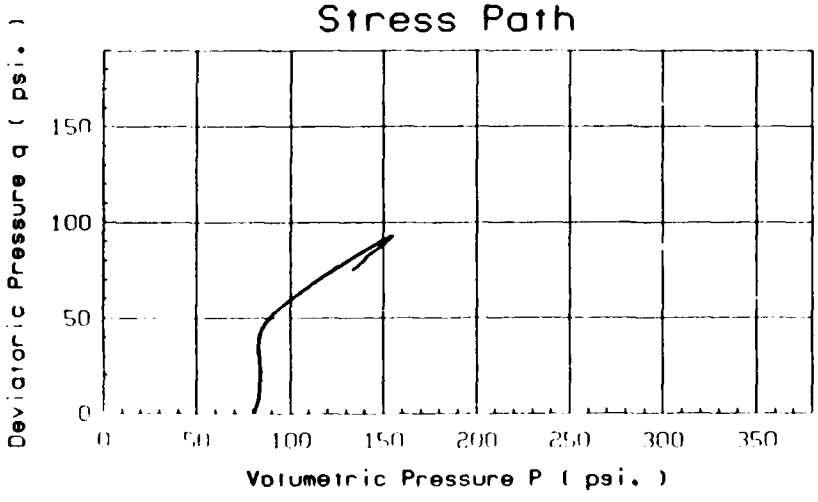

Test No. : BS3-3
Test Date : 5/28/86
Material : Bulk Sample #3
Silty Sand (SM), 8.1% fines.
γ_d = 107.40 pcf
$\overline{B}$ = 0.994
$\sigma_{3,c}'$ = 79.9 psi
Strain RATE = 25.7% per hour

Figure A-3: IC-$\overline{U}$ TRIAXIAL TEST NO. BS3-3

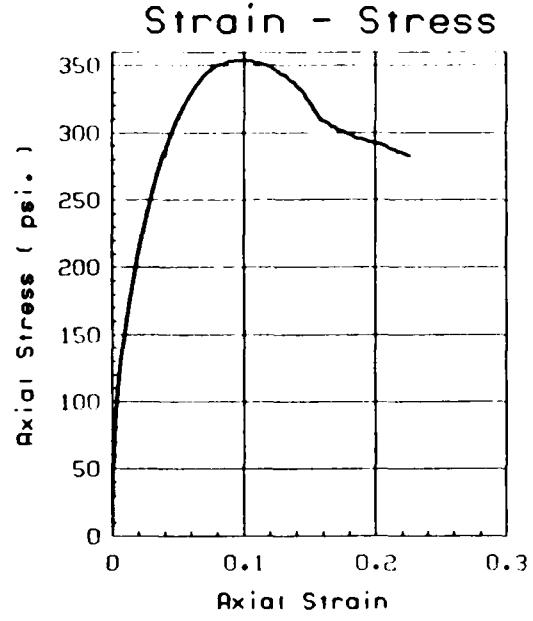

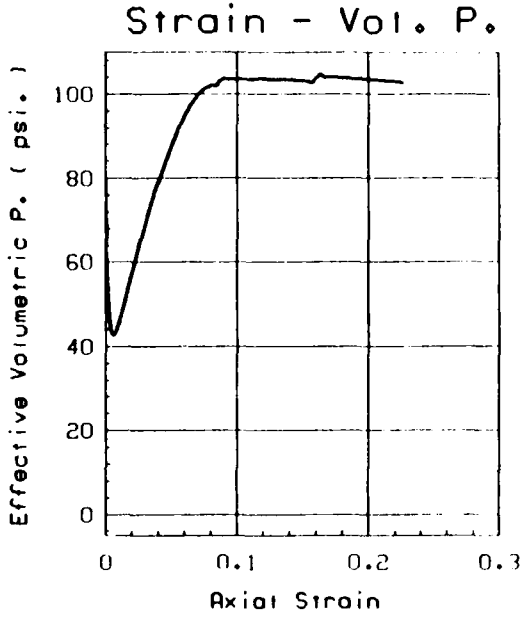

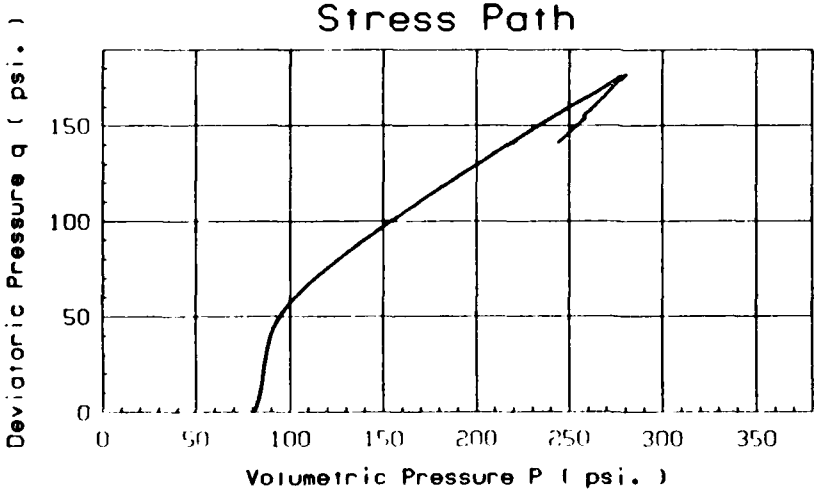

Test No. : BS3-4

Test Date : 5/29/86

Material : Bulk Sample #3

Silty Sand (SM), 8.1% fines.

γ_d = 110.57 pcf

$\bar{B}$ = 0.985

$\sigma_{3,c}'$ = 80.1 psi

Strain RATE = 25.2% per hour

Figure A-4: IC-$\bar{U}$ TRIAXIAL TEST NO. BS3-4

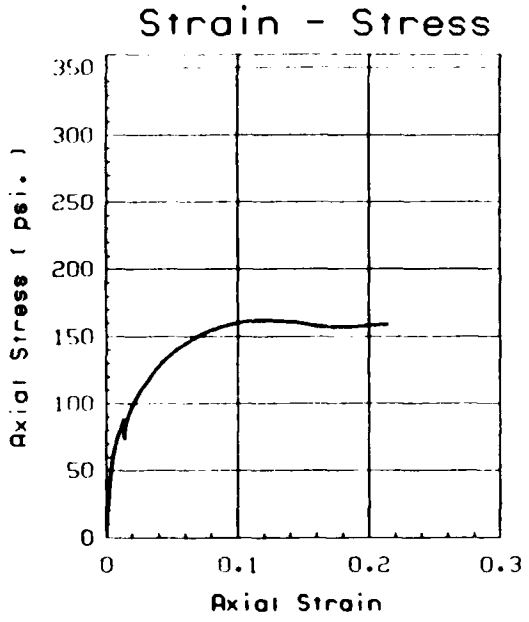

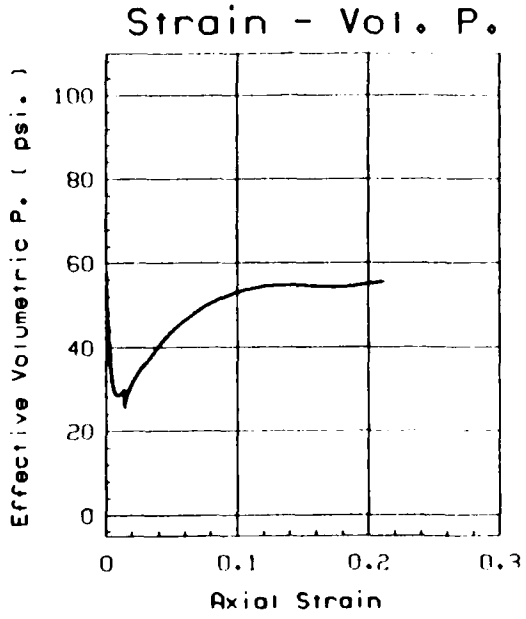

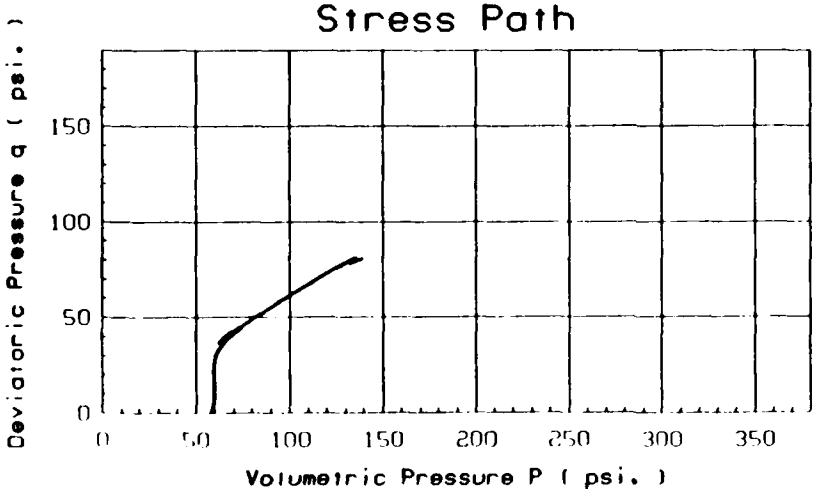

Test No. : BS3-5
Test Date : 7/26/86
Material : Bulk Sample #3
Silty Sand (SM), 8.1% fines.
γ_d = 105.24 pcf
$\bar{B}$ = 0.989
$\sigma_{3,c}'$ = 57.8 psi
Strain RATE = 24.5% per hour

Figure A-5: IC-$\bar{U}$ TRIAXIAL TEST NO. BS3-5

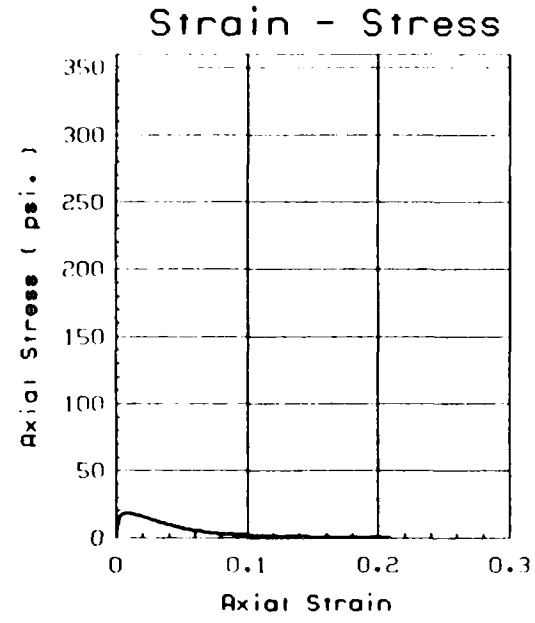

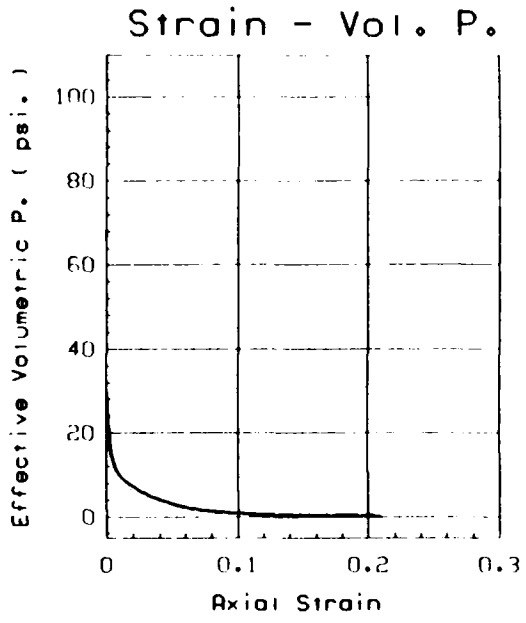

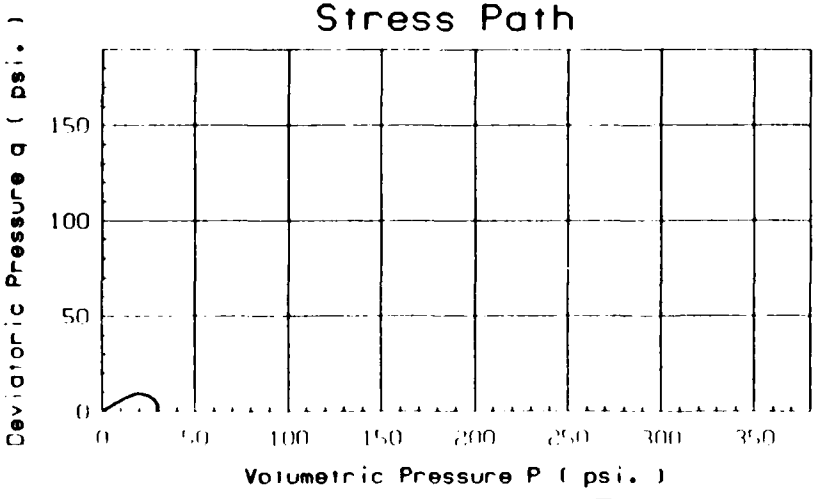

Test No. : BS3-6
Test Date : 9/30/86
Material : Bulk Sample #3
Silty Sand (SW), 8.0% fines.
γ_d = 94.77 pcf
$\overline{B}$ = 0.991
$\sigma_{3,c}'$ = 29.8 psi
Strain RATE = 27.36% per hour

Figure A-6: IC-$\overline{U}$ TRIAXIAL TEST NO. BS3-6

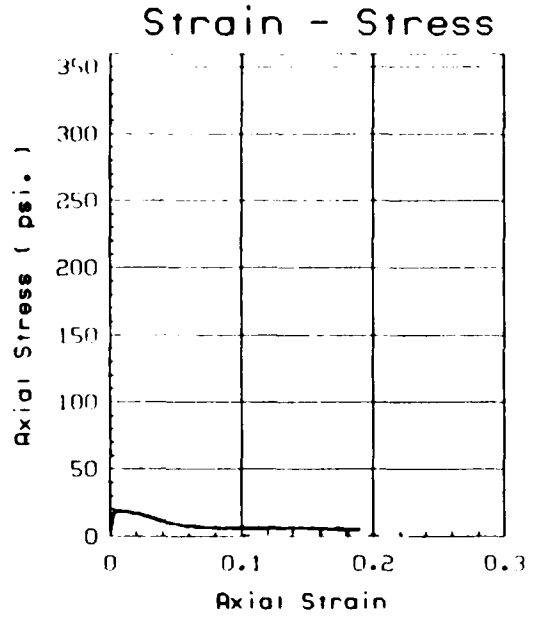

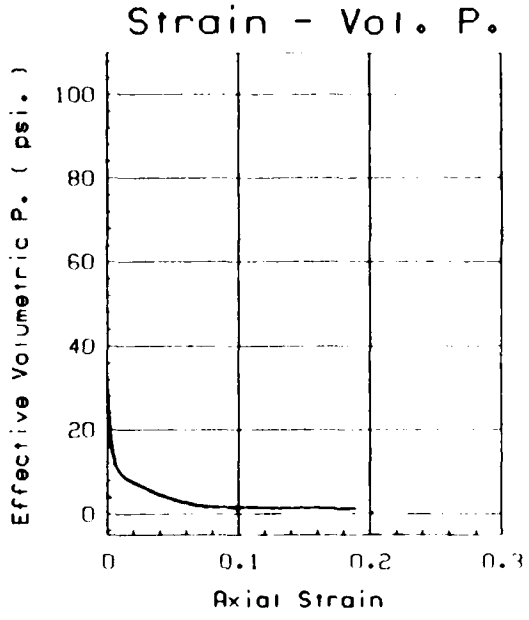

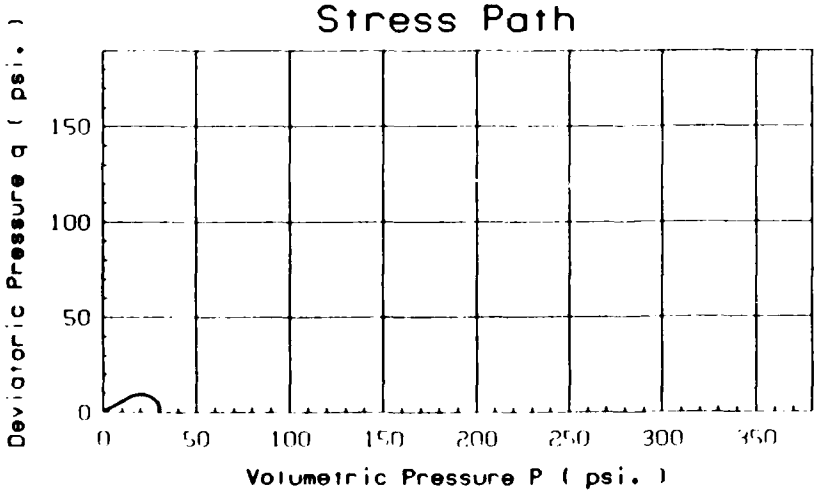

Test No. : BS3-7

Test Date : 10/1/86

Material : Bulk Sample #3

Sand (SW), 8.0% fines.

γ_d = 96.86 pcf

$\overline{B}$ = 0.995

$\sigma_{3,c}'$ = 29.6 psi

Strain RATE = 27.21% per hour

Figure A-7: IC-$\overline{U}$ TRIAXIAL TEST NO. BS3-7

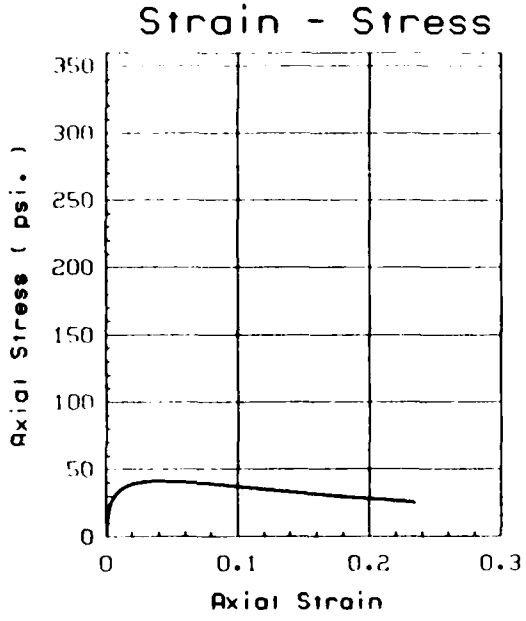

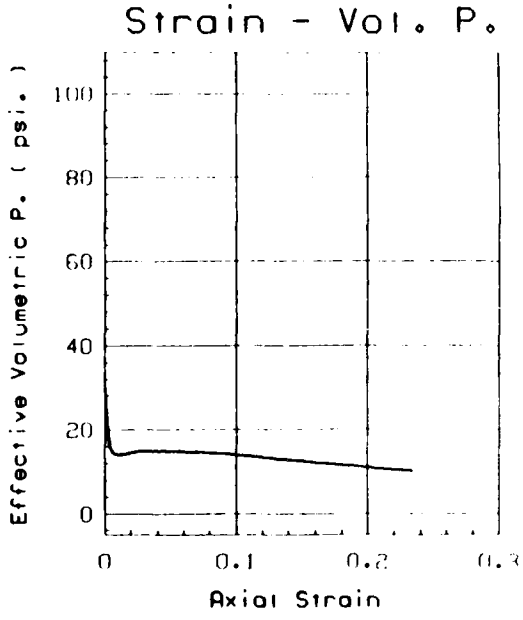

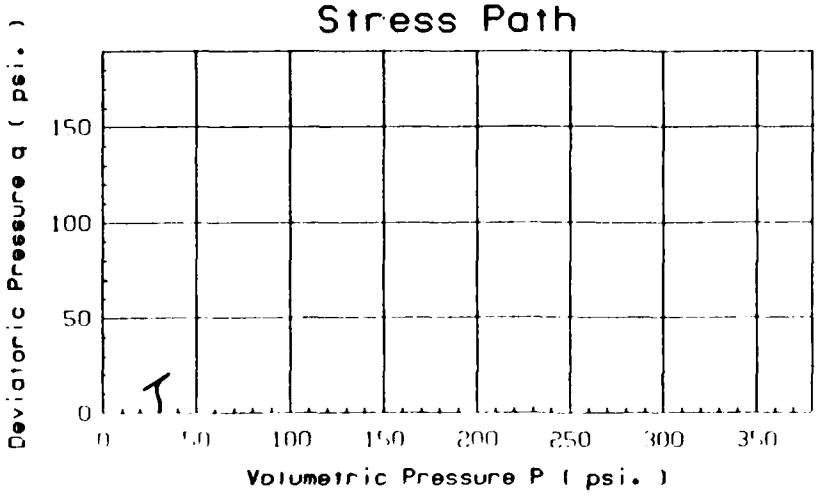

Test No. : BS3-8
Test Date : 10/6/86
Material : Bulk Sample #3
Sand (SW), 8.0% fines.
γ_d = 100.56 pcf
$\bar{B}$ = 0.993
$\sigma_{3,c}'$ = 29.9 psi
Strain RATE = 27.20% per hour

Figure A-8: IC-$\bar{U}$ TRIAXIAL TEST NO. BS3-8

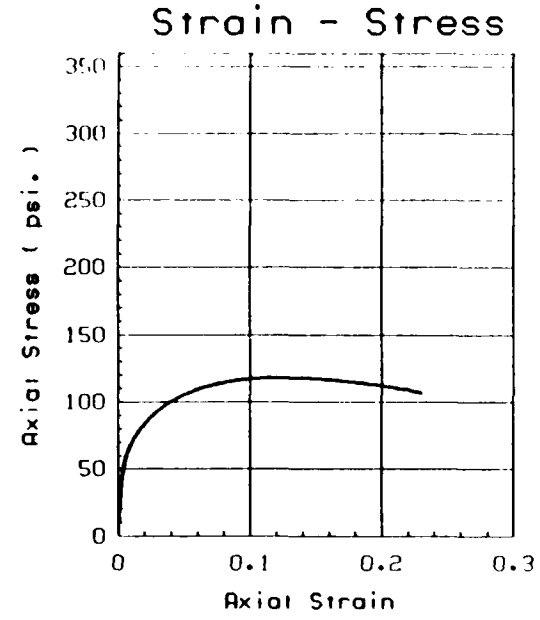

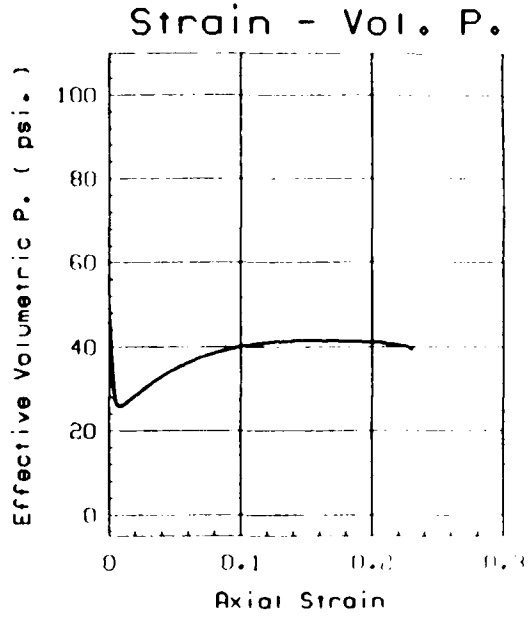

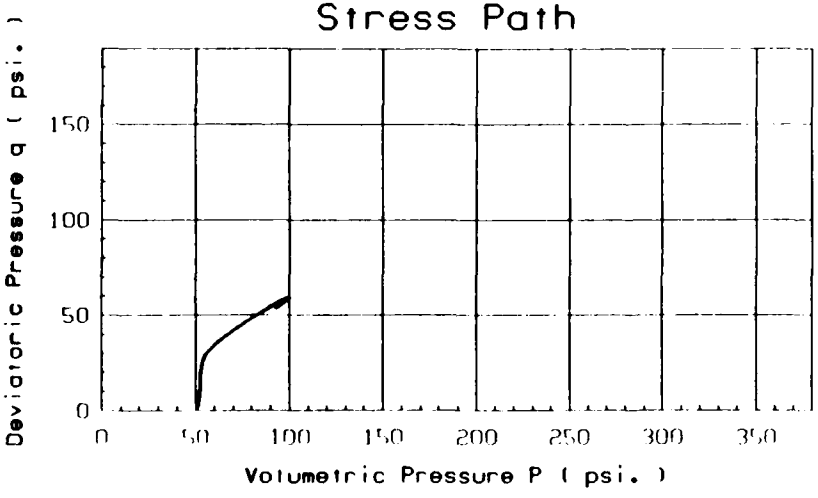

Test No. : BS3-9
Test Date : 10/7/86
Material : Bulk Sample #3
Sand (SW), 8.0% fines.
γ_d = 104.37 pcf
B = 0.992
$\sigma_{3,c}'$ = 49.7 psi
Strain RATE = 27.12% per hour

Figure A-9: IC-$\bar{U}$ TRIAXIAL TEST NO. BS3-9

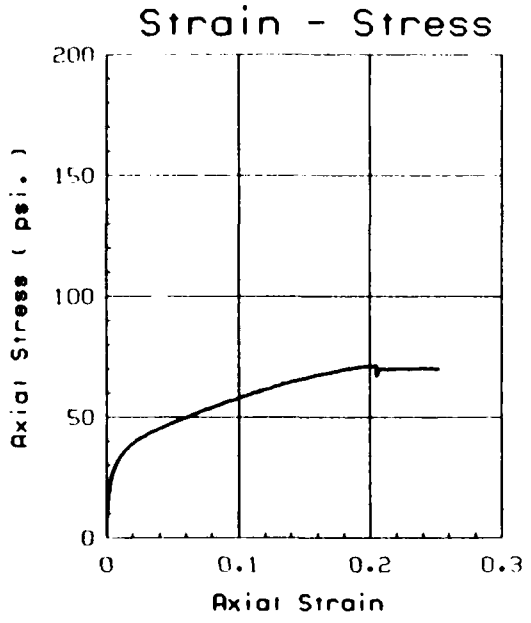

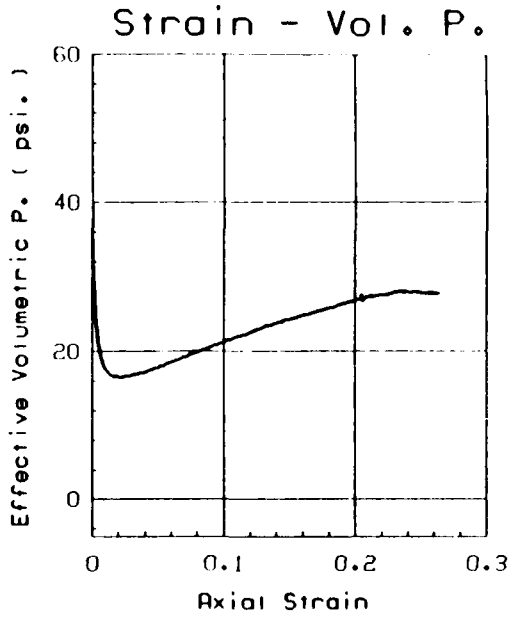

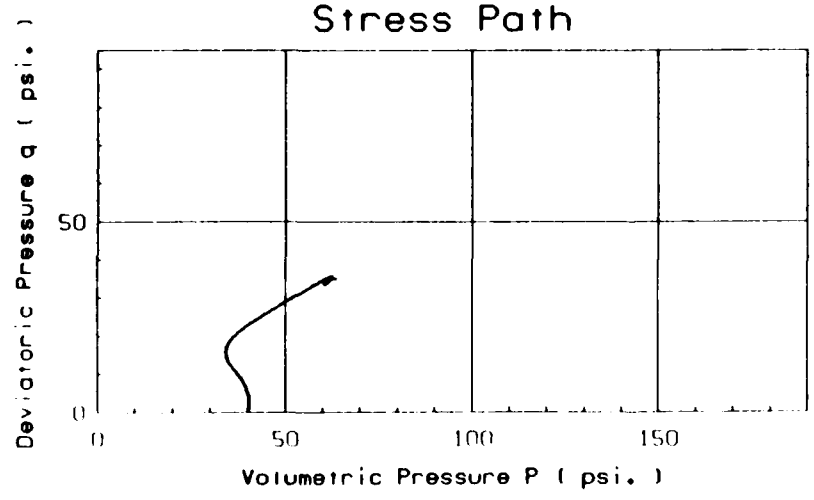

Test No. : BS7-1

Test Date : 6/22/86

Material : Bulk Sample #7

Silty Sand (SM), 48.0% fines.

γ_d = 108.57 pcf

B = 0.983

$\sigma_{3,c}'$ = 39.9 psi

Strain RATE = 4.5% per hour

Figure A-10: IC-$\bar{U}$ TRIAXIAL TEST NO. BS7-1

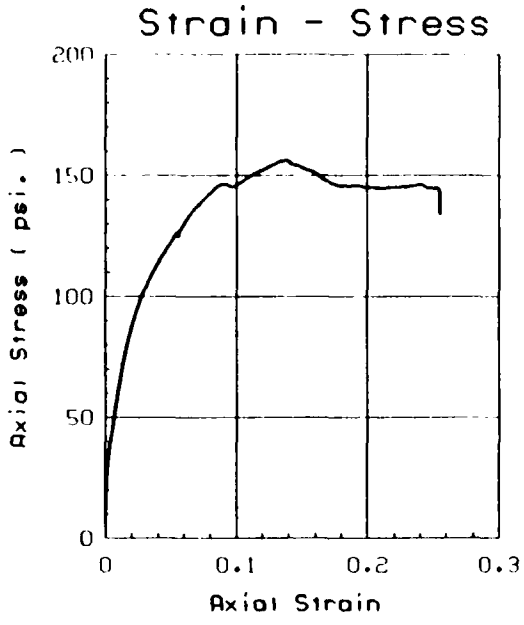

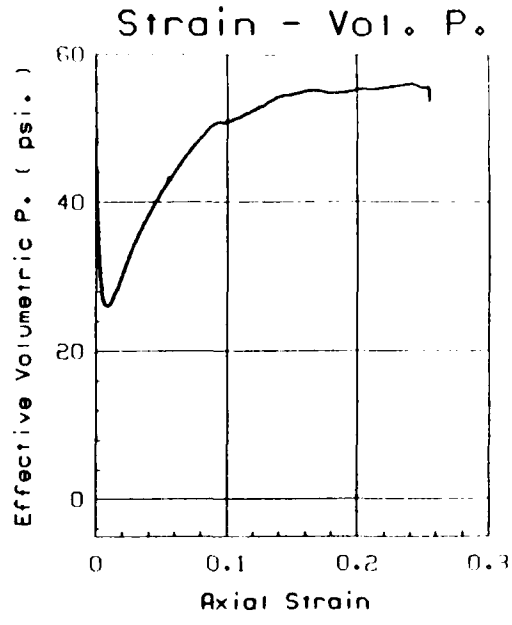

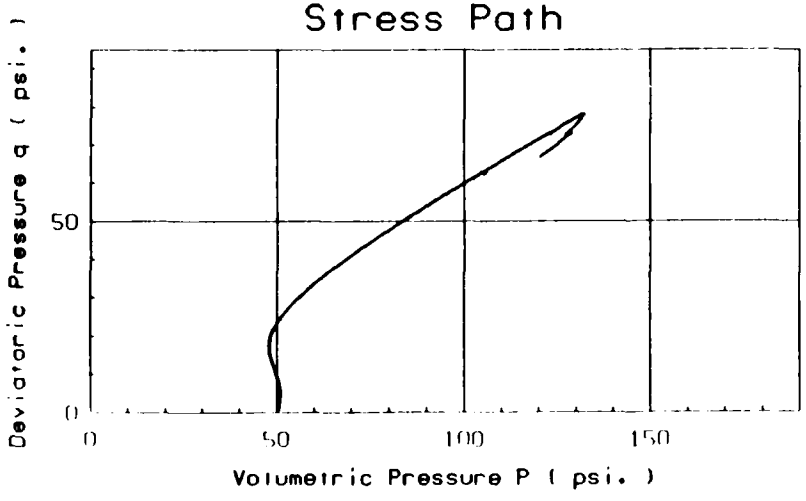

Test No. : BS7-2
Test Date : 6/26/86
Material : Bulk Sample #7
Silty Sand (SM), 48.0% fines
γ_d = 112.20 pcf
$\bar{B}$ = 0.982
$\sigma_{3,c}'$ = 49.9 psi
Strain RATE = 4.3% per hour

Figure A-11: IC-$\bar{U}$ TRIAXIAL TEST NO. BS7-2

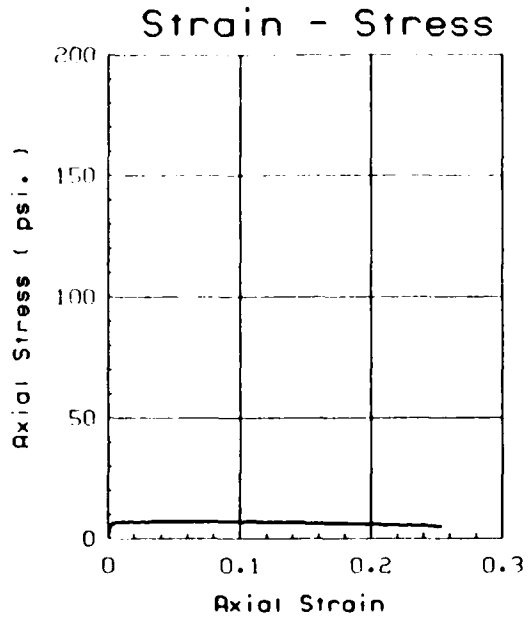

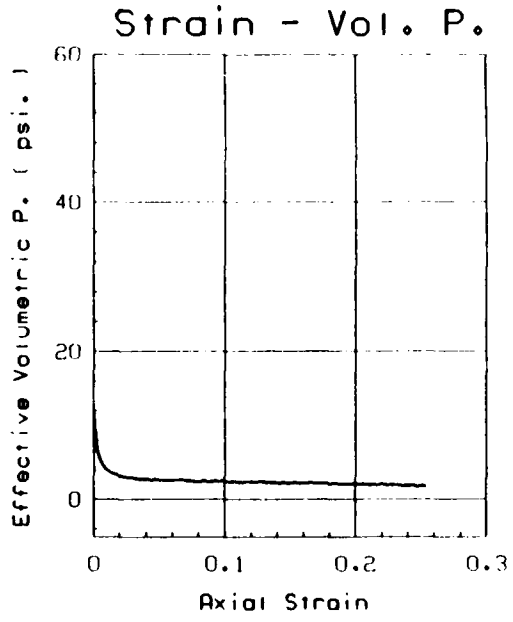

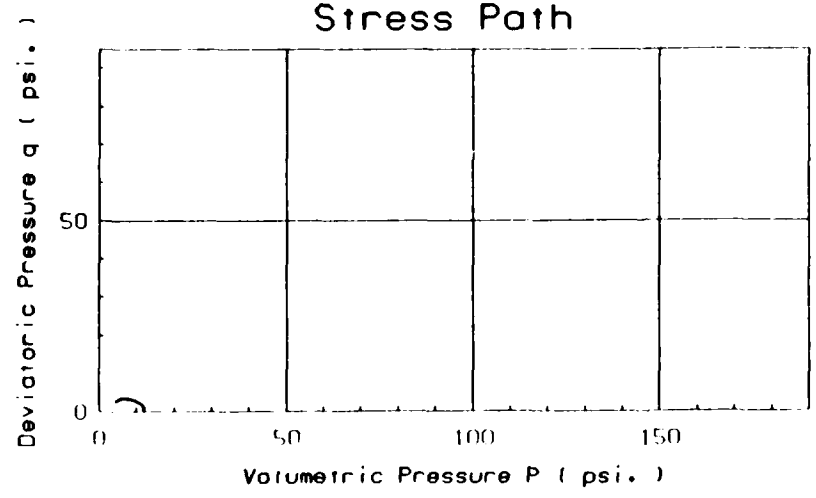

Test No. : BS7-3

Test Date : 6/30/86

Material : Bulk Sample #7

Silty Sand (SM), 48.0% fines.

γ_d = 101.78 pcf

$\overline{B}$ = 0.984

$\sigma_{3,c}'$ = 12.0 psi

Strain RATE = 4.5% per hour

Figure A-12: IC-$\overline{U}$ TRIAXIAL TEST NO. BS7-3

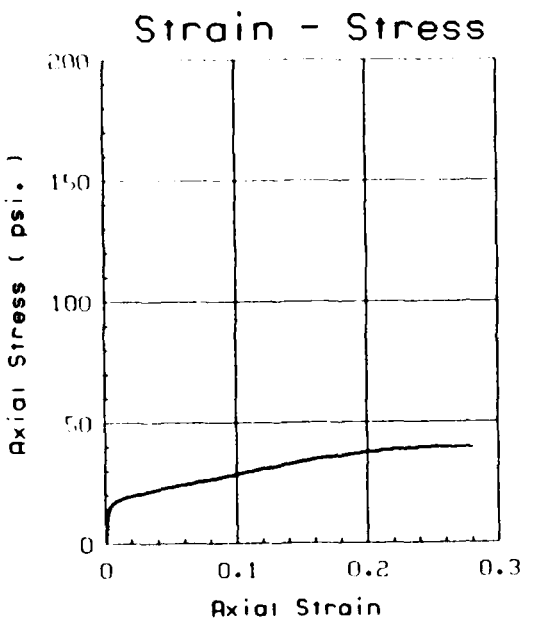

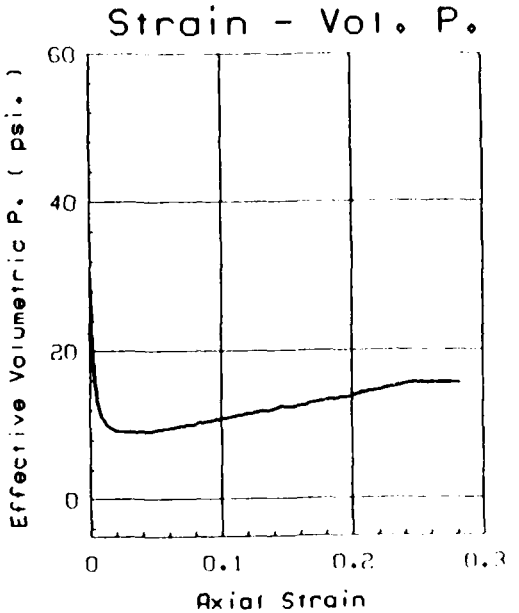

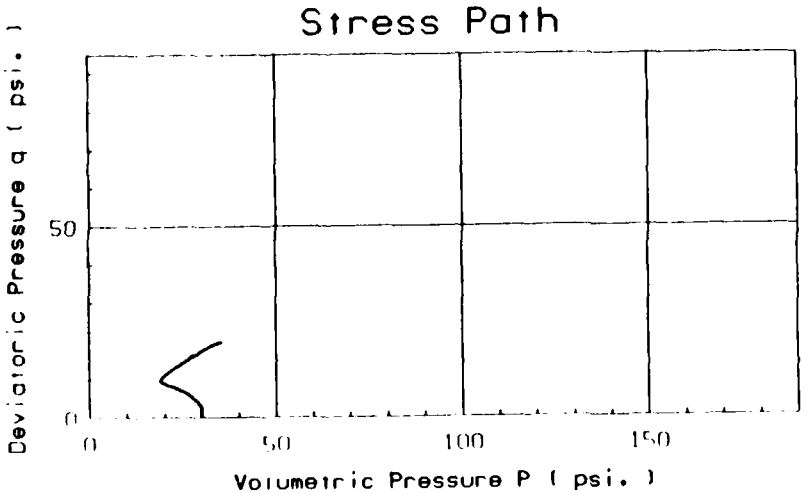

Test No. : BS7-4
Test Date : 7/5/86
Material : Bulk Sample #7
Silty Sand (SM), 48.0% fines.
γ_d = 106.85 pcf
$\overline{B}$ = 0.975
$\sigma_{3,c}'$ = 29.9 psi
Strain RATE = 4.6% per hour

Figure A-13: IC-$\overline{U}$ TRIAXIAL TEST NO. BS7-4

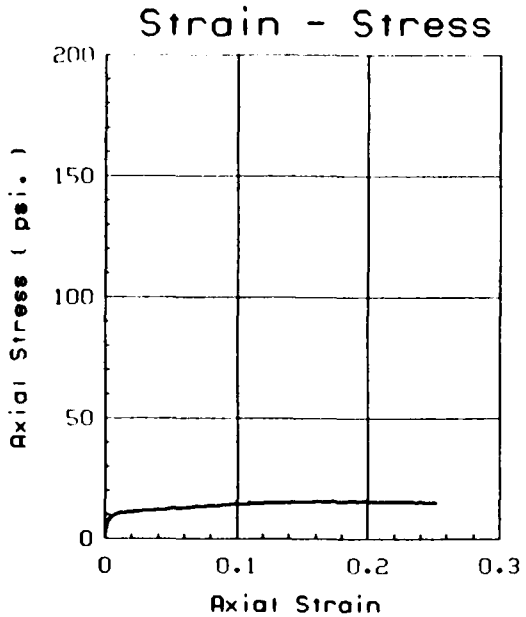

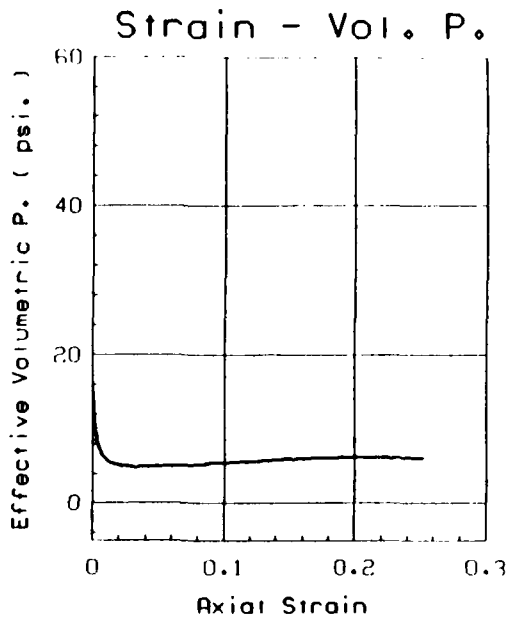

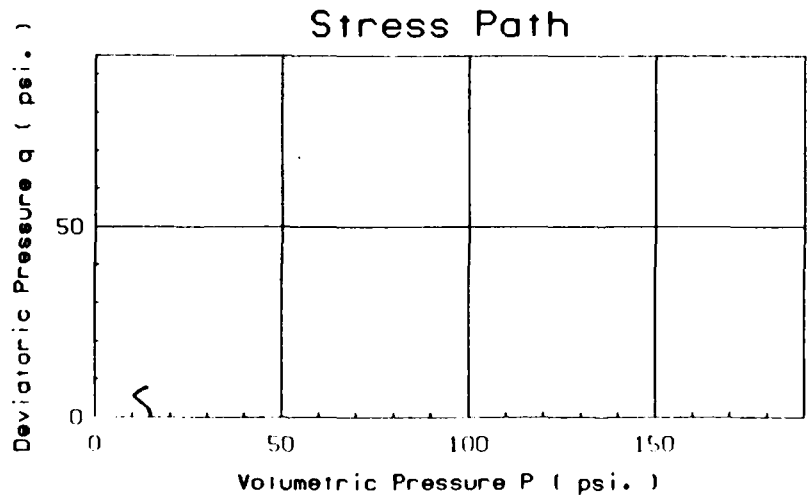

Test No. : BS7-5

Test Date : 7/12/86

Material : Bulk Sample #7

Silty Sand (SM), 48.0% fines.

γ_d = 104.24 pcf

$\bar{B}$ = 0.974

$\sigma_{3,c}'$ = 15.0 psi

Strain RATE = 4.5% per hour

Figure A-14: IC-$\bar{U}$ TRIAXIAL TEST NO. BS7-5

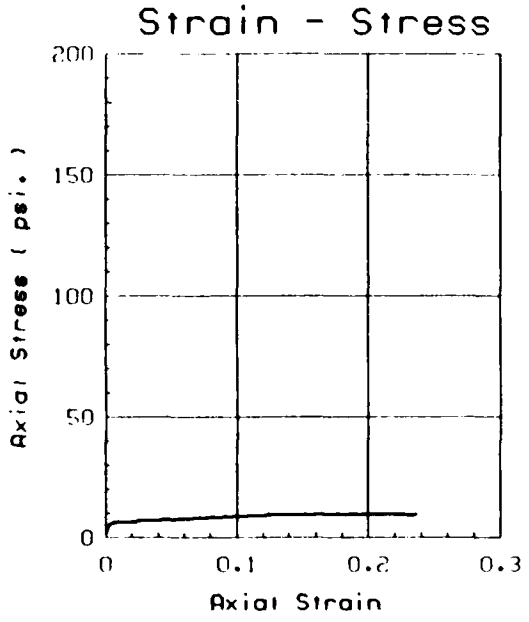

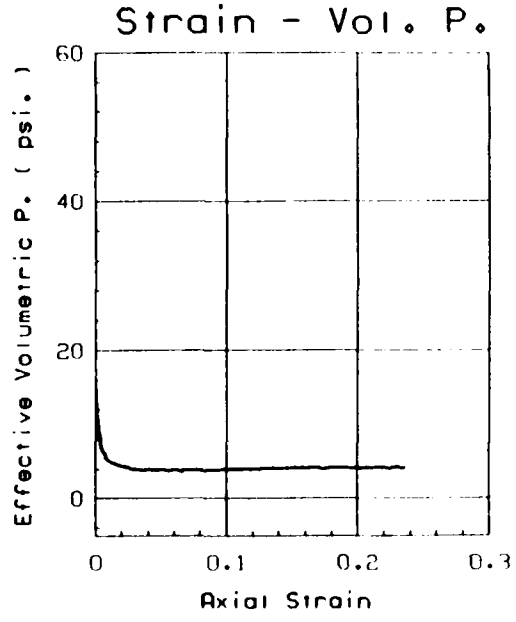

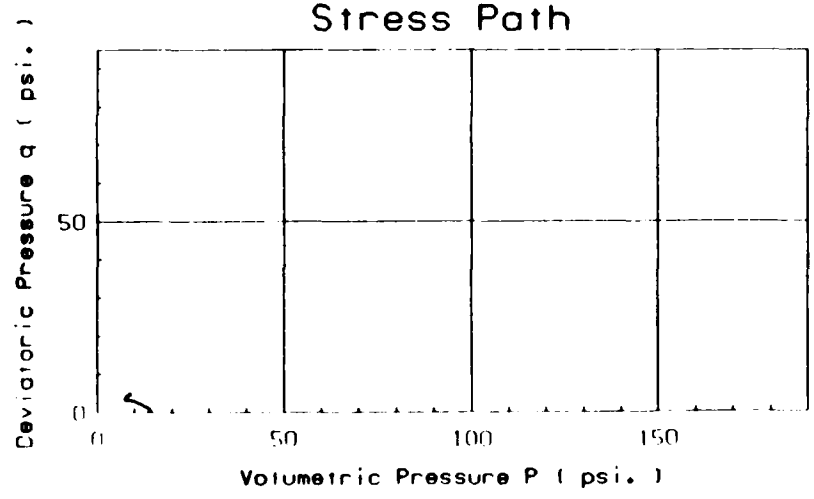

Test No. : BS7-6
Test Date : 10/26/86
Material : Bulk Sample #7
Silty Sand (SM), 48.0% fines.
γ_d = 103.23 pcf
$\overline{B}$ = 0.996
$\sigma_{3,c}'$ = 14.8 psi
Strain RATE = 5.05% per hour

Figure A-15: IC-$\overline{U}$ TRIAXIAL TEST NO. BS7-6

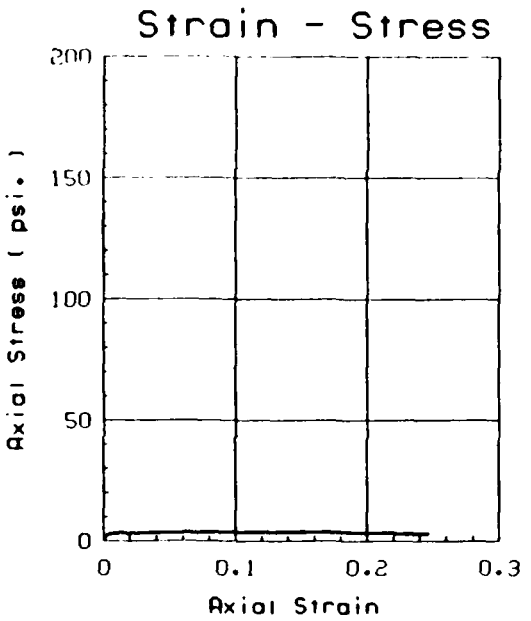

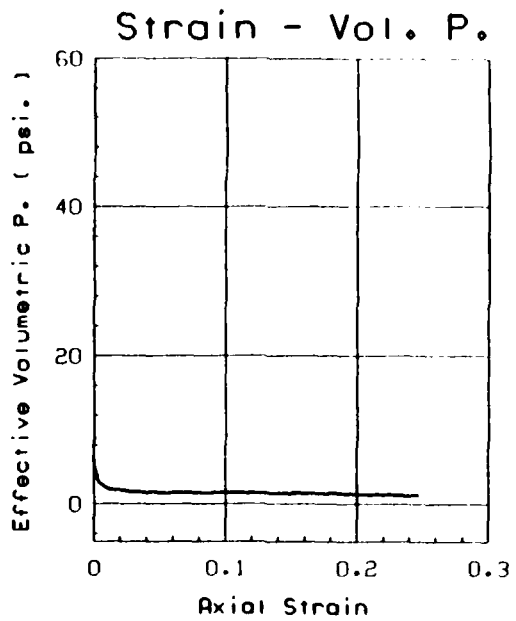

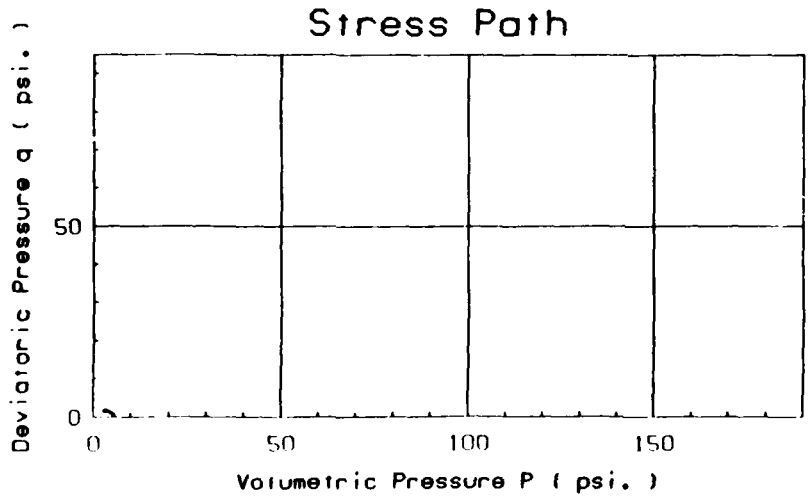

Test No. : BS7-7

Test Date : 10/28/86

Material : Bulk Sample #7

Silty Sand (SM), 48.0% fines.

γ_d = 98.84 pcf

$\overline{B}$ = 0.991

$\sigma_{3,c}'$ = 6.0 psi

Strain RATE = 5.01% per hour

Figure A-16: IC-$\bar{U}$ TRIAXIAL TEST NO. BS7-7

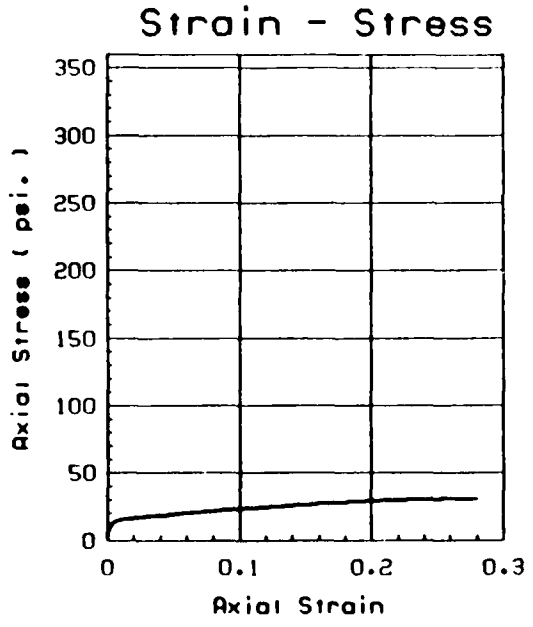

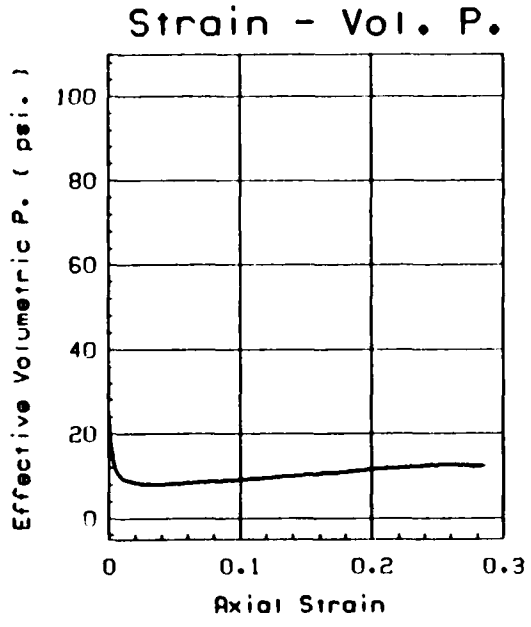

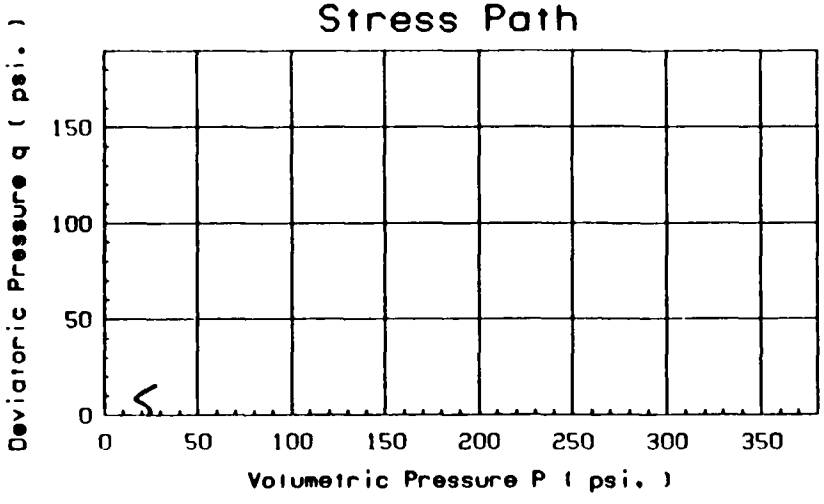

Test No. : BS7-8
Test Date : 10/24/86
Material : Bulk Sample #7
Silty Sand (SM), 48.0% fines.
γ_d = 105.11 pcf
$\overline{B}$ = 0.94
$\sigma_{3,c}'$ = 24.2 psi
Strain RATE = 4.4% per hour

Figure A-17: IC-$\overline{U}$ TRIAXIAL TEST NO. BS7-8

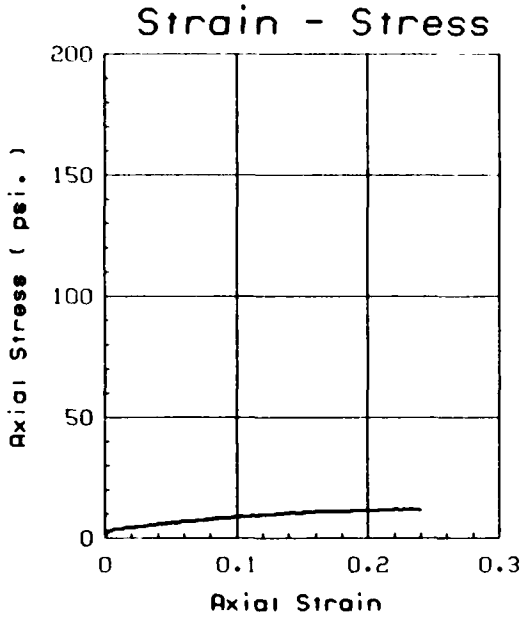

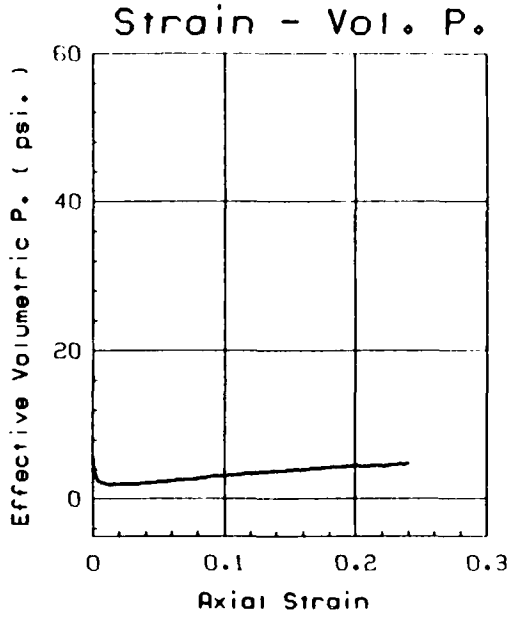

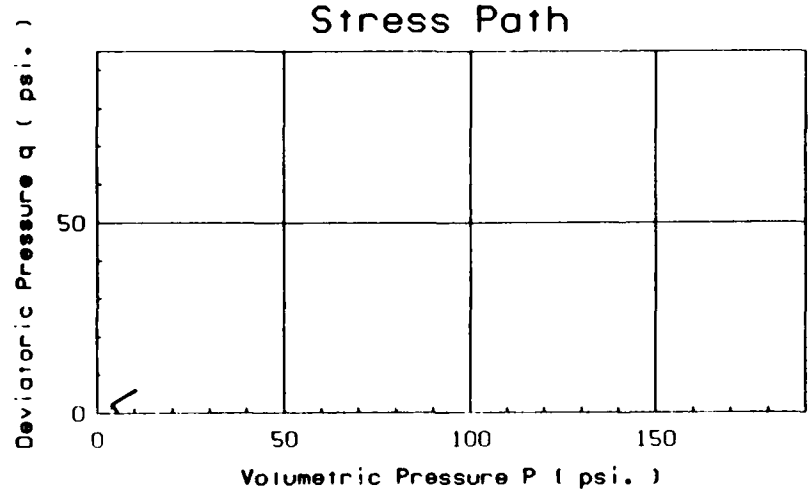

Test No. : BS7-2W
Test Date : 12/24/86
Material : Bulk Sample #7
Silty Sand (SM), 48.0% fines.
γ_d = 103.85 pcf
$\overline{B}$ = 0.989
$\sigma_{3,c}'$ = 5.5 psi
Strain RATE = 6.5% per hour

Figure A-18: IC-$\overline{U}$ TRIAXIAL TEST NO. BS7-2W

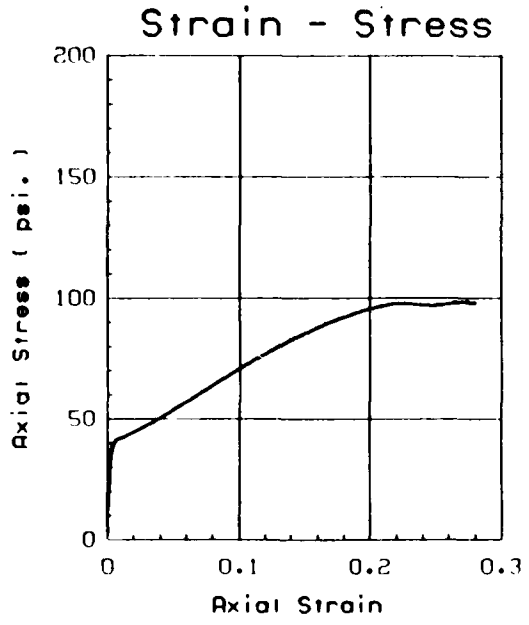

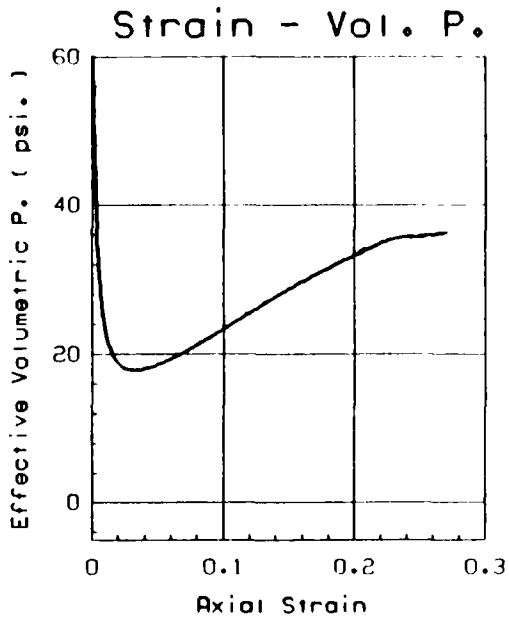

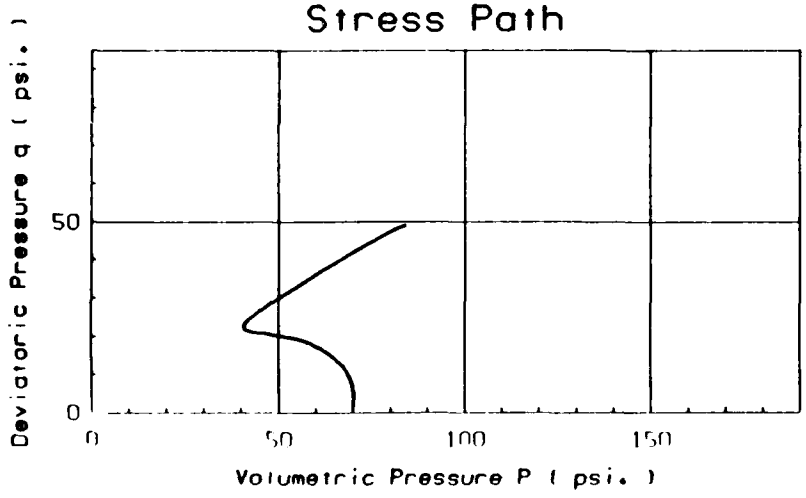

Test No. : BS7-3W
Test Date : 12/26/86
Material : Bulk Sample #7
Silty Sand (SM), 48.0% fines.
γ_d = 109.96 pcf
$\bar{B}$ = 0.991
$\sigma_{3,c}'$ = 69.3 psi
Strain RATE = 6.3% per hour

Figure A-19: IC-$\bar{U}$ TRIAXIAL TEST NO. BS7-3W

Section I-B: HANDLING AND TESTING OF UNDISTURBED SAMPLES

"Undisturbed" samples of hydraulic fill from the intact downstream portion of Lower San Fernando Dam were provided by Geotechnical Engineers, Inc. Sample void ratio changes during sampling, extrusion, test set-up and consolidation were continuously monitored so that steady-state strengths measured in laboratory IC-$\overline{U}$ triaxial tests could be "corrected" for void ratio changes in order to derive estimates of in-situ steady-state undrained strengths. Sample retrieval, handling and set-up procedures employed were designed to minimize both sample disturbance and sample volume (void ratio) changes.

B.1 Sampling

Two different sampling procedures were employed: (a) 2.8-inch diameter piston sampling with thinwalled Shelby-type tubes in conventional boreholes, and (b) 2.8-inch diameter hand-carved sampling within a large-diameter exploratory test shaft.

Void ratio changes during piston sampling were evaluated based on consideration of: (a) the ratio of the average diameter inside the lead cutting edge of the thinwall Shelby tube vs. the internal tube diameter, and (b) the ratio between the length of sampling tube penetration vs. the length of the sample inside the tube following removal from the borehole. Typical sampling penetration lengths were approximately 2 feet, so that 2-foot long samples were retrieved. Void ratio changes (Δe) during sampling were generally small; typical $\Delta e < 0.02$. Most piston samples were slightly densified during sampling, through a few samples dilated slightly.

Hand-carved samples were obtained by carving 2.8-inch diameter cylindrical block samples ahead of an advancing 2.8-inch diameter sampling tube. The tube was suspended by a sampling tripod, and was periodically lowered as hand-trimming progressed. Hand-carved samples were typically 14 inches in length. Volume changes during hand-carved sampling were evaluated using measurements similar to those used to evaluate piston sampling-induced volume changes. Void ratio changes during hand-carved sampling were generally small, and most samples densified slightly during sampling through some samples dilated slightly.

Following sampling, all samples were trimmed and the length from the tube ends to the ends of the samples were recorded so that sample volume changes during transport could be monitored. After trimming and measuring, fixed "packers" were inserted in the sample tubes to confine the samples during transport. Most of the samples arrived at Stanford University having undergone no volume change during transport.

B.2 Sample Extrusion and Test Set-Up:

Prior to sample extrusion, x-ray photographs of each sample tube were consulted to identify attractive sample zones. Sample zones showing striations due to layering between distinct soil zones of different gradation were not tested. Attractive sample zones were marked on the tube, and the end packers were briefly removed so that sample volume changes during transport could be evaluated. Any measured changes in sample length were assumed to represent volume change distributed uniformly over the full length of the sample. Measured transportation volume changes were typically negligible.

The tubes were next clamped vertically in a chain vise for cutting, with a free-moving packer plate on top of the sample as a measuring reference and a fixed packer supporting the base of the sample in the tube. All cuts were made approximately 2 to 3 cm from the preliminary "desired" final triaxial test sample ends, and the chain vise was applied approximately one inch from the cutting locations. A pair of circumferential ring stiffeners were applied approximately one and two inches above the cutting location, respectively. Each stiffener consisted of a steel ring with six radial screws which were lightly hand-tightened to provide radial pressure and confinement to minimize tube distortion during cutting. The tube was cut by hand using a rotary pipe cutter. Light cutting contact pressure was applied and the cutter was rotated slowly to minimize tube distortions. Cutting pressure and rate were further decreased immediately prior to "break-through". Each tube "cut" required approximately 30 to 60 minutes. All cutting was performed by two personnel who were rigorously drilled and practiced on numerous "dummy" tubes prior to being allowed to work on actual sample tubes. The care taken in cutting the sample tubes appears to have been successful, as sample volume changes during tube cutting were typically negligible. (Volume changes were evaluated by measuring the distance from the top of the tube to the free-moving packer plate at the top of the sample both before and after cutting.) In the few instances that minor volume changes were measured, these were assumed to be distributed within the top "triaxial sample length" within the tube, as tube movements (distortions) during cutting were localized at the tube end being cut.

The cutting process resulted in a slight inward rotation at the new lip of the cut tube, and some minor "burring" of this lip. The sample was next trimmed to approximately one to two centimeters from the newly cut tube end, and this lip was reduced and "de-burred" by hand using a sharp surgical knife and a tungsten machinist's hand cutting blade. Measurements before and after de-burring consistently showed that this process caused no sample volume change.

Next the tube was advanced vertically and re-clamped in the chain vise, and similar procedures were used to make a second tube cut approximately at the base of the "desired" triaxial sample. This lower end cut was not de-burred, as the sample would be subsequently extruded through the upper end of the newly produced short tube section. A thin steel plate with a sharp cutting edge was passed through the lower cut to separate the new short tube section and sample from the parent tube. Lower cuts were consistently found to produce no measurable sample volume change.

This process resulted in production of short tube (and sample) sections, with sample volume changes and dimensions of known (and typically negligible) magnitude. These short tube sections were then clamped vertically in a chain vise, and a stiff steel loading plate with a diameter almost equal to the sample diameter was placed beneath the sample. A hand-operated hydraulic jack was used to extrude the sample by applying force to this steel base plate. Samples were extruded in the direction of sample ingress during initial sampling to avoid shear reversal, and were extruded through the "de-burred" ends of the short sample tube sections. Some samples were placed overnight on porous stones in a shallow water bath to draw water by capillary rise

prior to extrusion, as this was found to be beneficial in reducing sample/tube wall interface friction, particularly in "sandy" samples.

Samples were extruded into a confining membrane held by external vacuum pressure to the sides of a forming mold with a diameter slightly larger than the sample diameter so that no sample/membrane contact occurred during extrusion. A gap between the top of the short sample tube and the base of the forming mold permitted examination of the sample during extrusion so that striated samples with distinct layers of variable gradation could be avoided. A number of samples were discarded because of such striation or layering at this stage, and several additional samples had one end trimmed "short" resulting in occasional testing of "short" triaxial samples with height: diameter ratios as low as 1.8:1 to optimize sample homogeneity.

Following extrusion, the vacuum pressure holding the membrane to the sides of the forming mold was released so that this membrane applied a light lateral confining stress to the sides of the extruded sample. A top cap and base plate were applied to the ends of the sample, and the membrane was sealed to these with O-rings. A vacuum pressure of 0.25 ksc was then applied to primarily "sandy" samples, but none to primarily "silty" samples, and the samples were then placed in a triaxial cell for testing. The average sample diameter and sample height were measured at this stage to evaluate sample volume changes during extrusion. These were usually found to be small but not negligible, and were typically compressive though a few sandy samples dilated during extrusion.

A number of samples were difficult to extrude, apparently due to sample/tube wall interface friction associated with rust accumulation

on the tube walls. This was observed only with predominantly "sandy" samples. Several samples which were difficult to extrude were also found to suffer significant volume change during extrusion, and these samples were discarded at this stage.

B.3 C-$\bar{U}$ Triaxial Testing:

Samples were saturated using the vacuum/back pressure saturation techniques described in Section 2.2.1. A number of undisturbed samples with high fines content were found to have high initial degrees of saturation immediately after extrusion, and the vacuum application stage of the vacuum/back pressure saturation process was omitted for these samples. Upon completion of back-pressure saturation, samples were consolidated to the desired initial effective confining stress conditions ($\sigma'_{1,c}$ and $\sigma'_{3,c}$). Volume changes were measured during consolidation.

Two types of undrained loading were applied to samples following initial consolidation: (a) monotonic axial loading to large strain for undrained residual or steady-state strength evaluation, or (b) cyclic axial loading for evaluation of undrained cyclic pore pressure generation and cyclic strain behavior. Monotonic loading was strain-controlled, and axial strain rates for each sample were selected to permit equalization of the internal sample pore pressure field during testing. Cyclic loading was computer-controlled/stress-controlled loading with uniform sinusoidal loading cycles. Cyclic loading rates varied from sample to sample, and were between 0.1 Hz and 0.5 Hz.

After completion of undrained shear testing, the final sample void ratio was determined by measuring and drying the entire sample. Void ratio estimates based on final dry unit weight and final sample volume

were found to be in close agreement with void ratio estimates based on final (fully saturated) water content.

Section I-C: IC-$\bar{U}$ TRIAXIAL TESTS ON UNDISTURBED SAMPLES

A total of 16 isotropically consolidated-undrained triaxial tests were performed on "undisturbed" samples of hydraulic fill from the downstream shell of Lower San Fernando Dam. Sample extrusion and testing procedures employed are described in Section I-B. All samples tested had a nominal diameter of 2.8-inches. Table I-4 summarizes testing conditions as well as the results of these IC-$\bar{U}$ tests. Figures C-1 through C-32 present plots of (a) axial stress vs. axial strain, (b) effective confining stress (σ_3') vs. axial strain, (c) deviatoric stress $(1/2)(\sigma_1 - \sigma_3)$ vs. $(1/2)(\sigma_1' - \sigma_3')$ and (d) soil gradation for each of the samples tested.

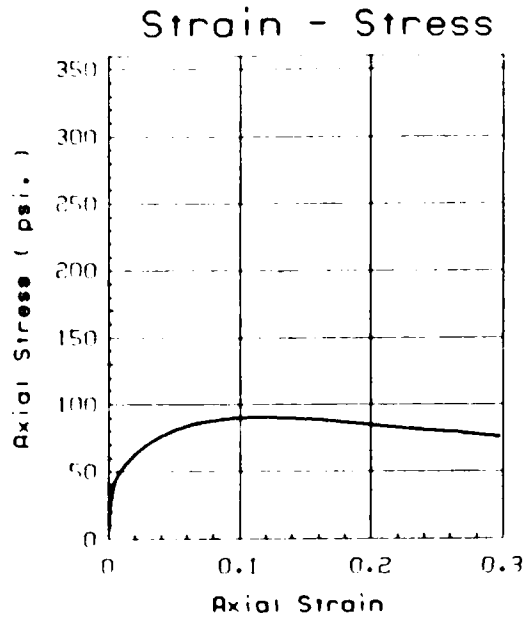

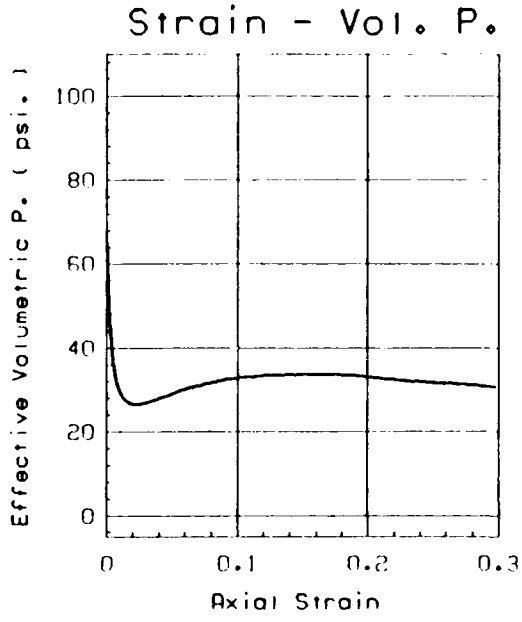

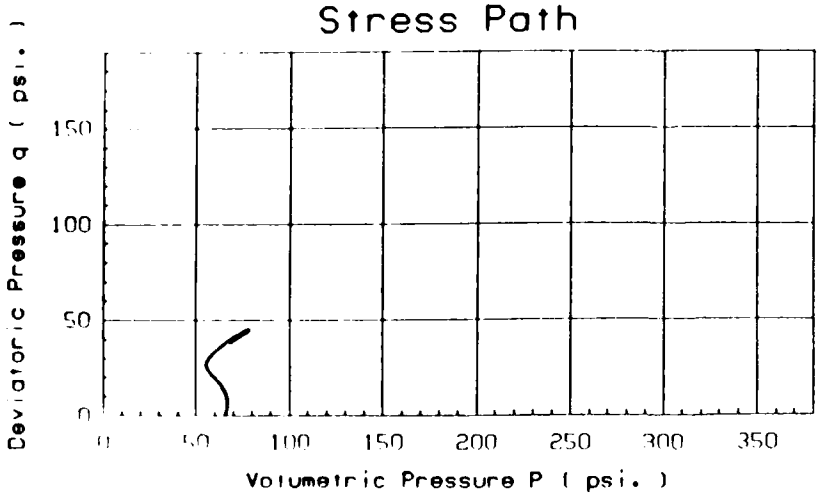

Test No. : 4

Test Date : 7/25/86

Material : Tube U111A-UF18

Silty Sand (SM-ML), 22% fines.

γ_d = 106.42 pcf

$\bar{B}$ = 0.994

$\sigma_{3,c}'$ = 65.1 psi

Strain RATE = 33.6% per hour

Figure C-1: IC-$\bar{U}$ TRIAXIAL TEST NO. 4: HYDRAULIC FILL

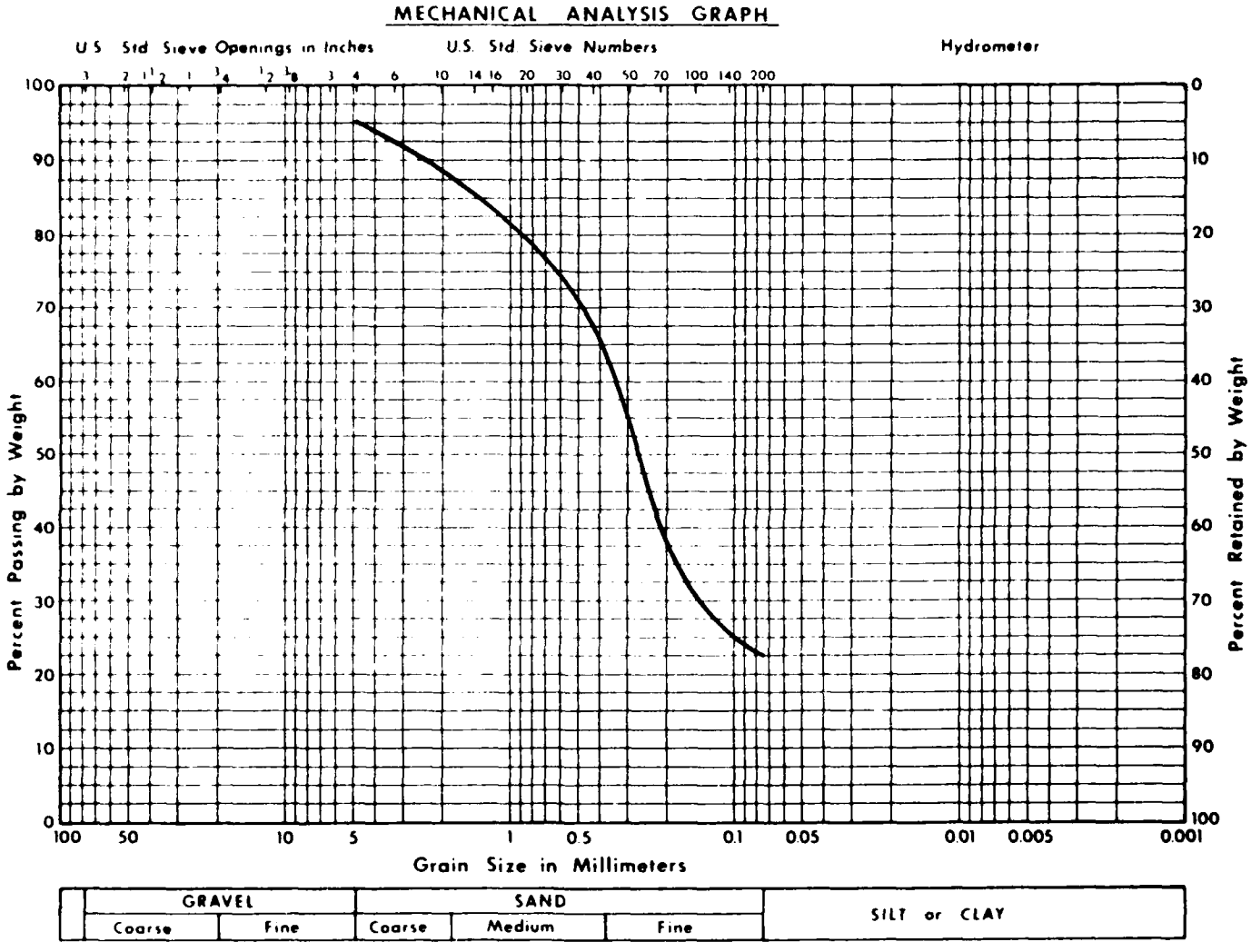

Figure C-2: GRAIN SIZE DISTRIBUTION; IC-$\bar{U}$ TEST SAMPLE NO. 4

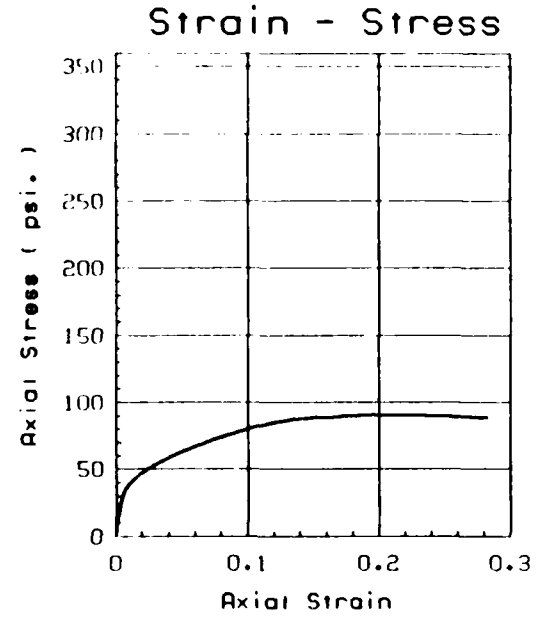

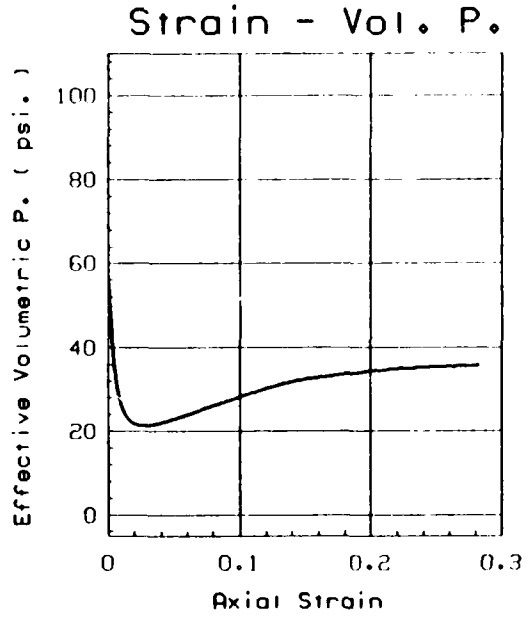

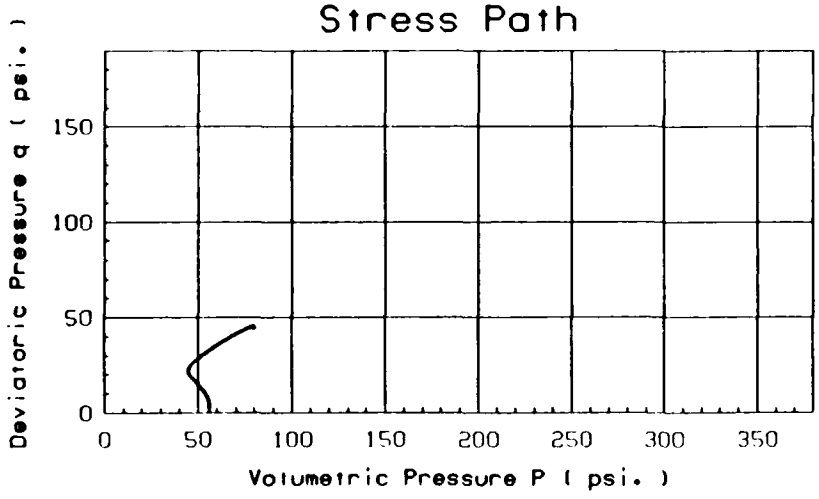

Test No. : 7

Test Date : 7/29/86

Material : Tube U111-UF18

Sandy Clayey Silt (ML), 70% fines.

γ_d = 100.88 pcf

$\bar{B}$ = 0.995

$\sigma_{3,c}'$ = 55.3 psi

Strain RATE = 6.82% per hour

Figure C-3: IC-$\bar{U}$ TRIAXIAL TEST NO. 7: HYDRAULIC FILL

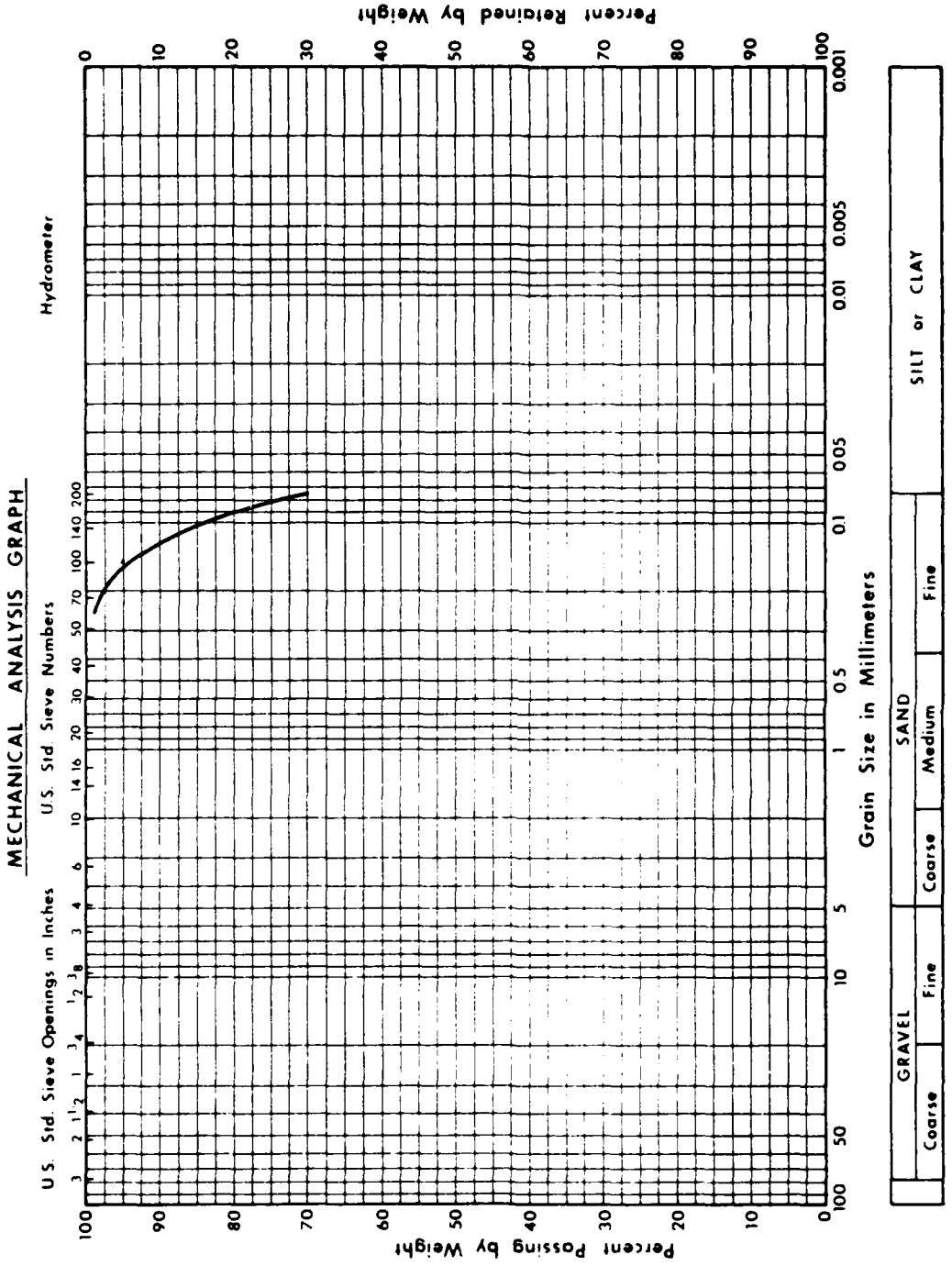

Figure C-4: GRAIN SIZE DISTRIBUTION; IC-$\bar{U}$ TEST SAMPLE NO. 7

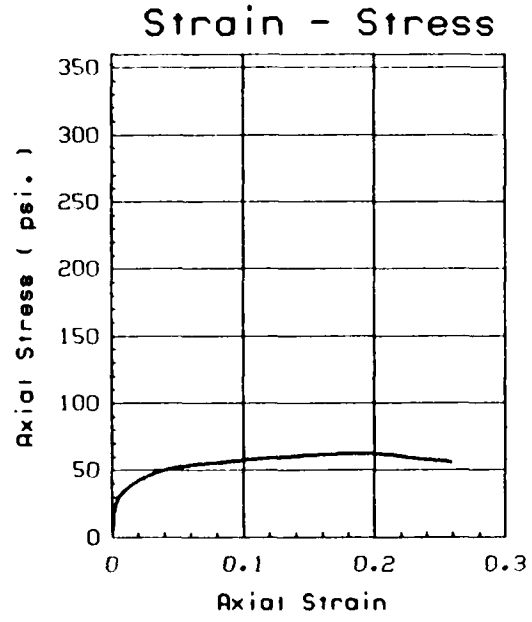

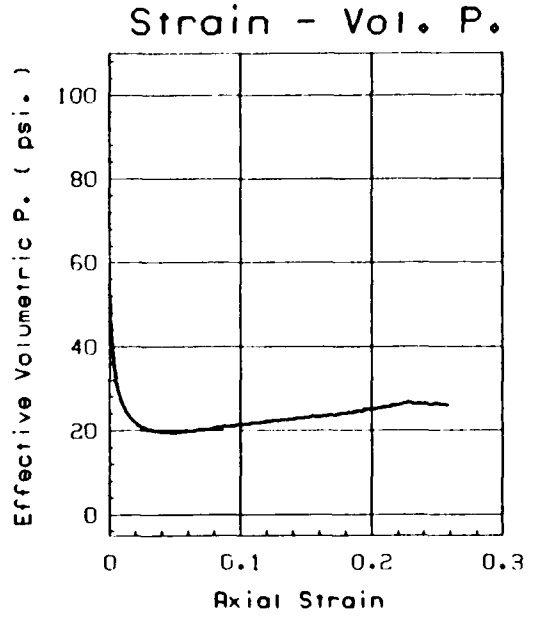

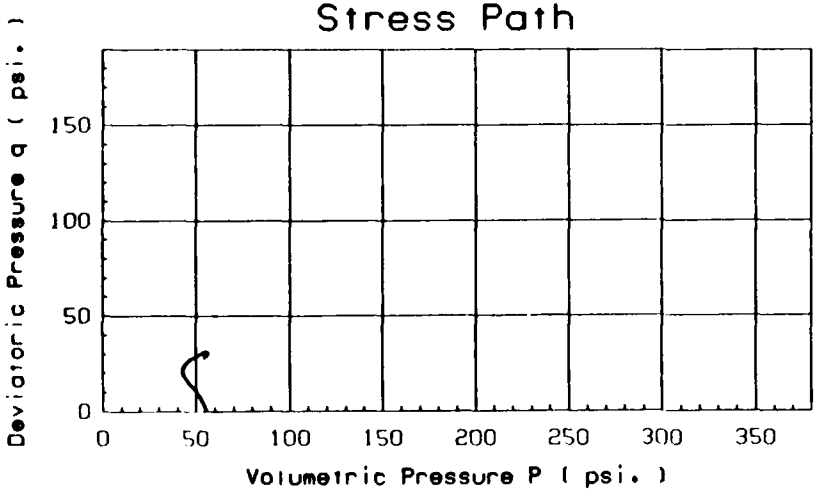

Test No. : 10

Test Date : 8/2/86

Material : Tube U104-UF4

Sandy Clayey Silt (ML), 85% fines.

γ_d = 94.21 pcf

$\bar{B}$ = 0.996

$\sigma_{3,c}'$ = 54.9 psi

Strain RATE = 6.5% per hour

Figure C-5: IC-$\bar{U}$ TRIAXIAL TEST NO. 10: HYDRAULIC FILL

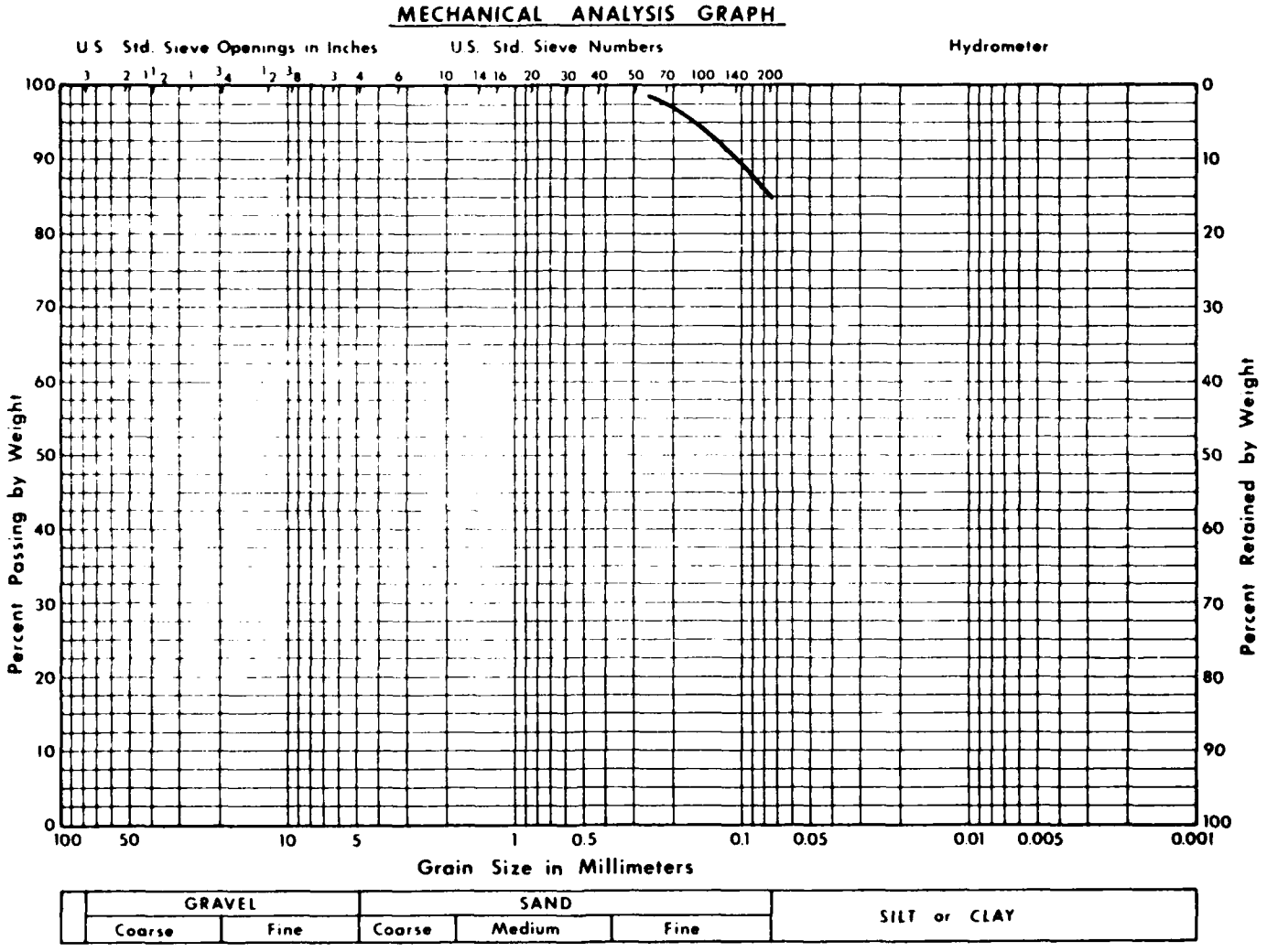

Figure C-6: GRAIN SIZE DISTRIBUTION; IC-$\bar{U}$ TEST SAMPLE NO. 10

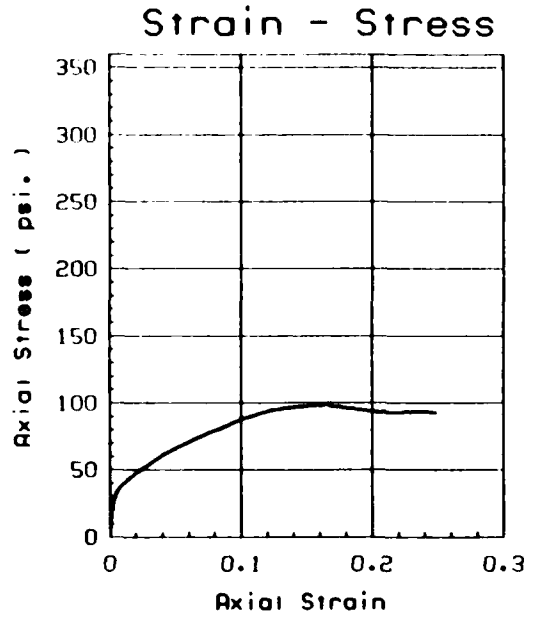

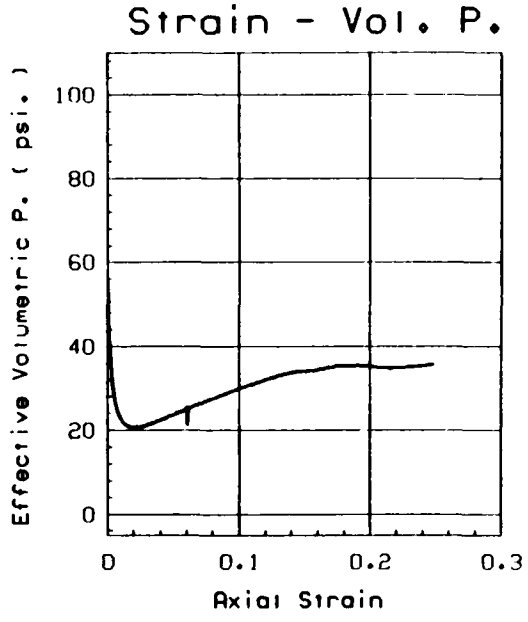

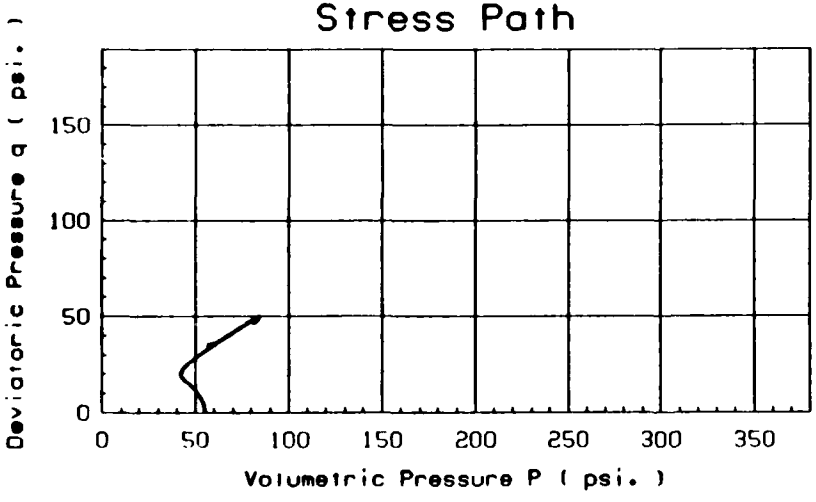

Test No. : 11

Test Date : 8/5/86

Material : Tube U104-UF4

Sandy Clayey Silt (ML), 78% fines.

γ_d = 97.51 pcf

$\overline{B}$ = 0.986

$\sigma_{3,c}'$ = 53.4 psi

Strain RATE = 7.9% per hour

Figure C-7: IC-$\overline{U}$ TRIAXIAL TEST NO. 11: HYDRAULIC FILL

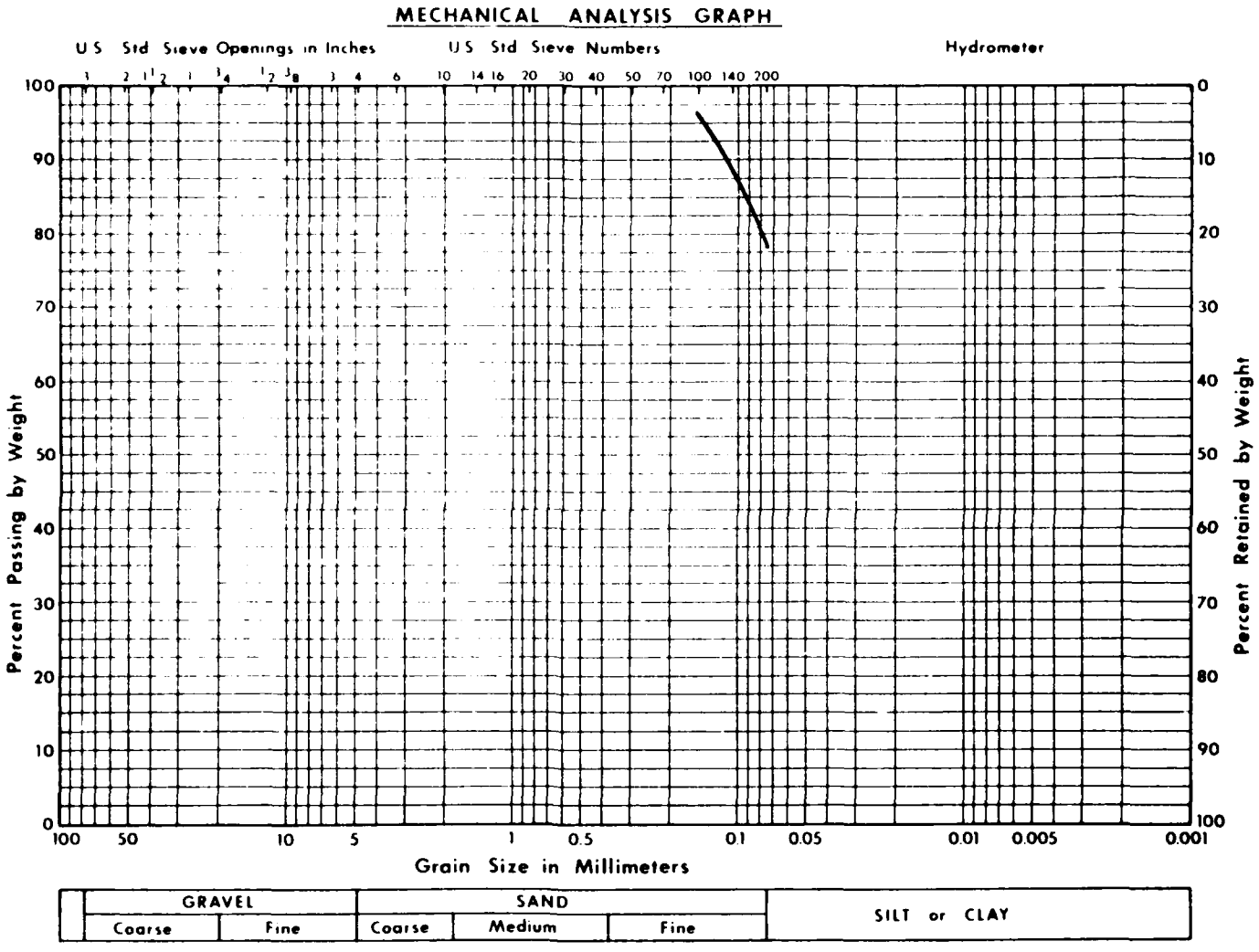

Figure C-8: GRAIN SIZE DISTRIBUTION; IC-$\bar{U}$ TEST SAMPLE NO. 11

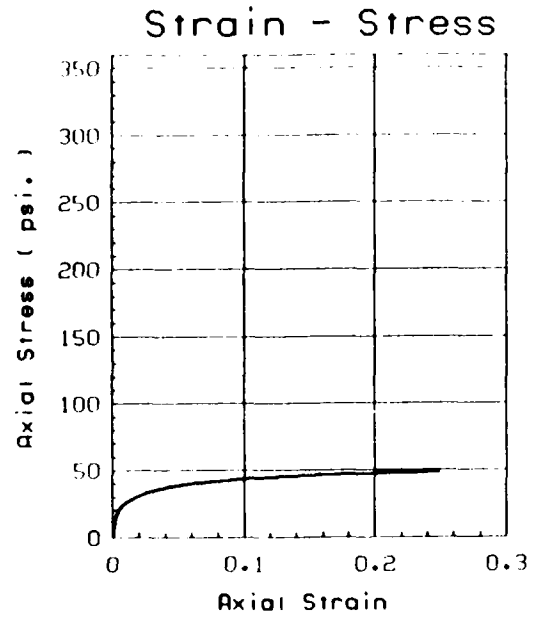

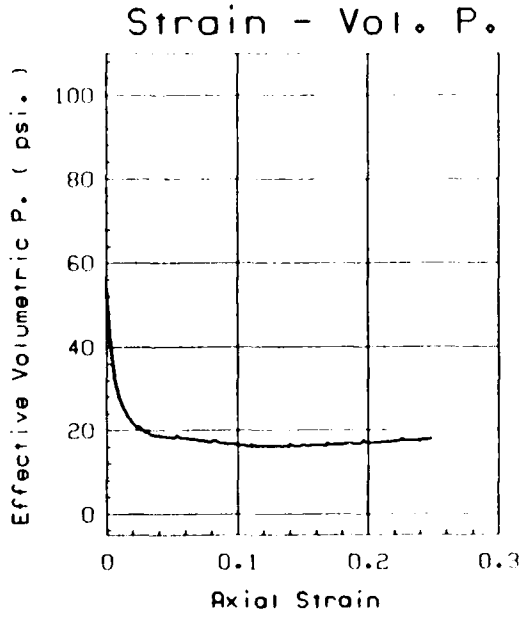

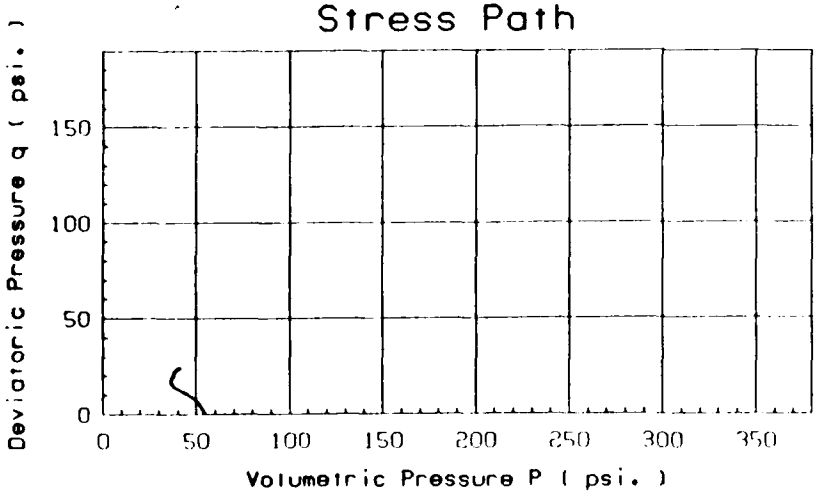

Test No. : 12

Test Date : 8/7/86

Material : Tube U111-UF6

Sandy Clayey Silt (ML), 78% fines.

γ_d = 97.02 pcf

$\bar{B}$ = 0.991

$\sigma_{3,c}'$ = 54.5 psi

Strain RATE = 8.6% per hour

Figure C-9: IC-$\bar{U}$ TRIAXIAL TEST NO. 12: HYDRAULIC FILL

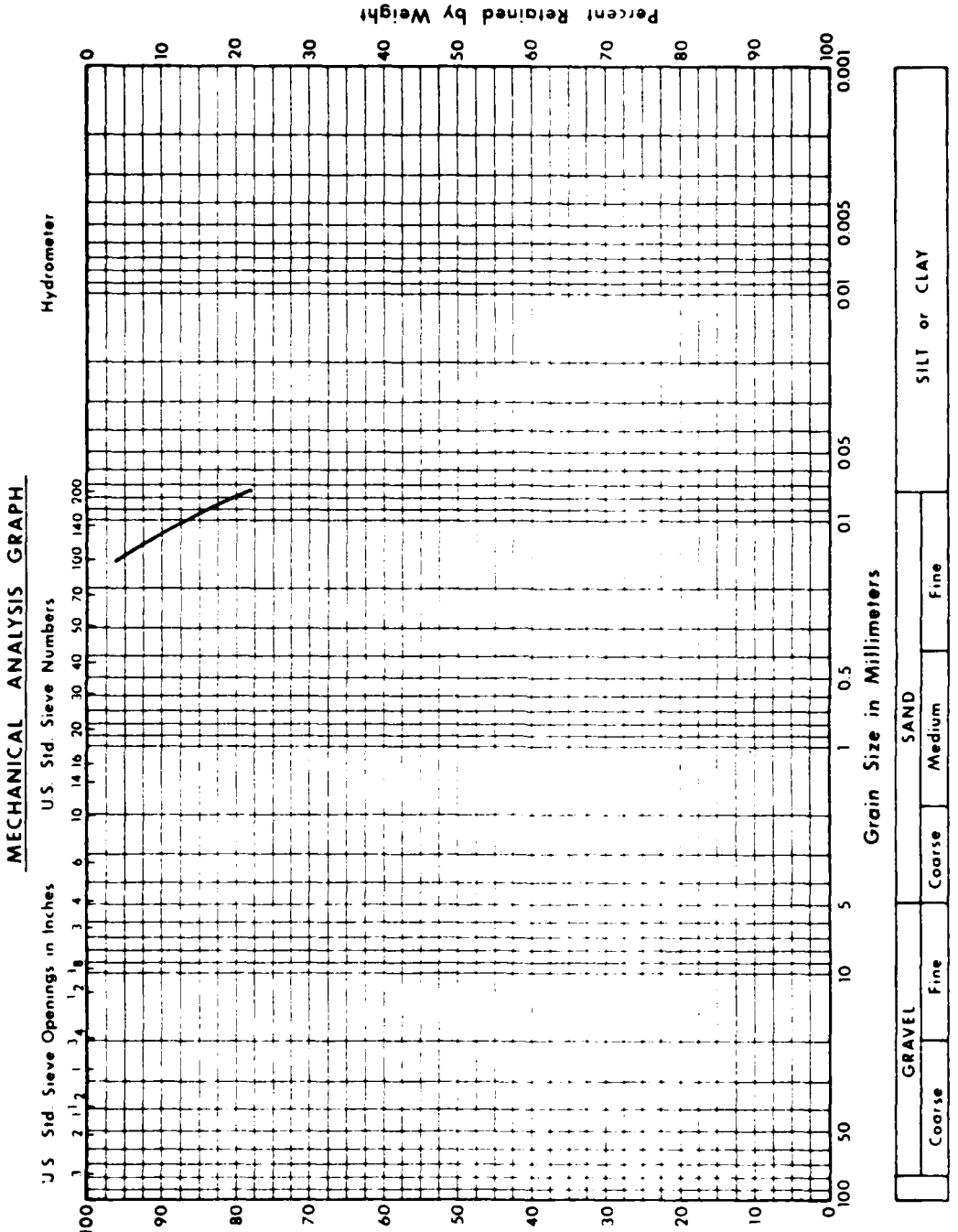

Figure C-10: GRAIN SIZE DISTRIBUTION; IC-$\bar{U}$ TEST SAMPLE NO. 12

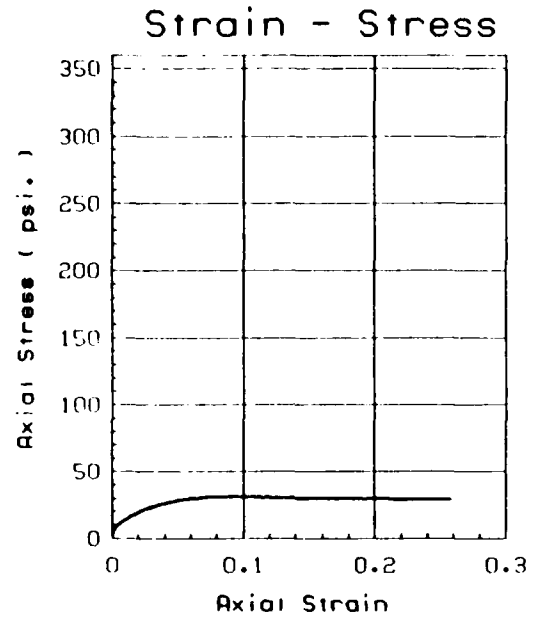

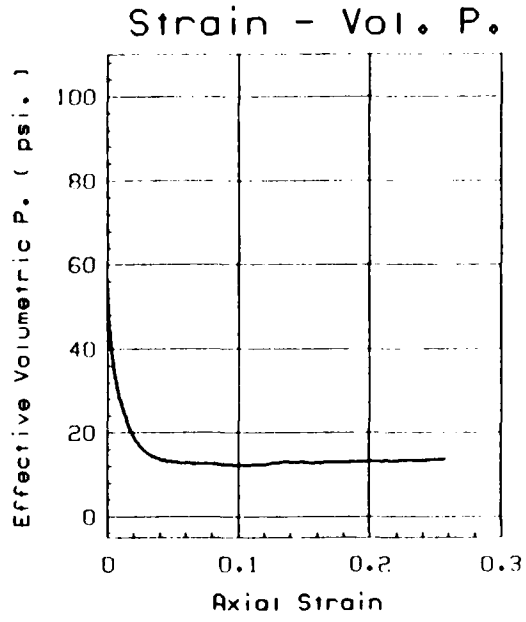

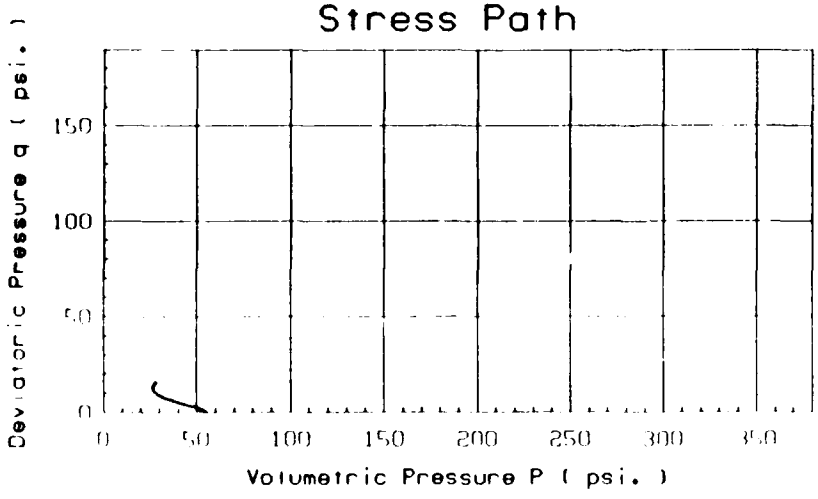

Test No. : 14

Test Date : 8/12/86

Material : Tube U102-UF1

Sandy Clayey Silt (ML), 83% fines.

γ_d = 95.36 pcf

$\bar{B}$ = 0.998

σ_3' = 54.6 psi

Strain RATE = 8.9% per hour

Figure C-11: IC-$\bar{U}$ TRIAXIAL TEST NO. 14: HYDRAULIC FILL

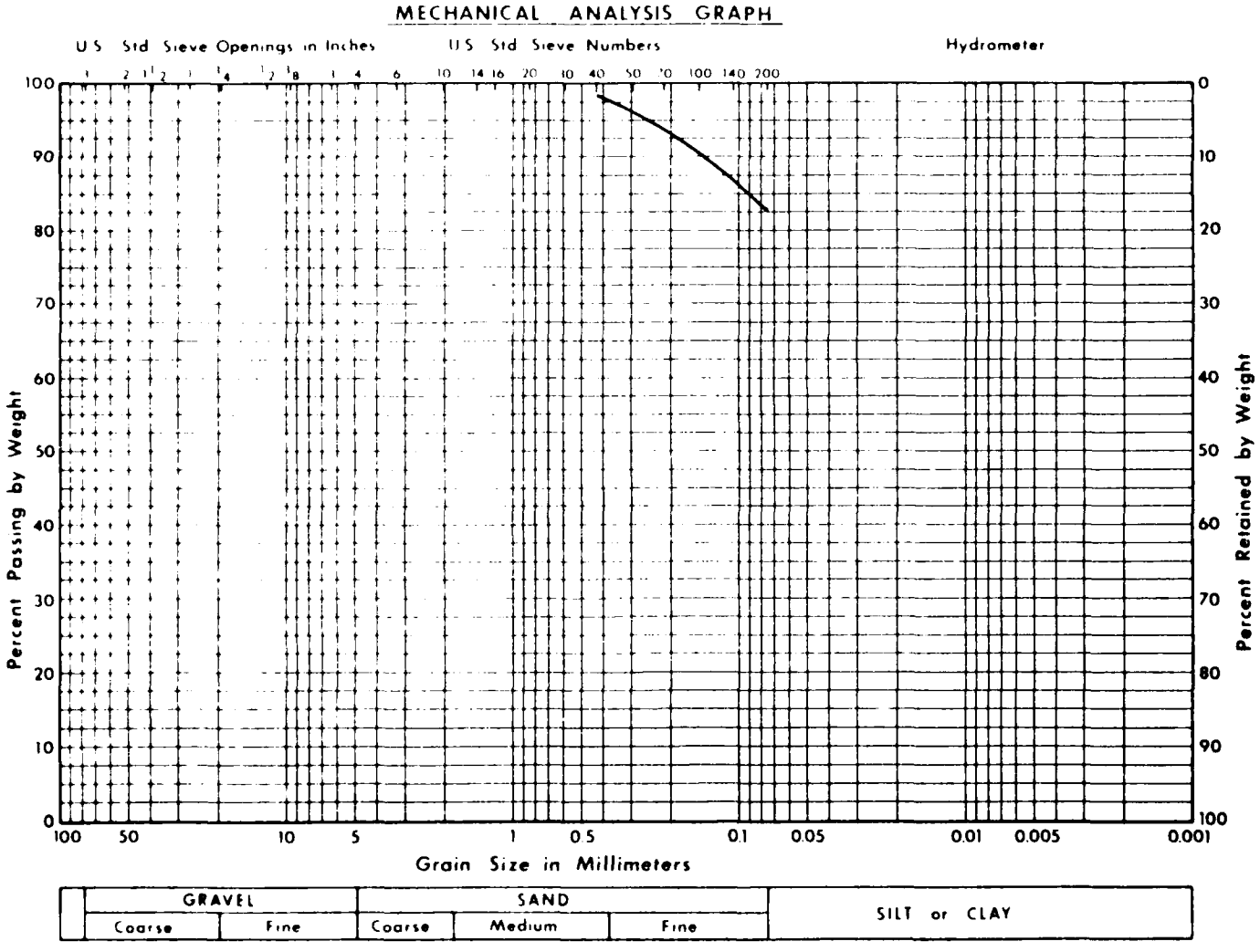

Figure C-12: GRAIN SIZE DISTRIBUTION; IC-$\bar{U}$ TEST SAMPLE NO. 14

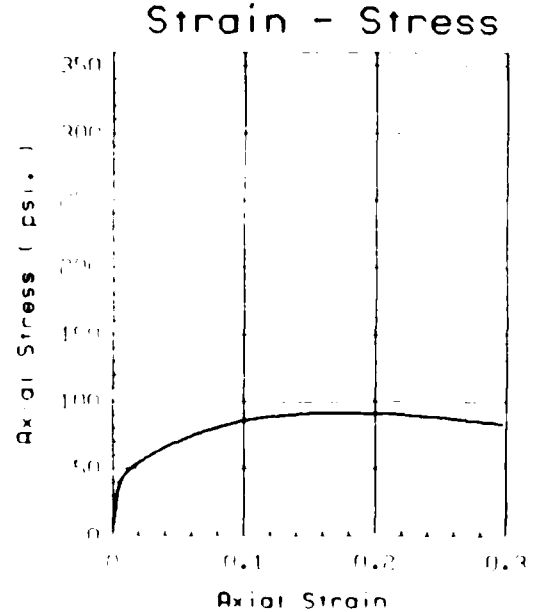

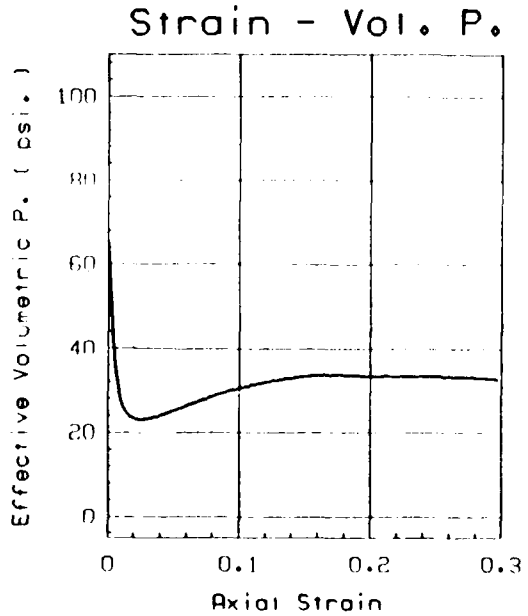

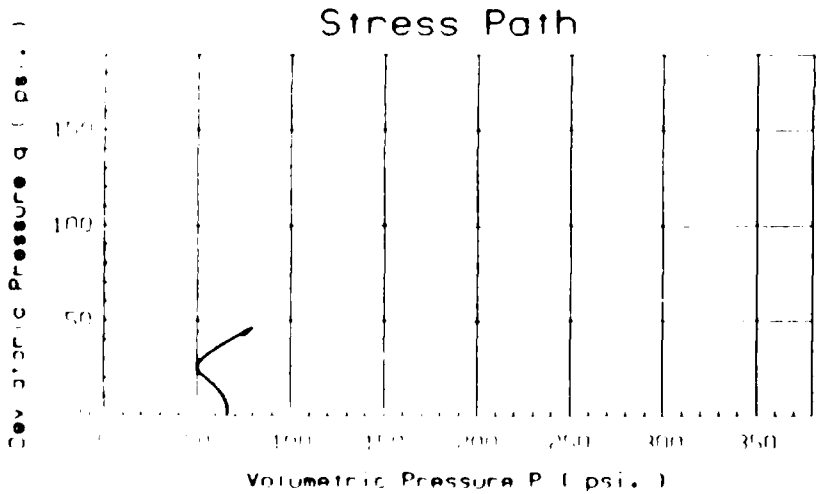

Test No. : 16

Test Date : 8/13/86

Material : Tube U111-UF21

Silty Sand (SM-ML), 12% fines.

γ_d = 110.81 pcf

$\bar{B}$ = 0.991

$\sigma_{3,c}'$ = 65.1 psi

Strain RATE = 8.8% per hour

Figure C-13: IC-$\bar{U}$ TRIAXIAL TEST NO. 16: HYDRAULIC FILL

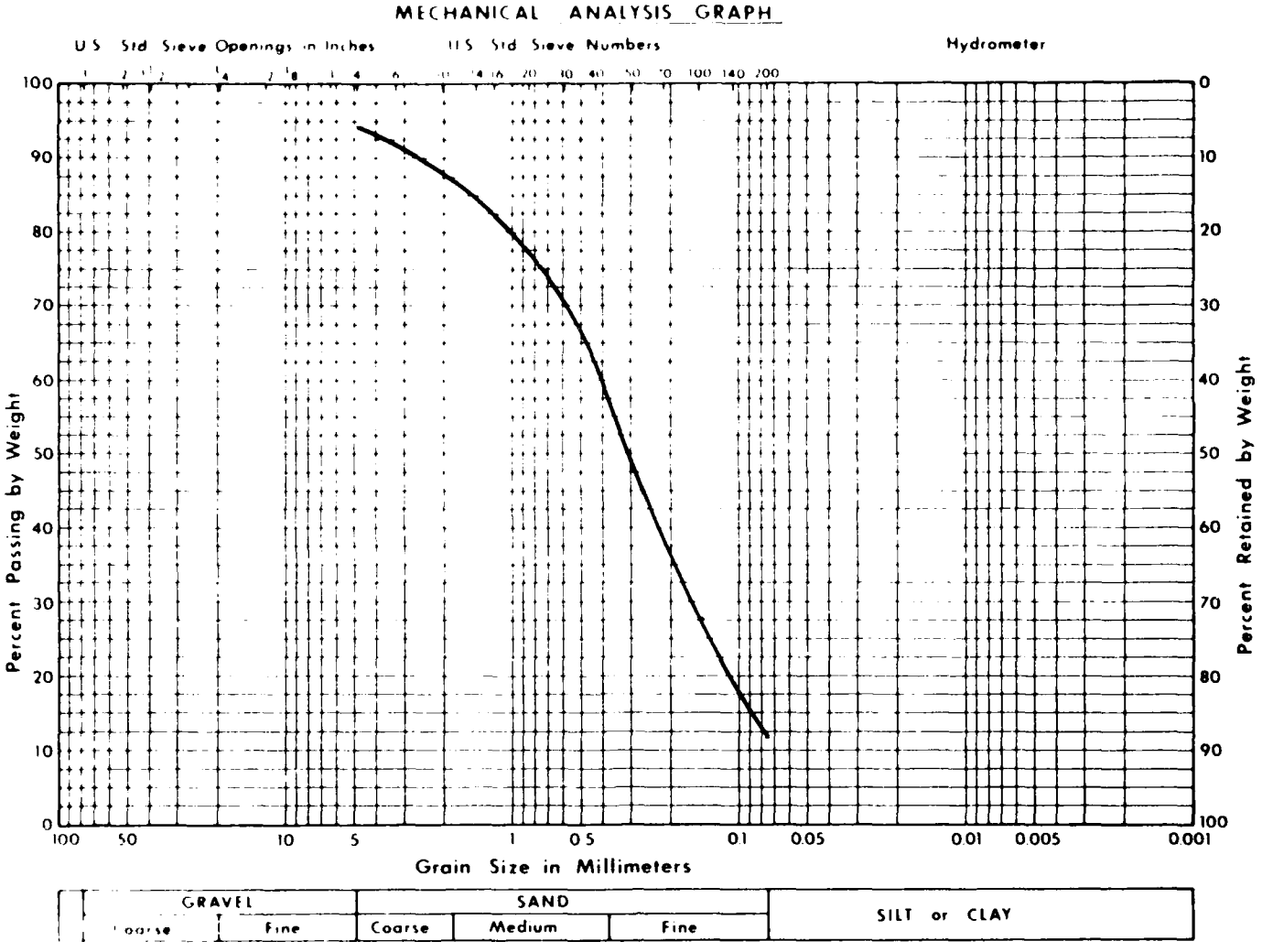

FIG. C 14: GRAIN SIZE DISTRIBUTION; IC-$\bar{U}$ TEST SAMPLE NO. 16

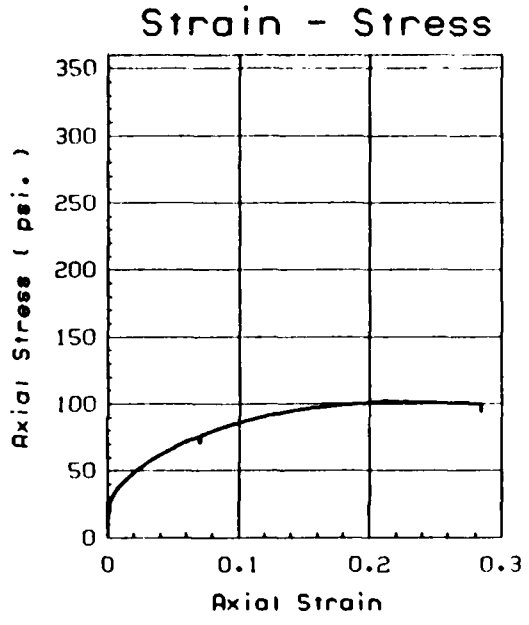

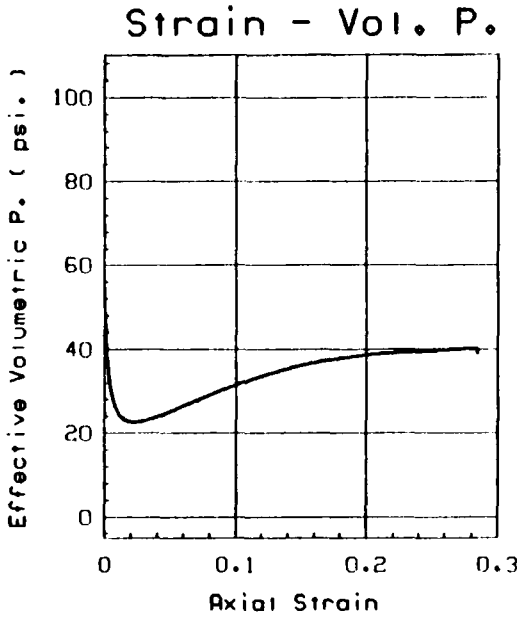

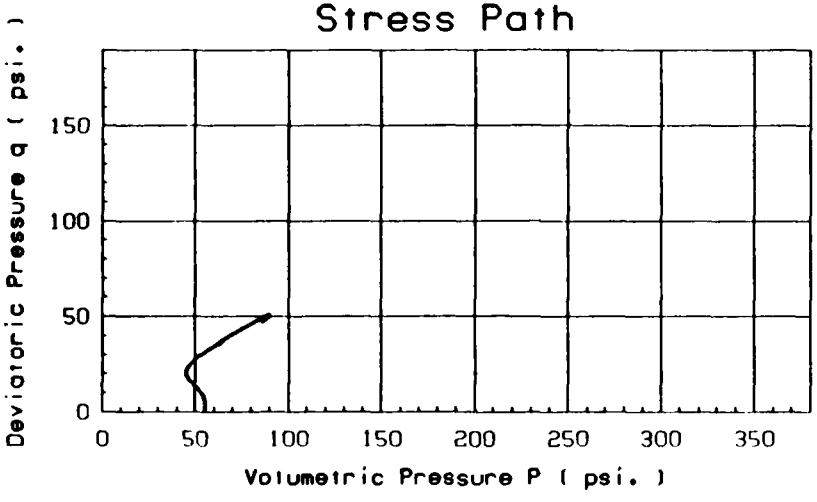

Test No. : 20
Test Date : 8/17/86
Material : Tube U104-UF10
Sandy Clayey Silt (ML), 61% fines.
γ_d : 104.22 pcf
$\bar{B}$: 0.996
$\sigma_{3,c}'$ = 54.7 psi
Strain RATE = 7.9% per hour

Figure C-15: IC-$\bar{U}$ TRIAXIAL TEST NO. 20: HYDRAULIC FILL

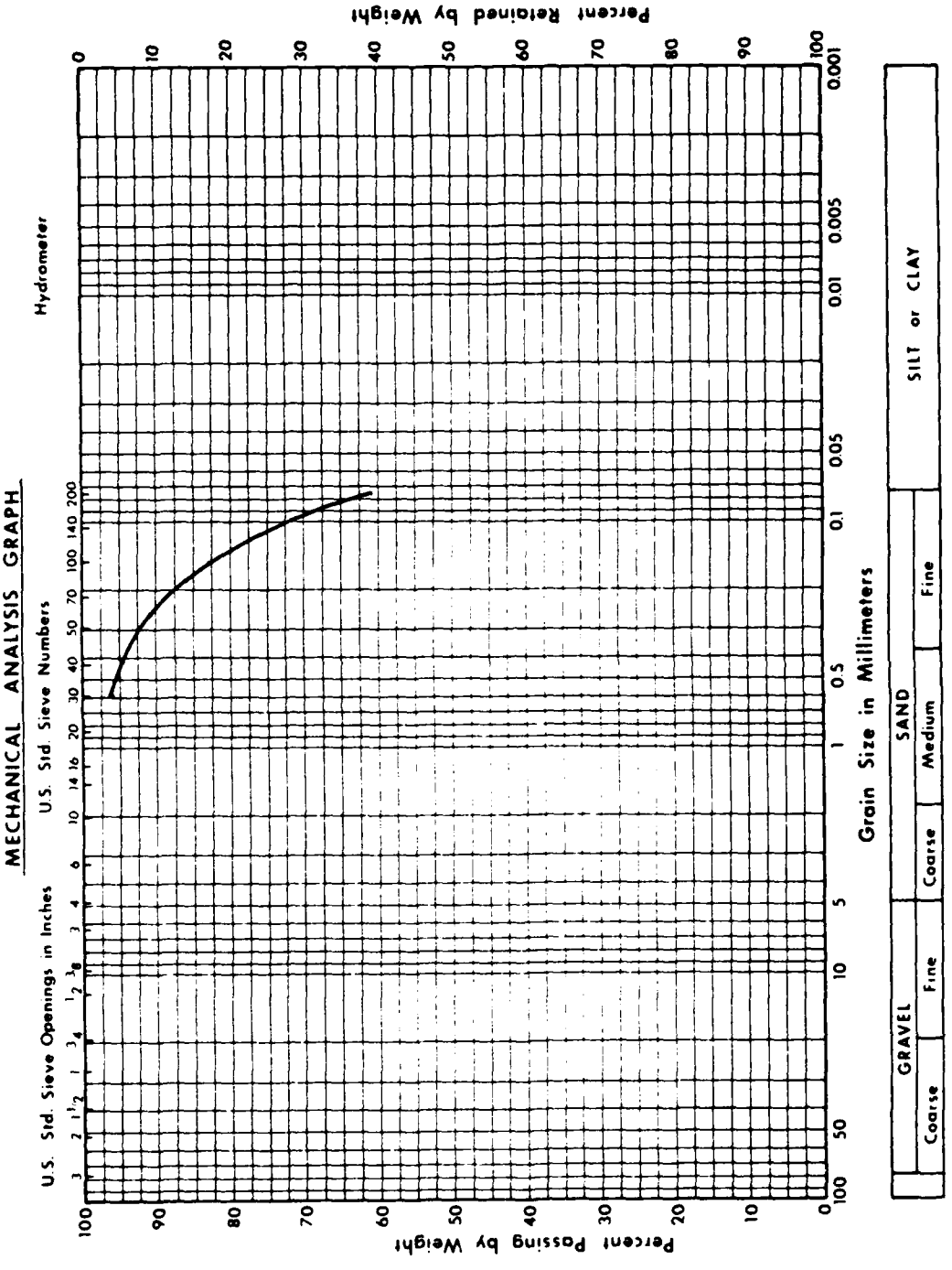

Figure C-16: GRAIN SIZE DISTRIBUTION; IC-$\bar{U}$ TEST SAMPLE NO. 20

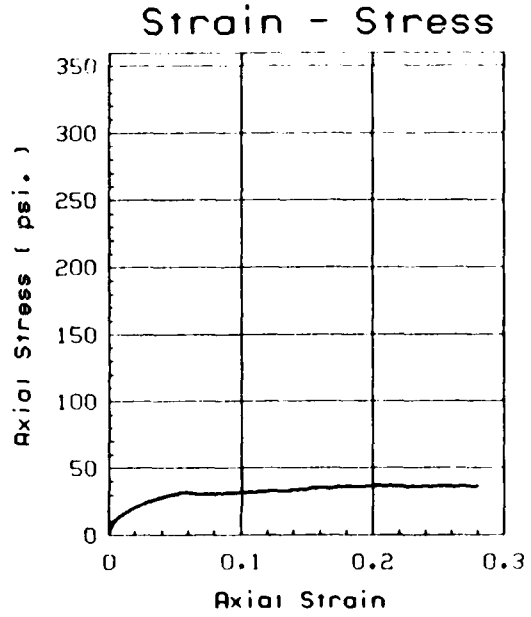

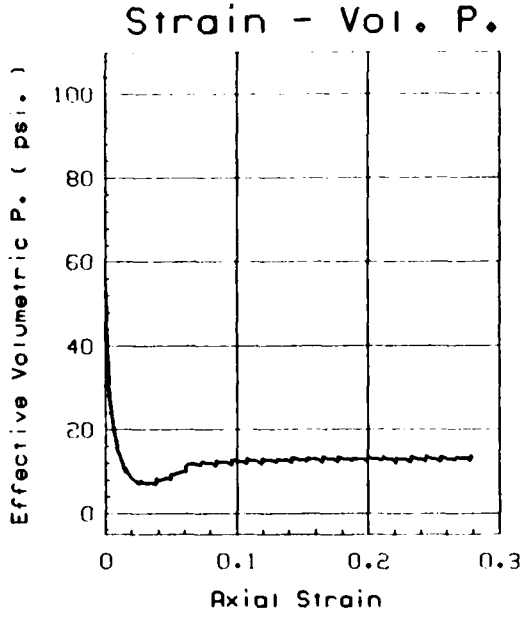

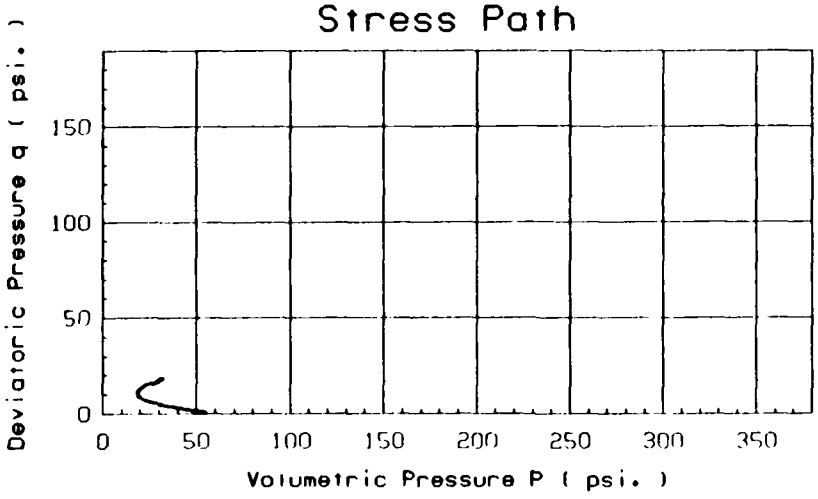

Test No. : 28

Test Date : 8/20/86

Material : Tube U105-UF12

Silty Clayey Sand (SM-ML), 43% fines.

γ_d = 93.47 pcf

$\bar{B}$ = 0.996

$\sigma_{3,c}'$ = 54.6 psi

Strain RATE = 3.9% per hour

Figure C-17: IC-$\bar{U}$ TRIAXIAL TEST NO. 28: HYDRAULIC FILL

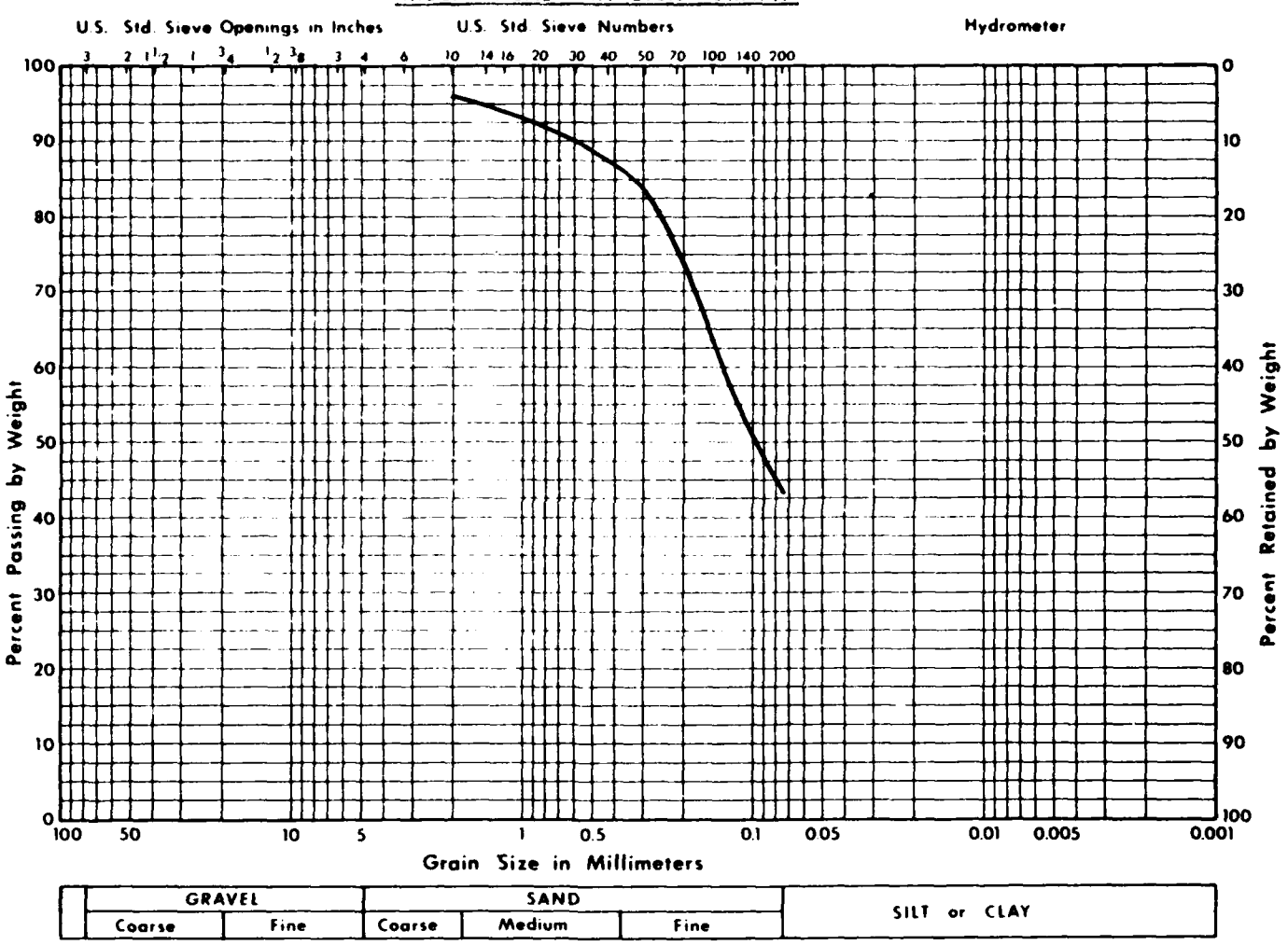

Figure C-18: GRAIN SIZE DISTRIBUTION; IC-$\bar{U}$ TEST SAMPLE NO. 28

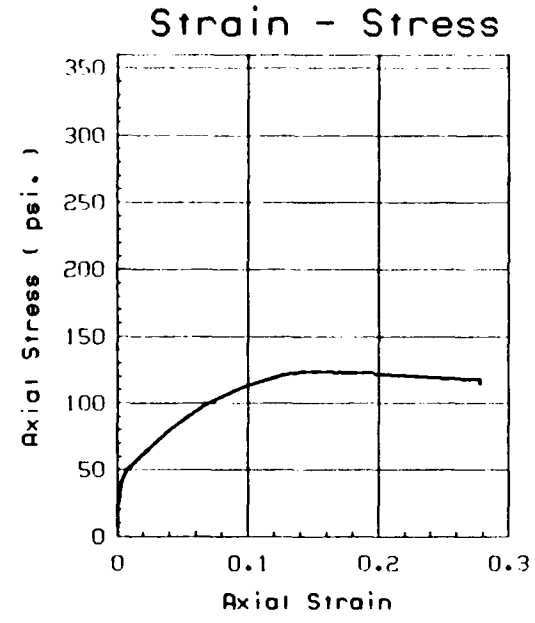

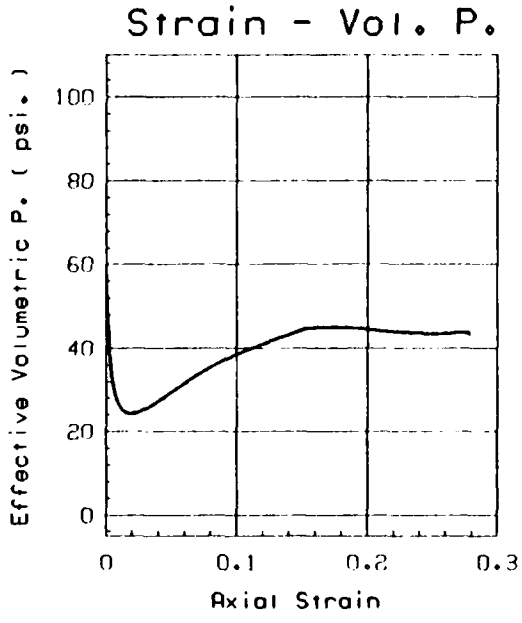

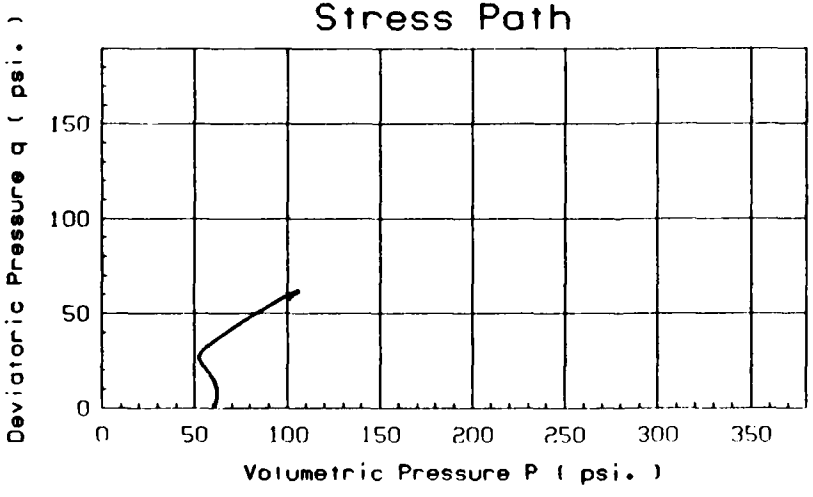

Test No. : 43
Test Date : 8/31/86
Material : Tube TS101
Silty Sand (SM-ML), 22% fines.
γ_d = 101.46 pcf
$\bar{B}$ = 0.997
$\sigma_{3,c}'$ = 60.2 psi
Strain RATE = 13.8% per hour

Figure C-19: IC-$\bar{U}$ TRIAXIAL TEST NO. 43: HYDRAULIC FILL

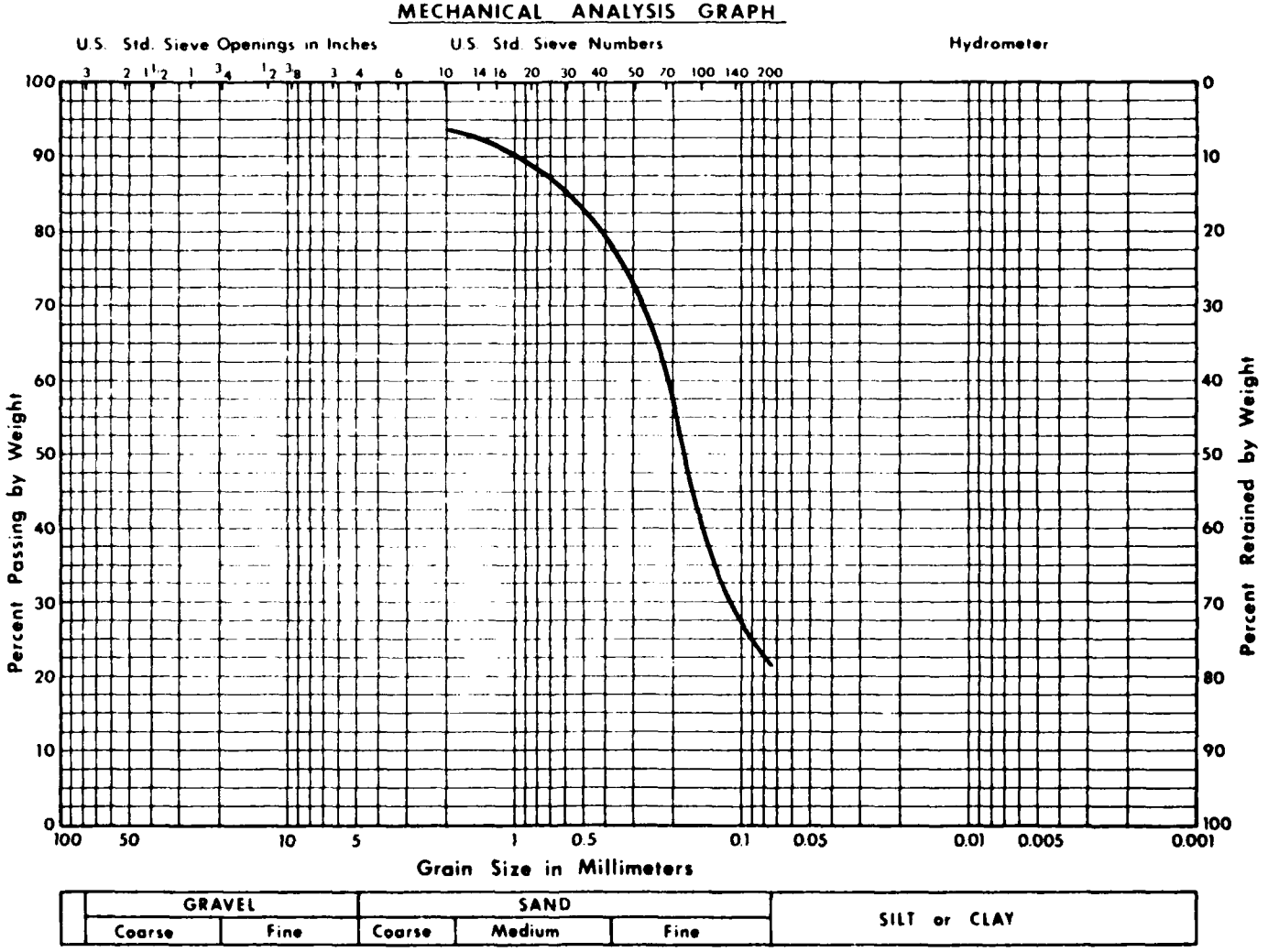

Figure C-20: GRAIN SIZE DISTRIBUTION; IC-$\bar{U}$ TEST SAMPLE NO. 43

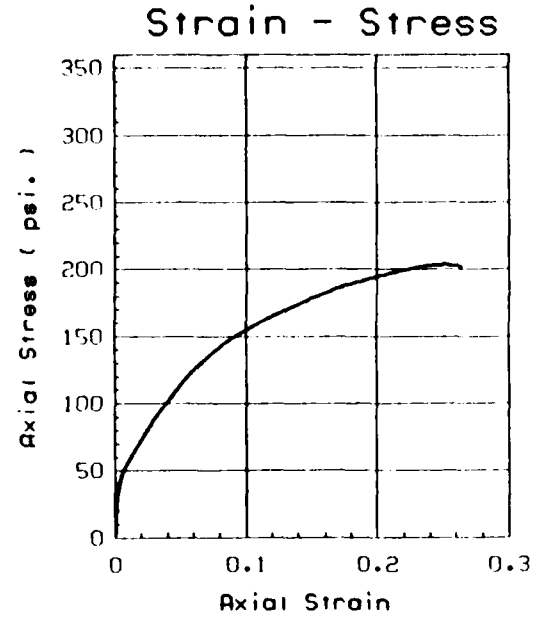

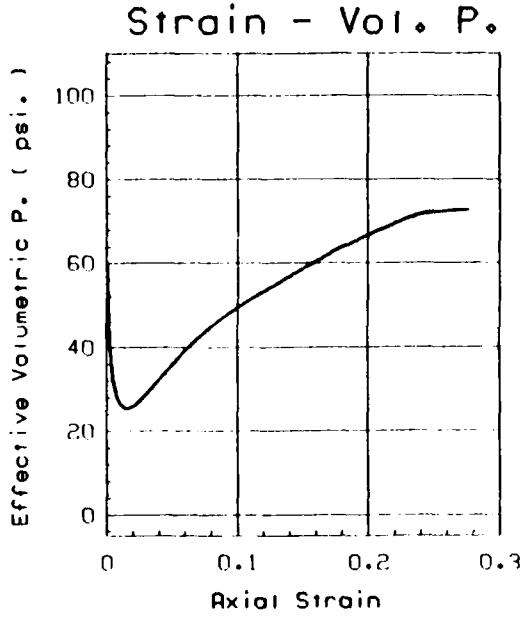

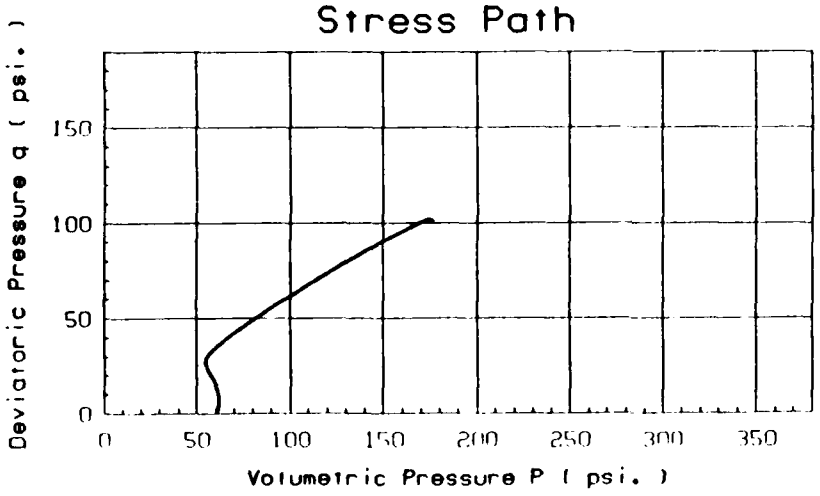

Test No. : 44
Test Date : 8/31/86
Material : Tube TS106
Silty Sand (SM-ML), 16% fines.
γ_d = 103.21 pcf
$\overline{B}$ = 0.988
$\sigma_{3,c}'$ = 60.2 psi
Strain RATE = 14.9% per hour

Figure C-21: IC-$\overline{U}$ TRIAXIAL TEST NO. 44: HYDRAULIC FILL

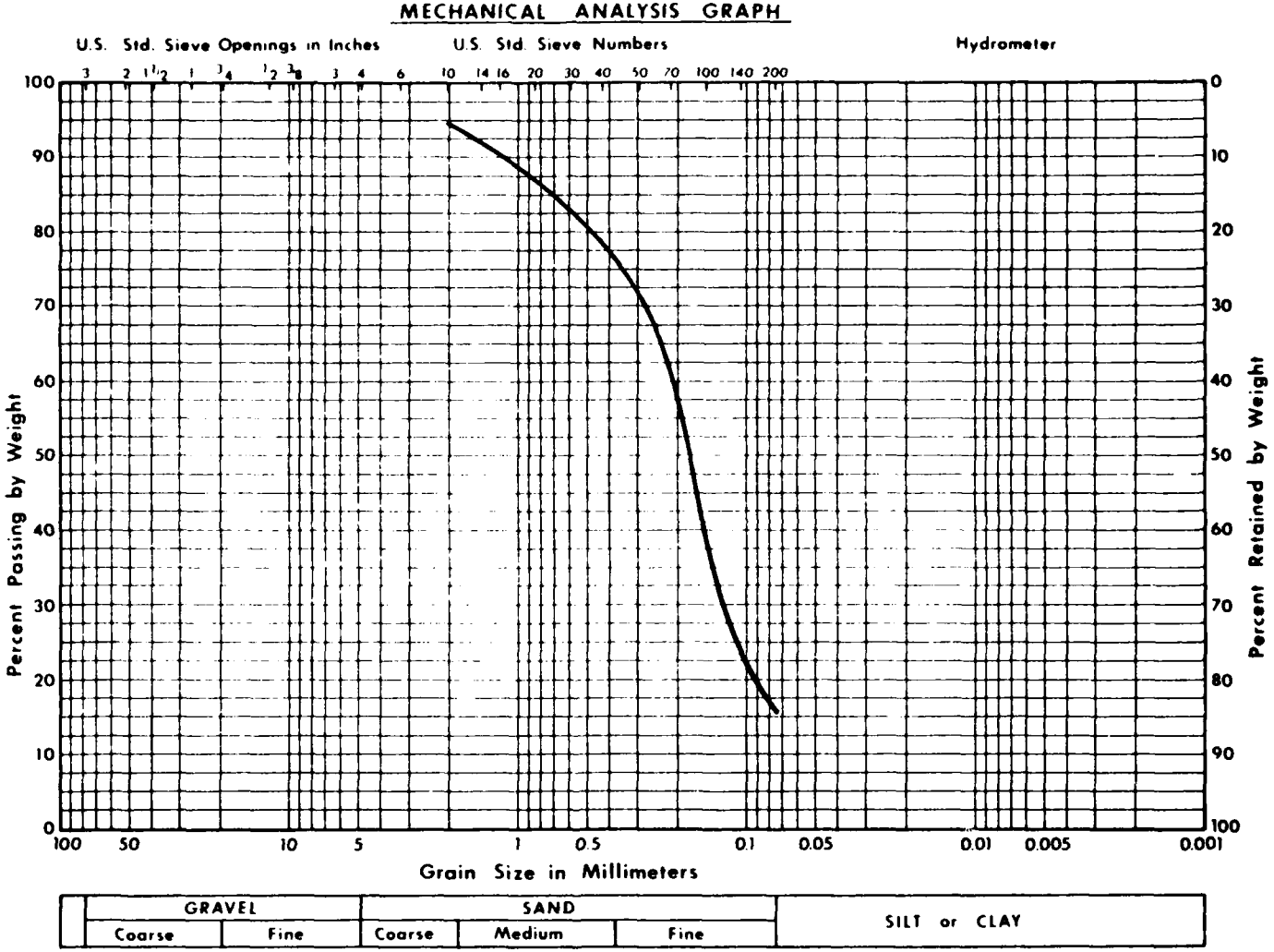

Figure C-22: GRAIN SIZE DISTRIBUTION; IC-$\bar{U}$ TEST SAMPLE NO. 44

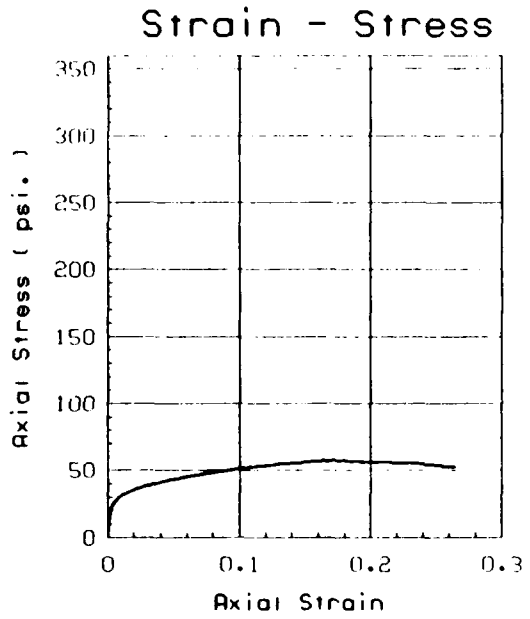

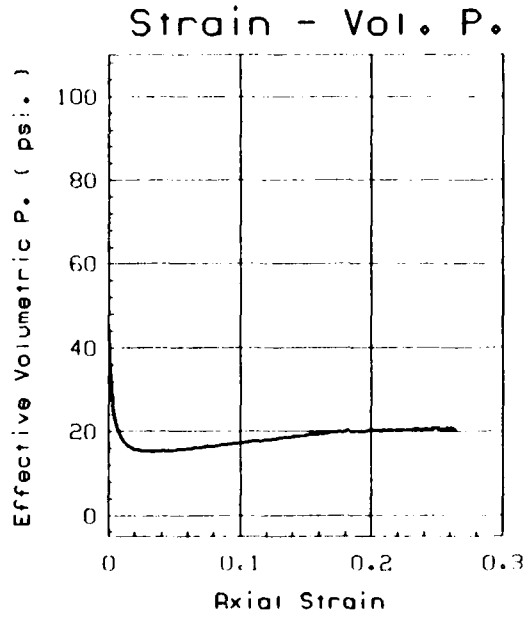

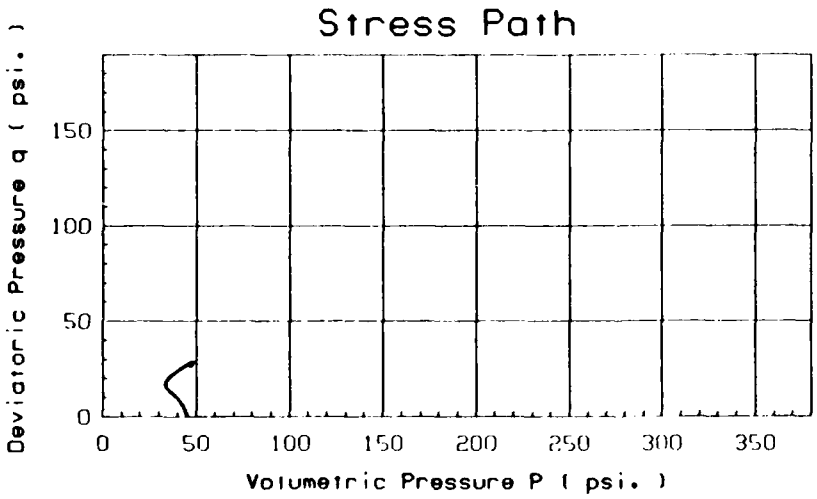

Test No. : 45
Test Date : 9/2/86
Material : Tube TS111
Sandy Clayey Silt (ML), 84% fines.
γ_d = 102.65 pcf
$\bar{B}$ = 0.982
$\sigma_{3,c}'$ = 45.0 psi
Strain RATE = 6.2% per hour

Figure C-23: IC-$\bar{U}$ TRIAXIAL TEST NO. 45: HYDRAULIC FILL

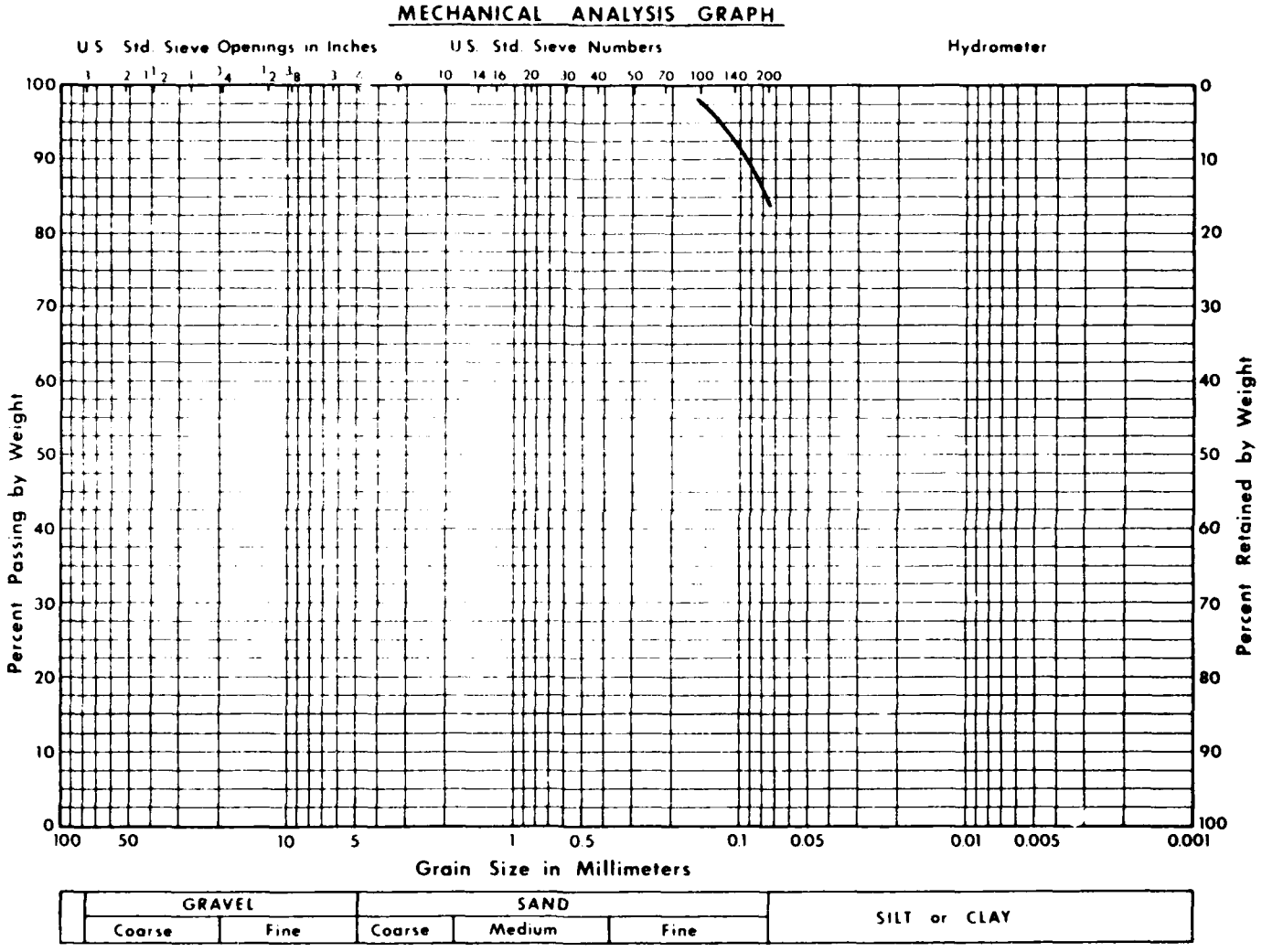

Figure C-24: GRAIN SIZE DISTRIBUTION; IC-$\bar{U}$ TEST SAMPLE NO. 45

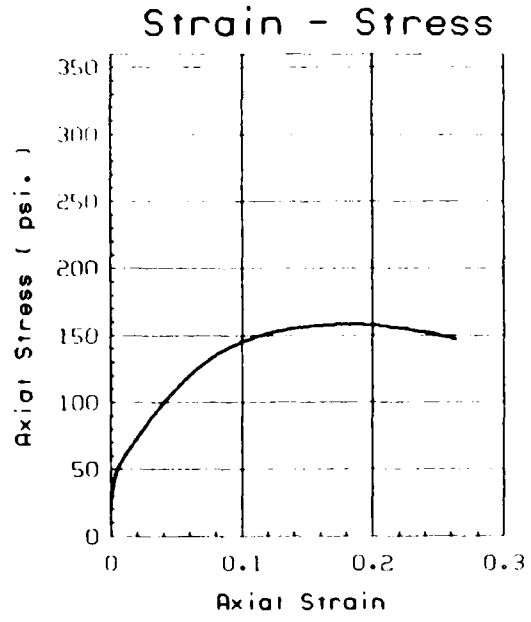

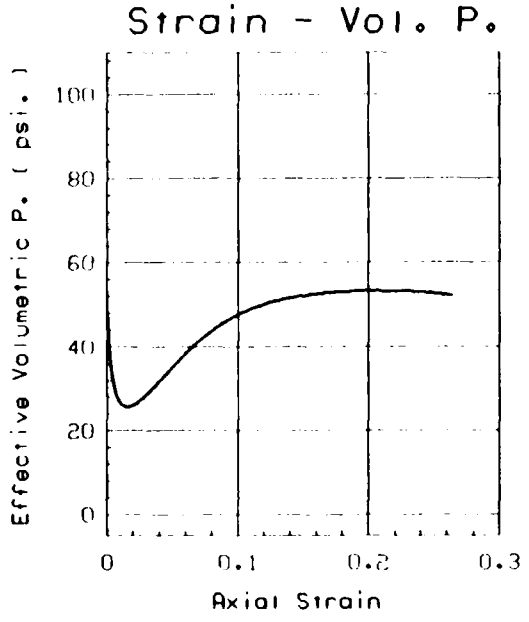

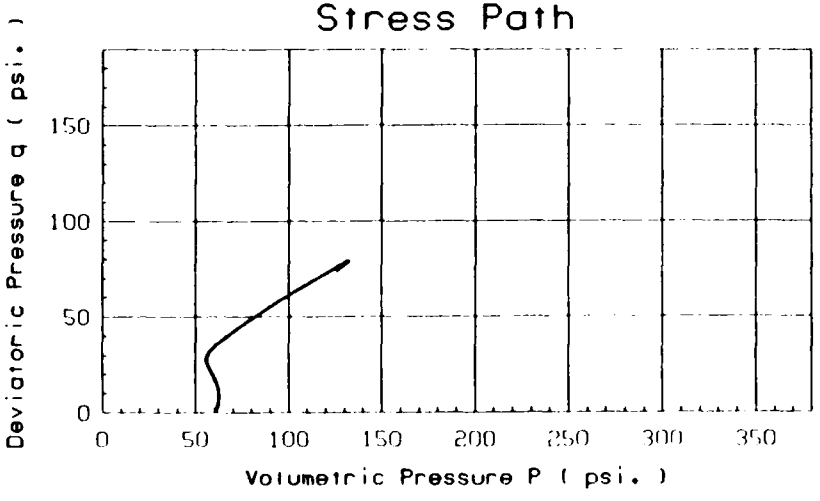

Test No. : 46
Test Date : 9/2/86
Material : Tube TS113
Silty Sand (SM-ML), 14% fines.
γ_d = 108.68 pcf
$\bar{B}$ = 0.994
$\sigma_{3,c}'$ = 60.1 psi
Strain RATE = 31.0% per hour

Figure C-25: IC-$\bar{U}$ TRIAXIAL TEST NO. 46: HYDRAULIC FILL

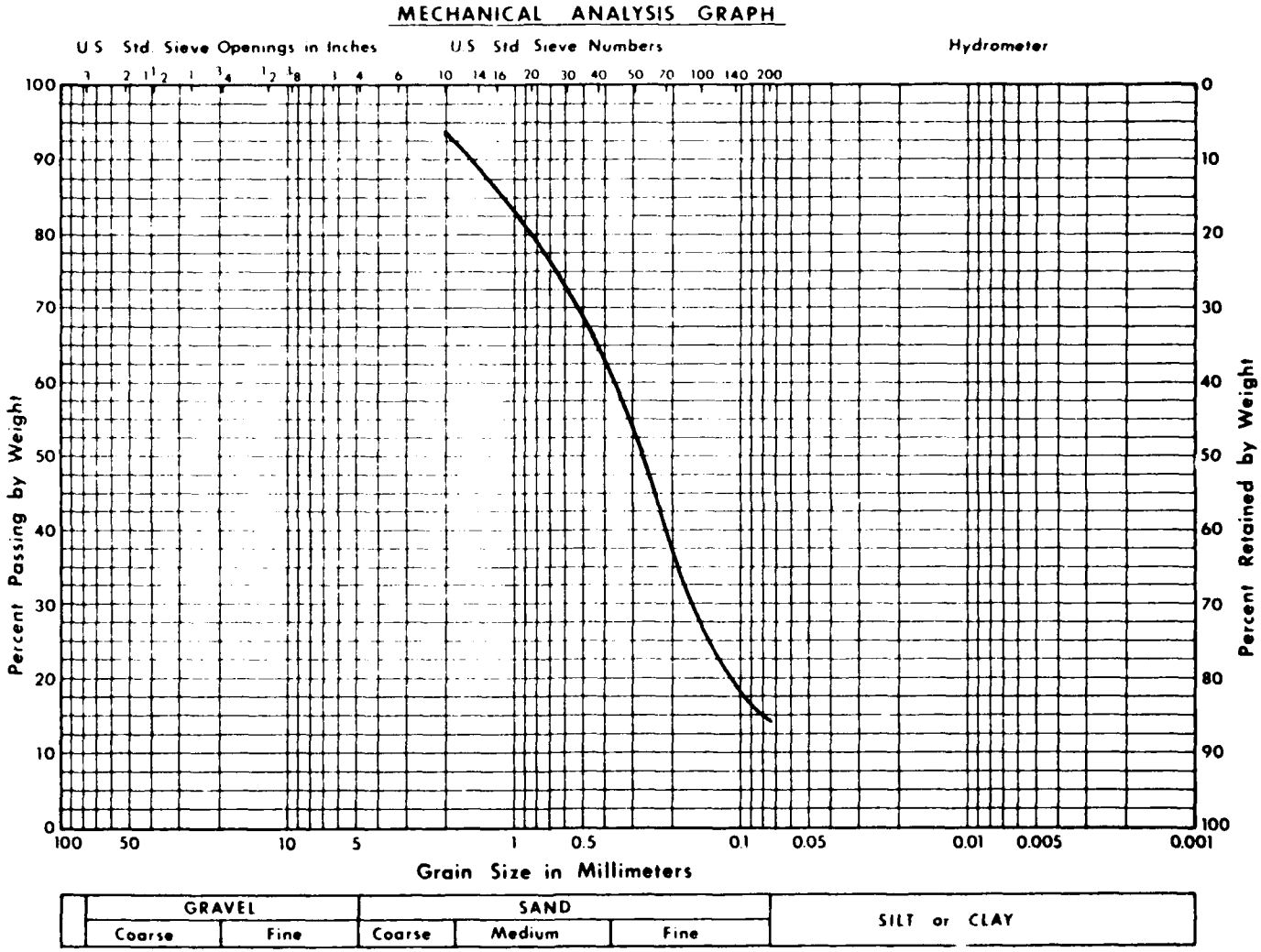

Figure C-26: GRAIN SIZE DISTRIBUTION; IC-$\bar{U}$ TEST SAMPLE NO. 46

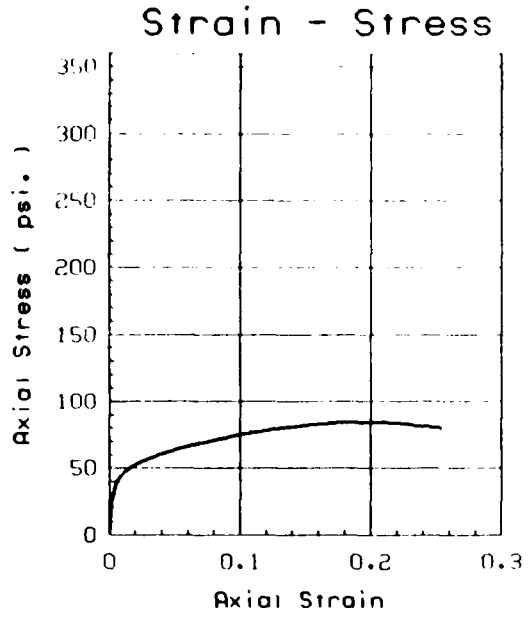

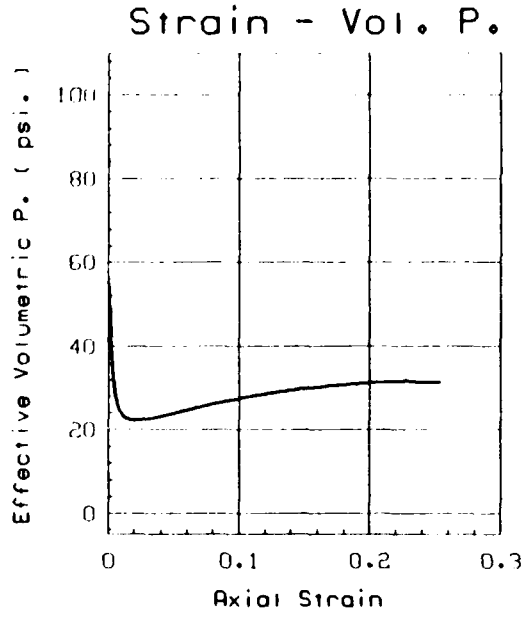

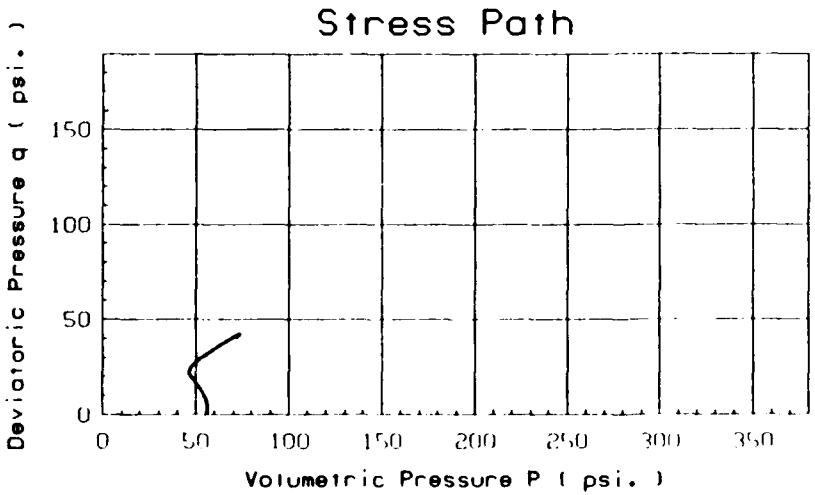

Test No. : 50

Test Date : 9/5/86

Material : Tube TS303

Sandy Clayey Silt (ML), 51% fines.

γ_d = 101.69 pcf

$\bar{B}$ = 0.991

$\sigma_{3,c}'$ = 55.1 psi

Strain RATE = 9.0% per hour

Figure C-27: IC-$\bar{U}$ TRIAXIAL TEST NO. 50: HYDRAULIC FILL

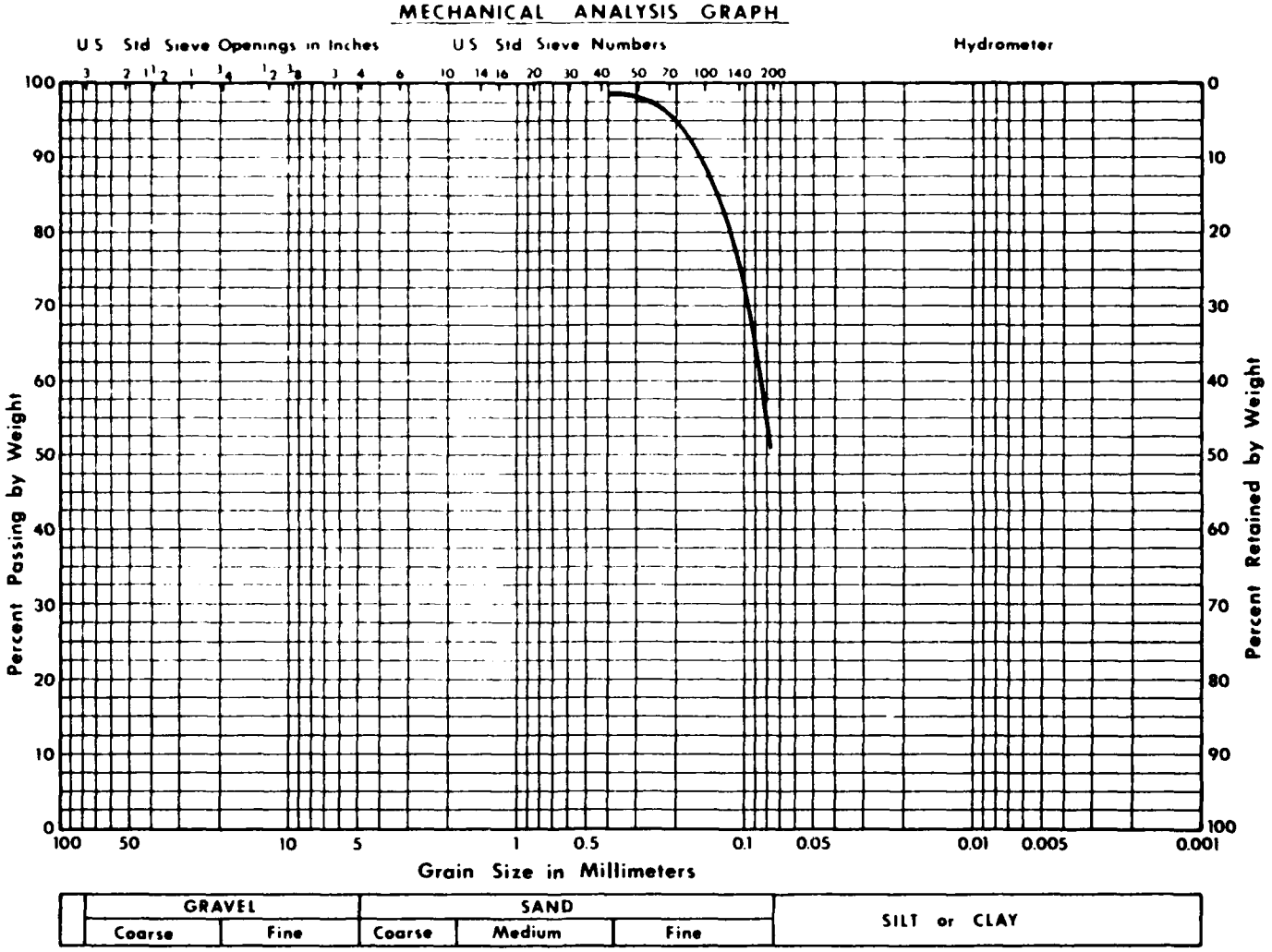

Figure C-28: GRAIN SIZE DISTRIBUTION; IC-$\bar{U}$ TEST SAMPLE NO. 50

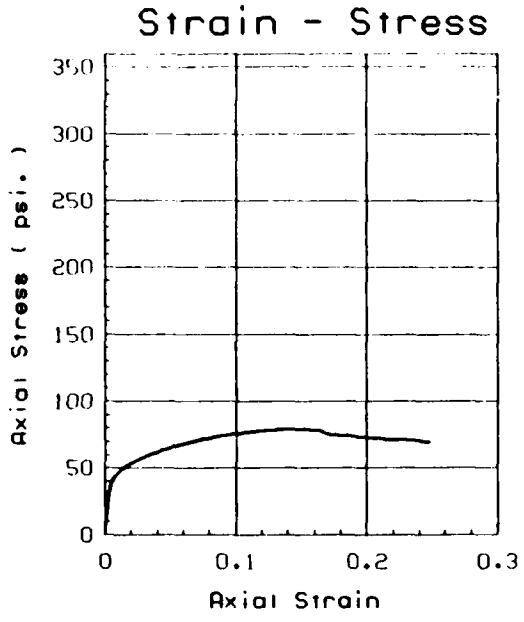

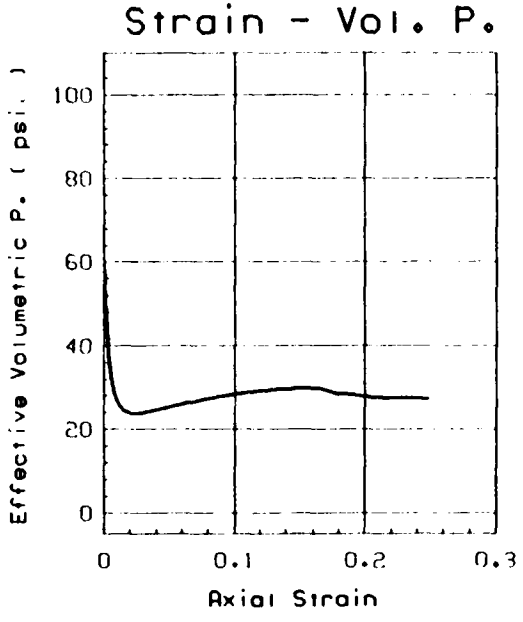

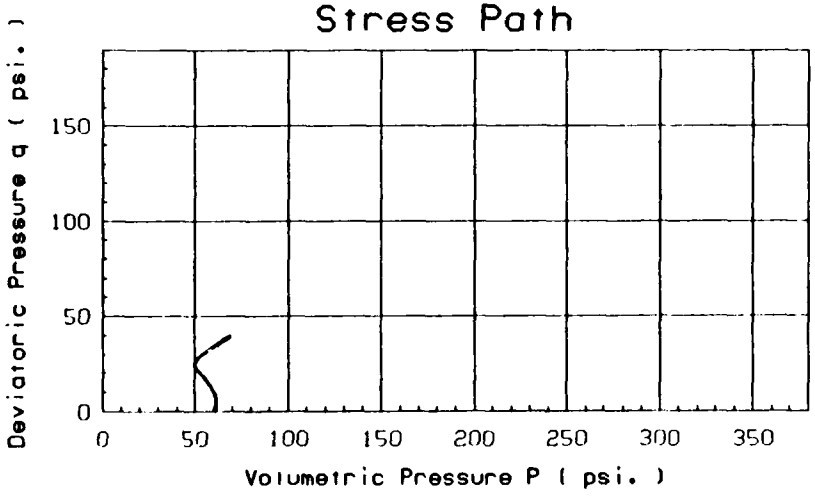

Test No. : 51
Test Date : 9/6/86
Material : Tube TS308
Silty Sand (SM-ML), 44% fines.
γ_d = 103.00 pcf
$\bar{B}$ = 0.993
$\sigma_{3,c}'$ = 60.2 psi
Strain RATE = 17.2% per hour

Figure C-29: IC-$\bar{U}$ TRIAXIAL TEST NO. 51: HYDRAULIC FILL

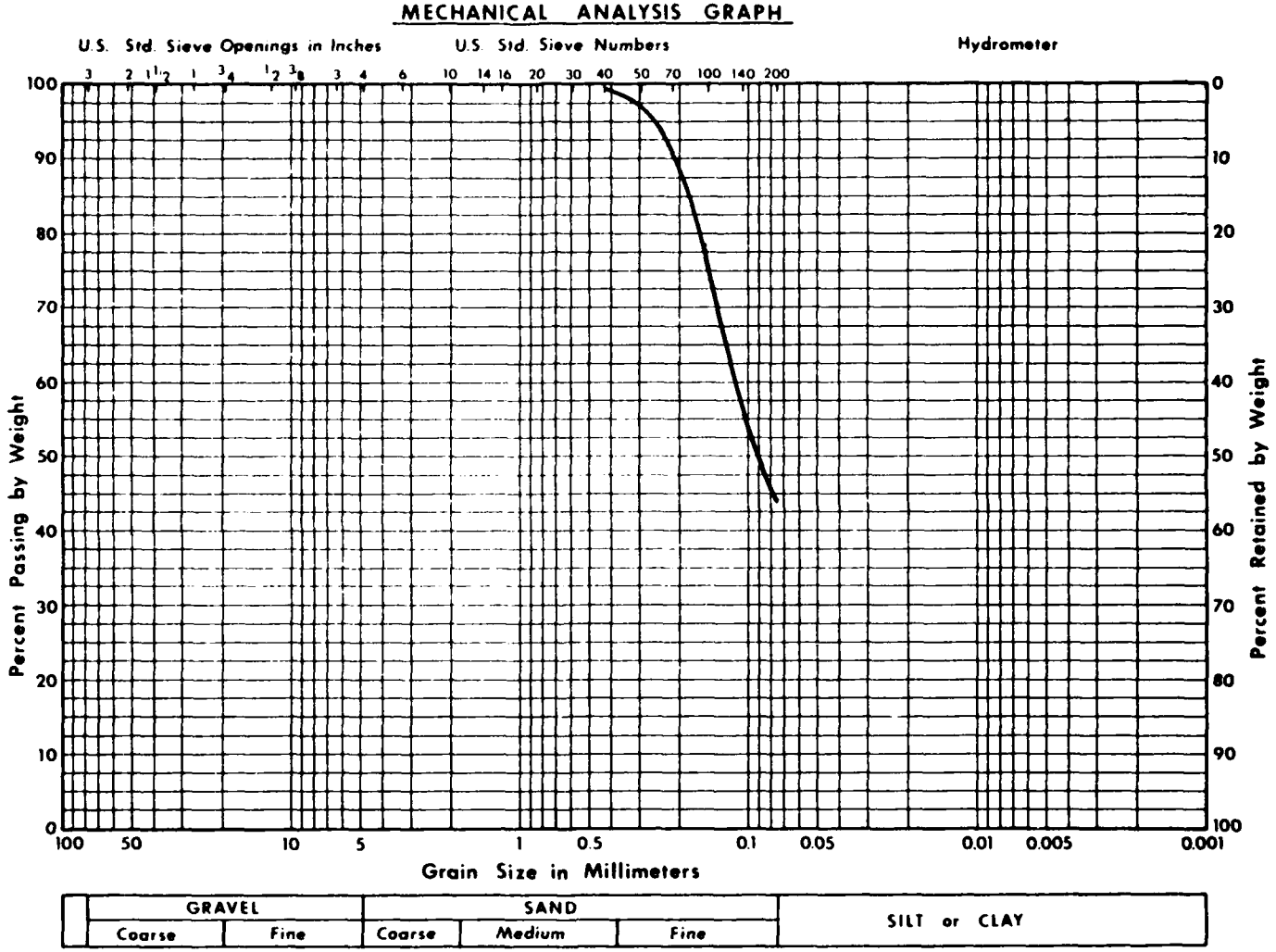

Figure C-30: GRAIN SIZE DISTRIBUTION; IC-$\bar{U}$ TEST SAMPLE NO. 51

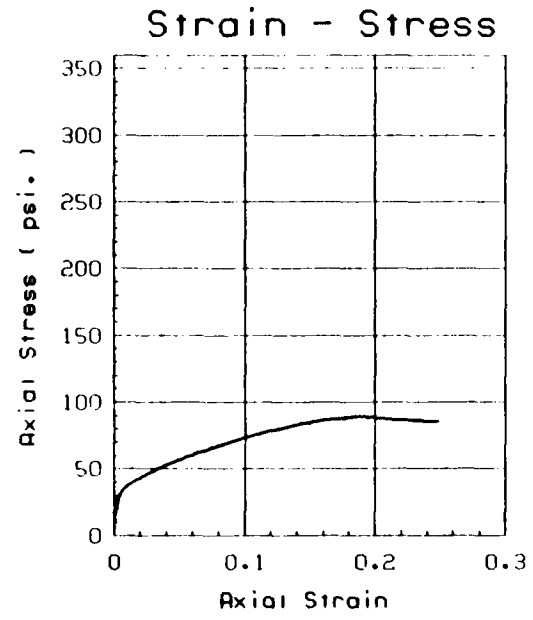

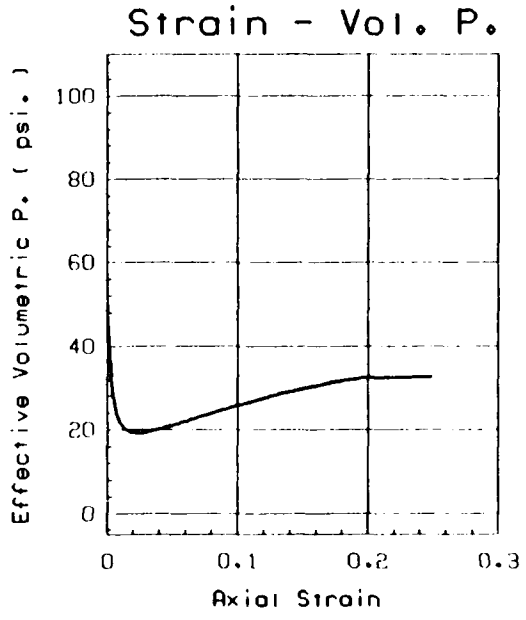

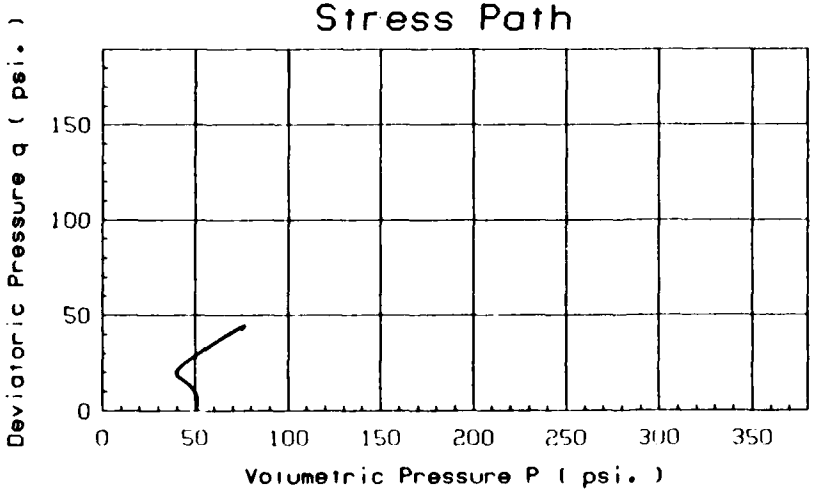

Test No. : 52
Test Date : 9/7/86
Material : Tube TS311
Sandy Silty (ML), 61% fines.
γ_d = 100.93 pcf
$\bar{B}$ = 0.994
$\sigma_{3,c}'$ = 50.0 psi
Strain RATE = 7.4% per hour

Figure C-31: IC-$\bar{U}$ TRIAXIAL TEST NO. 52: HYDRAULIC FILL

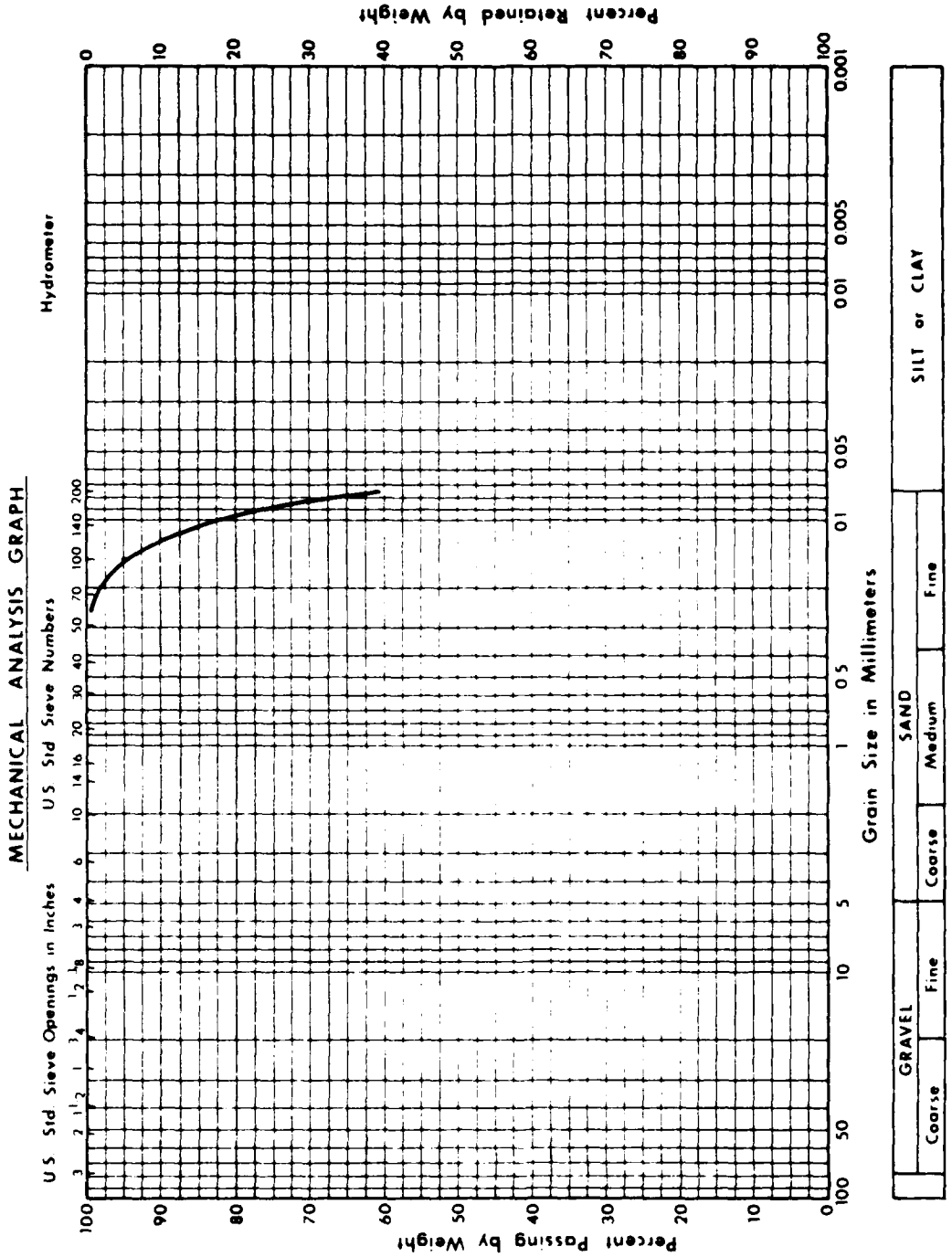

Figure C-32: GRAIN SIZE DISTRIBUTION; IC-$\bar{U}$ TEST SAMPLE NO. 52

Section I-D: UNDRAINED CYCLIC TRIAXIAL TESTS ON UNDISTURBED SAMPLES

A total of 19 cyclic triaxial tests were performed on undisturbed samples of hydraulic fill. Figure D-1 through D-48 present plots of (a) cyclic axial stress vs. time, (b) incremental pore pressure development vs. time, (c) axial strain vs. time, and (d) soil sample gradation for each cyclic test performed. On these figures; cyclic stress ratio is defined as CSR = $\sigma_{d,c}/2\sigma'_{3,i}$ and $K_c = \sigma'_{1,i}/\sigma'_{3,i}$ at the end of consolidation. The results of these tests are summarized in Figures 5-1 through 5-6, and I-2 as well as in Tables 5-1, 5-2 and I-5.

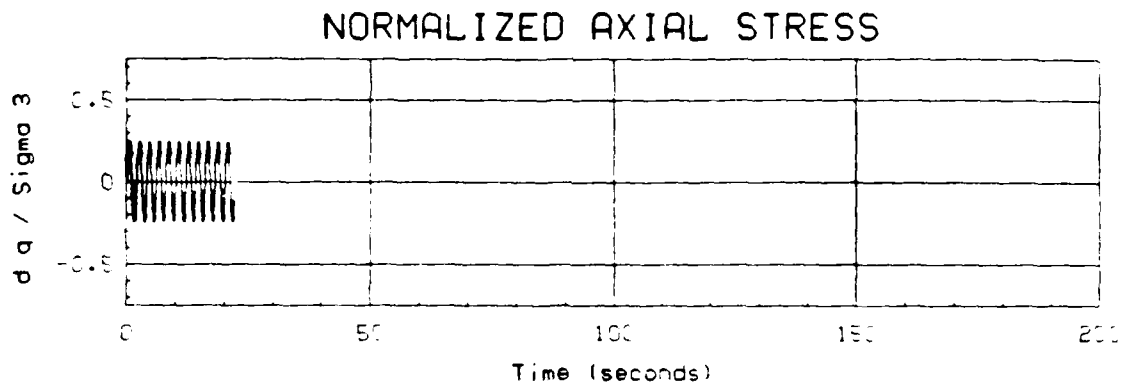

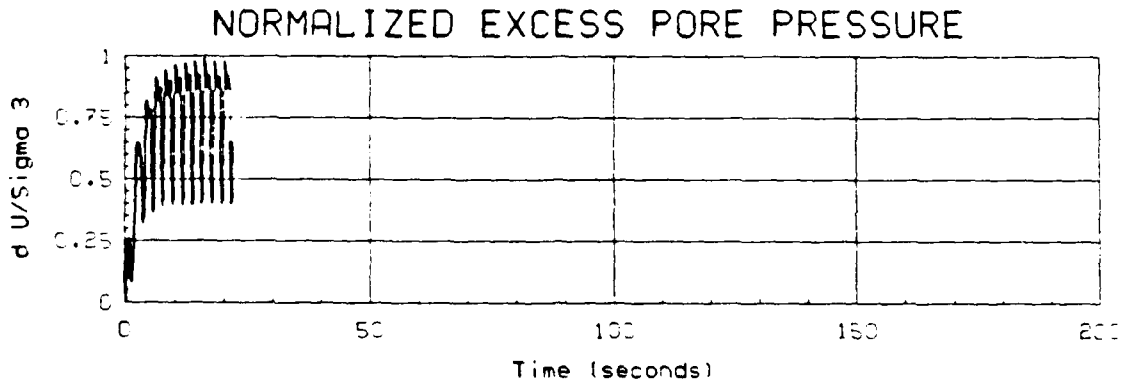

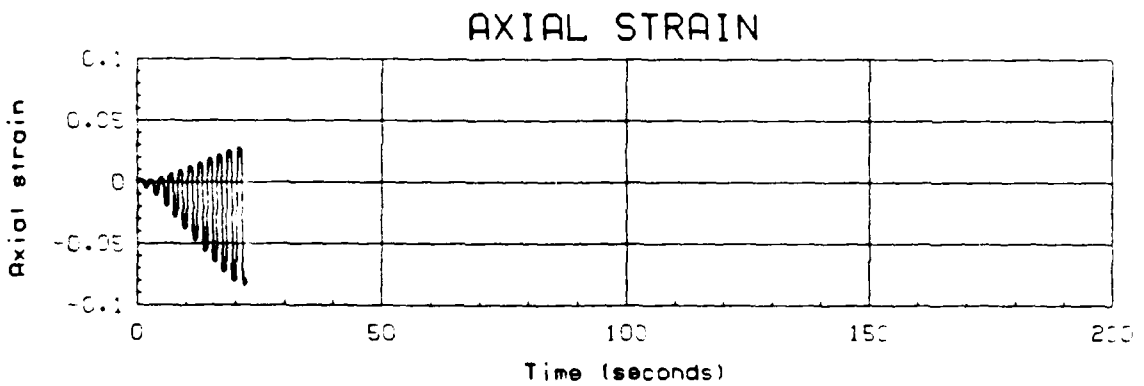

Test No.	: 1	B-value	: 0.989
Test Date	: 7/23/86	$\sigma_{3,i}'$	: 2.00 ksc
Material	: Tube U104-UF8	K_c	: 1.00
Silty Sand (SM-ML), 20% fines.		CSR	: 0.249

Figure D-1: UNDRAINED CYCLIC TRIAXIAL TEST NO. 1: HYDRAULIC FILL

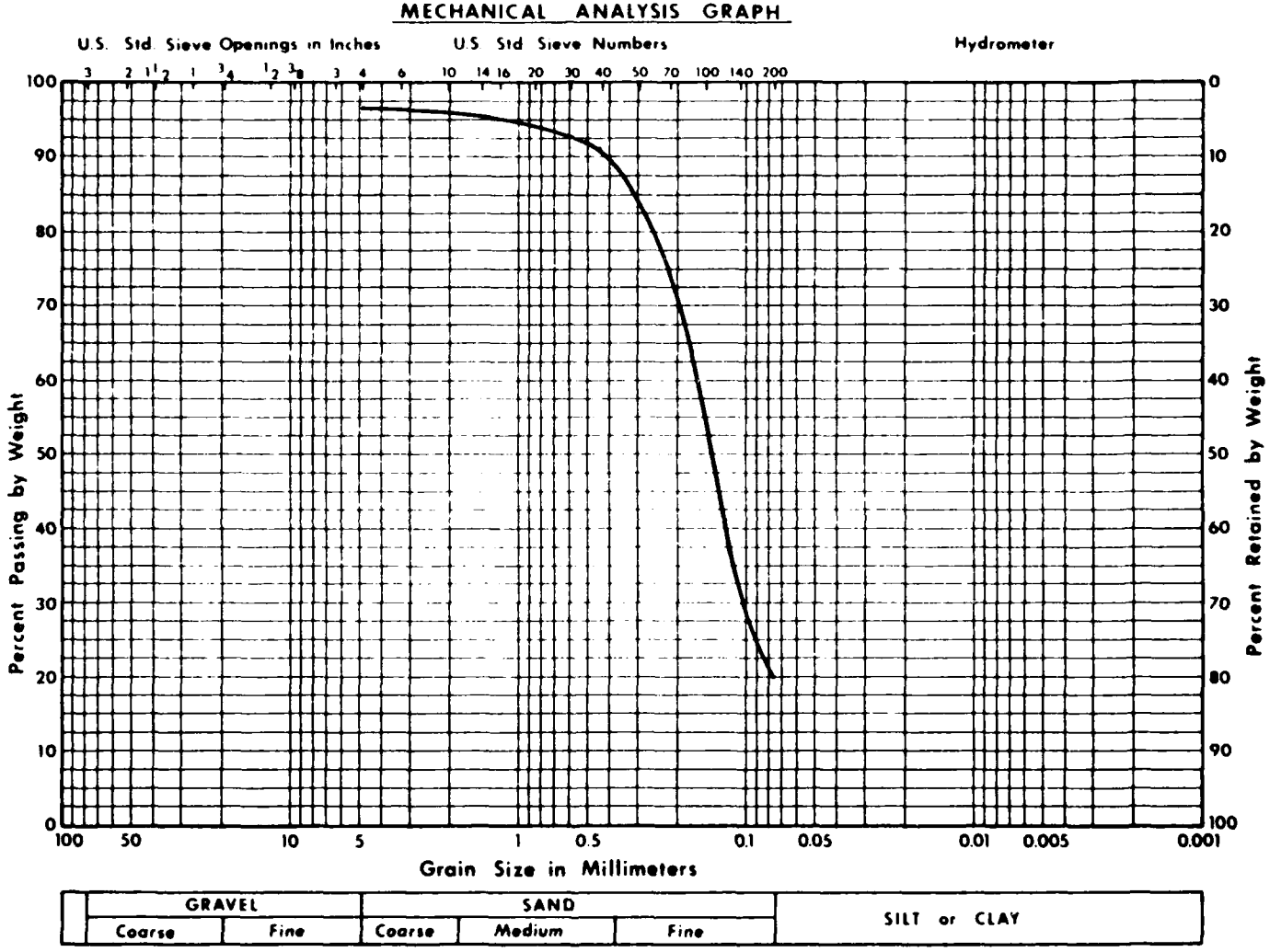

Figure D-2: GRAIN SIZE DISTRIBUTION; CYCLIC TRIAXIAL TEST NO. 1

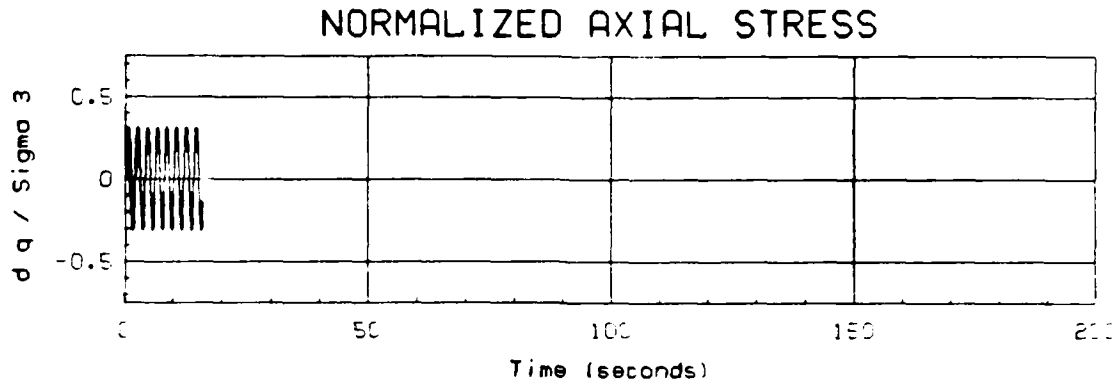

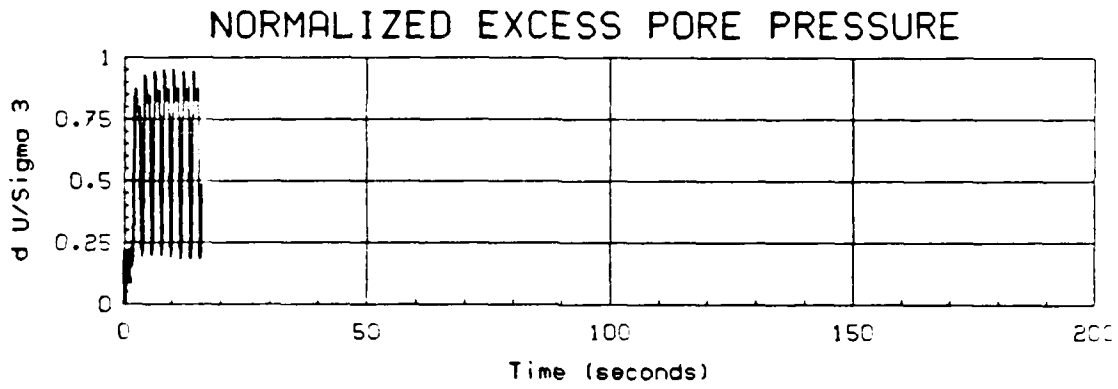

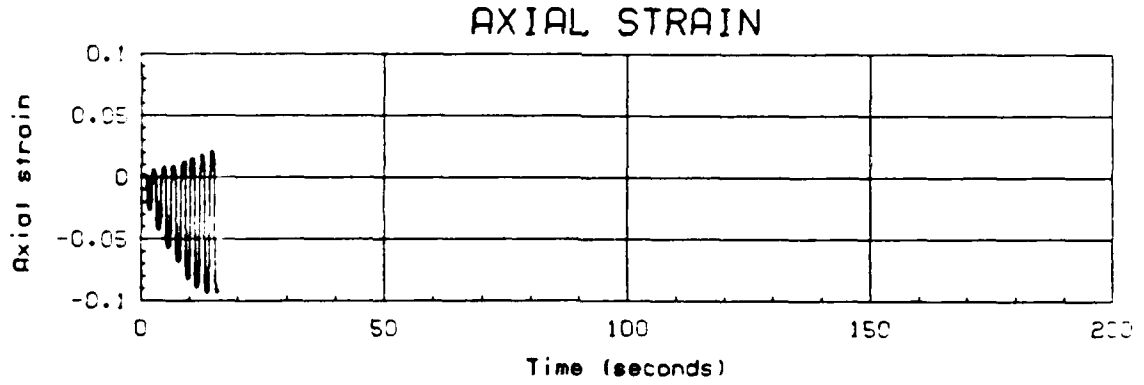

Test No.	: 2	B-value	: 0.996
Test Date	: 7/23/86	$\sigma_{3,i}'$	: 2.00 ksc
Material	: Tube U104-UF8	K_c	: 1.00
Silty Sand (SM-ML), 8% fines.		CSR	: 0.319

Figure D-3: UNDRAINED CYCLIC TRIAXIAL TEST NO. 2: HYDRAULIC FILL

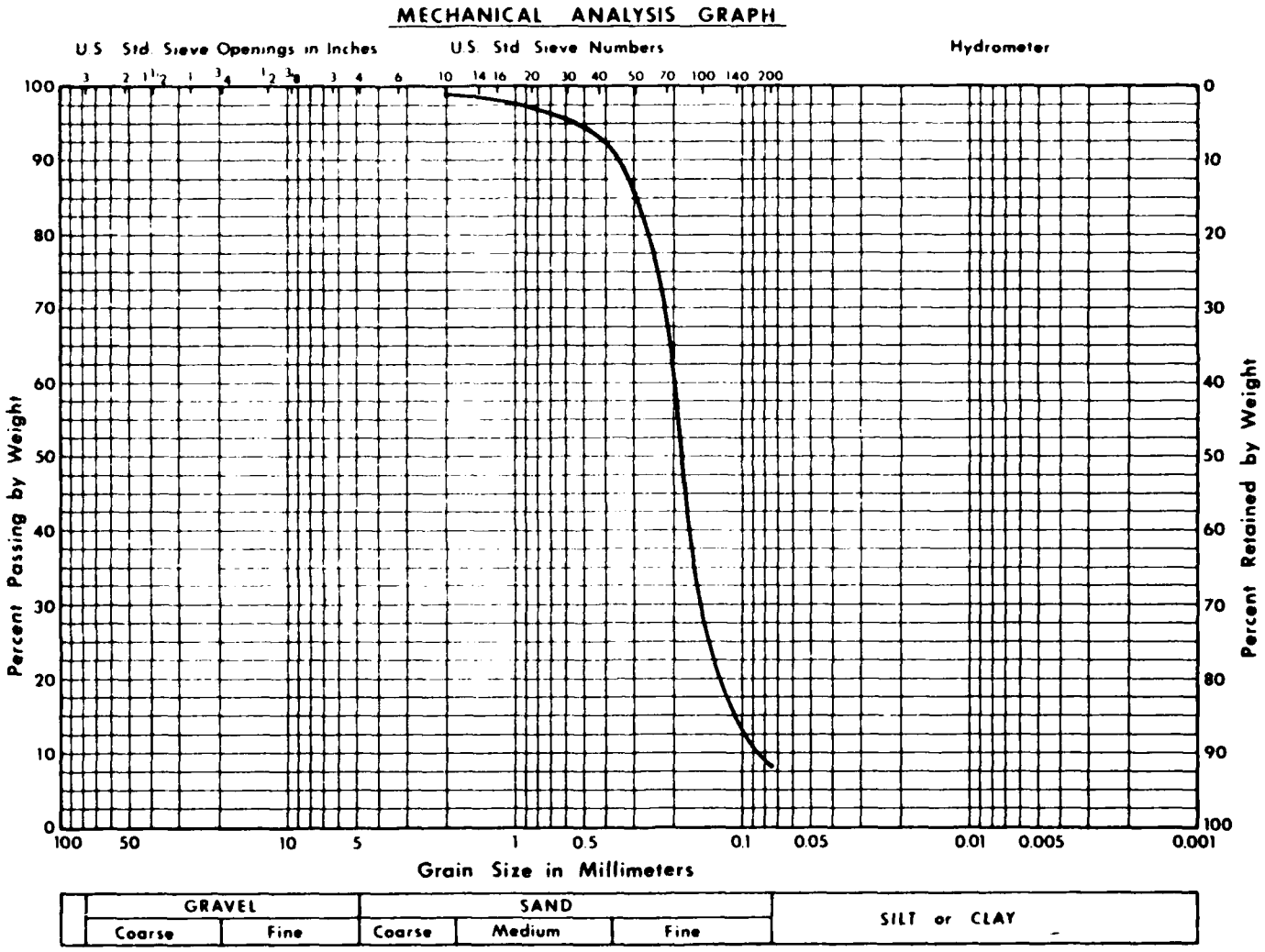

Figure D-4: GRAIN SIZE DISTRIBUTION; CYCLIC TRIAXIAL TEST NO. 2

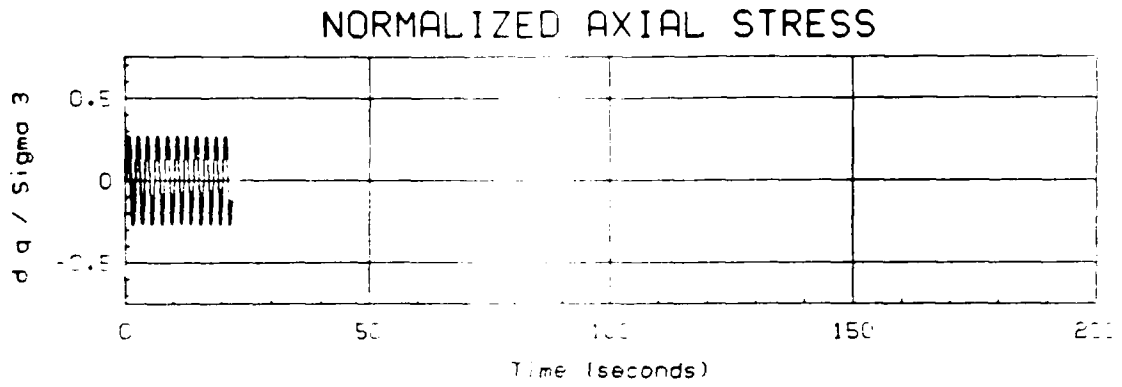

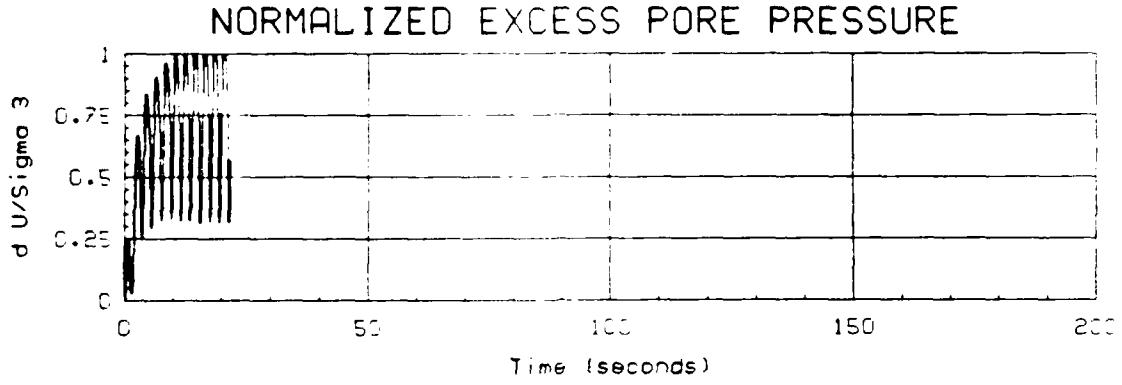

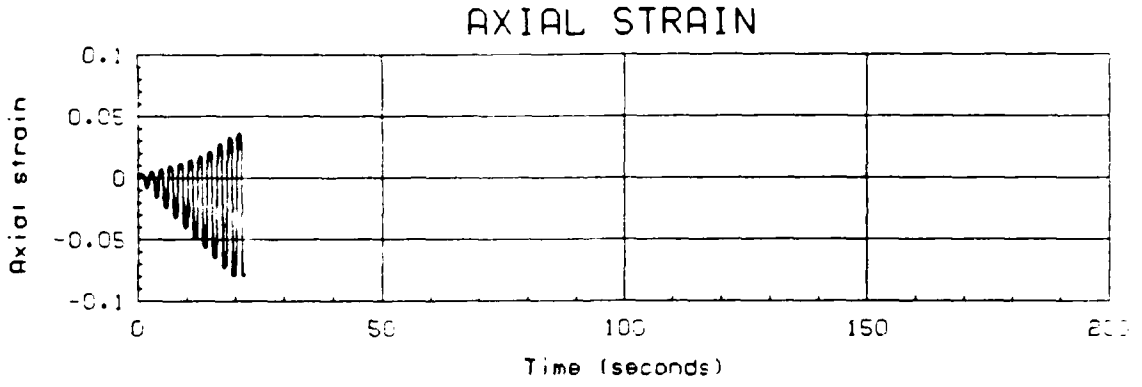

Test No.	: 3	B-value	: 0.997
Test Date	: 7/24/86	$\sigma_{3,i}'$	: 2.00 ksc
Material	: Tube U111A-UF18	K_c	: 1.00
Silty Sand (SM-ML), 15% fines.		CSR	: 0.270

Figure D-5: UNDRAINED CYCLIC TRIAXIAL TEST NO. 3: HYDRAULIC FILL

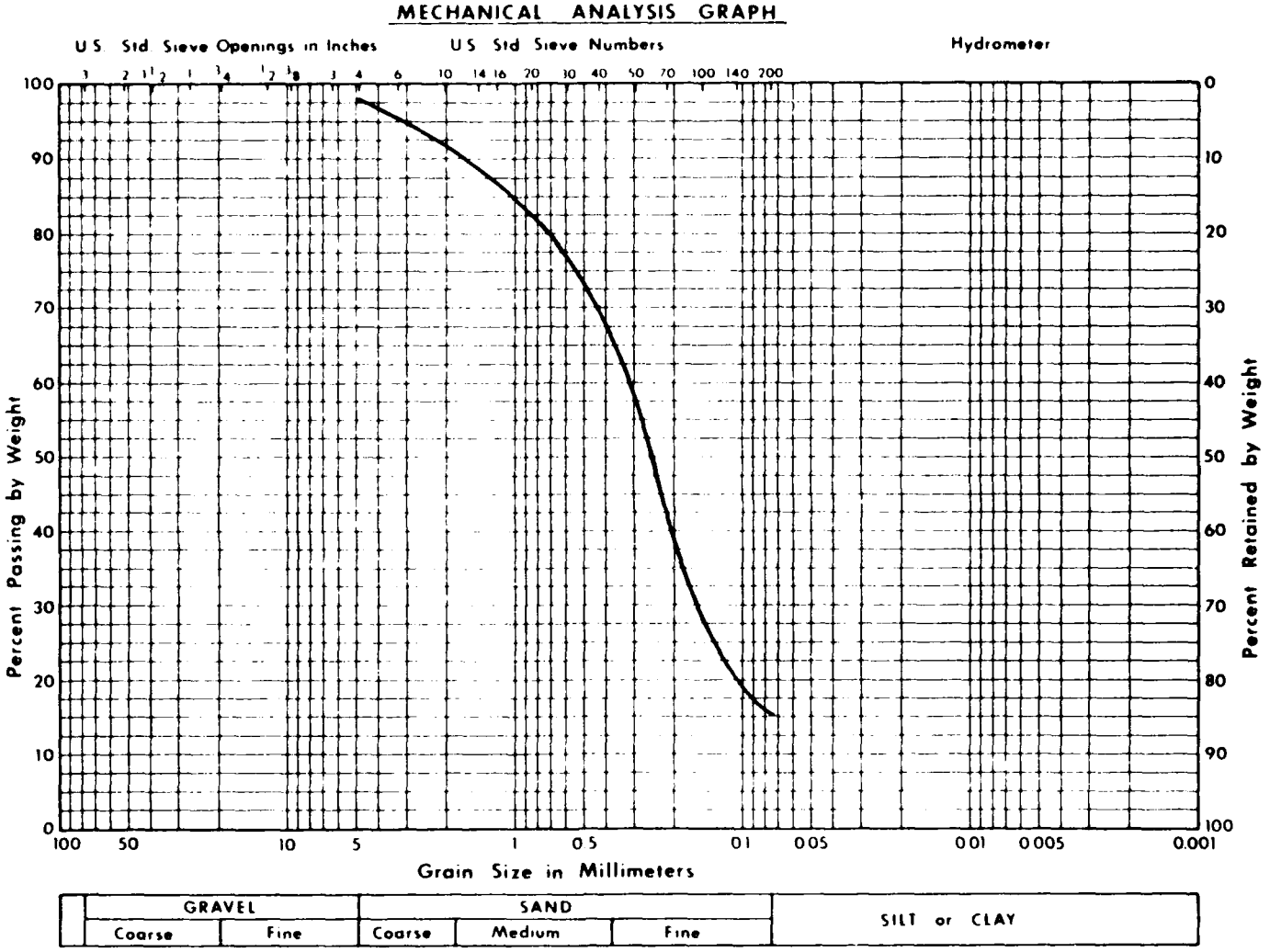

Figure D-6: GRAIN SIZE DISTRIBUTION; CYCLIC TRIAXIAL TEST NO. 3

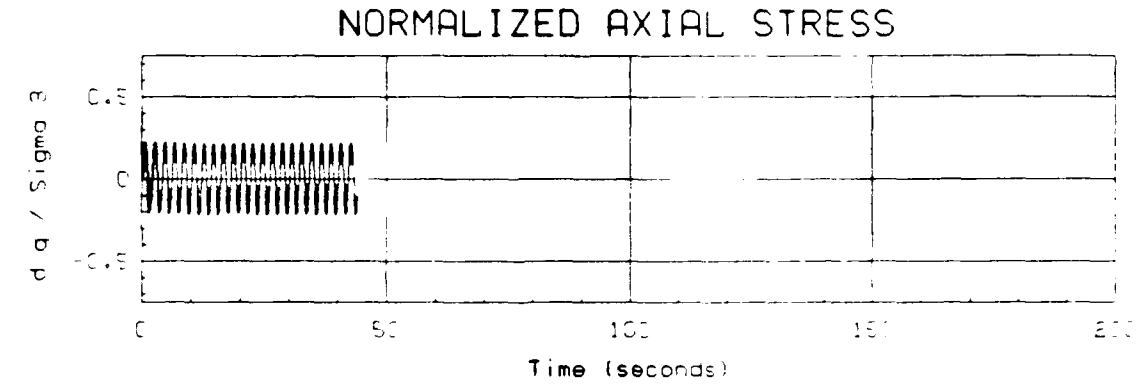

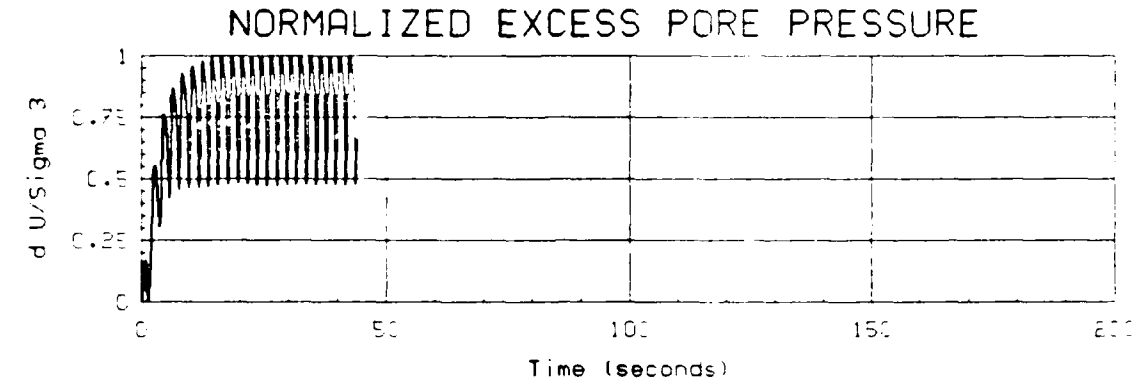

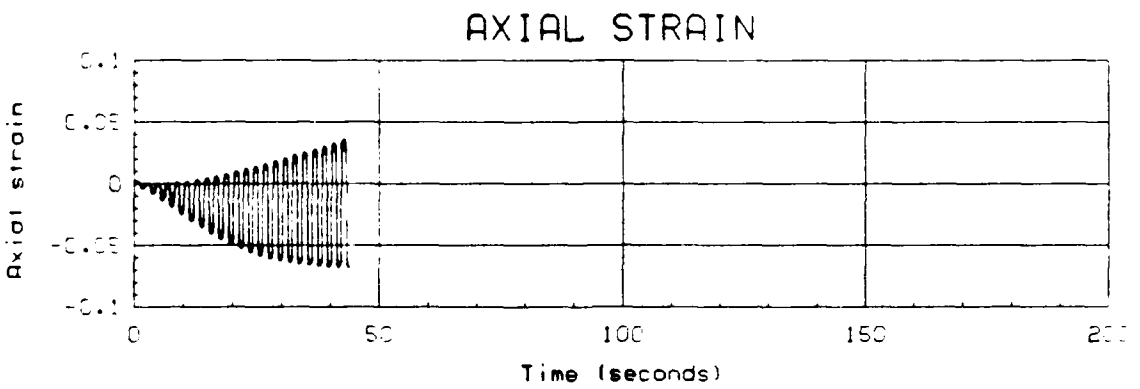

Test No.	:	5	B-value	:	0.995
Test Date	:	7/24/86	$\sigma_{3,i}'$	:	2.00 ksc
Material	:	Tube U111A-UF18	K_c	:	1.00
Silty Sand (SM-ML), 19% fines.			CSR	:	0.224

Figure D-7: UNDRAINED CYCLIC TRIAXIAL TEST NO. 5: HYDRAULIC FILL

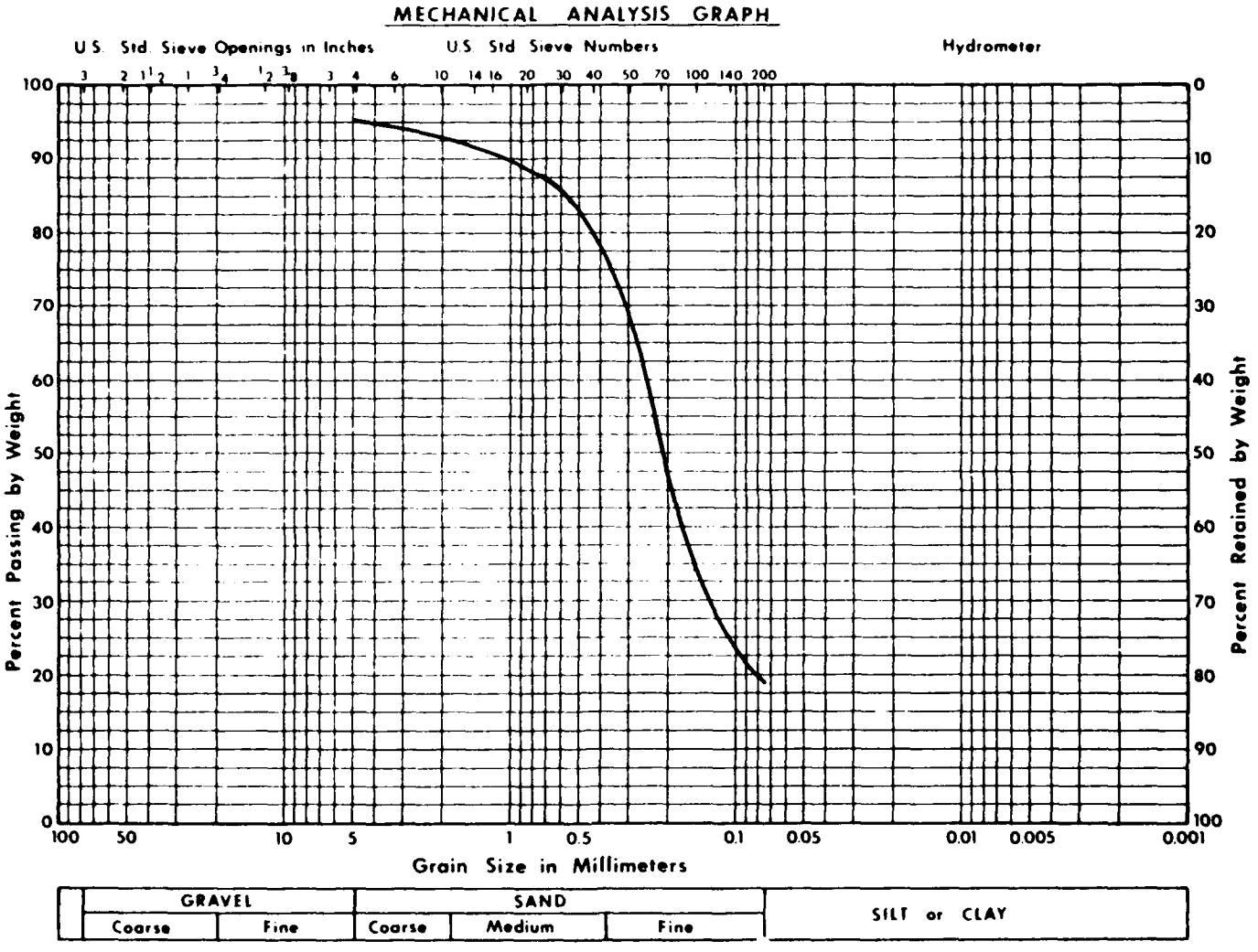

Figure D-8: GRAIN SIZE DISTRIBUTION; CYCLIC TRIAXIAL TEST NO. 5

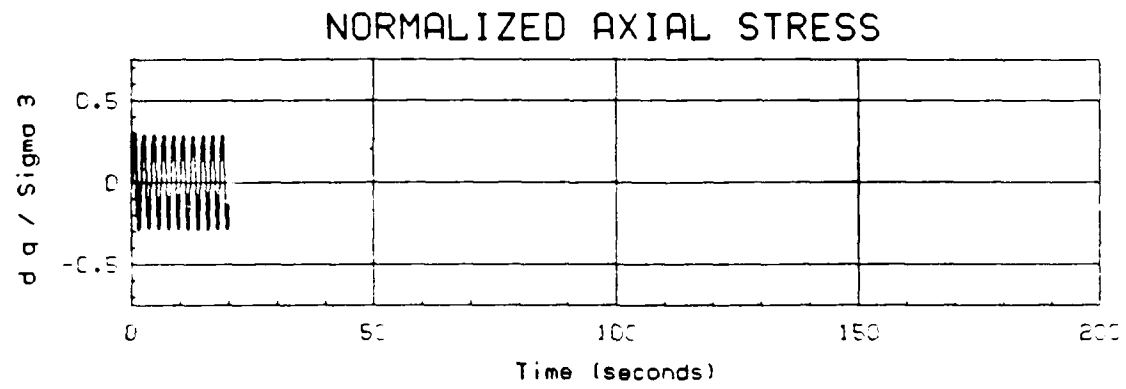

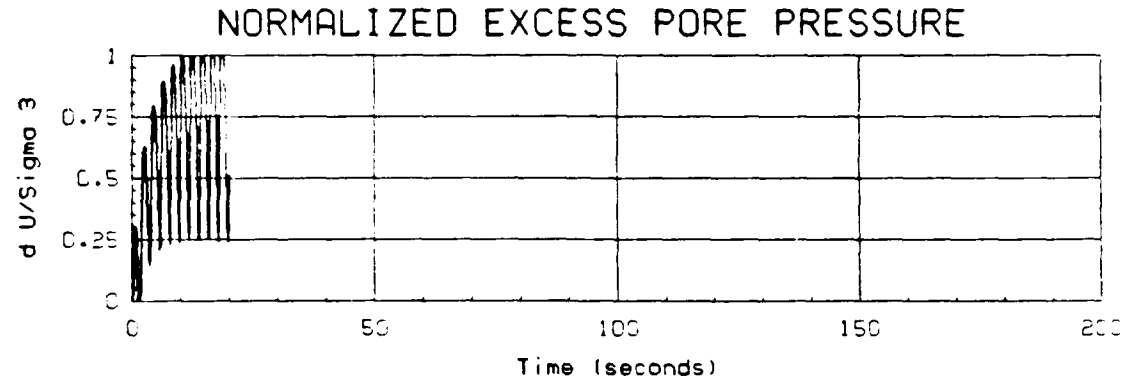

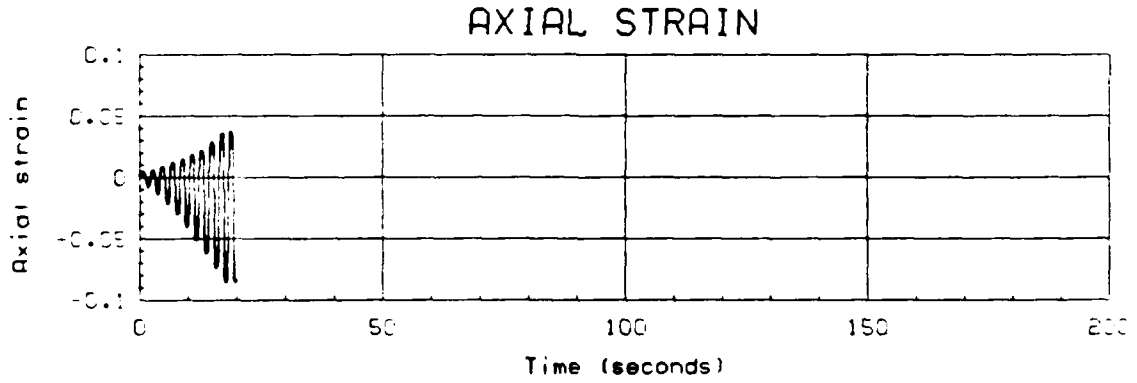

Test No.	:	8	B-value	:	0.995
Test Date	:	7/30/86	$\sigma_{3,i}'$	:	2.00 ksc
Material	:	Tube U111-UF18	K_c	:	1.00
Sandy Clayey Silt (ML), 56% fines.			CSR	:	0.288

Figure D-9: UNDRAINED CYCLIC TRIAXIAL TEST NO. 8: HYDRAULIC FILL

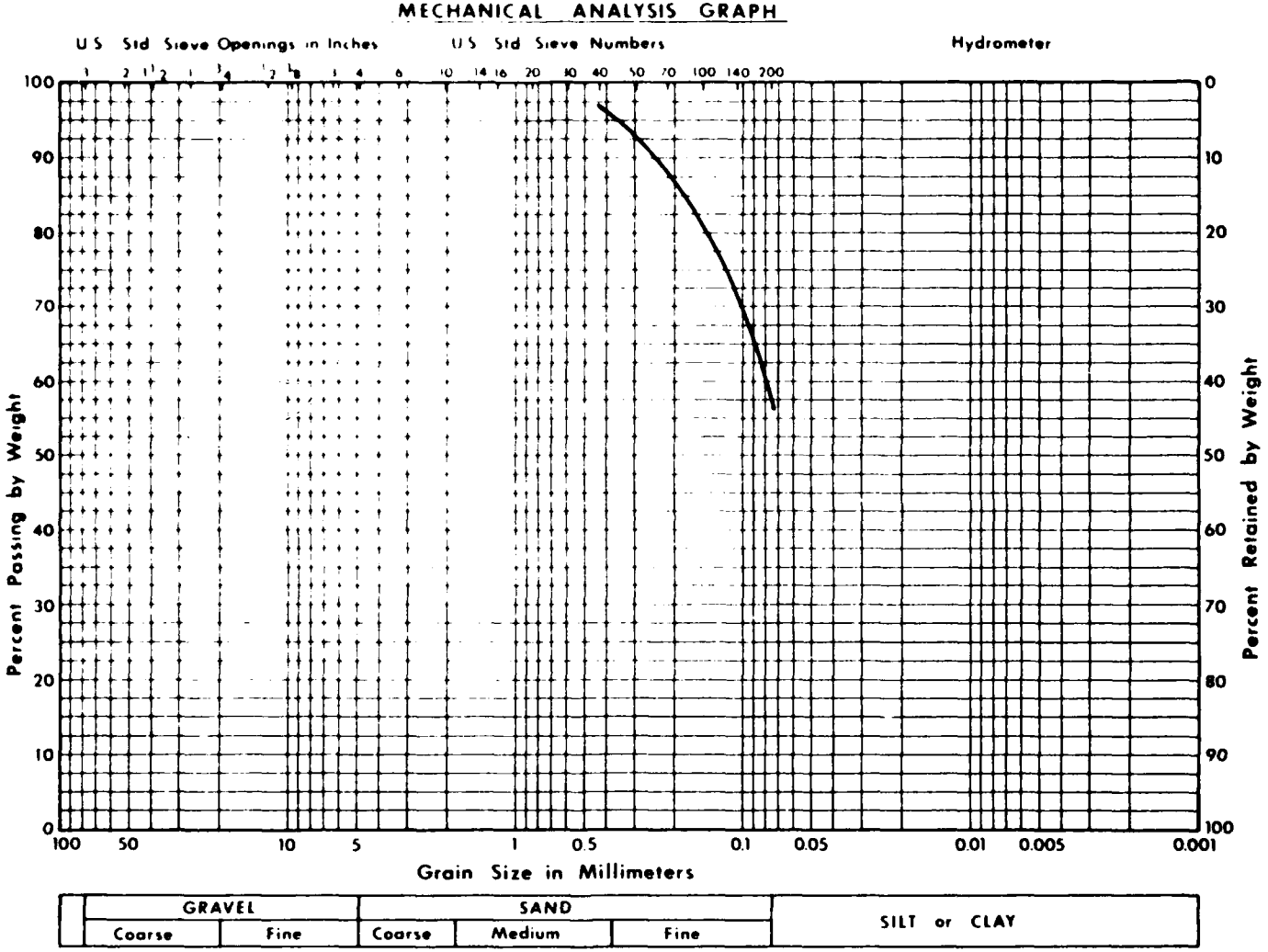

Figure D-10: GRAIN SIZE DISTRIBUTION; CYCLIC TRIAXIAL TEST NO.8

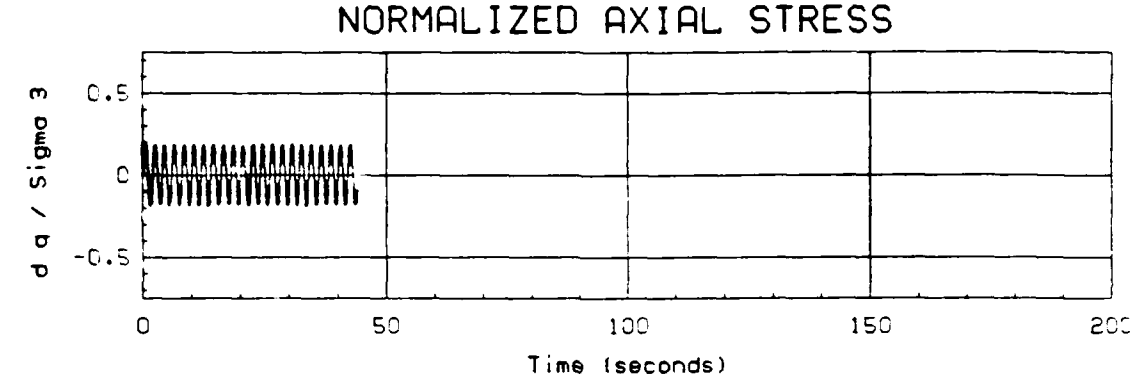

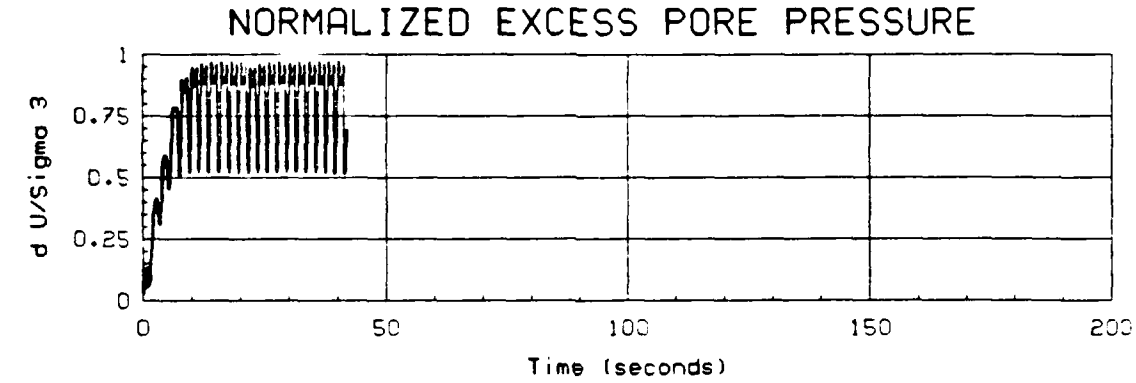

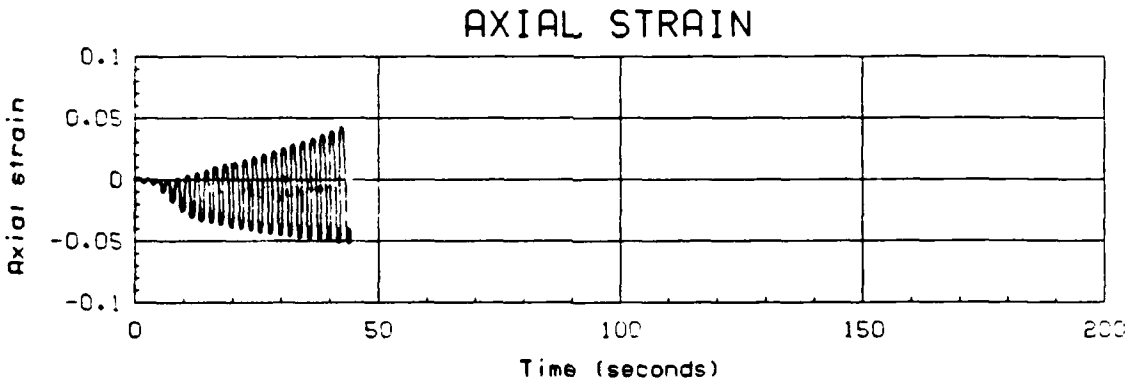

Test No.	:	15	B-value	:	0.986
Test Date	:	8/12/86	$\sigma_{3,i}'$	:	2.00 ksc
Material	:	Tube U102-UF1	K_c	:	1.00
Silty Sand (SM-ML), 35% fines.			CSR	:	0.193

Figure D-11: UNDRAINED CYCLIC TRIAXIAL TEST NO. 15: HYDRAULIC FILL

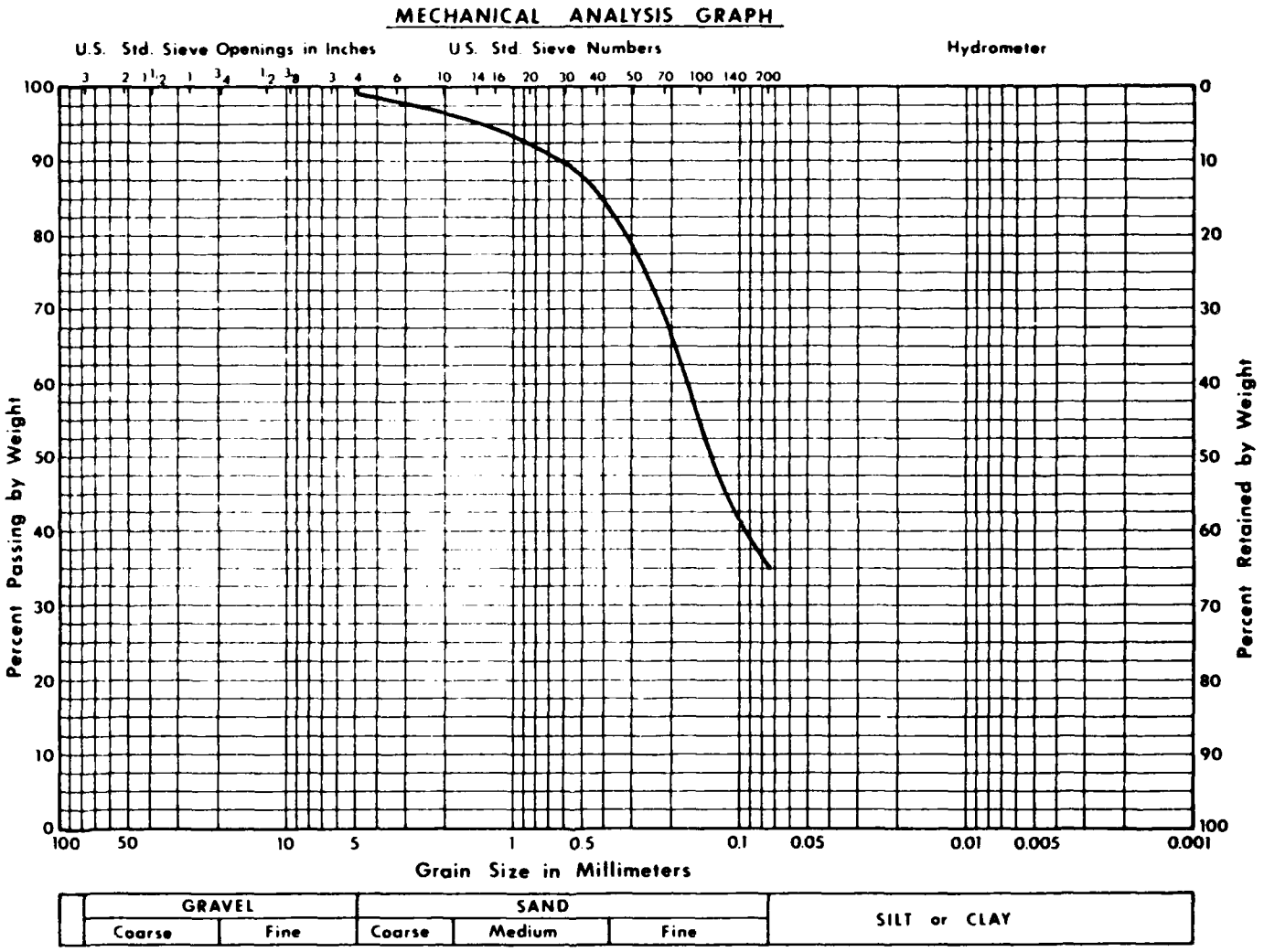

Figure D-12: GRAIN SIZE DISTRIBUTION; CYCLIC TRIAXIAL TEST NO. 15

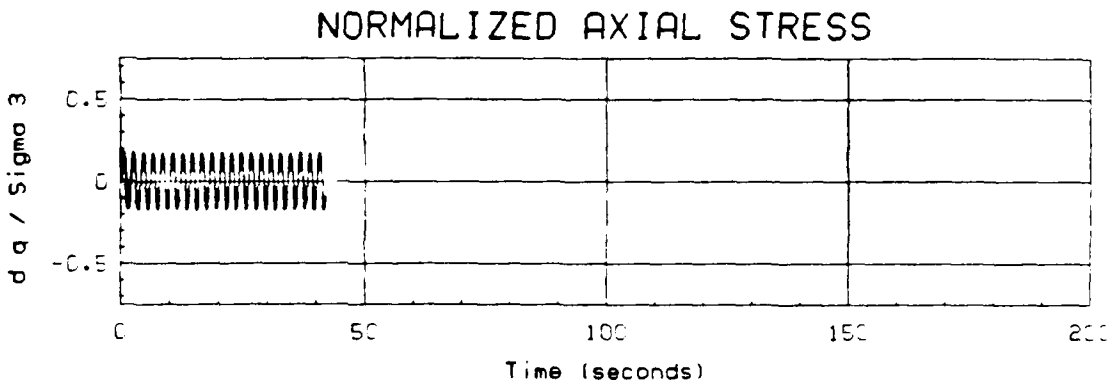

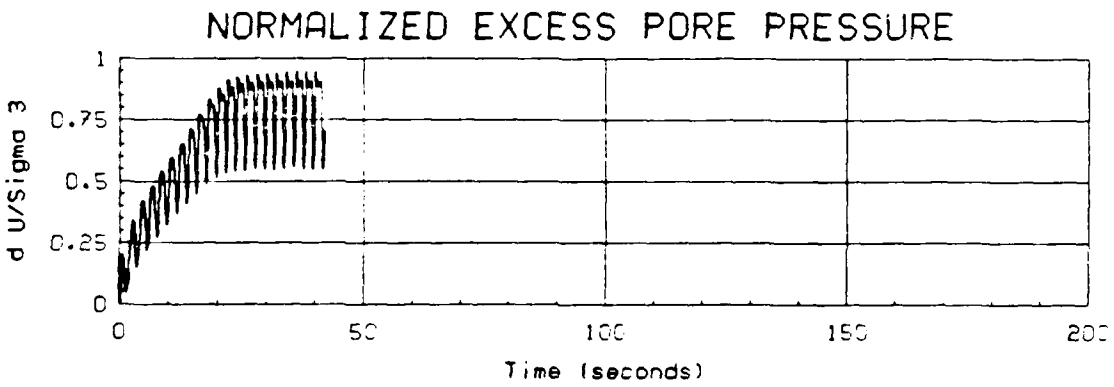

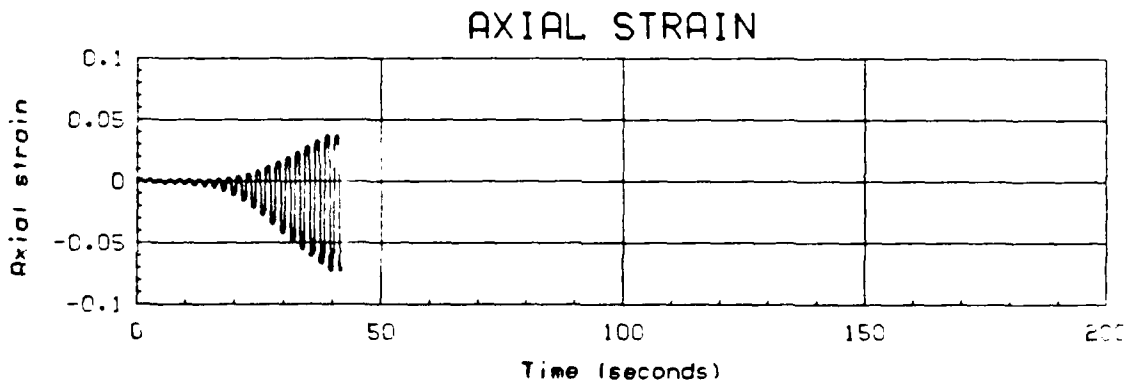

Test No.	:	17	B-value	:	0.989
Test Date	:	8/14/86	$\sigma_{3,i}'$	:	2.00 ksc
Material	:	Tube U111-UF21	K_c	:	1.00
Silty Sand (SM-ML), 25% fines.			CSR	:	0.184

Figure D-13: UNDRAINED CYCLIC TRIAXIAL TEST NO. 17: HYDRAULIC FILL

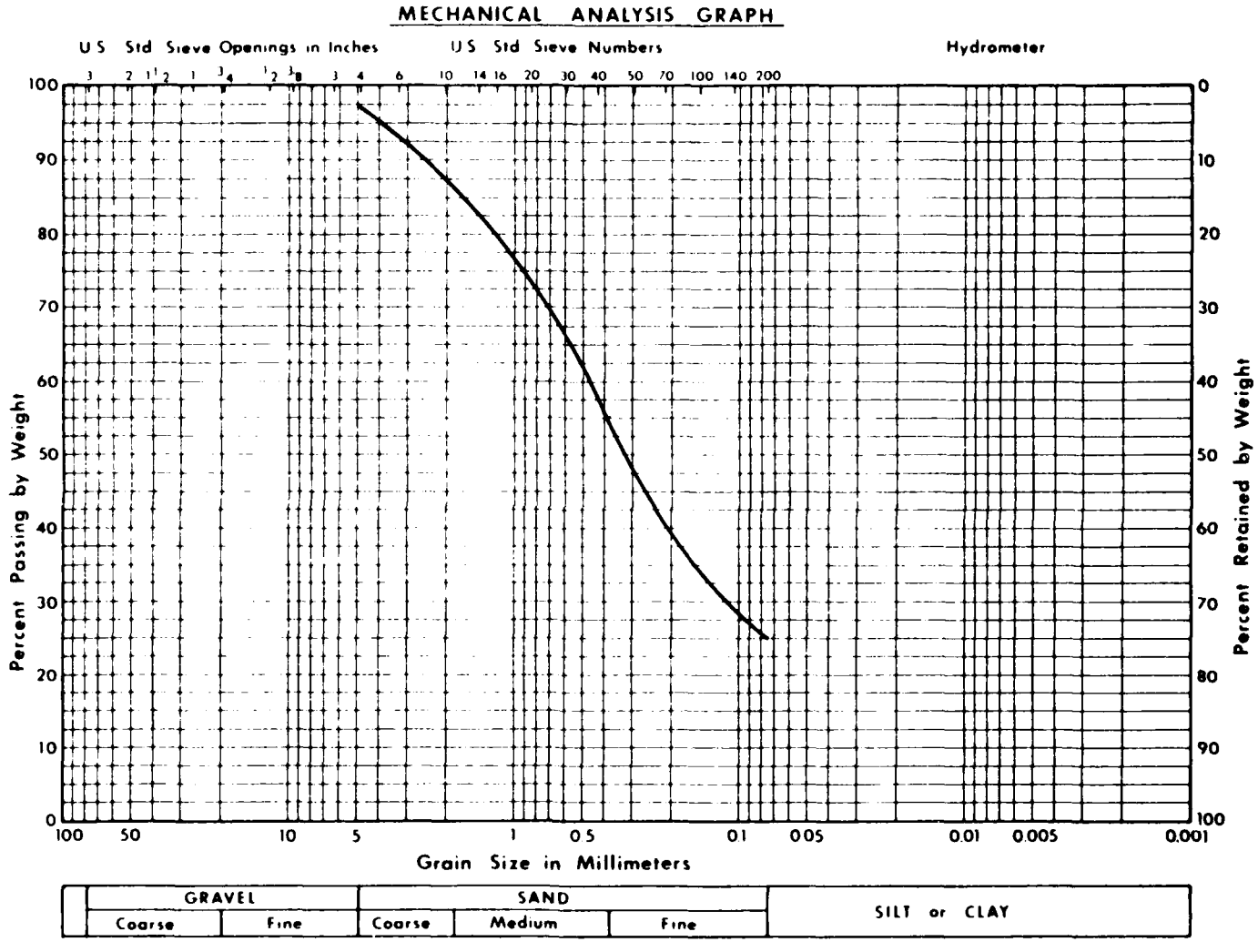

Figure D-14: GRAIN SIZE DISTRIBUTION; CYCLIC TRIAXIAL TEST NO. 17

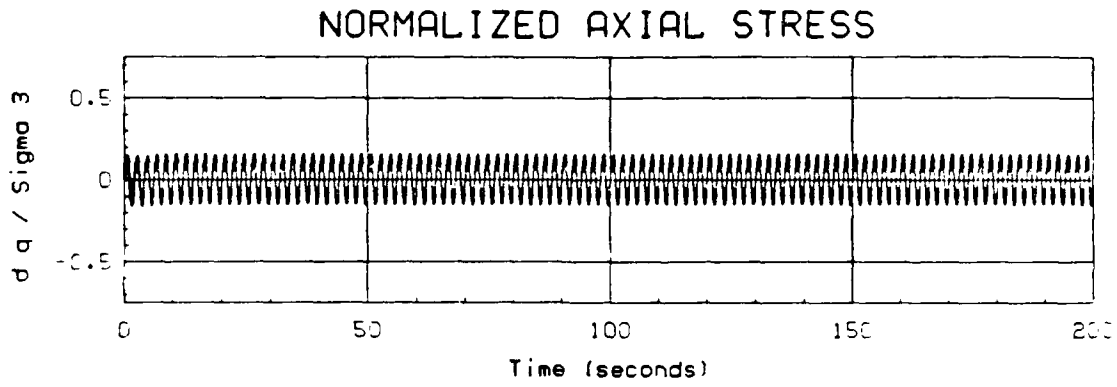

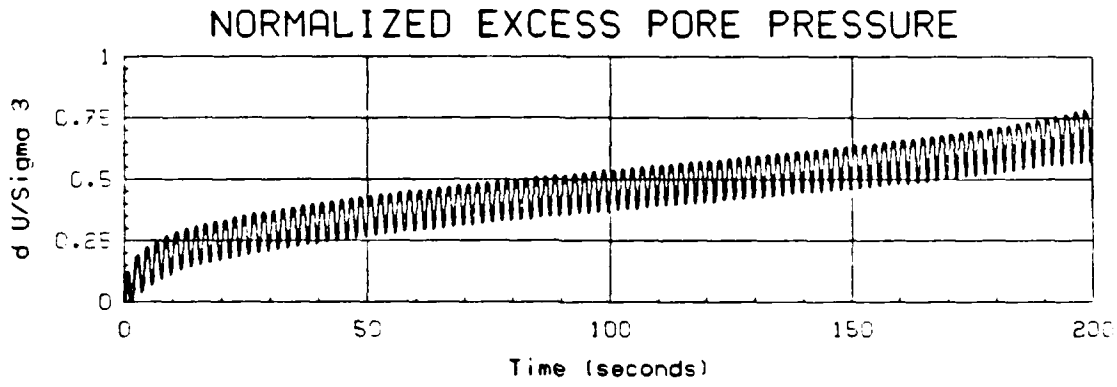

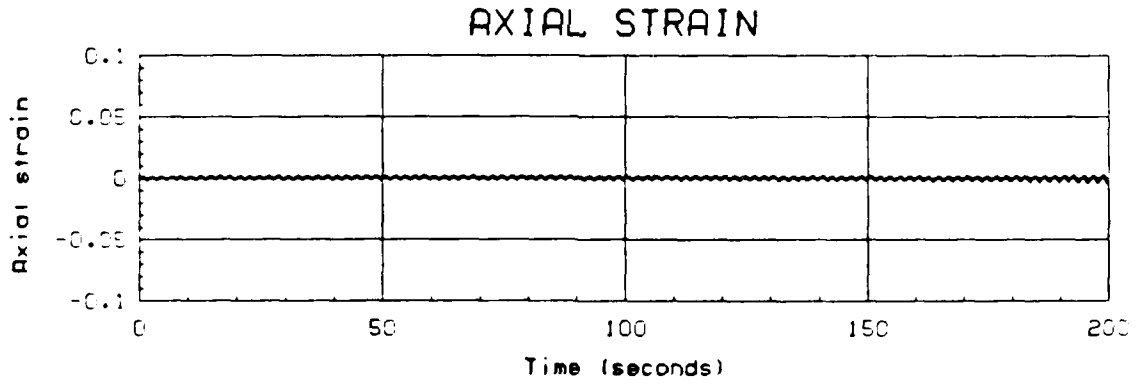

Test No.	:	18	B-value	:	0.998
Test Date	:	8/14/86	$\sigma_{3,i}'$	:	2.00 ksc
Material	:	Tube U111-UF21	K_c	:	1.00
Silty Sand (SM-ML), 17% fines.			CSR	:	0.162

Figure D-15: UNDRAINED CYCLIC TRIAXIAL TEST NO. 18: HYDRAULIC FILL

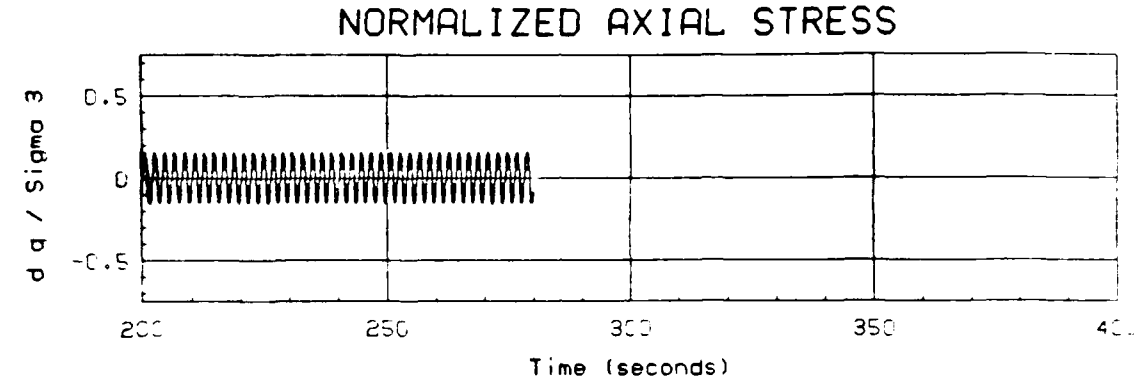

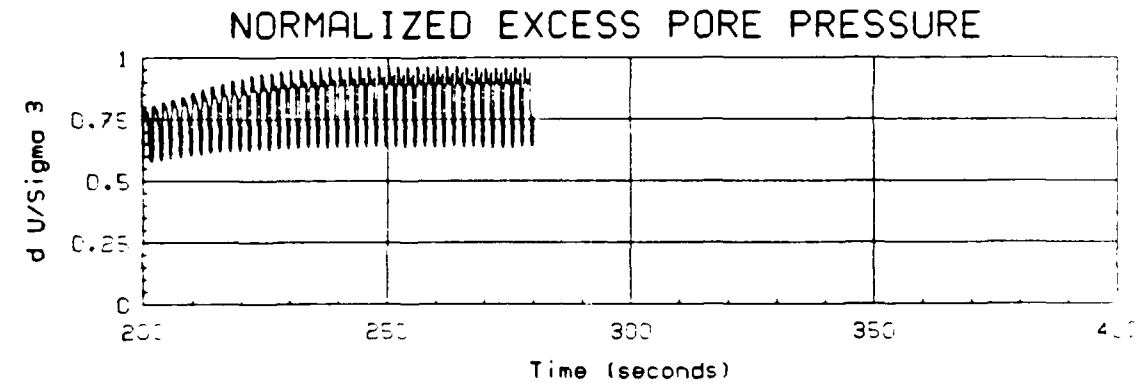

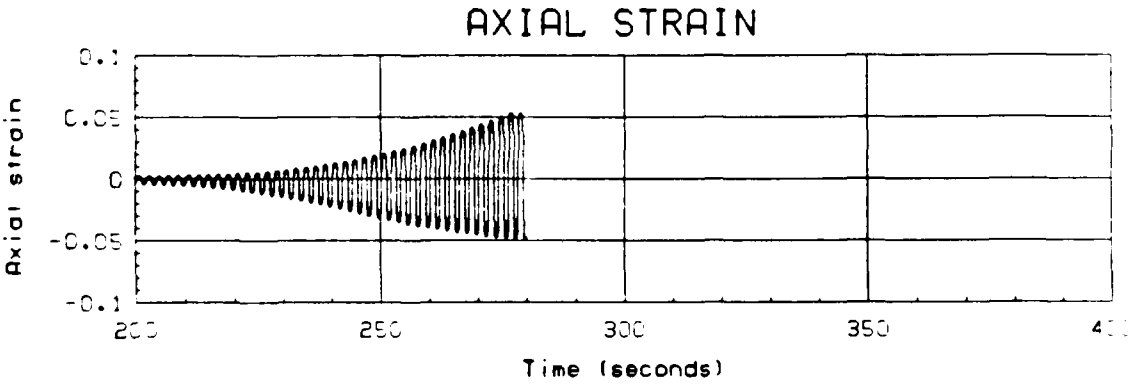

(Figure D-15, continued)

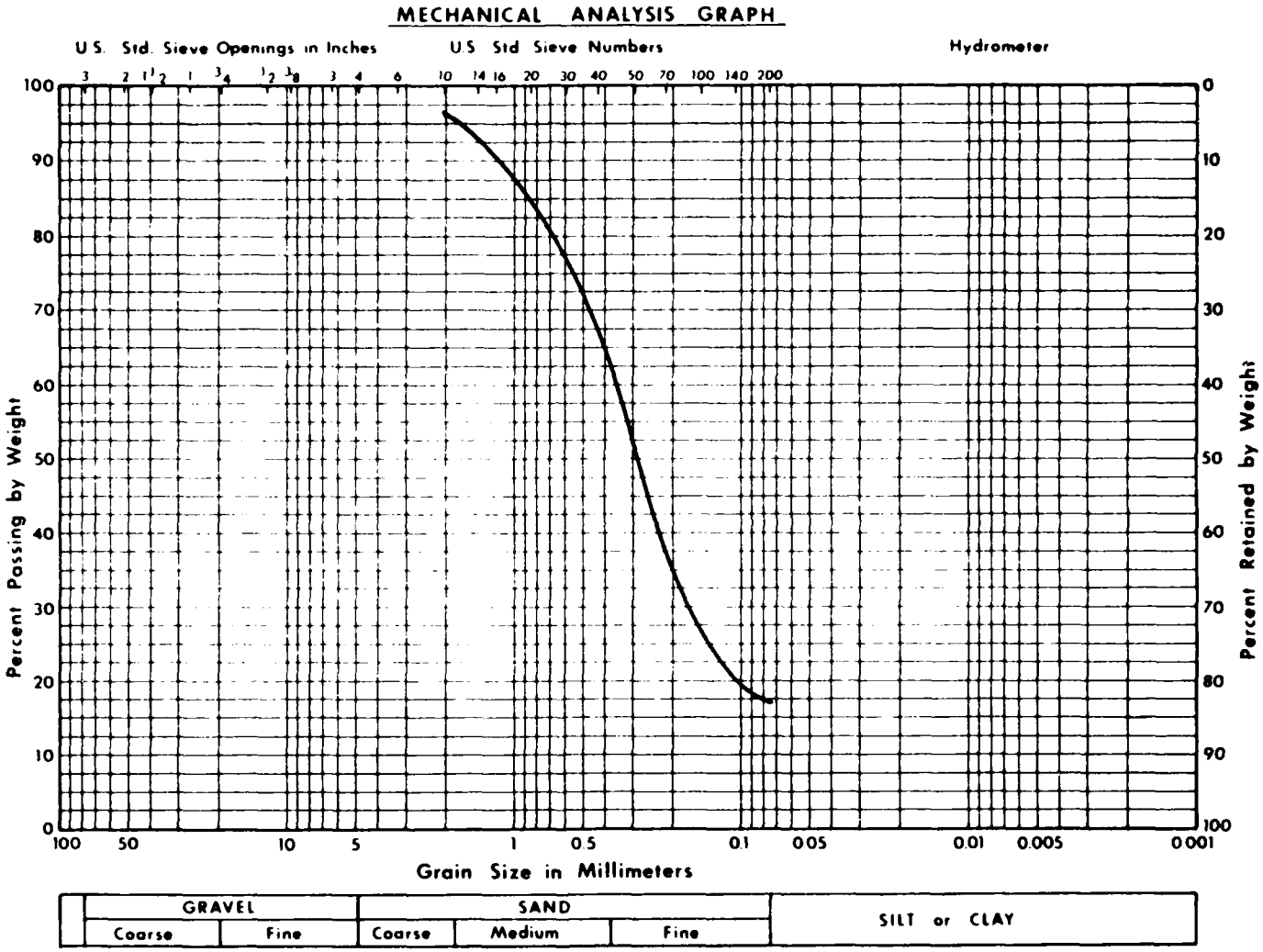

Figure D-16: GRAIN SIZE DISTRIBUTION; CYCLIC TRIAXIAL TEST NO. 18

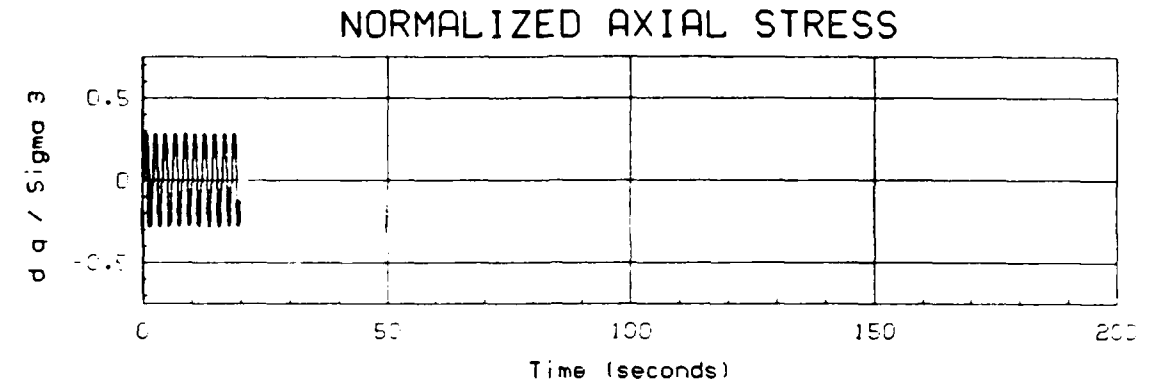

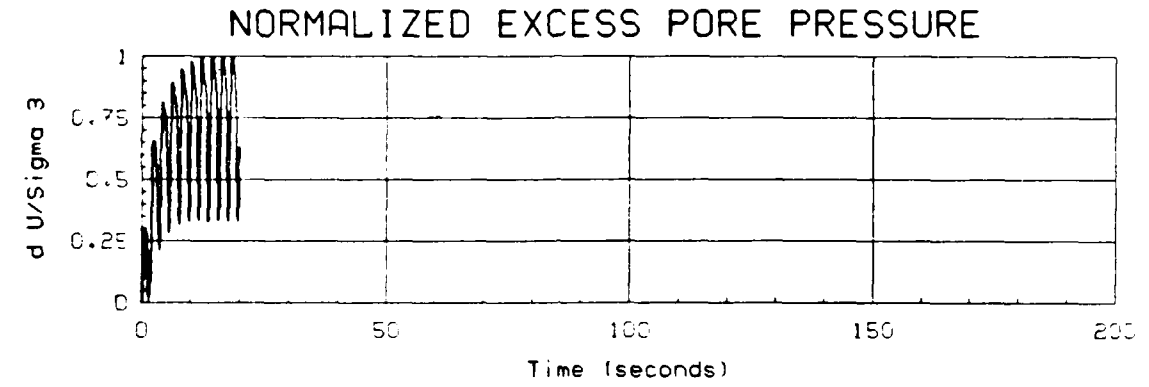

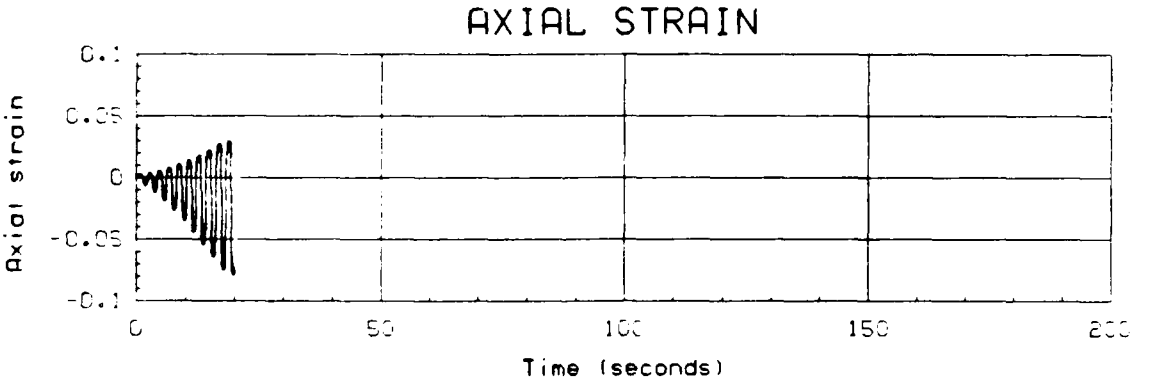

Test No.	:	21	B-value	:	0.988
Test Date	:	8/14/86	$\sigma_{3,i}'$	:	2.00 ksc
Material	:	Tube U103-UF4	K_c	:	1.00
Sandy Clayey Silt (ML), 63% fines.			CSR	:	0.282

Figure D-17: UNDRAINED CYCLIC TRIAXIAL TEST NO. 21: HYDRAULIC FILL

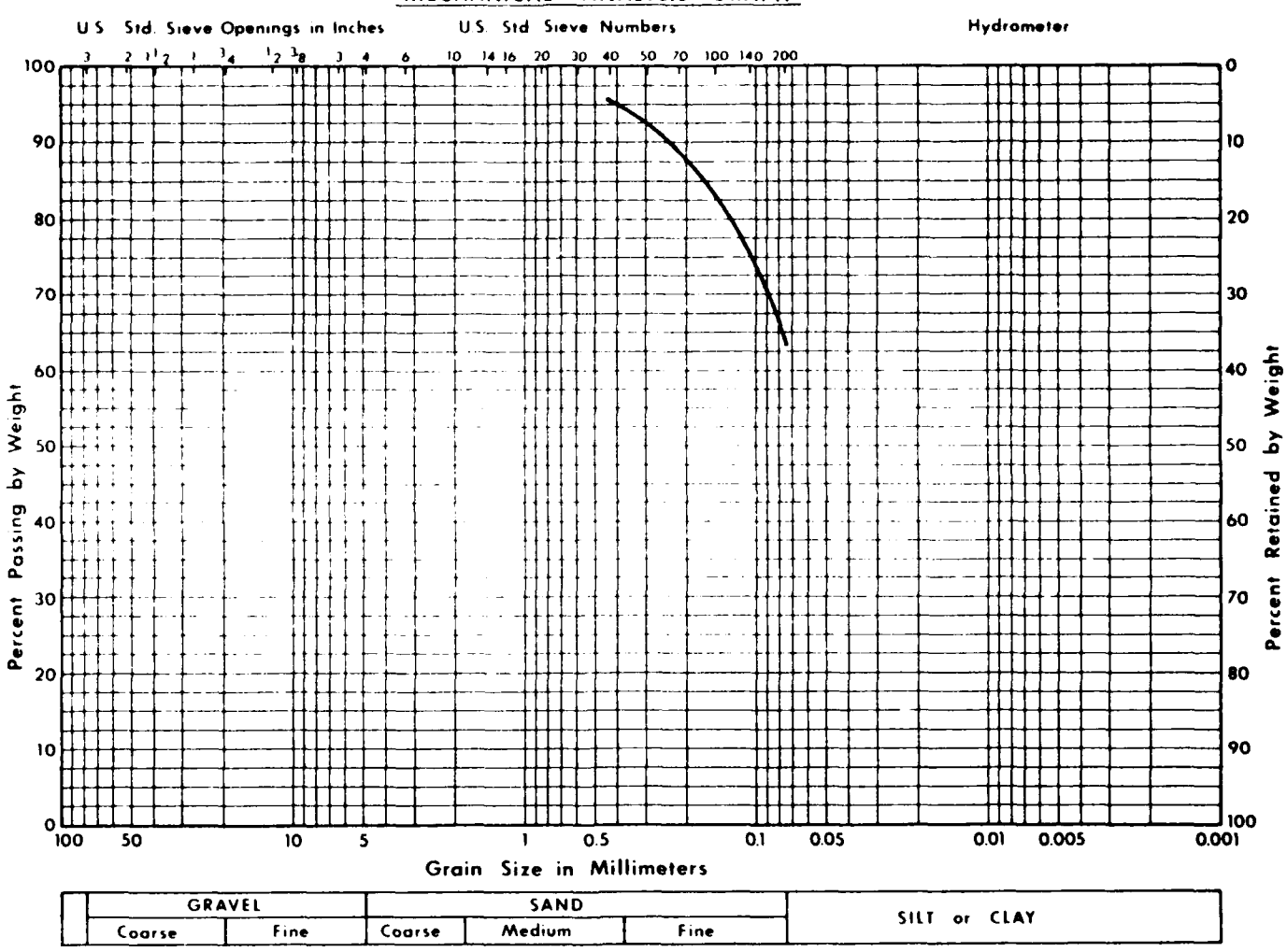

Figure D-18: GRAIN SIZE DISTRIBUTION; CYCLIC TRIAXIAL TEST NO. 21

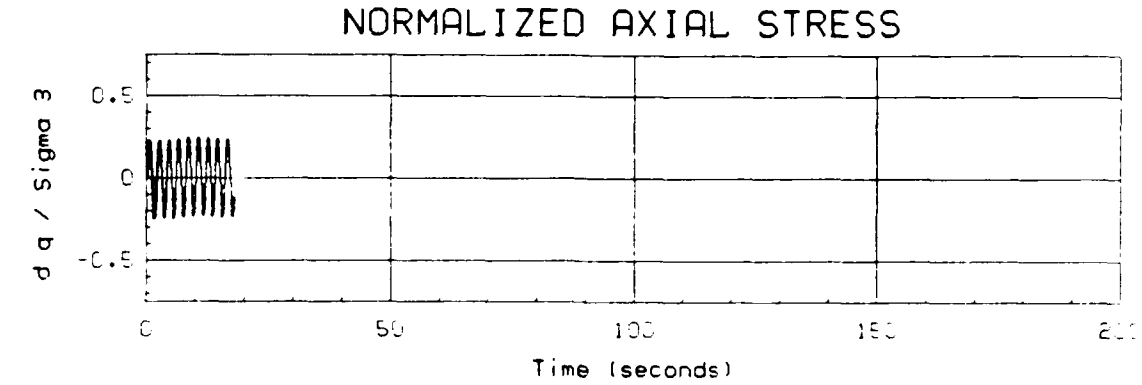

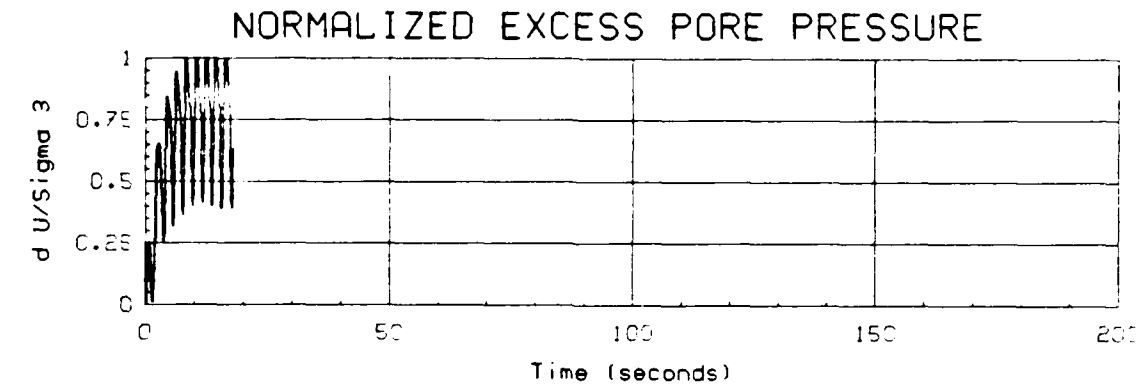

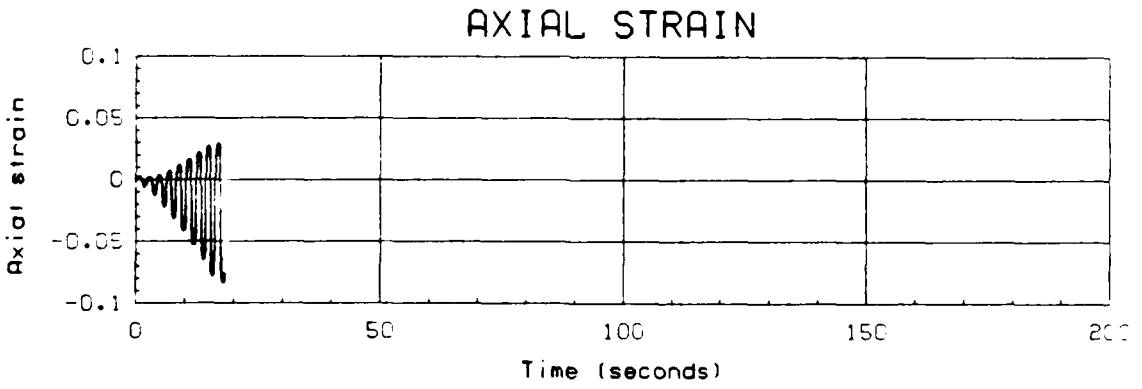

Test No.	:	22	B-value	:	0.996
Test Date	:	8/15/86	$\sigma_{3,i}'$	:	2.00 ksc
Material	:	Tube U103-UF4	K_c	:	1.00
		Silty Sand (SM-ML), 39% fines.	CSR	:	0.243

Figure D-19: UNDRAINED CYCLIC TRIAXIAL TEST NO. 22: HYDRAULIC FILL

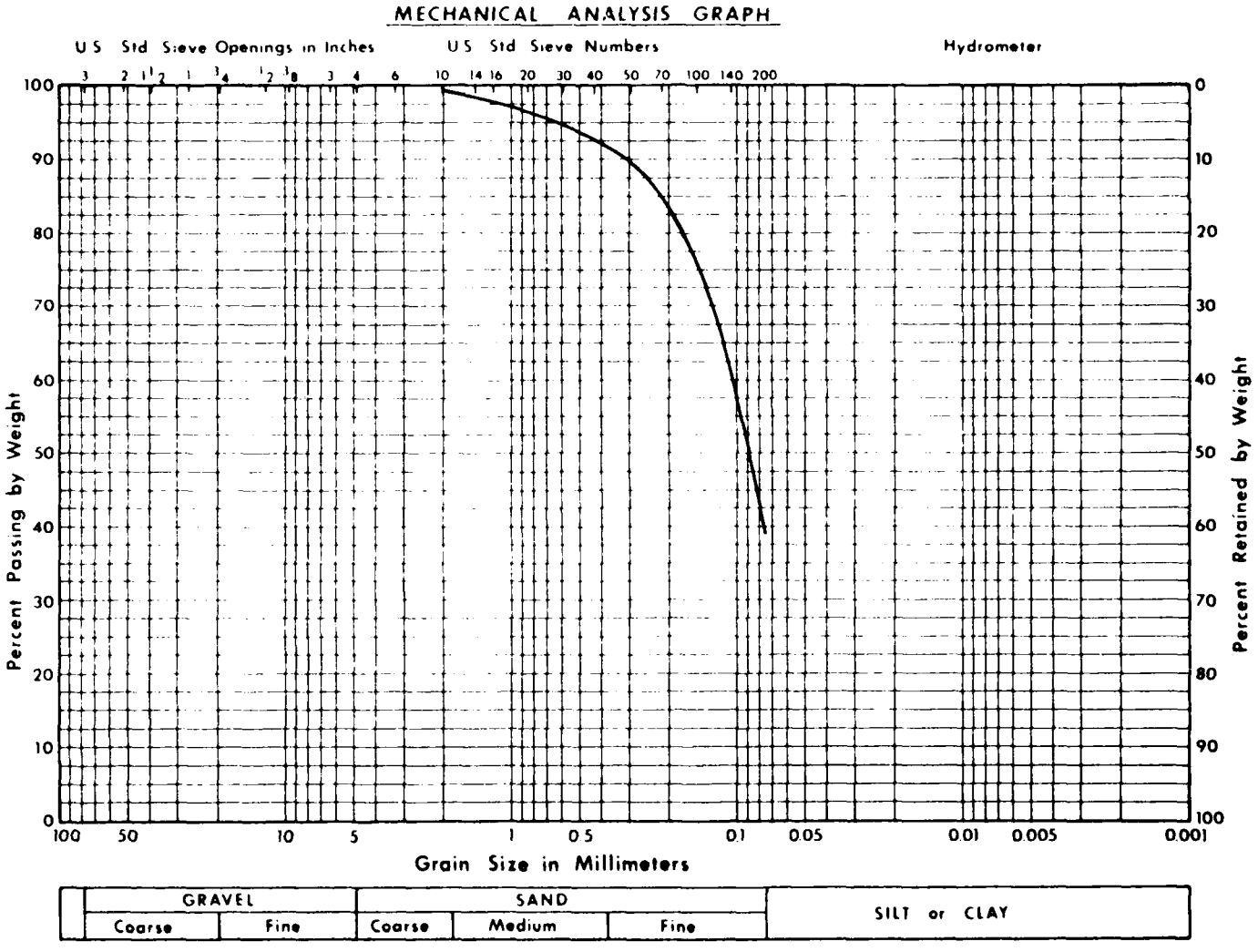

Figure D-20: GRAIN SIZE DISTRIBUTION; CYCLIC TRIAXIAL TEST NO. 22

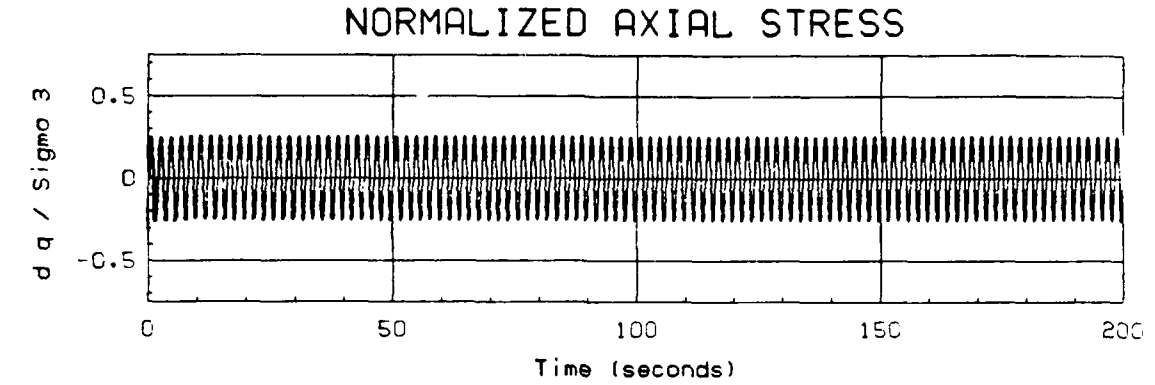

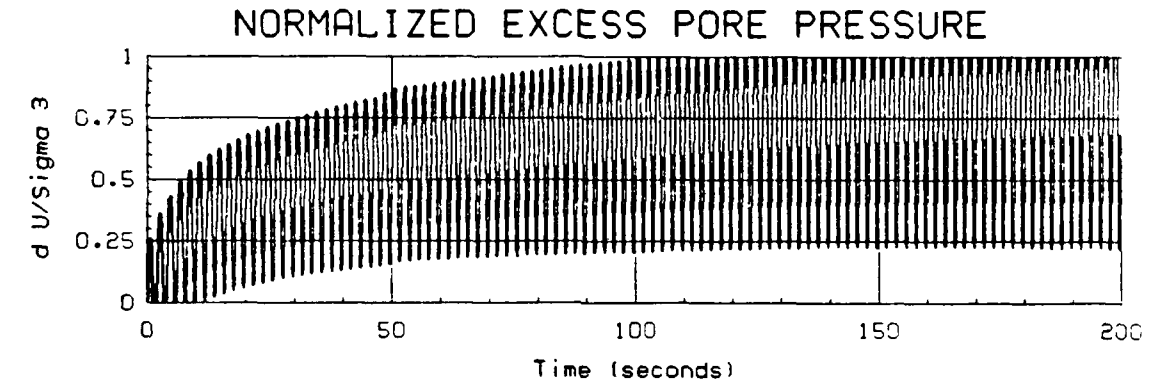

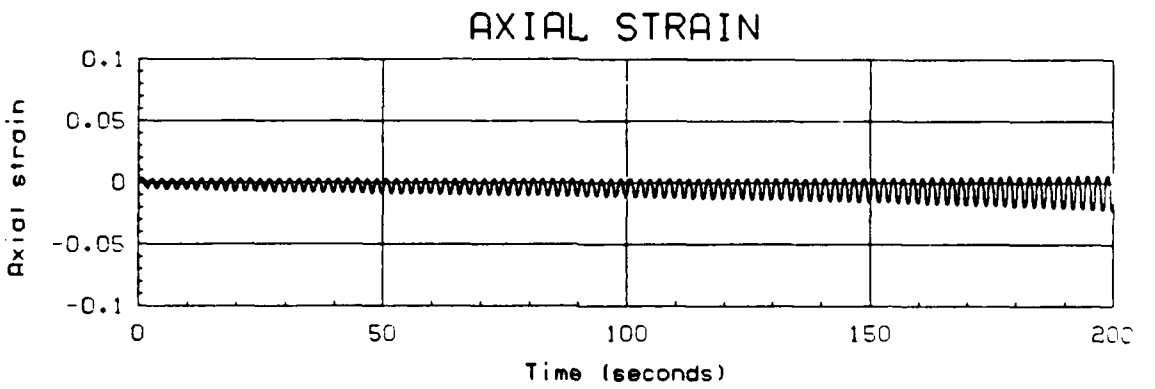

Test No.	: 27	B-value	: 0.990
Test Date	: 8/19/86	$\sigma_{3,i}'$	: 2.00 ksc
Material	: Tube U105-UF12	K_c	: 1.00
Silty Clay (CL), 99% fines.		CSR	: 0.255

Figure D-21: UNDRAINED CYCLIC TRIAXIAL TEST NO. 27: HYDRAULIC FILL

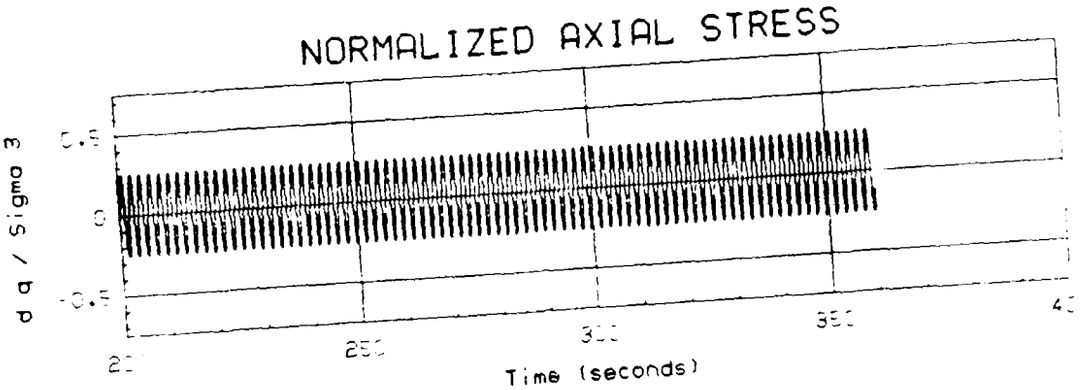

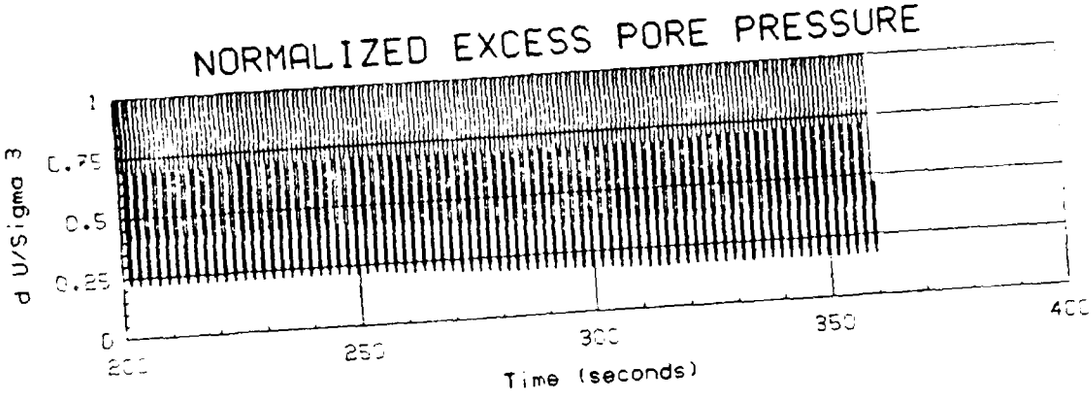

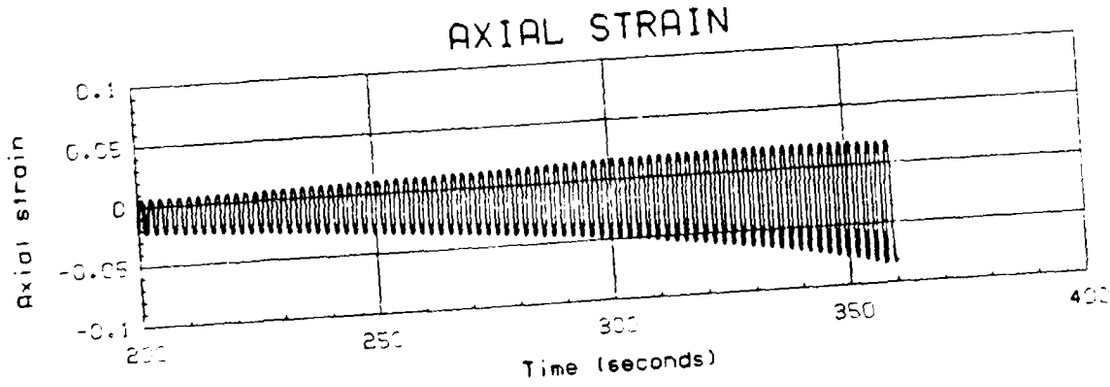

(Figure D-21, continued)

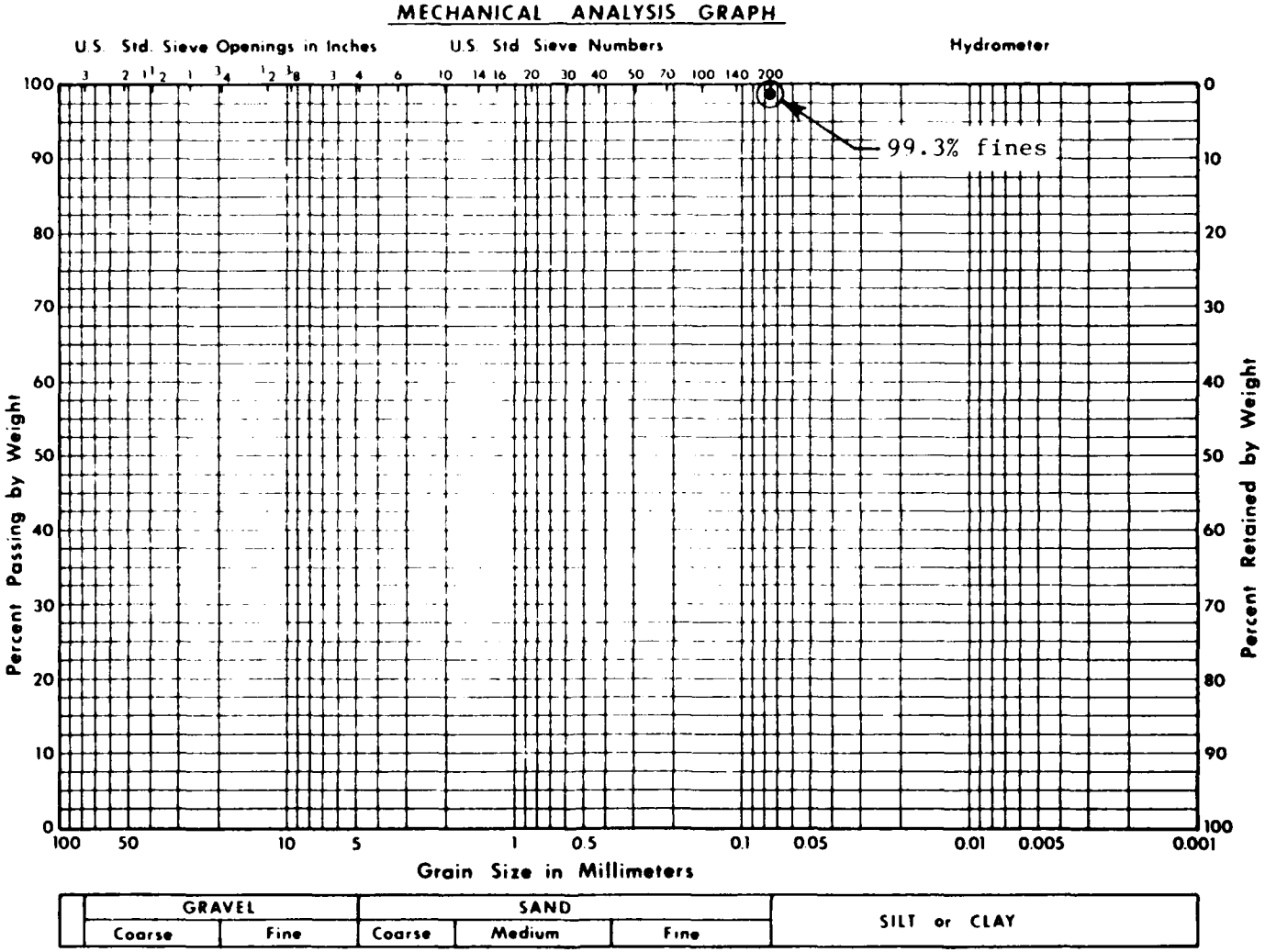

Figure D-22: GRAIN SIZE DISTRIBUTION; CYCLIC TRIAXIAL TEST NO. 27

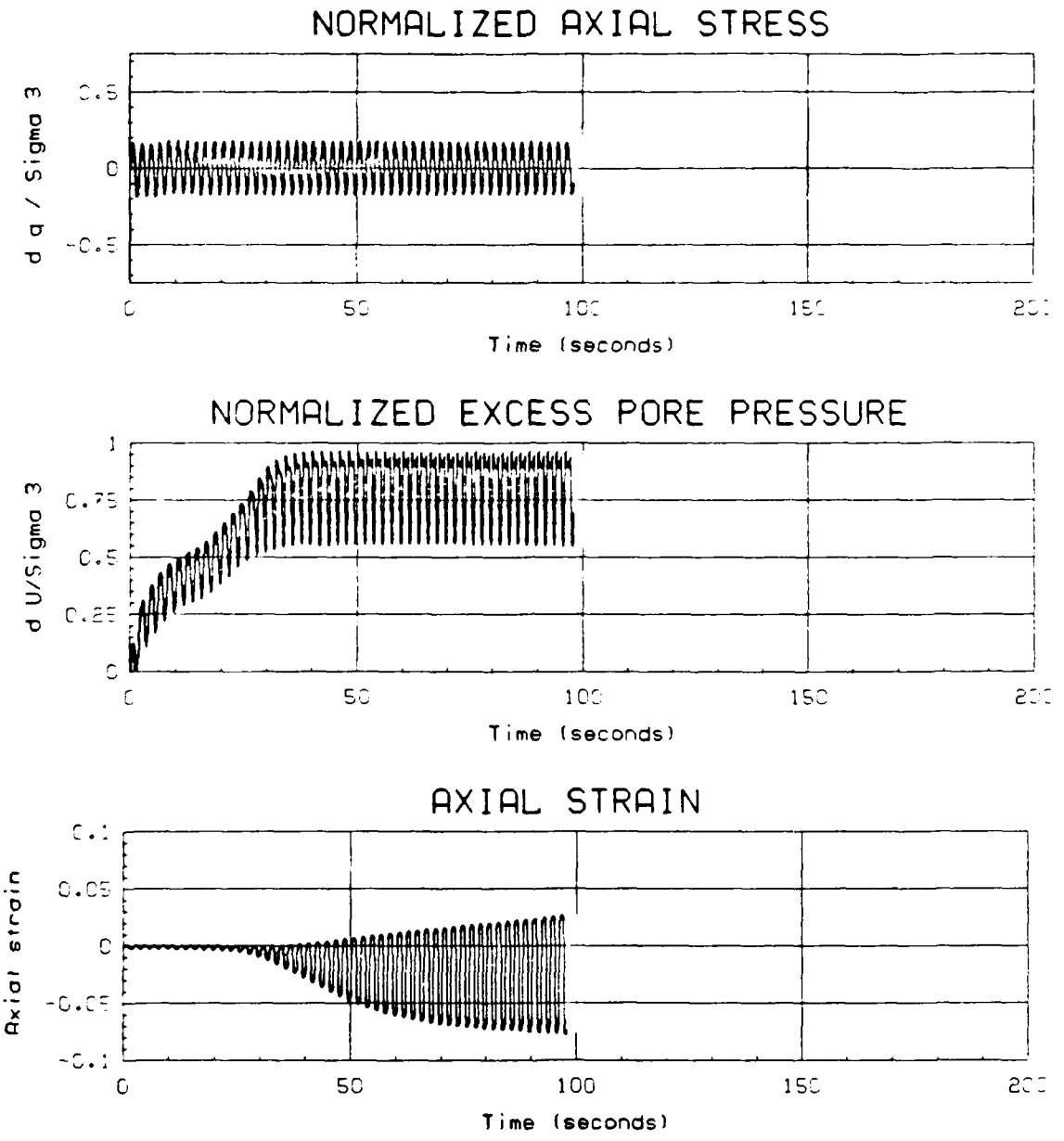

Test No.	:	30	B-value	:	0.987
Test Date	:	8/22/86	$\sigma_{3,i}'$	:	2.00 ksc
Material	:	Tube U111-UF4	K_c	:	1.00
Silty Sand (SM-ML), 24% fines.			CSR	:	0.183

Figure D-23: UNDRAINED CYCLIC TRIAXIAL TEST NO. 30: HYDRAULIC FILL

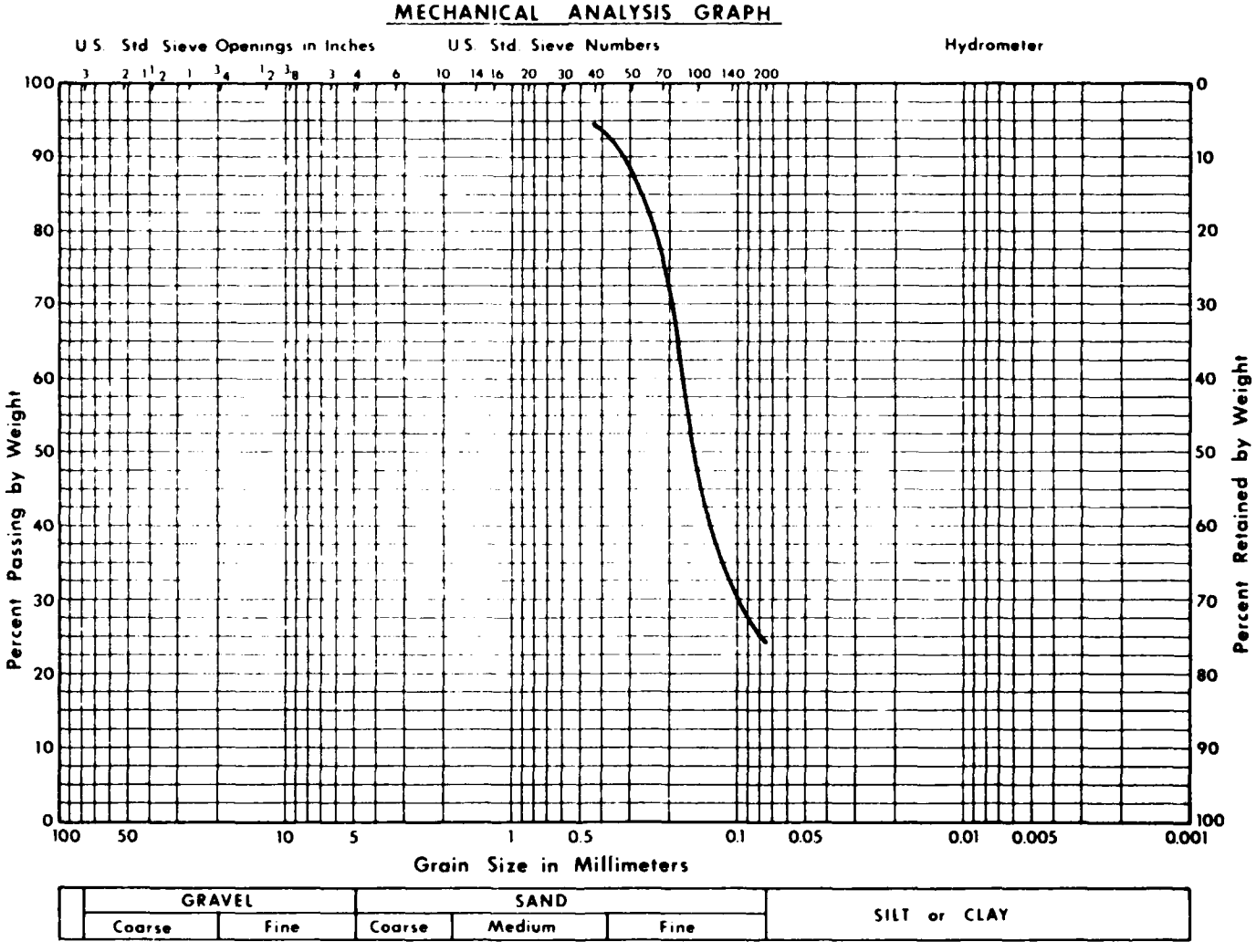

Figure D-24: GRAIN SIZE DISTRIBUTION; CYCLIC TRIAXIAL TEST NO. 30

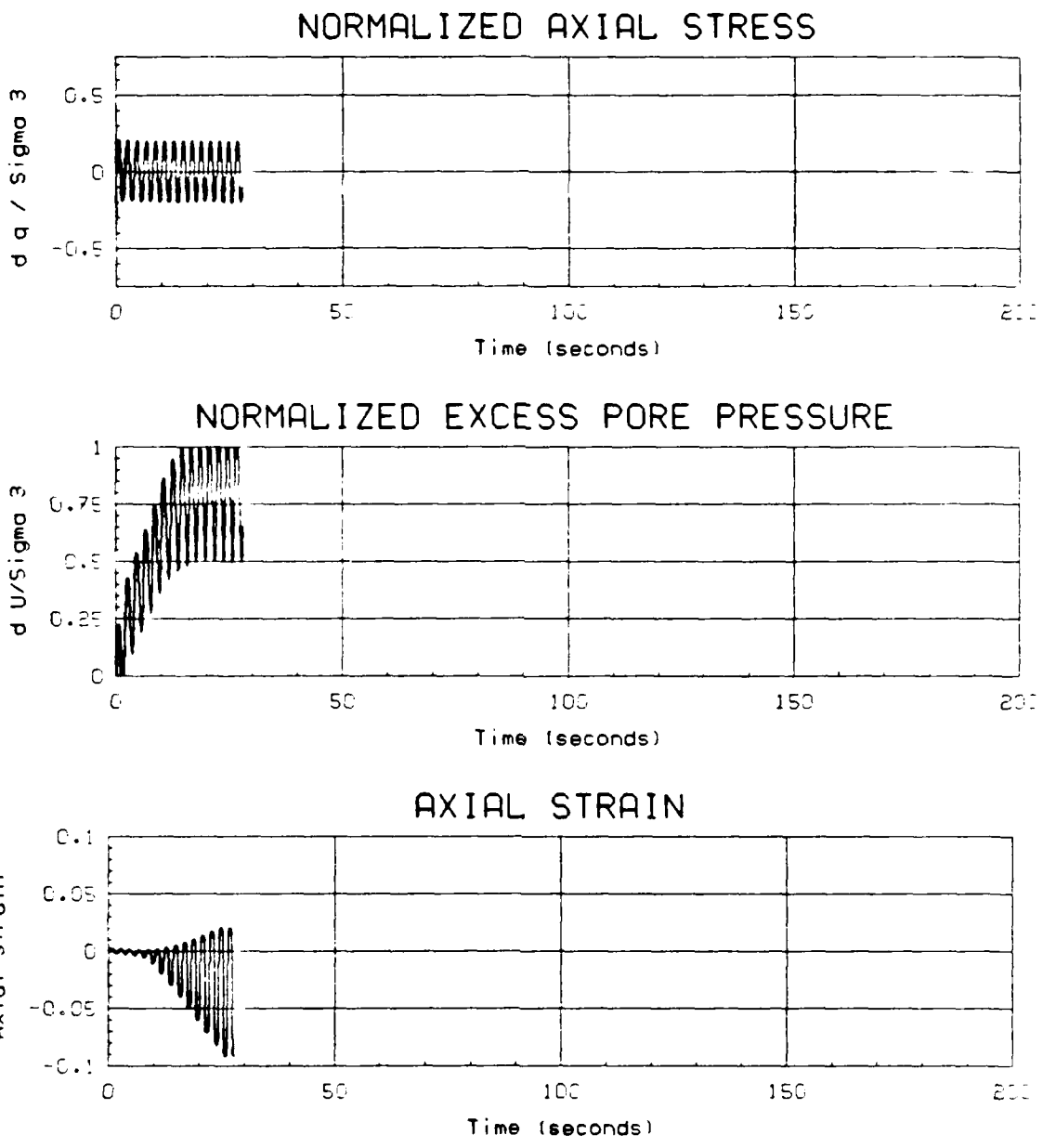

Test No.	:	31	B-value	:	0.994
Test Date	:	8/22/86	$\sigma_{3,i}'$	:	2.00 ksc
Material	:	Tube U111-UF4	K_c	:	1.00
Sandy Clayey Silt (ML), 58% fines.			CSR	:	0.208

Figure D-25: UNDRAINED CYCLIC TRIAXIAL TEST NO. 31: HYDRAULIC FILL

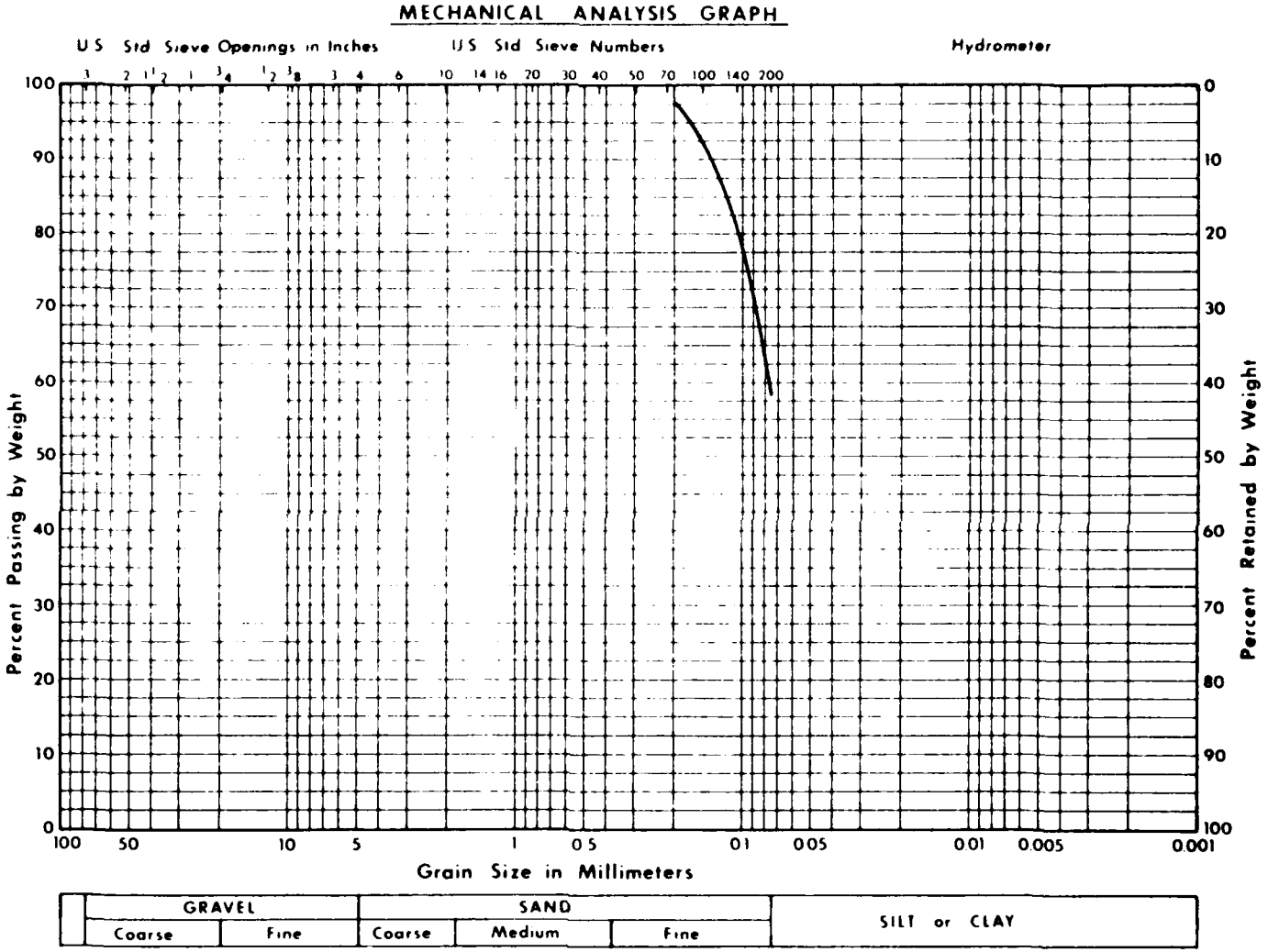

Figure D-26: GRAIN SIZE DISTRIBUTION; CYCLIC TRIAXIAL TEST NO. 31

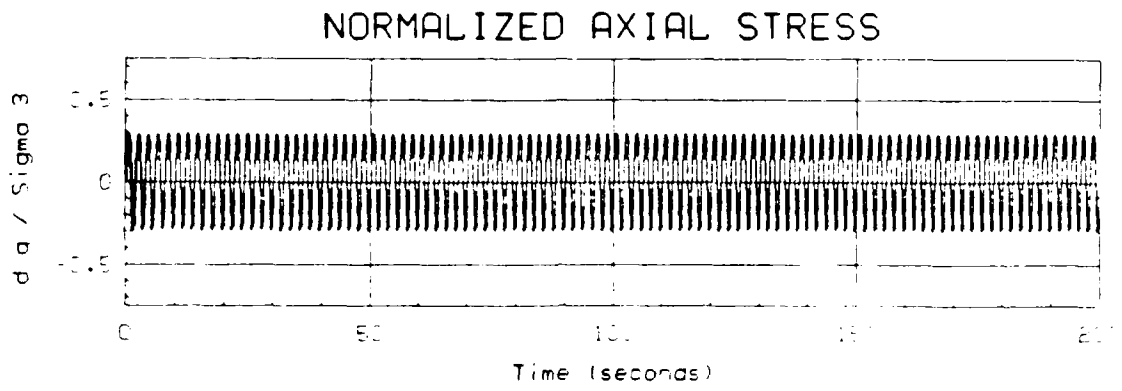

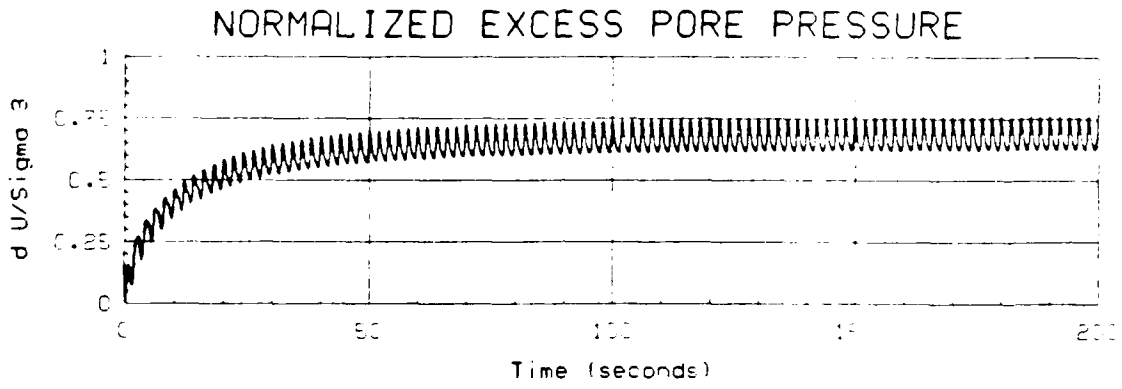

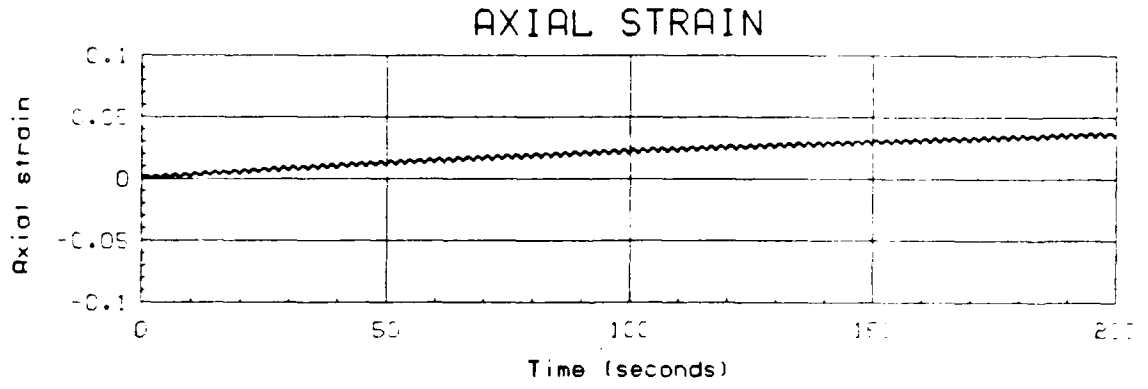

Test No.	:	32	B-value	:	0.993
Test Date	:	8/22/86	$\sigma_{3,i}'$	:	2.00 ksc
Material	:	Tube U111-UF9	K_c	:	1.75
Silty Sand (SM-ML), 24% fines.			CSR	:	0.293

Figure D-27: UNDRAINED CYCLIC TRIAXIAL TEST NO. 32: HYDRAULIC FILL

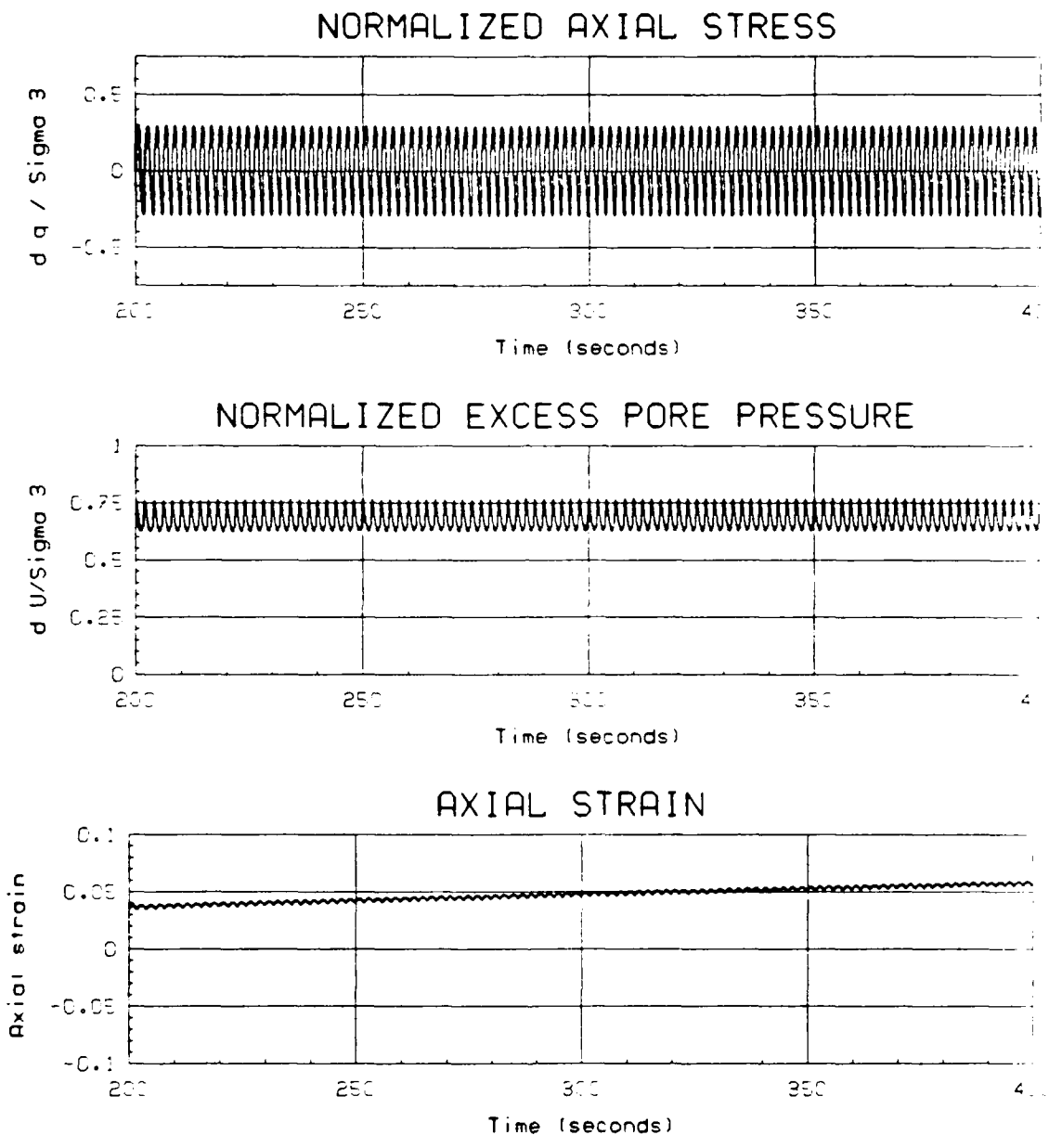

(Figure D-27, continued)

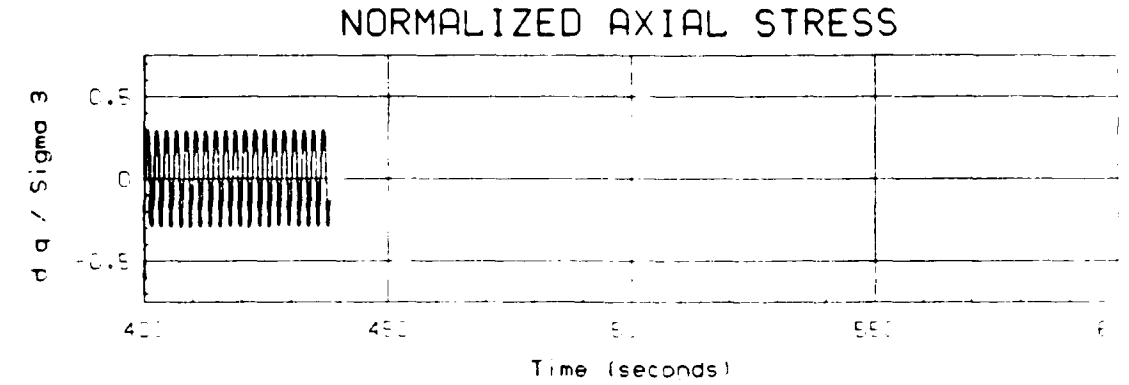

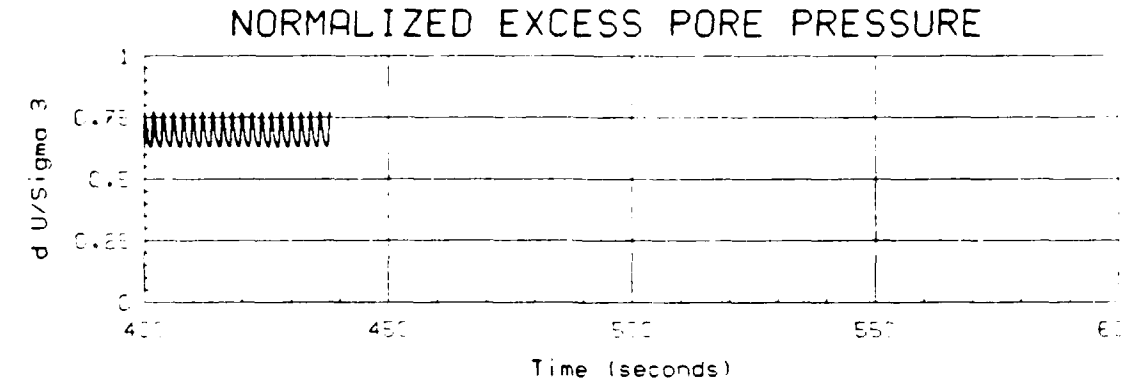

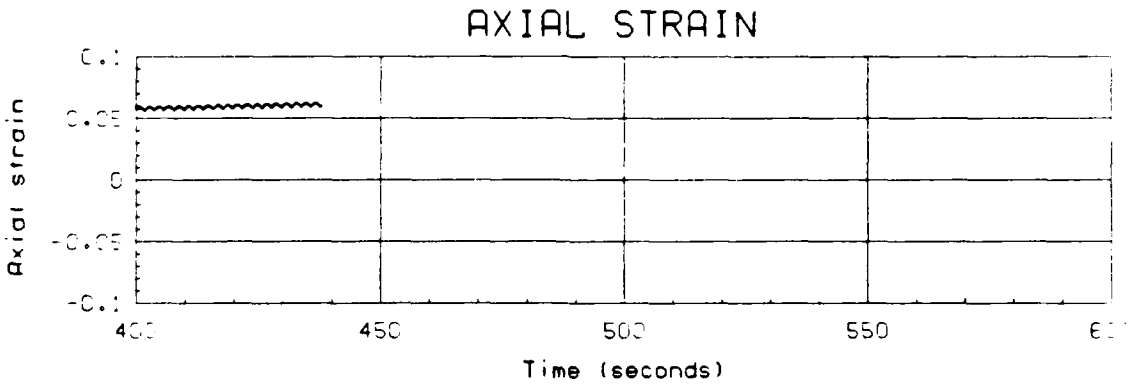

(Figure D-27, continued)

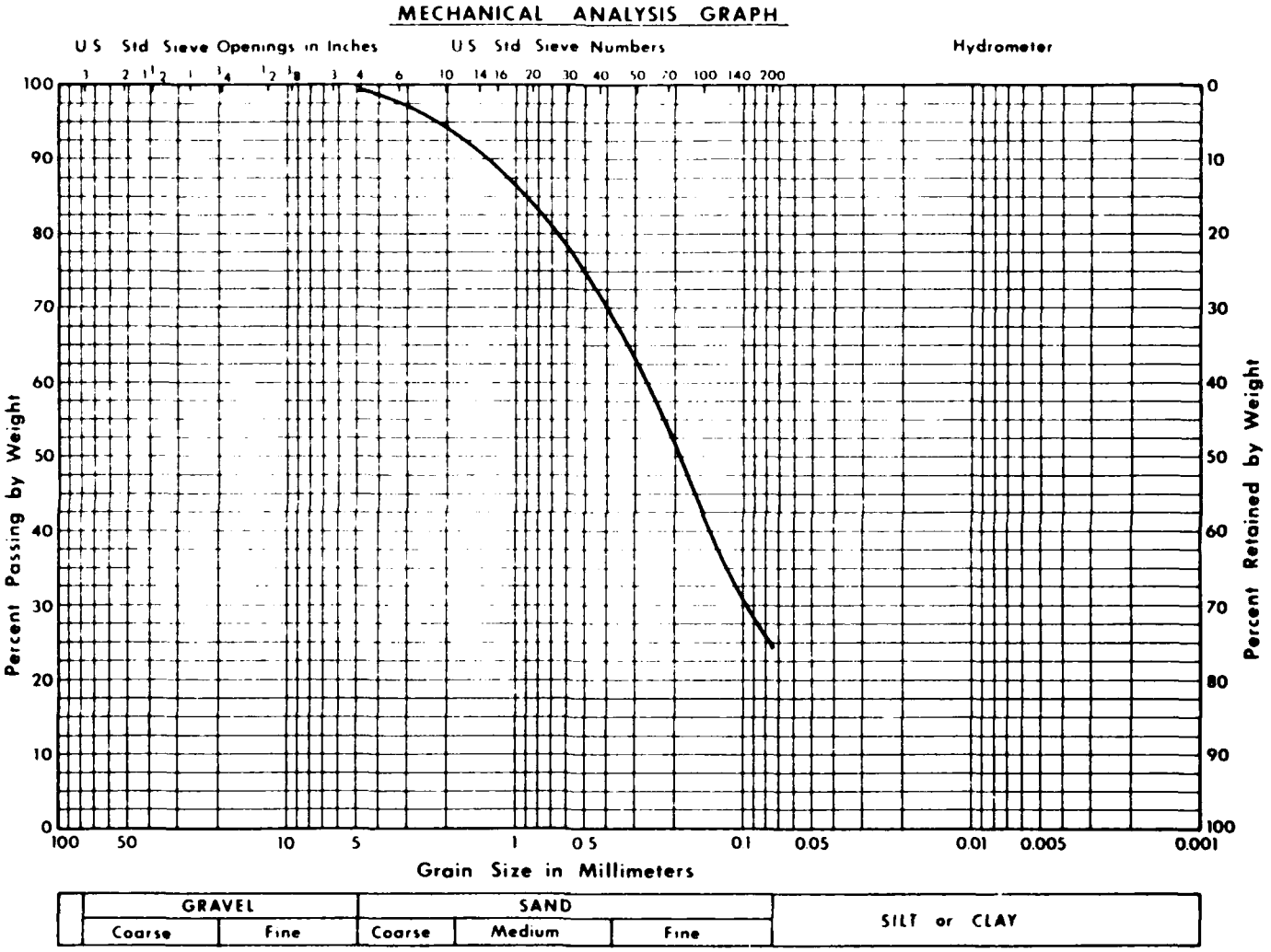

Figure D-28: GRAIN SIZE DISTRIBUTION; CYCLIC TRIAXIAL TEST NO. 32

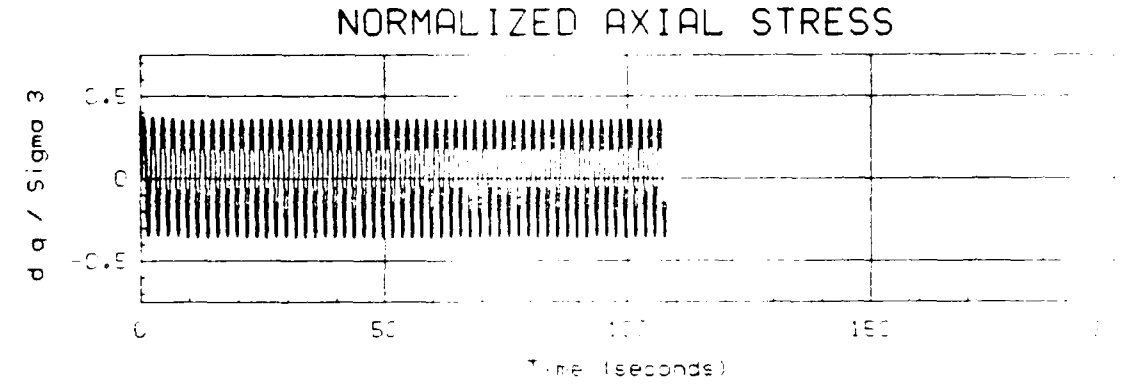

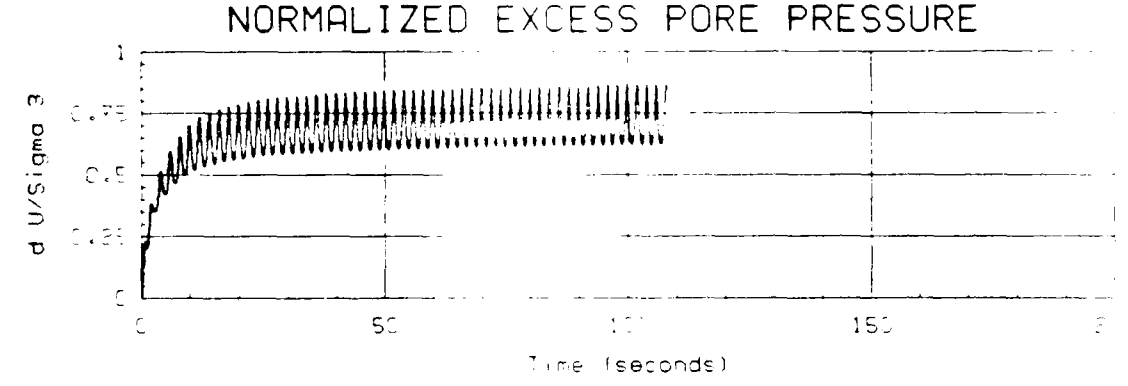

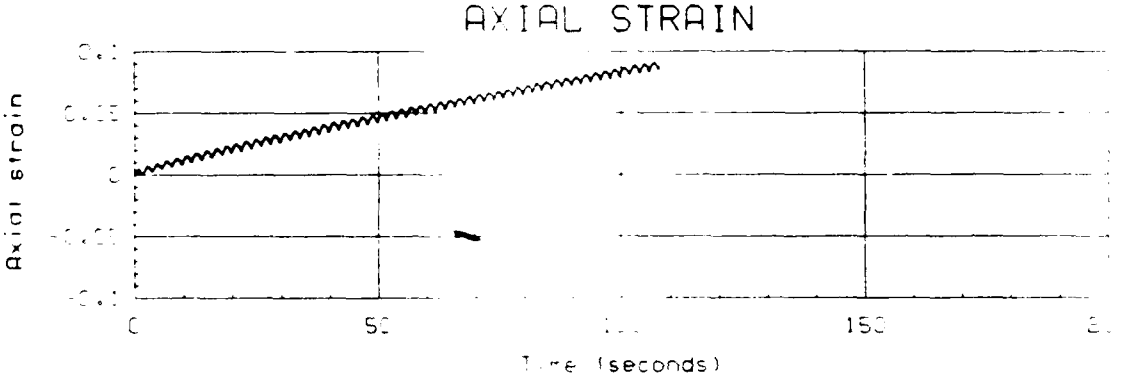

Test No.	:	33	B-value	:	0.991
Test Date	:	8/24/86	$\sigma_{3,i}'$	:	2.00 ksc
Material	:	Tube U11	K_c	:	1.75
		Silty Sand (SM-ML),	CSR	:	0.357

Figure D-29: UNDRAINED C TRIAXIAL TEST NO. 33: HYDRAULIC FILL

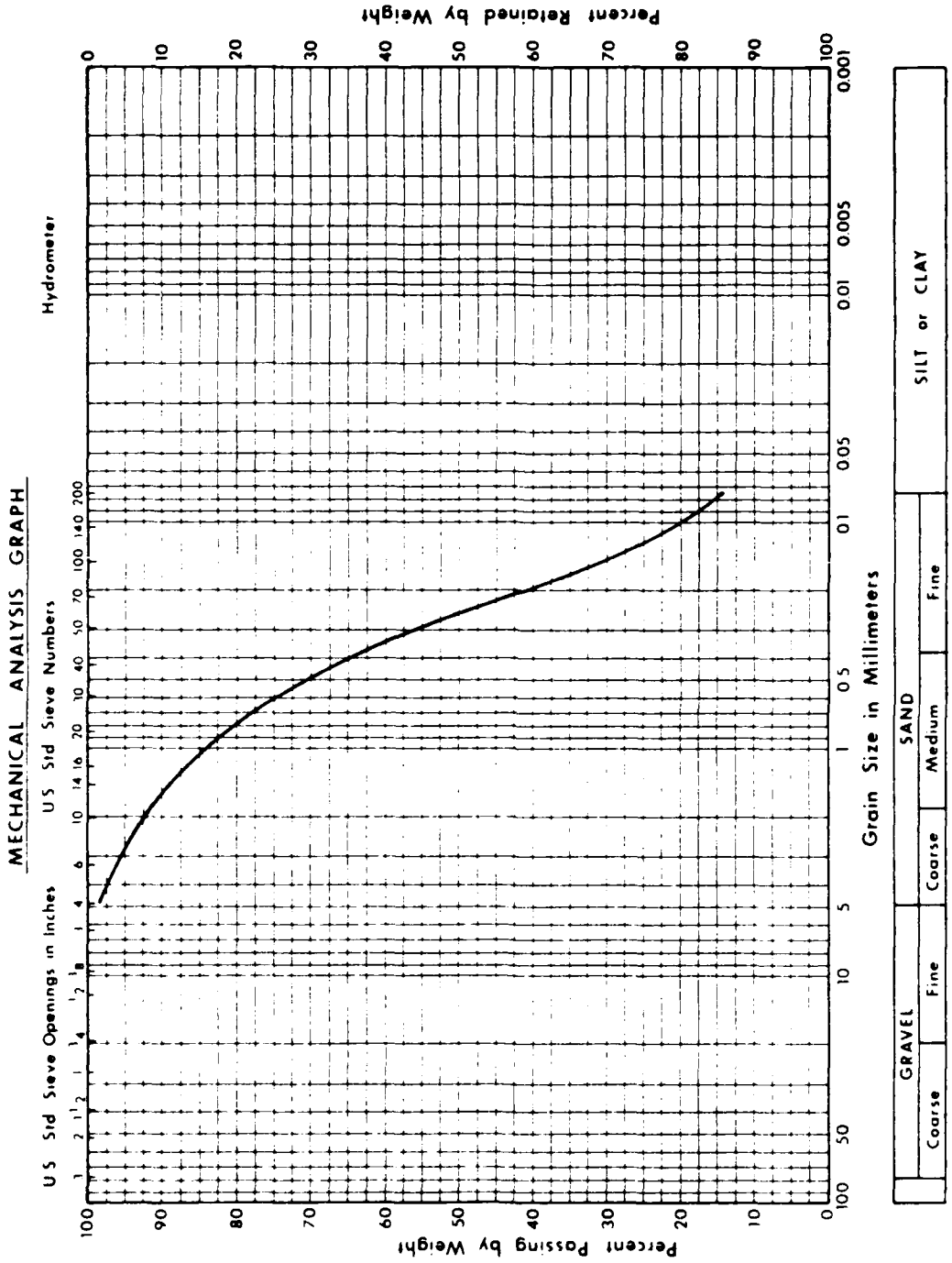

Figure D-30: GRAIN SIZE DISTRIBUTION; CYCLIC TRIAXIAL TEST NO. 33

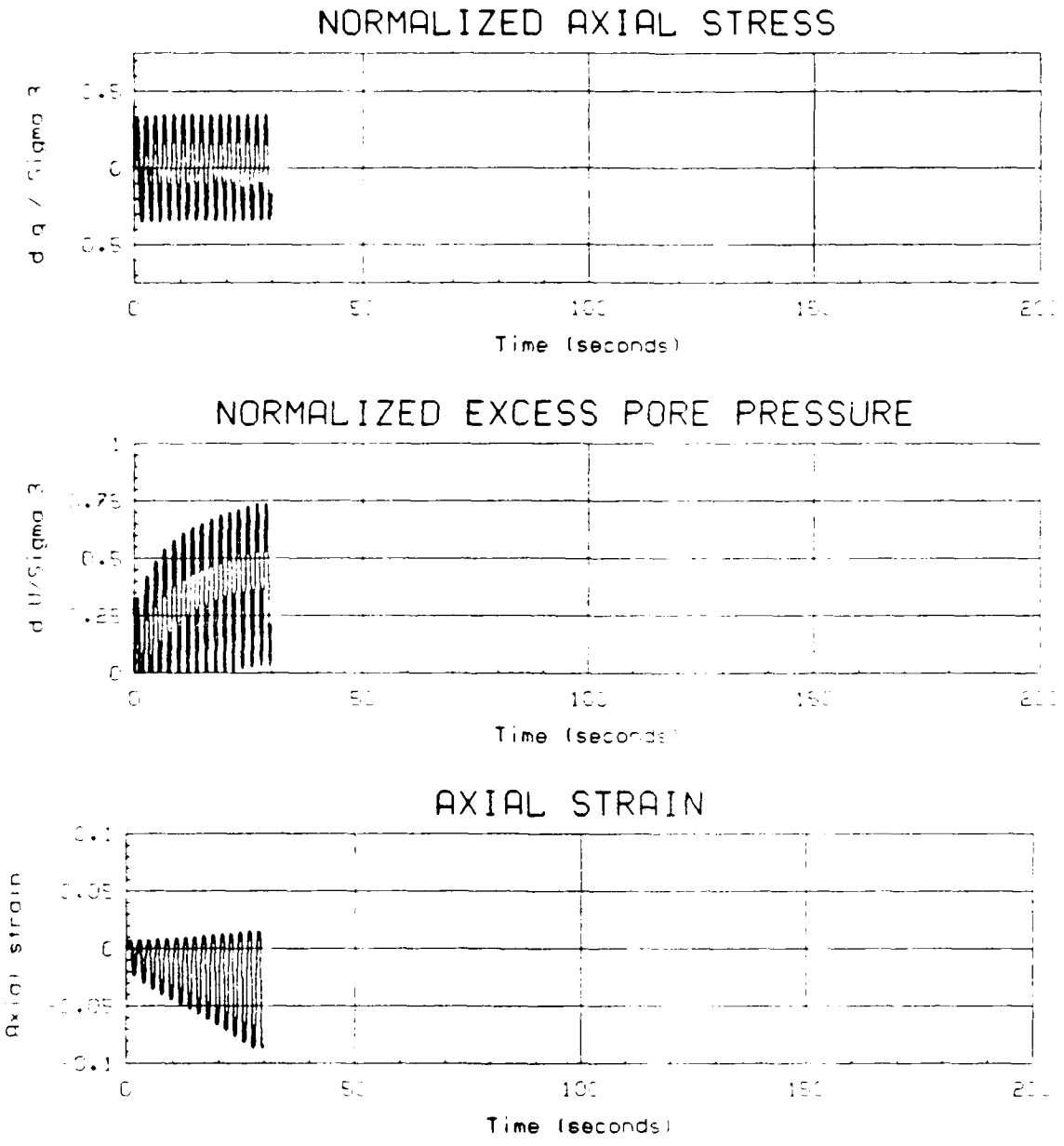

Test No.	:	34	B-value	:	0.988
Test Date	:	8/24/86	$\sigma_{3,i}'$	:	2.00 ksc
Material	:	Tube U105-UF11	K_c	:	1.00
		Silty Clay (CL), 99% fines.	CSR	:	0.345

Figure D-31: UNDRAINED CYCLIC TRIAXIAL TEST NO. 34: HYDRAULIC FILL

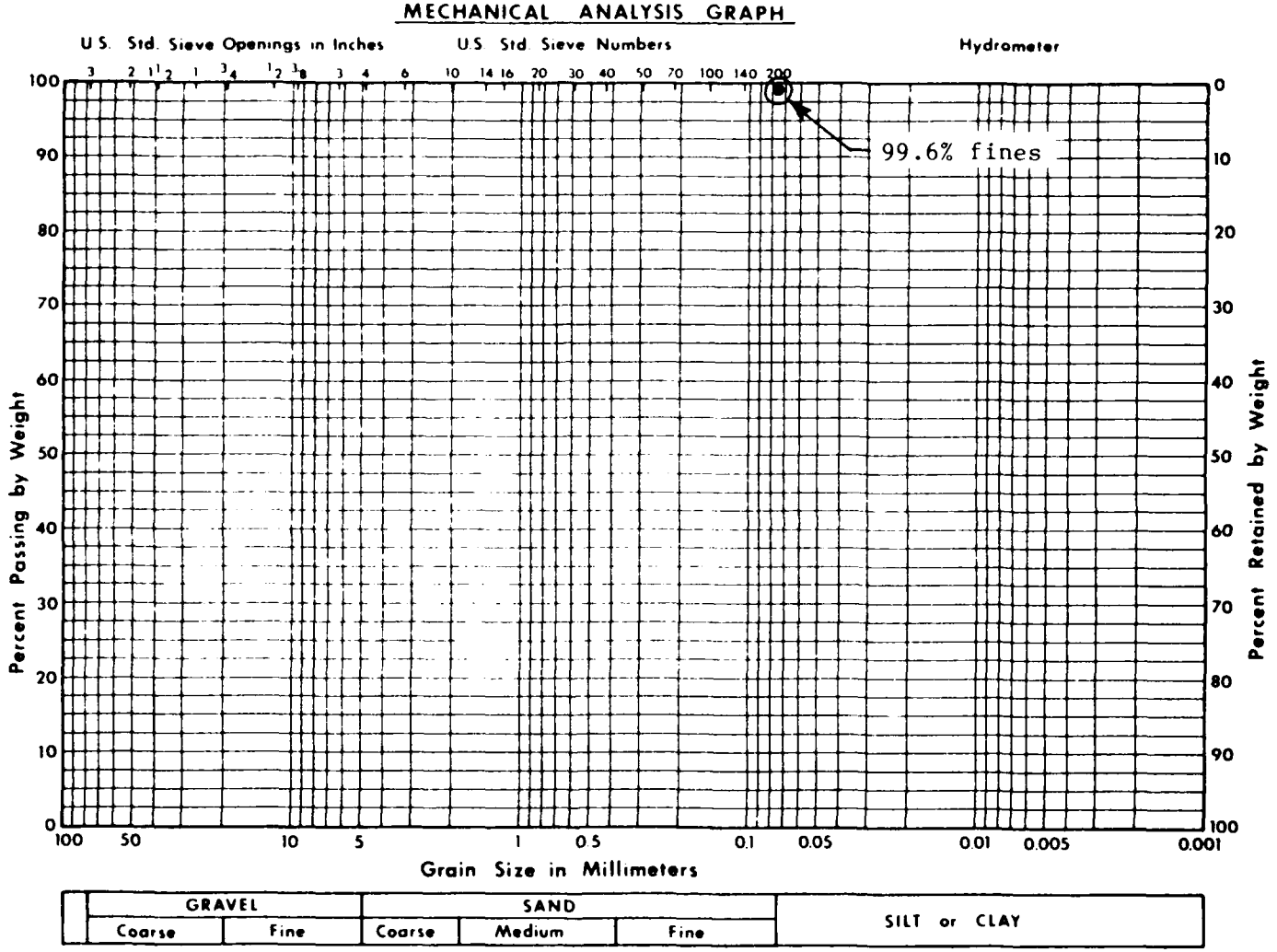

Figure D-32: GRAIN SIZE DISTRIBUTION; CYCLIC TRIAXIAL TEST NO. 34

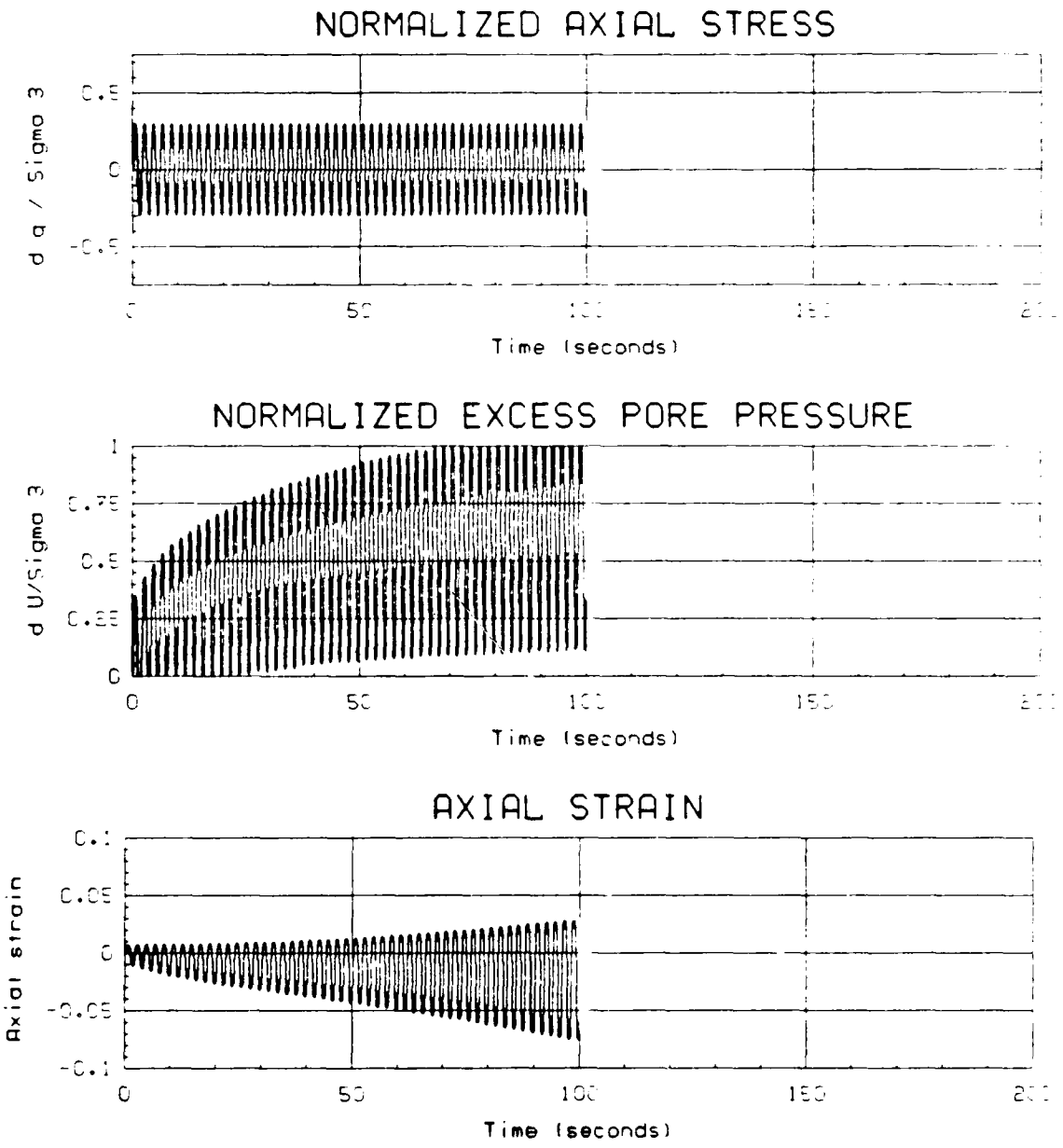

Test No.	:	35	B-value	:	0.981
Test Date	:	8/25/86	$\sigma_{3,i}'$	:	2.00 ksf
Material	:	Tube U105-UF11	K_c	:	1.00
Silty Clay (CL), 98% fines.			CSR	:	0.298

Figure D-33: UNDRAINED CYCLIC TRIAXIAL TEST NO. 35: HYDRAULIC FILL

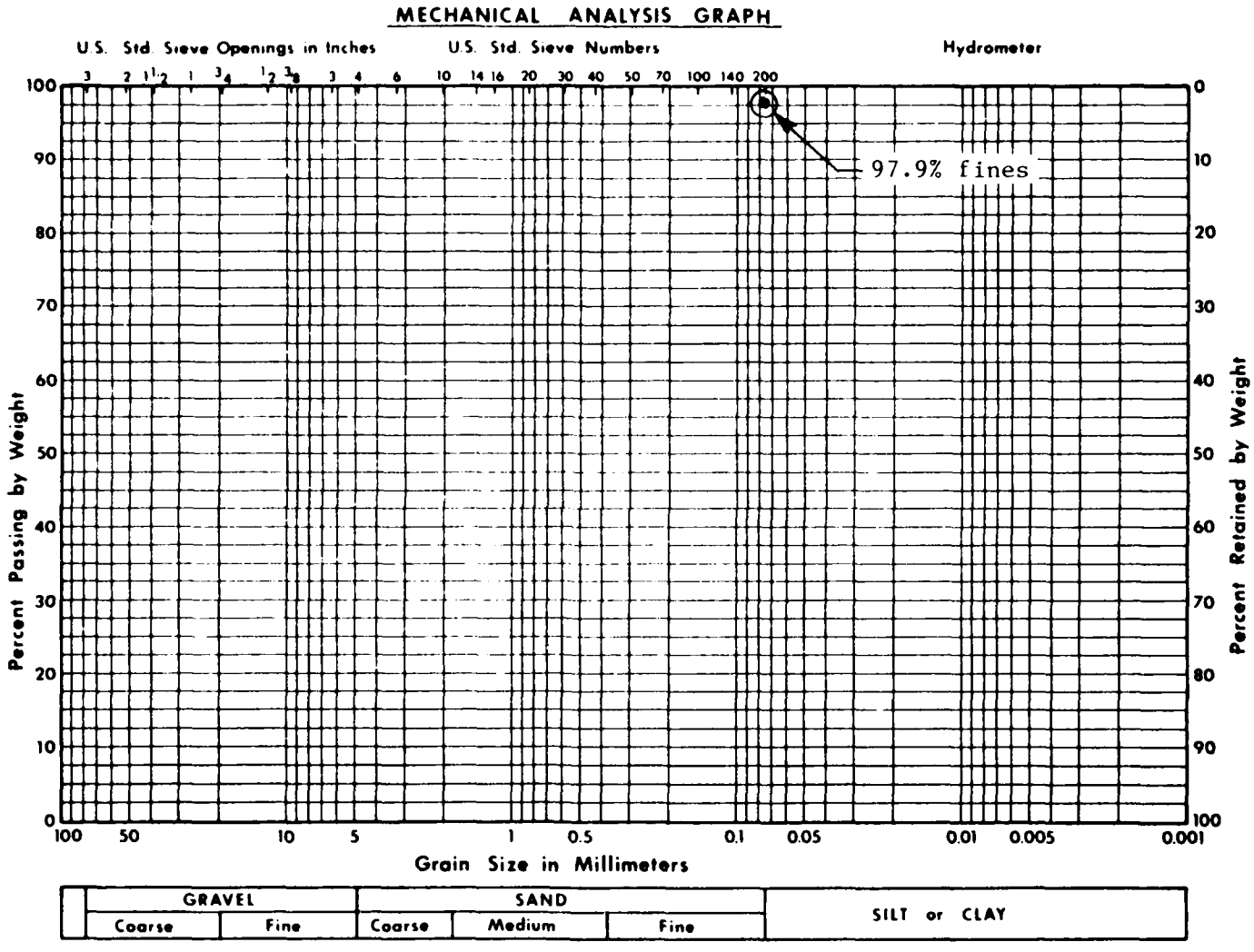

Figure D-34: GRAIN SIZE DISTRIBUTION; CYCLIC TRIAXIAL TEST NO. 35

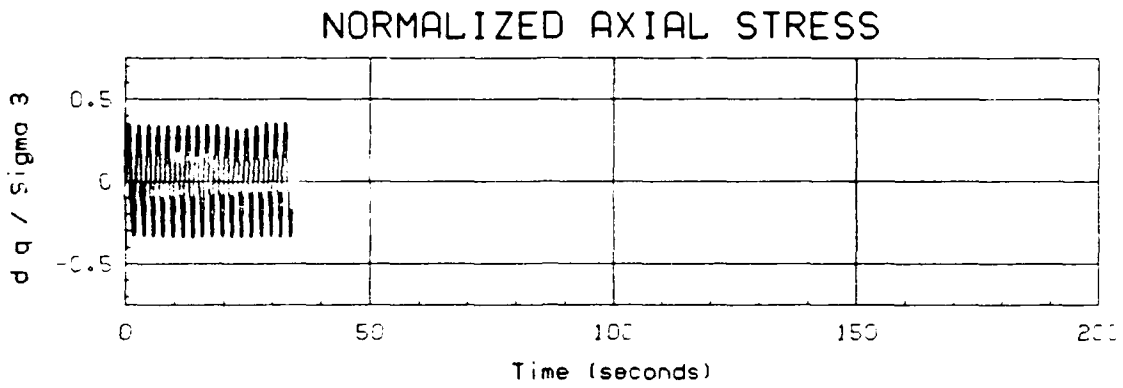

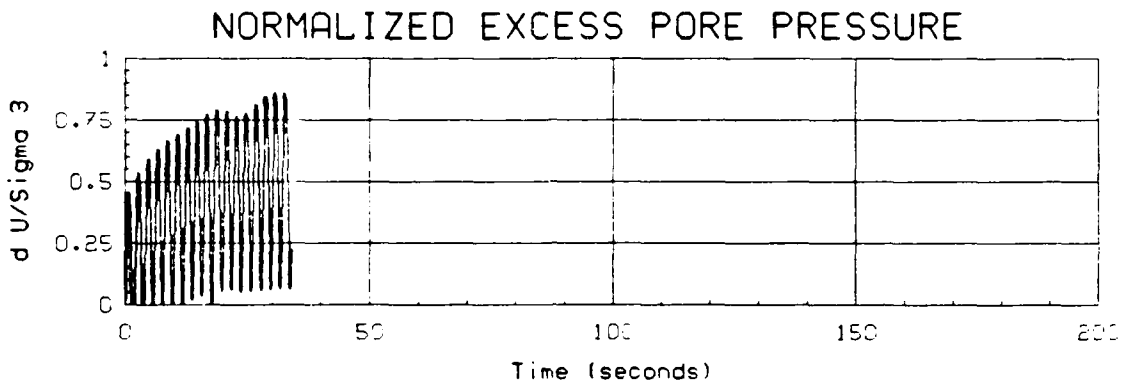

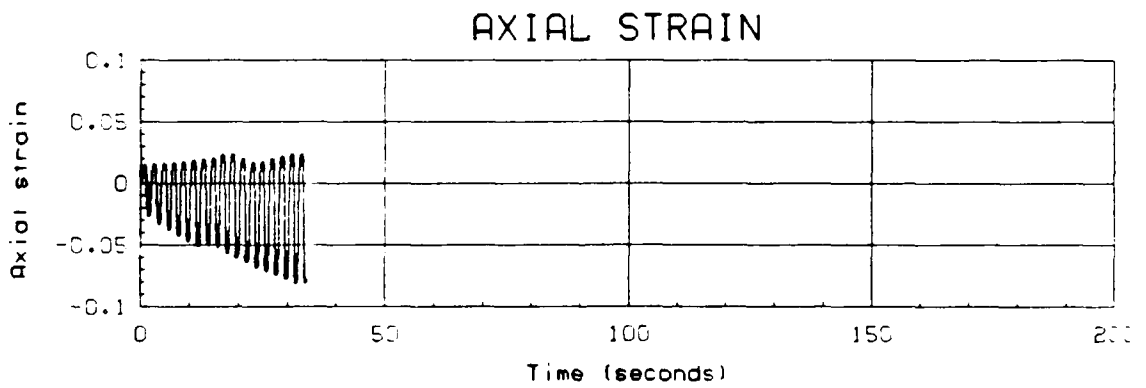

Test No.	:	36	B-value	:	0.991
Test Date	:	8/26/86	$\sigma_{3,i}'$	:	2.00 ksc
Material	:	U105-UF11	K_c	:	1.00
Silty Clay (CL), 99% fines.			CSR	:	0.339

Figure D-35: UNDRAINED CYCLIC TRIAXIAL TEST NO. 36: HYDRAULIC FILL

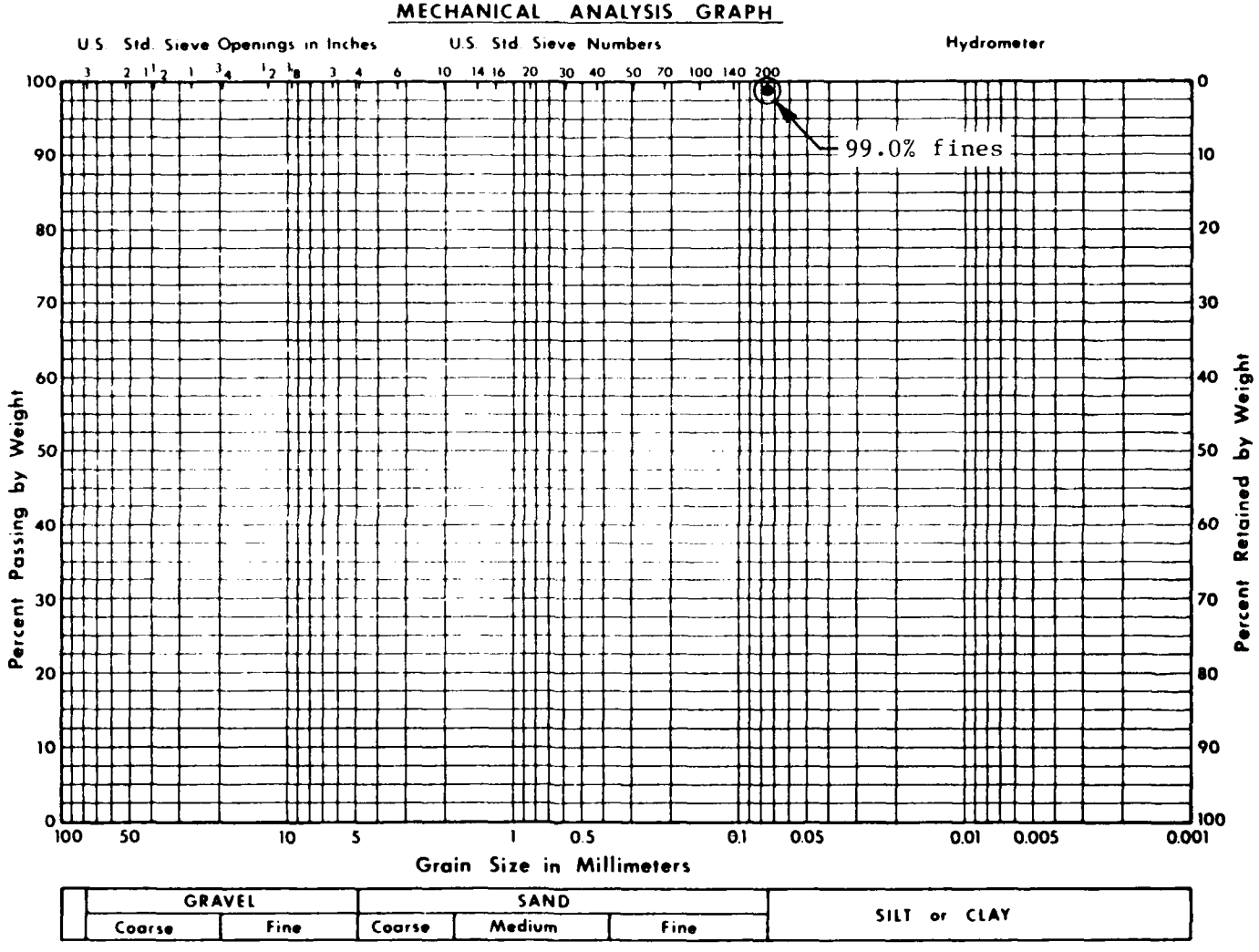

Figure D-36: GRAIN SIZE DISTRIBUTION; CYCLIC TRIAXIAL TEST NO. 36

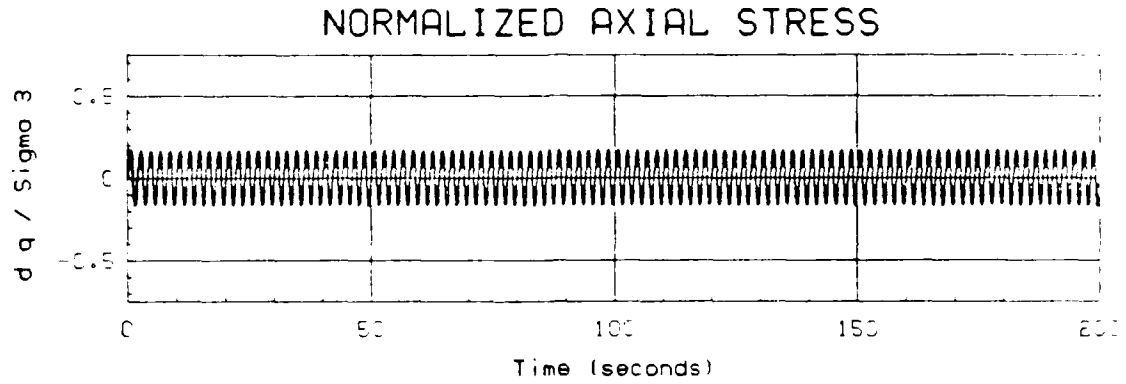

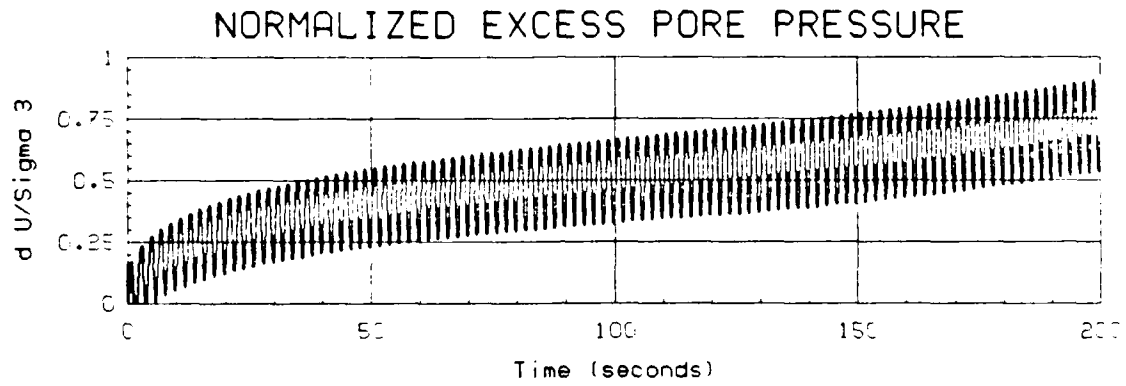

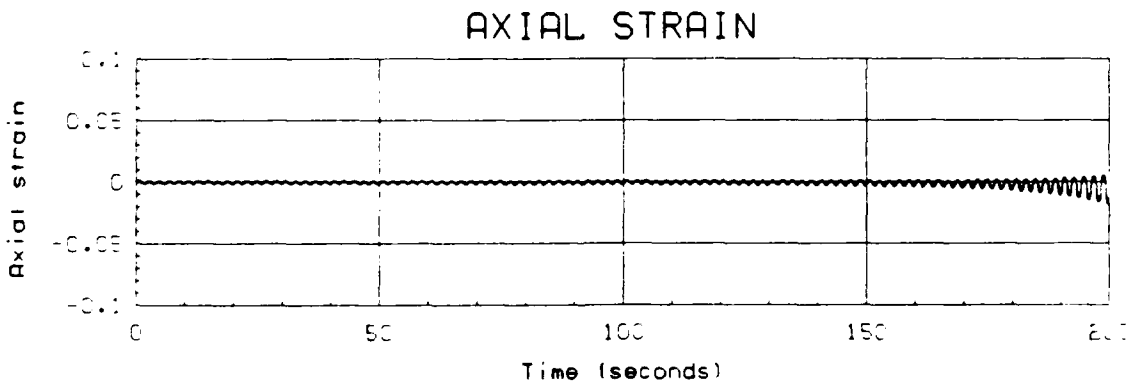

Test No.	:	39	B-value	:	0.995
Test Date	:	8/30/86	$\sigma_{3,i}'$	:	2.00 ksc
Material	:	Tube U111-UF16	K_c	:	1.00
Sandy Clayey Silt (ML), 83% fines.			CSR	:	0.174

Figure D-37: UNDRAINED CYCLIC TRIAXIAL TEST NO. 39: HYDRAULIC FILL

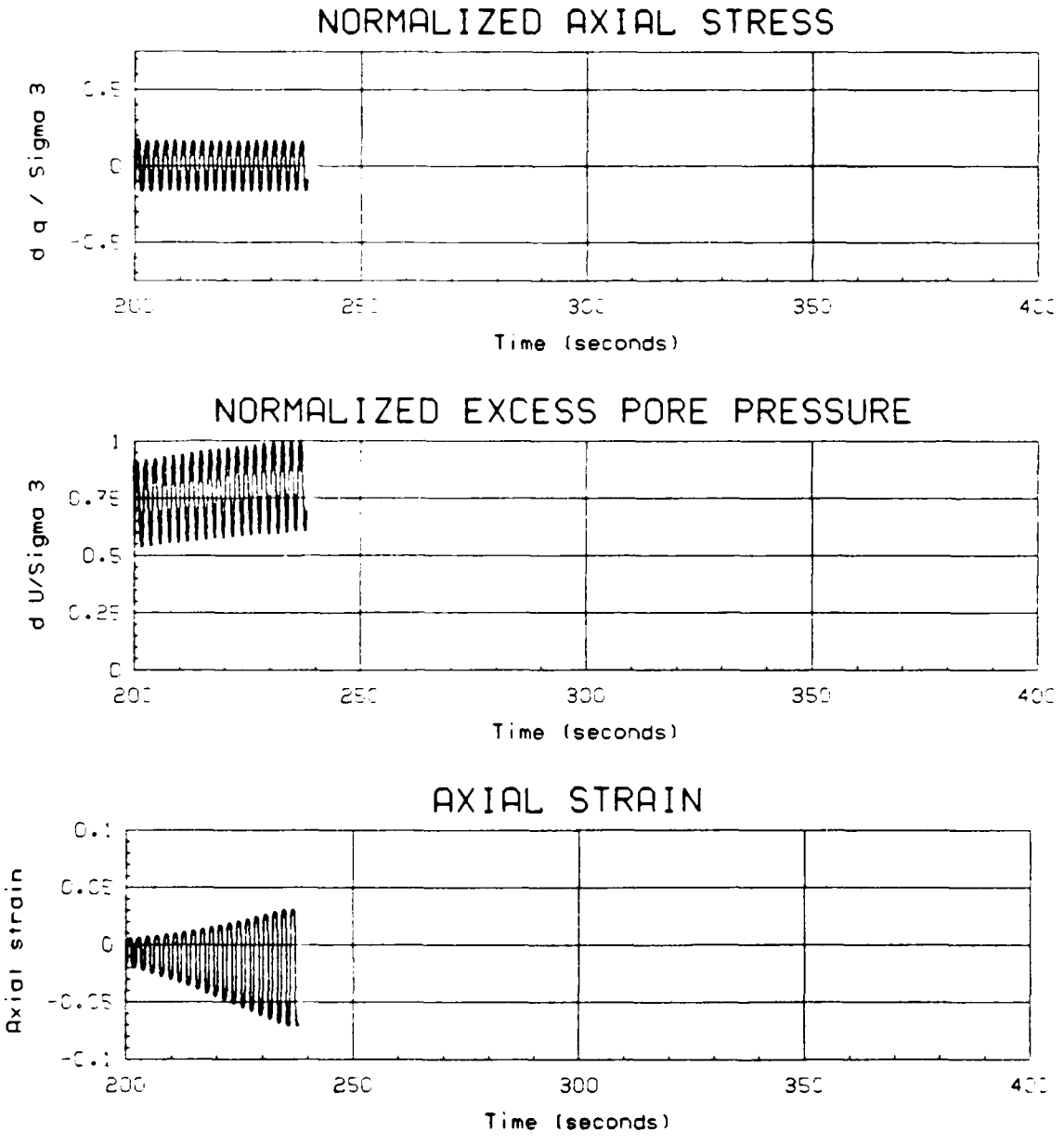

(Figure D-37, continued)

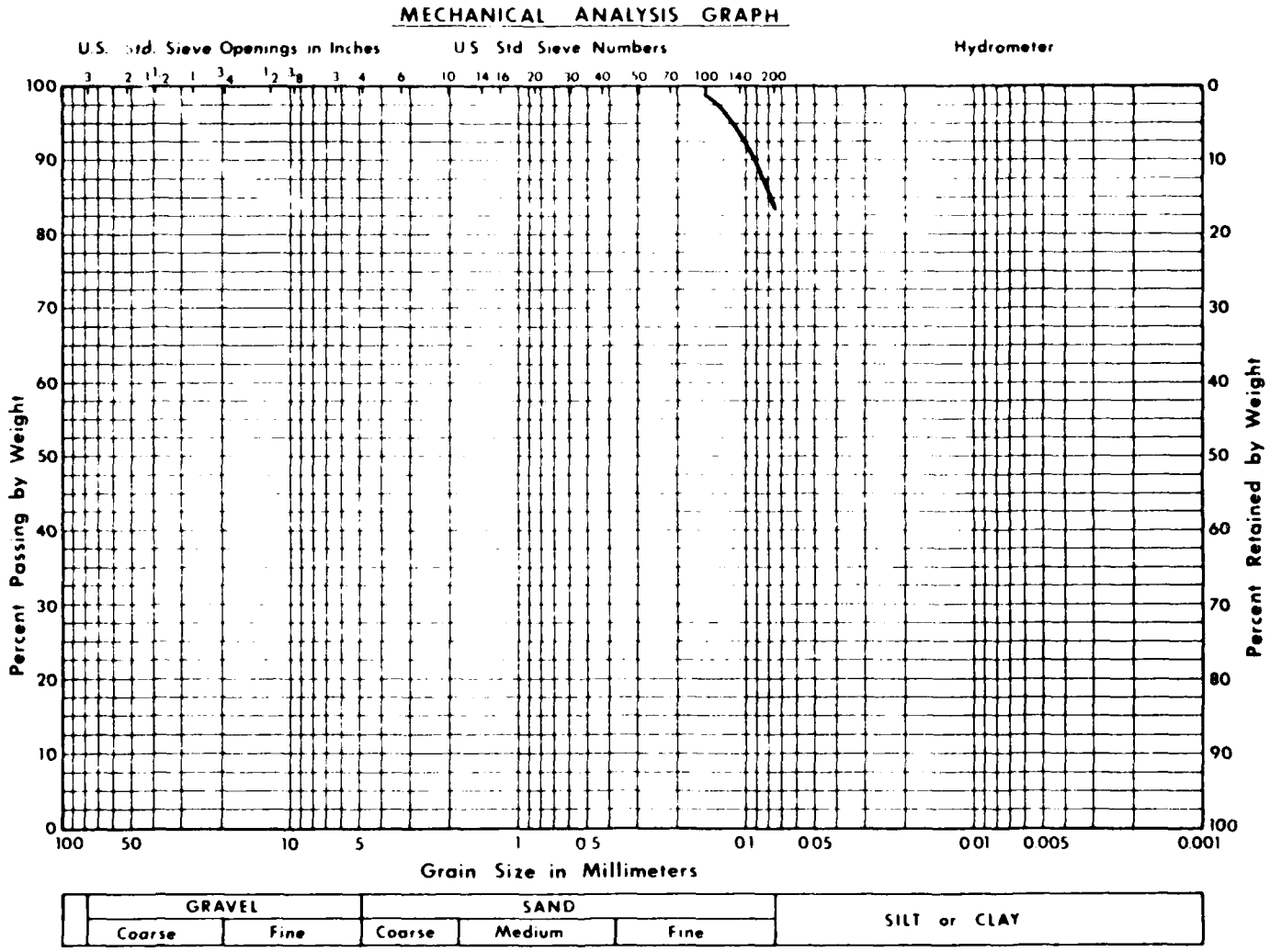

Figure D-38: GRAIN SIZE DISTRIBUTION; CYCLIC TRIAXIAL TEST NO. 39

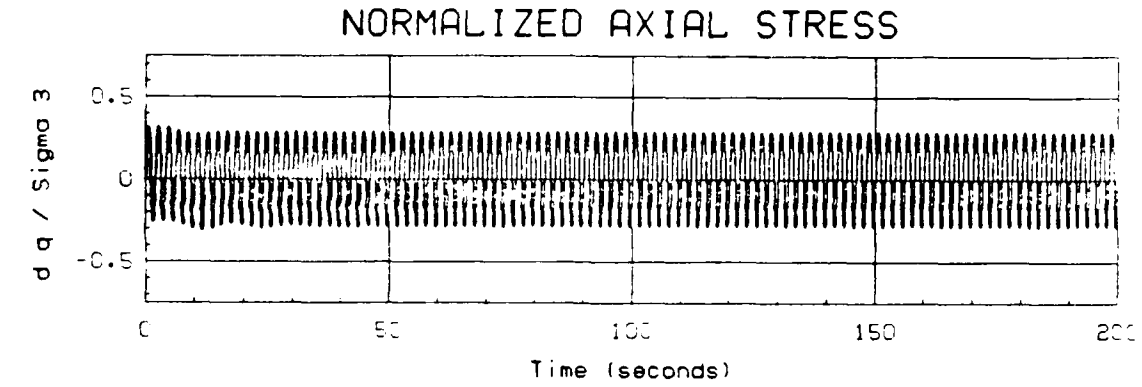

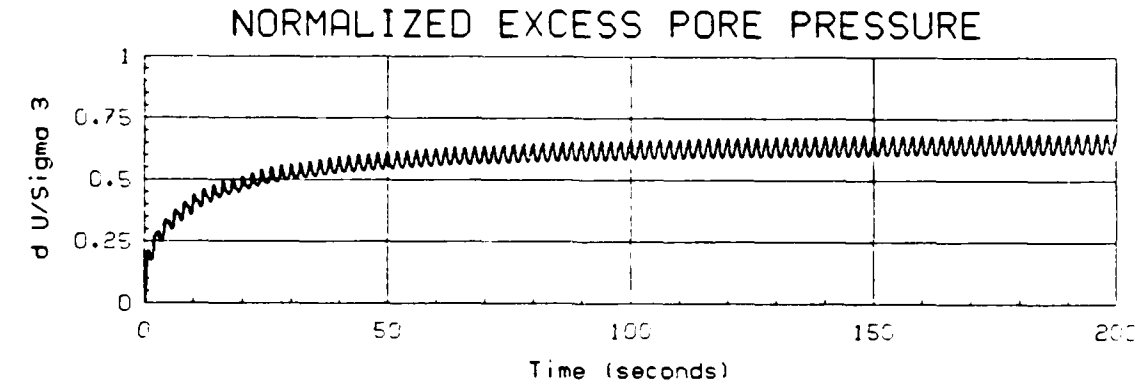

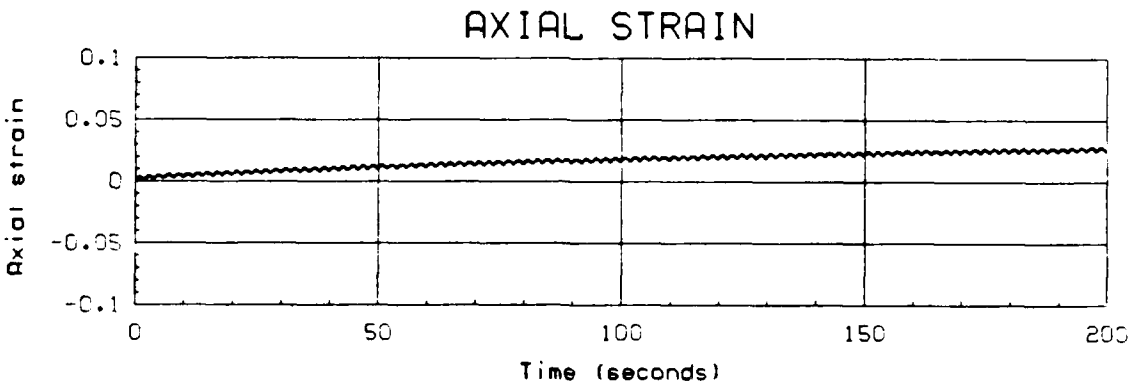

Test No.	:	40	B-value	:	0.989
Test Date	:	8/28/86	$\sigma_{3,i}'$	:	2.00 ksc
Material	:	Tube U111A-UF6	K_c	:	1.75
Silty Sand (SM-SP), 12% fines.			CSR	:	0.287

Figure D-39: UNDRAINED CYCLIC TRIAXIAL TEST NO. 40: HYDRAULIC FILL

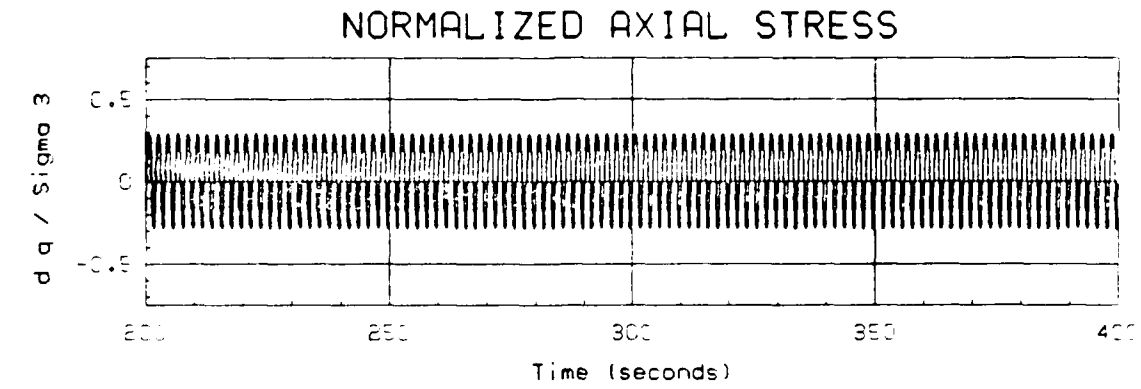

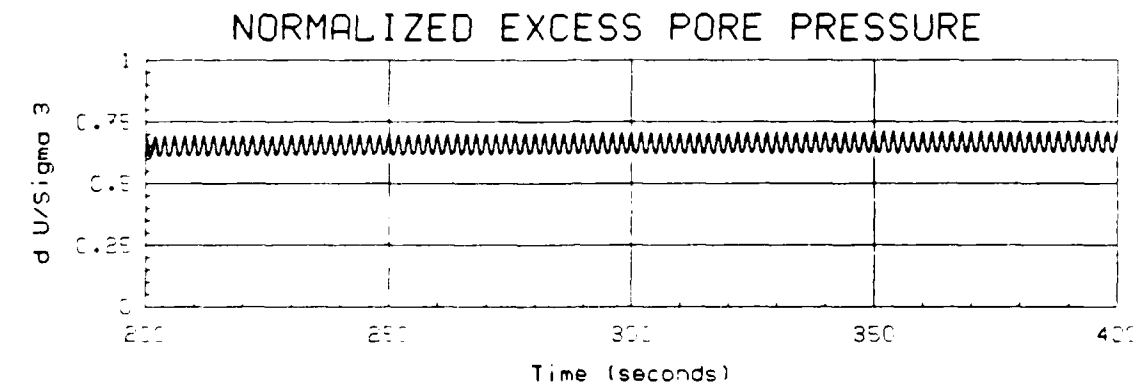

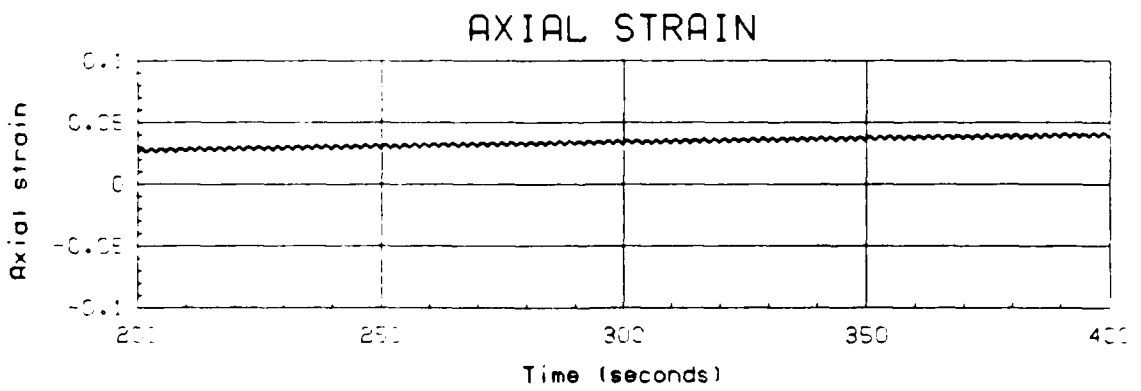

(Figure D-39, continued)

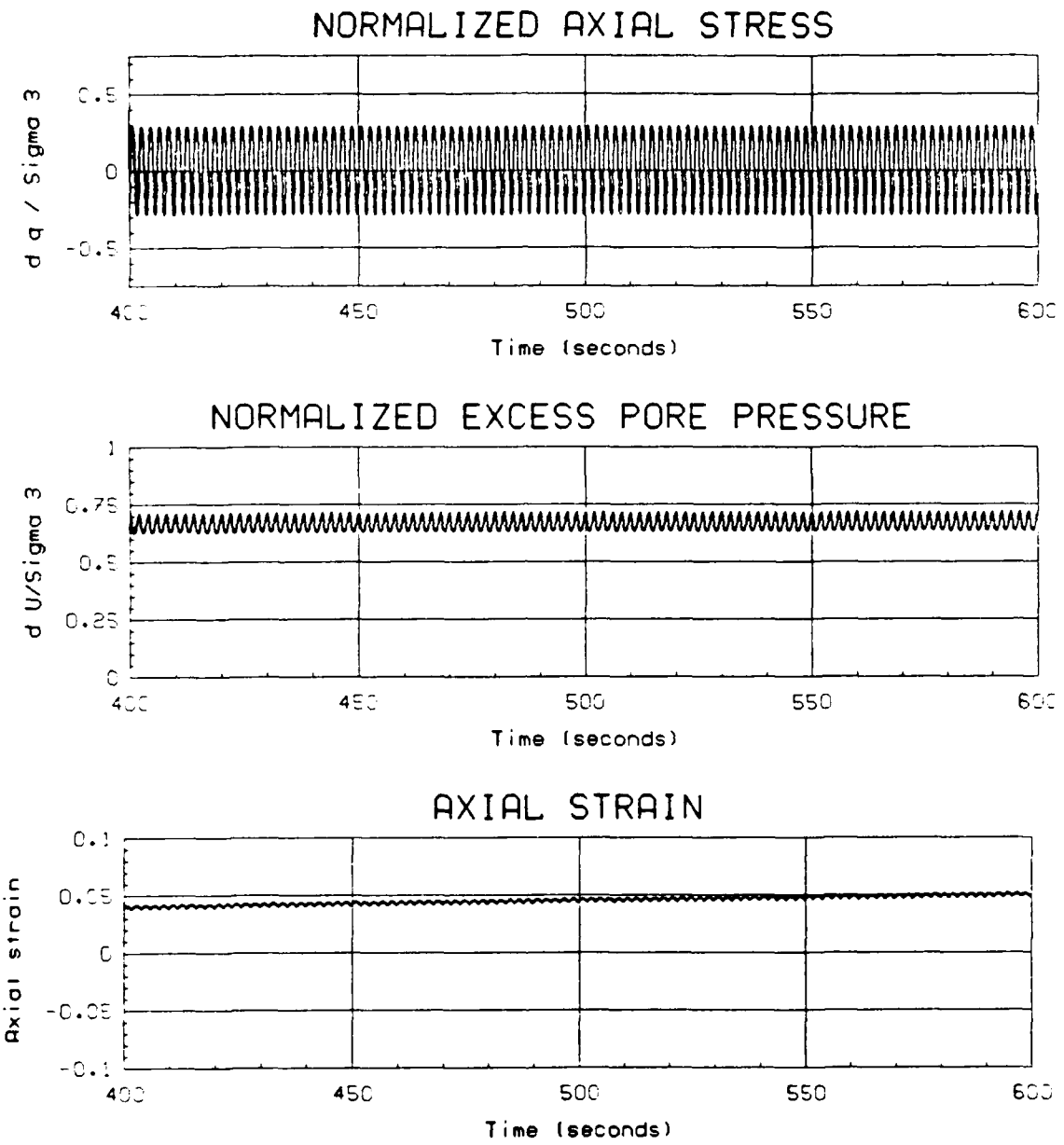

(Figure D-39, continued)

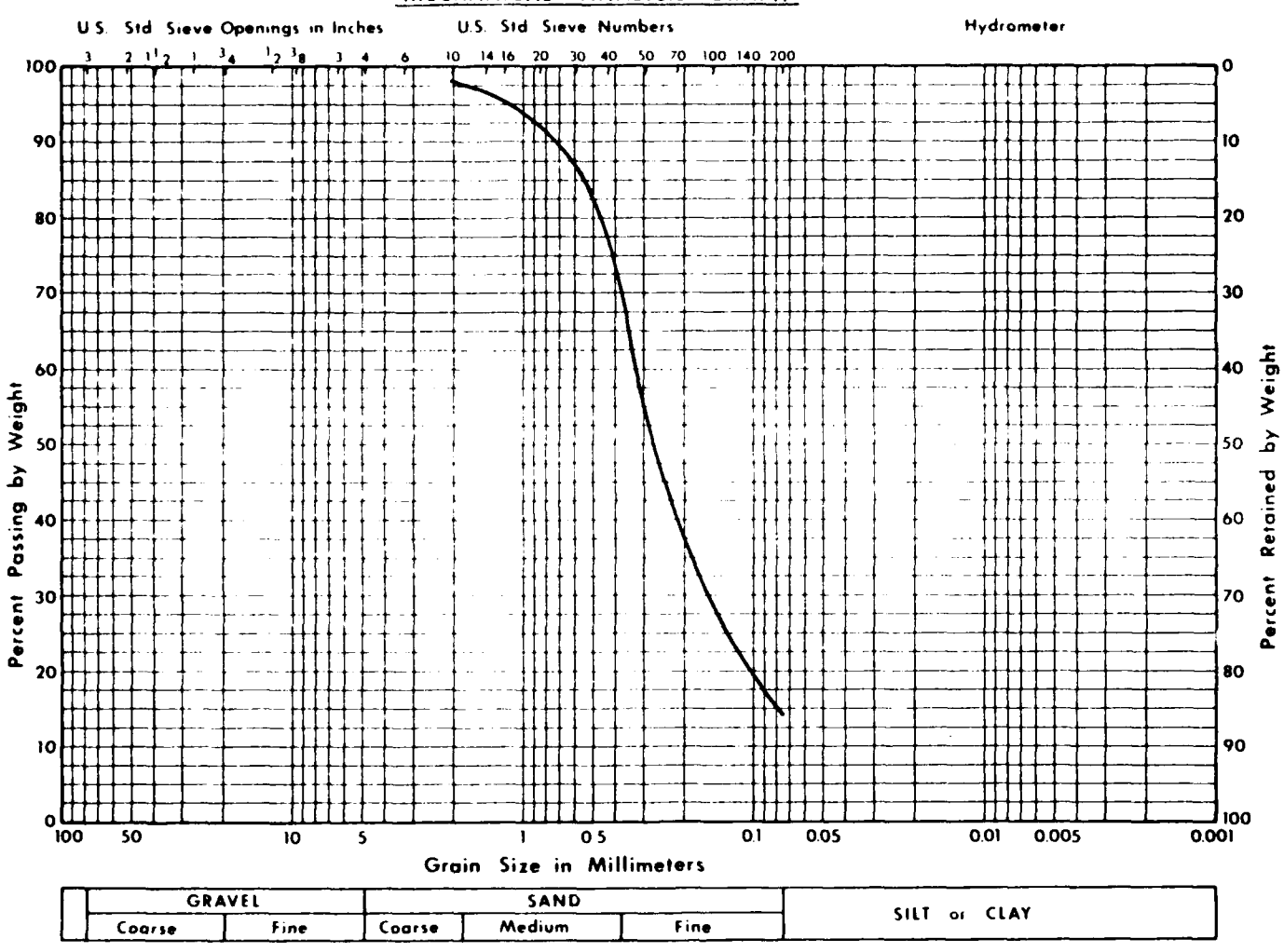

Figure D-40: GRAIN SIZE DISTRIBUTION; CYCLIC TRIAXIAL TEST NO. 40

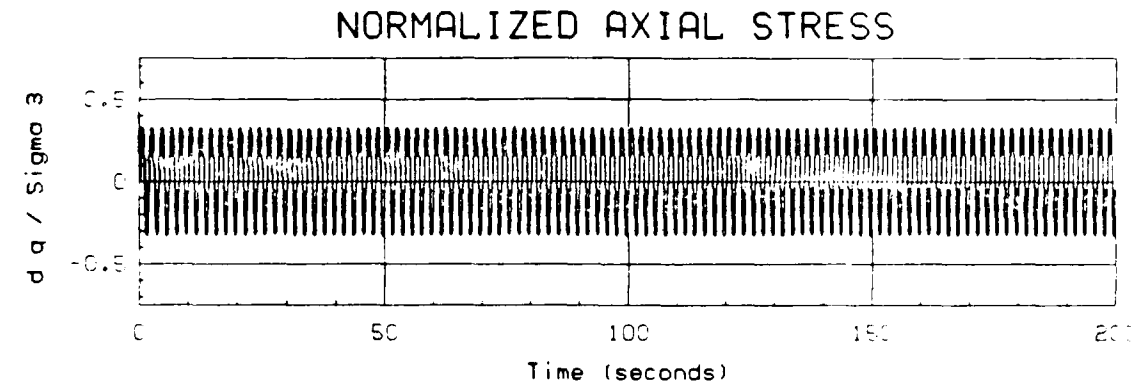

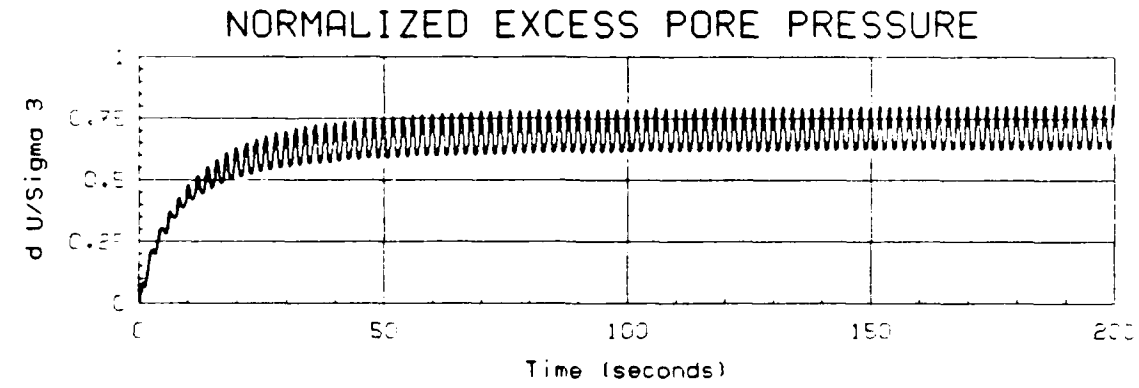

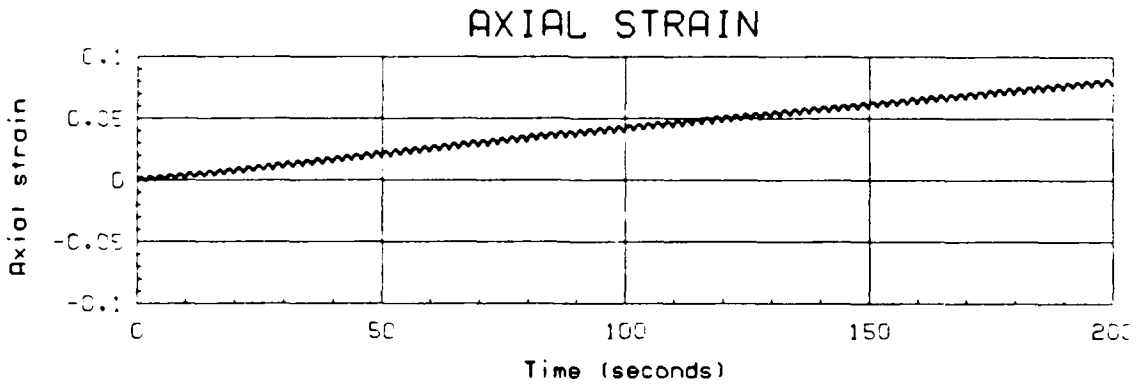

Test No.	:	41	B-value	:	0.974
Test Date	:	8/28/86	$\sigma_{3,i}'$	:	2.00 ksc
Material	:	Tube U111A-UF6	K_c	:	1.75
Silty Sand (SM-ML), 17% fines.			CSR	:	0.325

Figure D-41: UNDRAINED CYCLIC TRIAXIAL TEST NO. 41: HYDRAULIC FILL

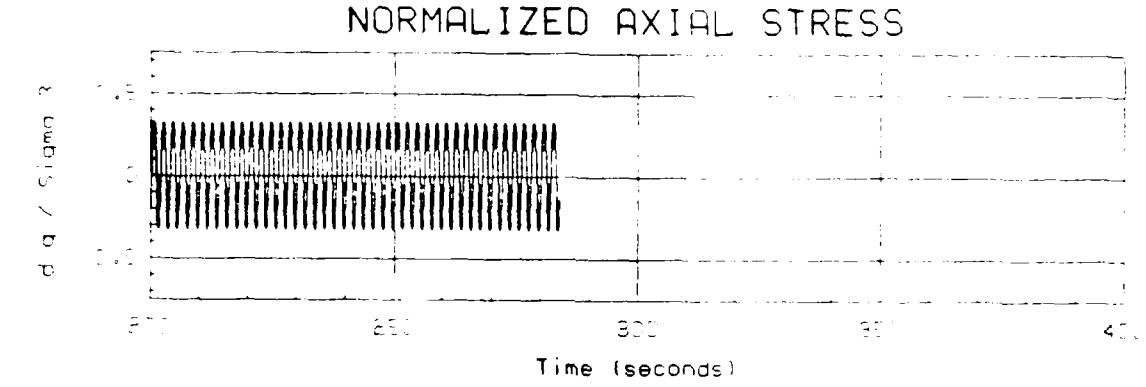

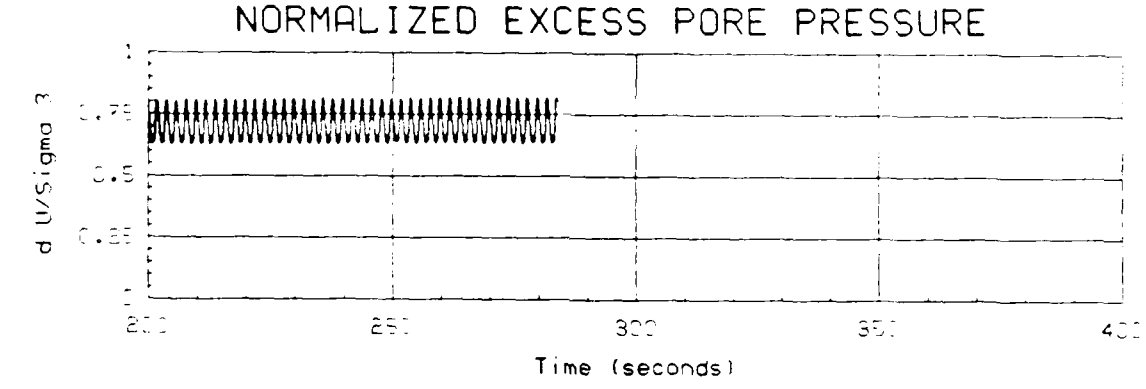

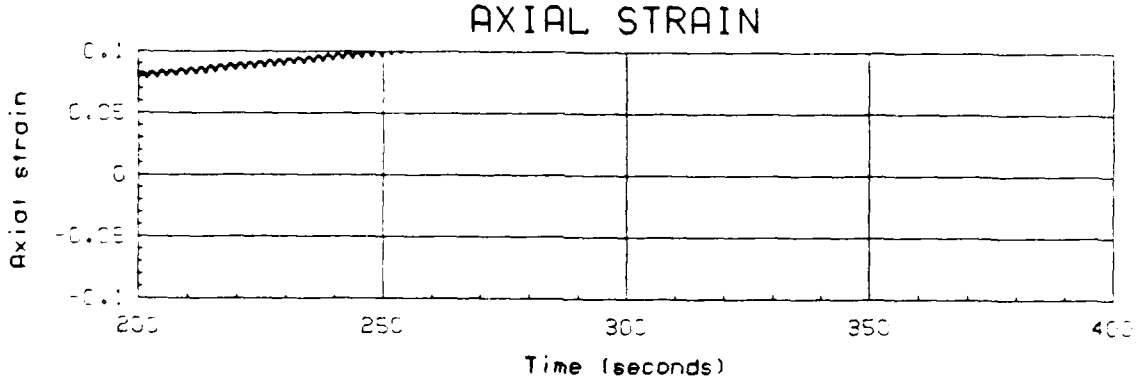

(Figure D-41, continued)

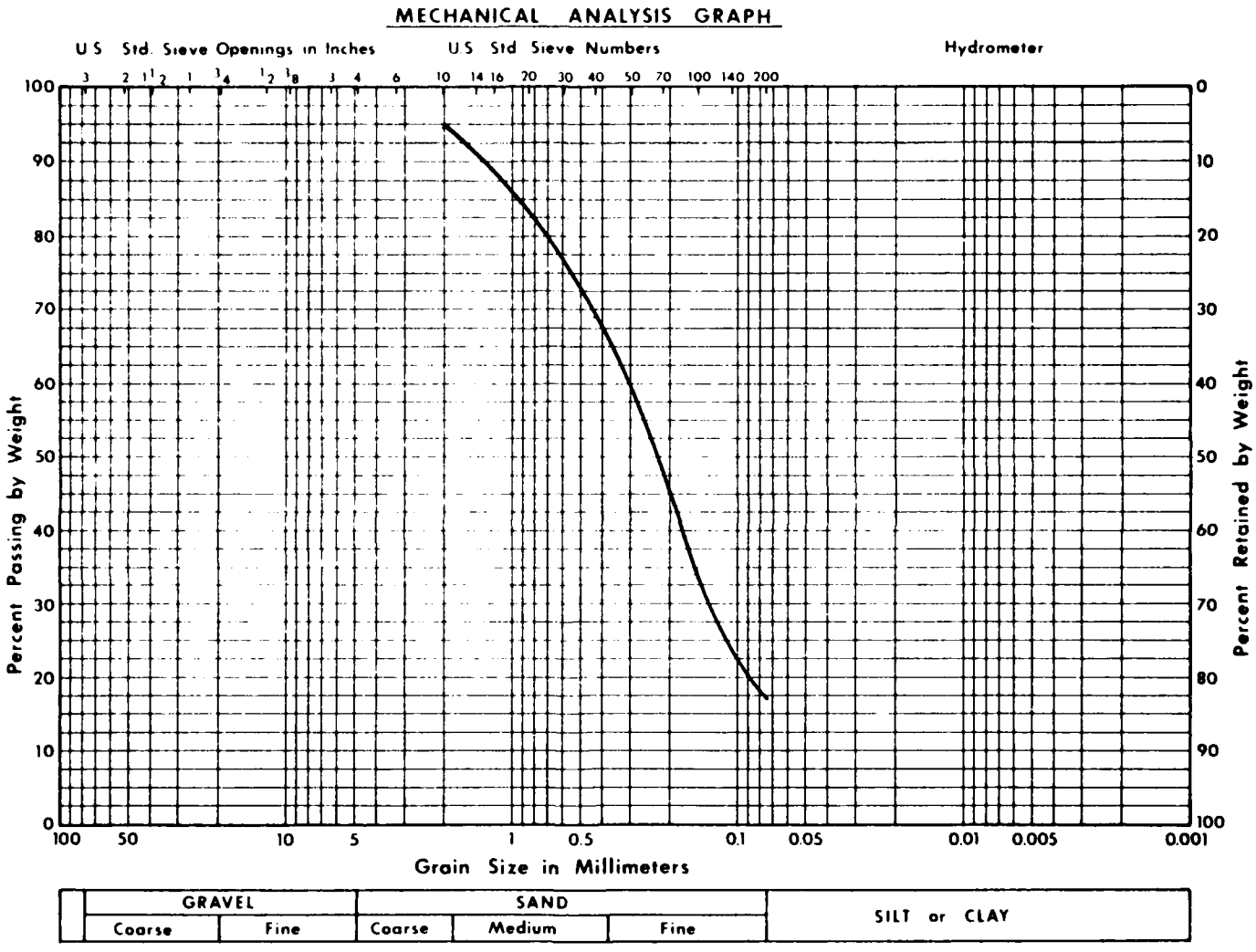

Figure D-42: GRAIN SIZE DISTRIBUTION; CYCLIC TRIAXIAL TEST NO. 41

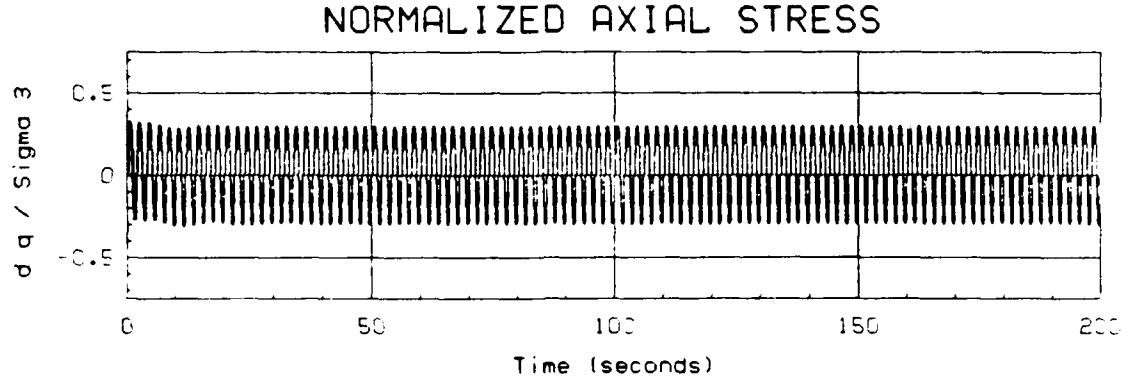

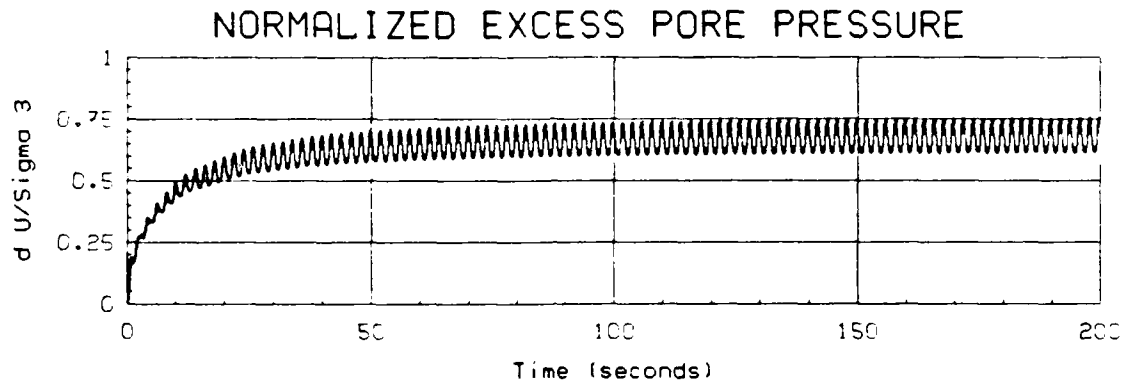

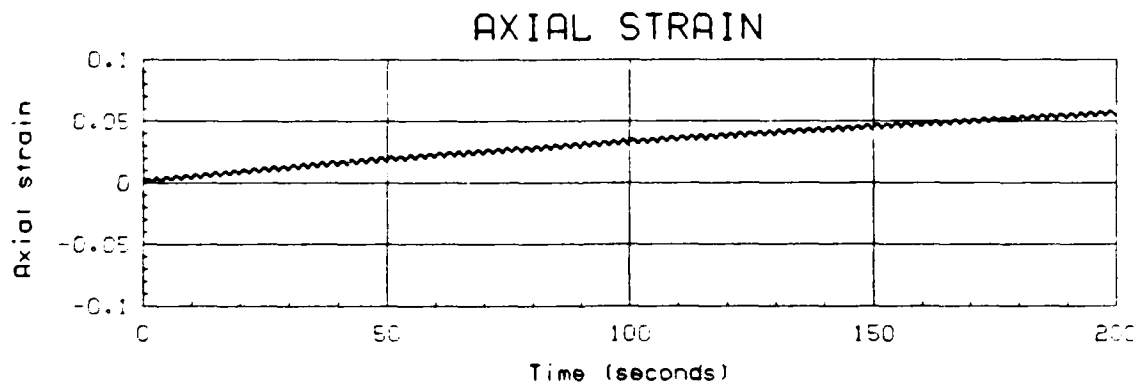

Test No.	:	42	B-value	:	0.997
Test Date	:	8/29/86	$\sigma_{3,i}'$	:	2.00 ksc
Material	:	Tube U111A-UF7	K_c	:	1.75
Silty Sand (SM-ML), 15% fines.			CSR	:	0.297

Figure D-43: UNDRAINED CYCLIC TRIAXIAL TEST NO. 42: HYDRAULIC FILL

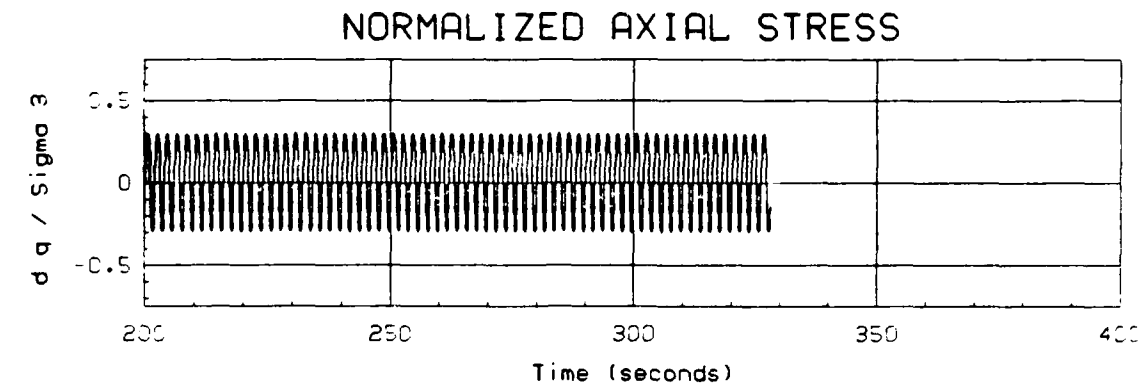

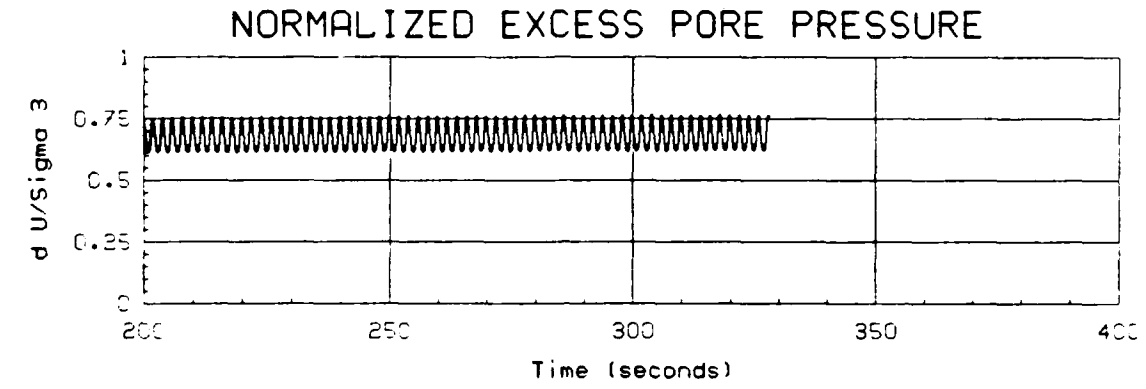

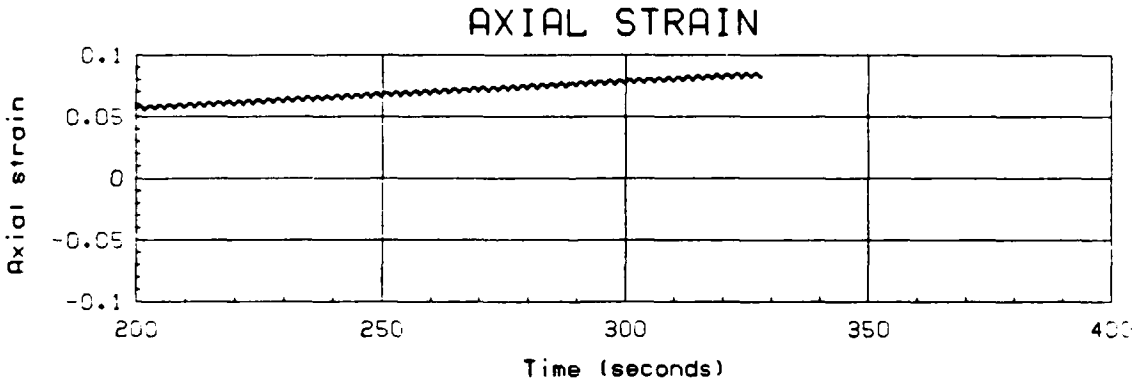

(Figure D-43, continued)

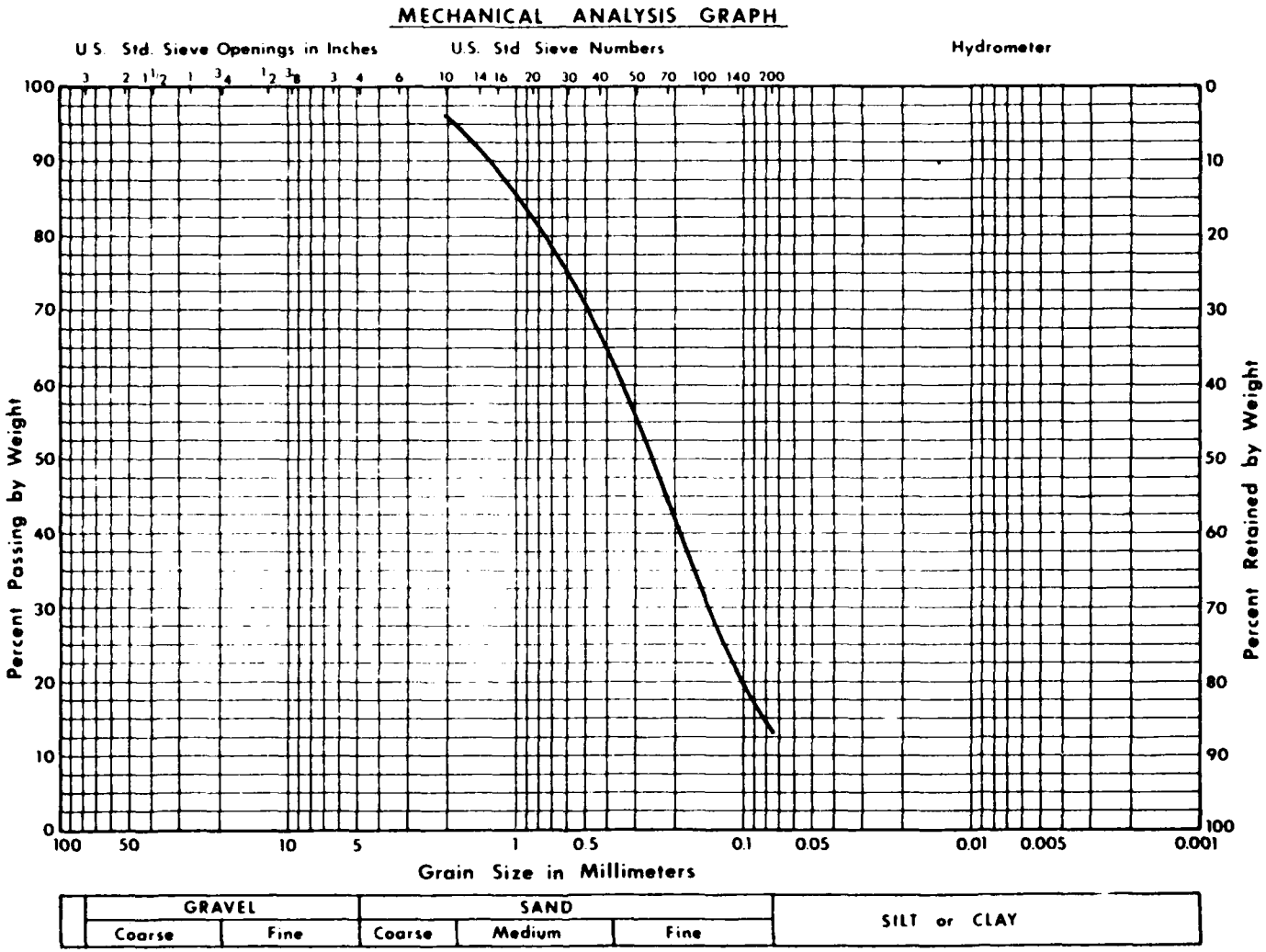

Figure D-44: GRAIN SIZE DISTRIBUTION; CYCLIC TRIAXIAL TEST NO. 42

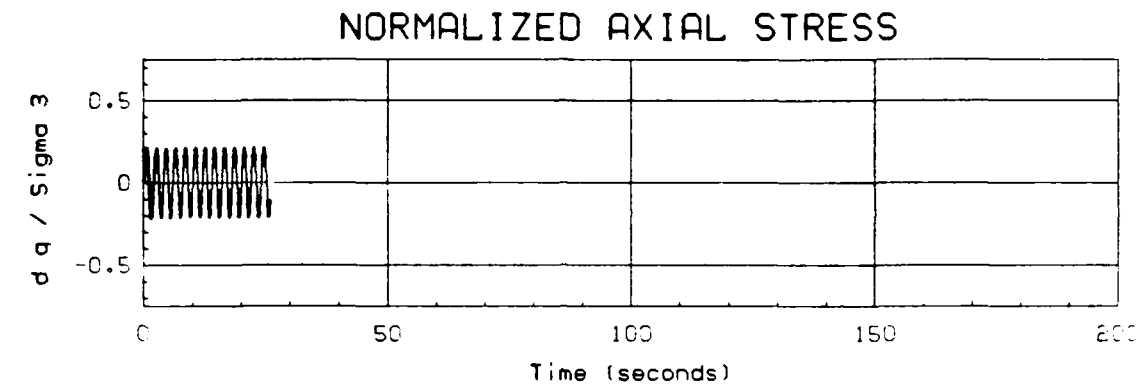

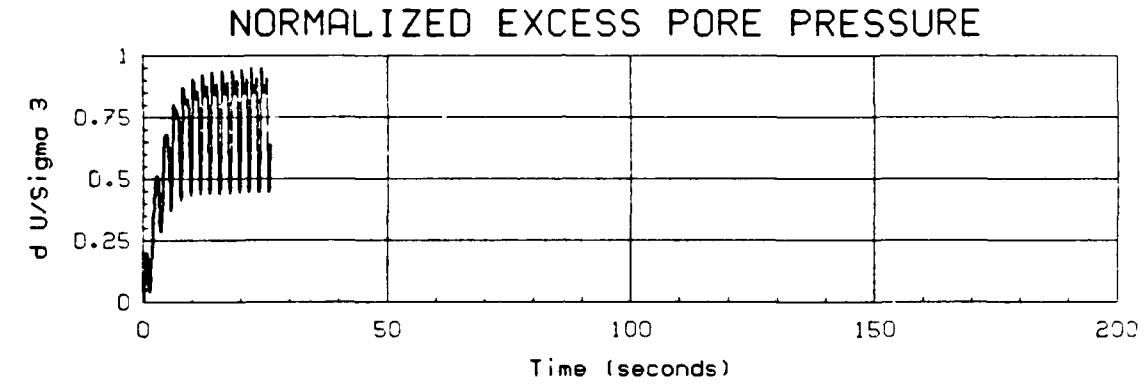

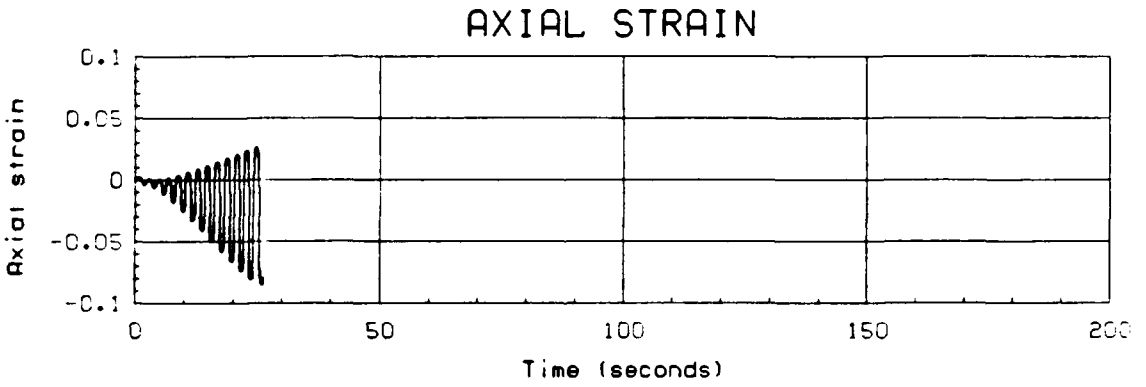

Test No.	: 47	B-value	: 0.991
Test Date	: 9/3/86	$\sigma_{3,i}'$	: 2.00 ksc
Material	: Tube TS117	K_c	: 1.00
Silty Sand (SM-ML), 22% fines.		CSR	: 0.221

Figure D-45: UNDRAINED CYCLIC TRIAXIAL TEST NO. 47: HYDRAULIC FILL

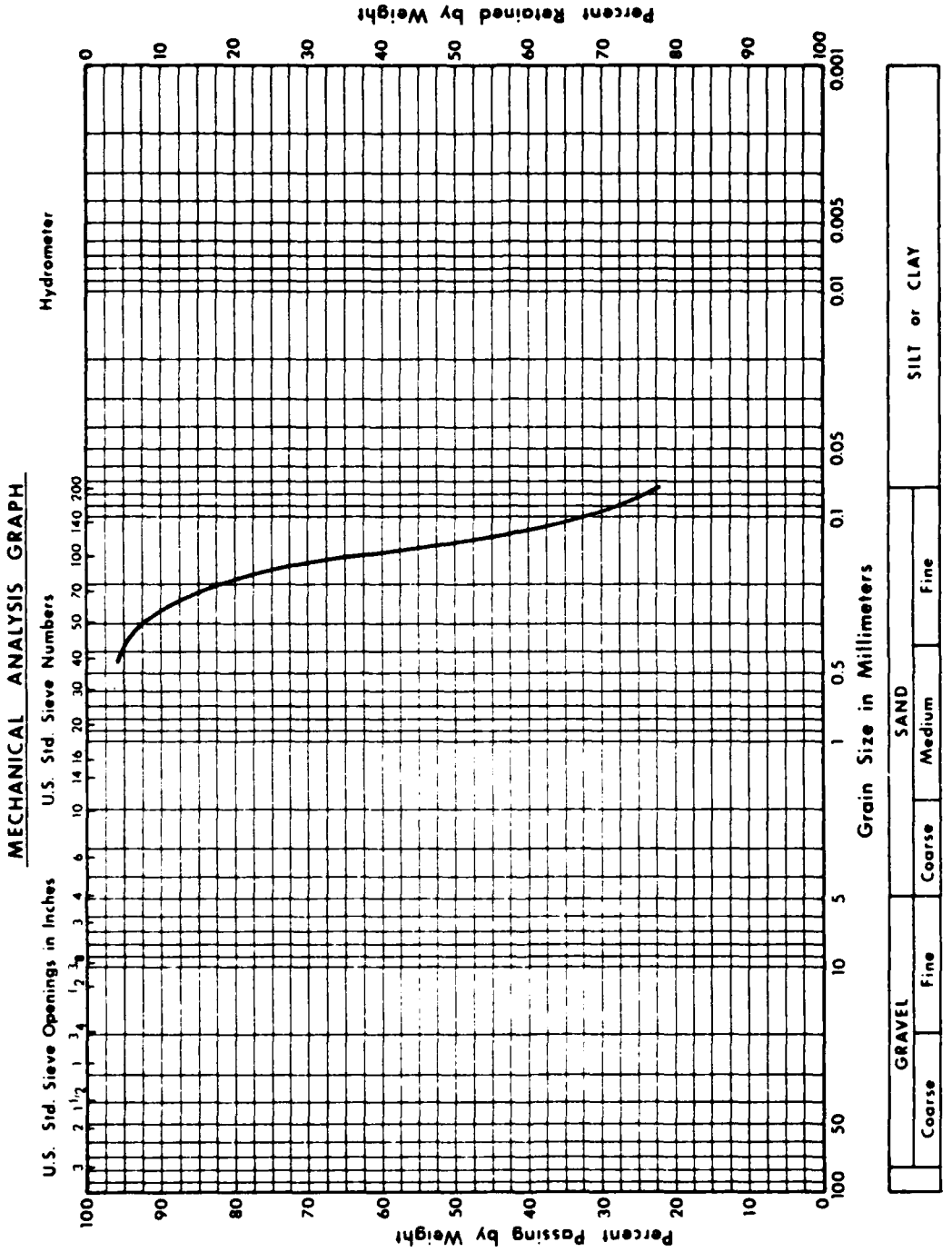

Figure D-46: GRAIN SIZE DISTRIBUTION; CYCLIC TRIAXIAL TEST NO. 47

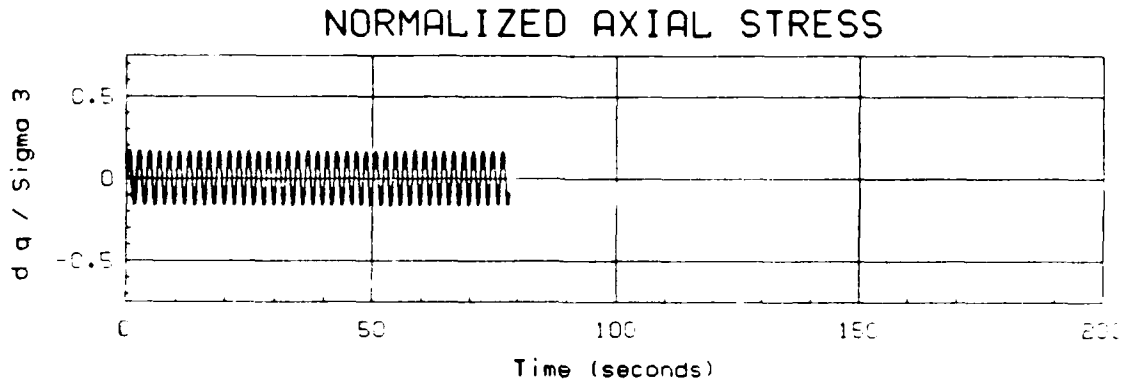

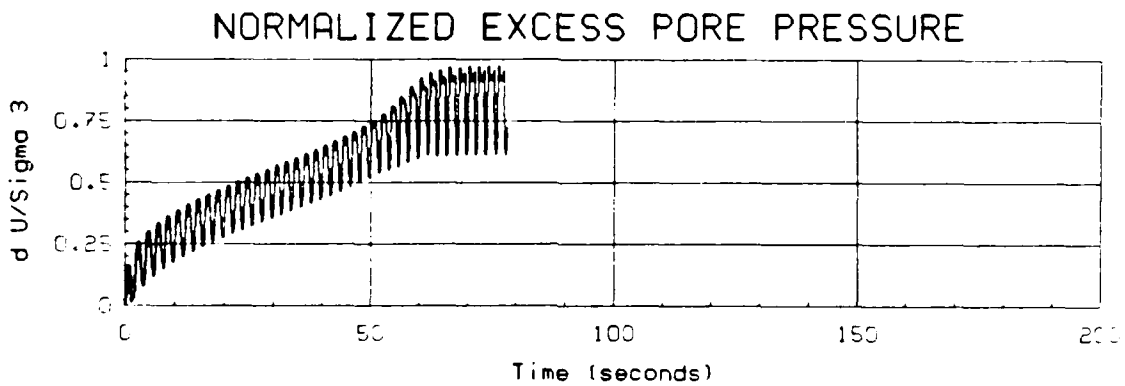

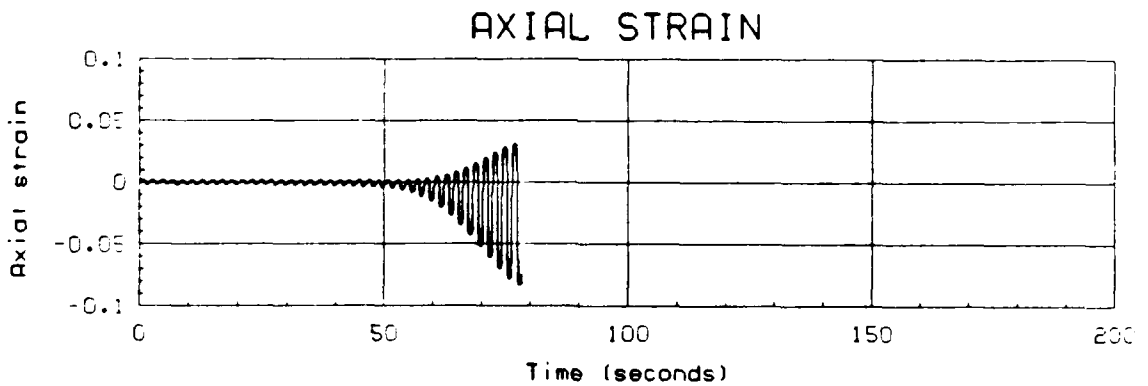

Test No.	: 49	B-value	: 0.998
Test Date	: 9/4/86	$\sigma_{3,i}'$	: 2.00 ksc
Material	: Tube TS211	K_c	: 1.00
Silty Sand (SM-ML), 36% fines.		CSR	: 0.172

Figure D-47: UNDRAINED CYCLIC TRIAXIAL TEST NO. 49: HYDRAULIC FILL

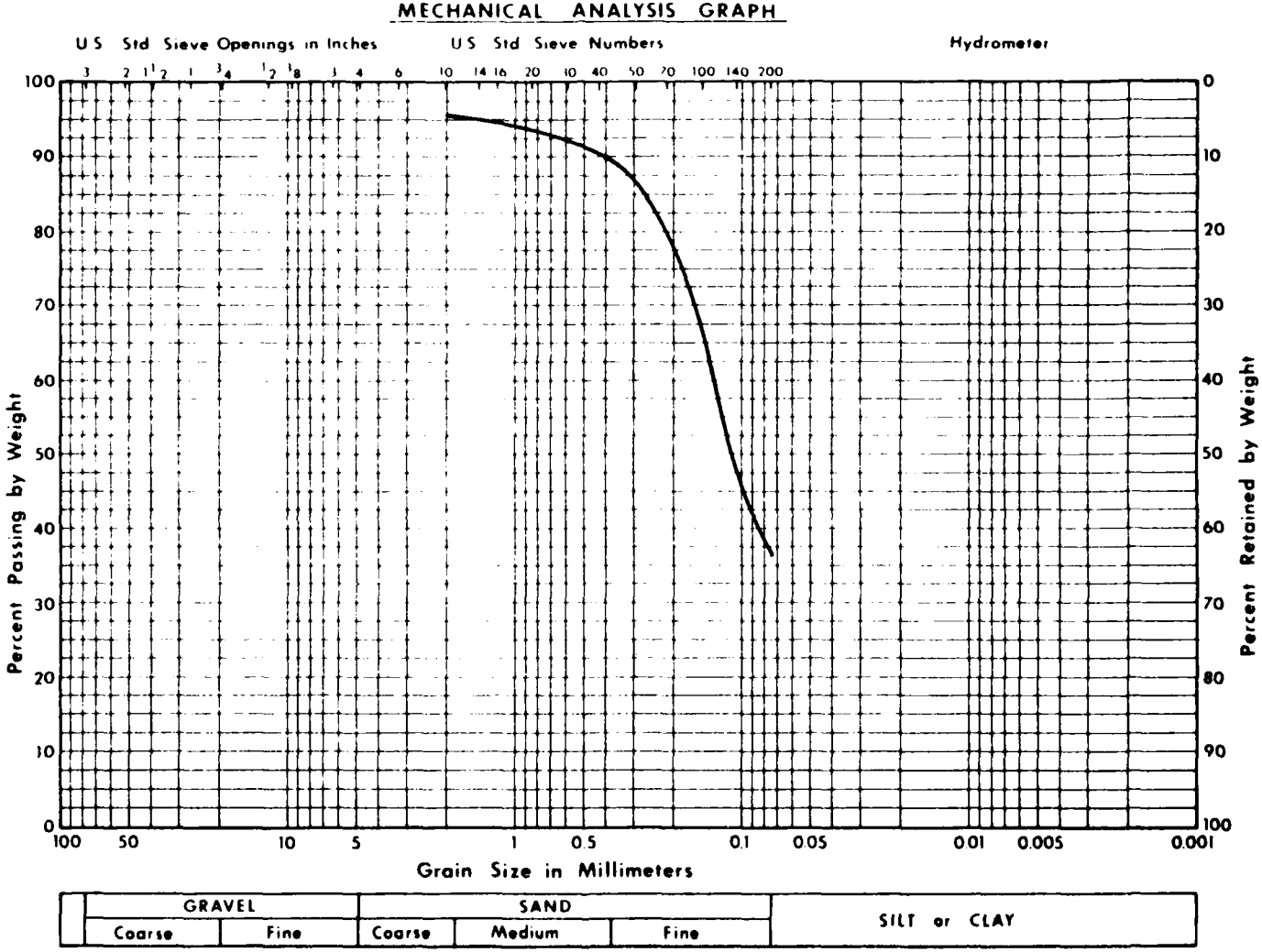

Figure D-48: GRAIN SIZE DISTRIBUTION; CYCLIC TRIAXIAL TEST NO. 49